UNIVERSITY OF CALIFORNIA
RIVERSIDE

Urban Air Pollution: Wastewater Treatment Sources and Impacts on Agriculture

A Dissertation submitted in partial satisfaction
of the requirements for the degree of

Doctor of Philosophy

in

Chemical and Environmental Engineering

by

Pedro Manuel Piqueras

June 2017

Dissertation Committee:
Dr. Akua Asa-Awuku, Chairperson
Dr. David Cocker
Dr. Mark Matsumoto

The Dissertation of Pedro Manuel Piqueras is approved:

_____

_____

_____

Committee Chairperson

University of California, Riverside

Acknowledgements

The work in this dissertation wouldn't have been possible without the help and guidance of my advisor, Akua Asa-Awuku, who continuously encouraged me to think for myself and to develop my project from scratch. Akua always knew that I could reach my true potential by applying my research to real world situations. She was a mentor and a friend in and outside of the laboratory and I truly appreciated her honesty, loyalty and helpfulness throughout the past four years. The following pages are the fruit of her advice on projects, and the end result of our publication ideas and career goals.

My colleagues, Ashley Vizenor, Emmanuel Fofie and Diep Vu provided important technical contributions in the laboratory as well as out of work discussions and experiences that helped me grow as a scientist. Thank you for all your involvement and suggestions. I look forward to continue our friendship for many years to come. I would also like to express my gratitude to Dr. Matsumoto, who contributed quite extensively with his expertise in wastewater and water quality during the bioreactor development and the field work in two chapters of this dissertation. His wisdom outside of the university also impacted my life both academically and personally. I must also thank Dr. David Cocker, who supplied me with air quality knowledge and laboratory instruction, as well as observations on my research. I am truly appreciative of the advice and relevant science that you have shared with me over the past four years. You gave valuable and insightful feedback on all of my work it has helped me enormously.

I would also like to specifically thank the staff of Orange County Sanitation District for access to the facilities, their assistance and cooperation. In addition, I must thank the numerous students (Jose, Wenyan, Tyler, Vincent, Derek, Mary, Carlos, Vincent) that helped me in and out of the laboratory. Thank you for always making sure that I had what I needed on time.

I am also very grateful for Rebecca Garland, who put so much work and effort on the phytotoxic study in Mpumalanga. Without her I would not have been able to accomplish the work in chapter 4 of this dissertation. Thank you for allowing this meaningful partnership to be a successful one. Additionally, I would like to express my gratitude to Seneca Naidoo, Mogesh Naidoo, and the rest of the team at the Council for Scientific and Industrial Research. It was an honor to work alongside South African scientists (especially Zane, Mthetho and Juanette) and I am thankful for the time spent in Pretoria. Thank you for friendliness, helpfulness and willingness to show me what I needed for my research and more. I look forward to continuing to have a strong relationship with you all for years to come.

I would also like to show my appreciation for Robiul Islam, Meredith Leigha and Betsy Stone from the University of Iowa for opening up to the idea of collaboration and for sending us the filter characterization data in chapter 2 of this dissertation. This also goes to Fengying Li from the Nanjing University of Information Science and Technology in China, who also decided to collaborate in our project and provided meaningful modeling results. My most sincere gratitude also goes to Katie Curnyn and Marylynn

Yates for the time that they spent teaching me MS2 propagation techniques, training me on biosafety procedures and for letting me use the microbiology laboratory.

A huge thank you goes to my wife, Sara Piqueras, who helped me to keep my head straight through the hardest times of this PhD. She provided a critical emotional support that was key to the success of my graduate studies. Countlessly, she listened to my long speeches, practice presentations, gave me ideas and often helped me at the laboratory. Yet she never expected anything in return. Thank you for sticking by my side for this wild journey.

I also would like to recognize my parents who listened to me and helped me get to where I am today. You devoted a tremendous amount of energy, time and money for me to pursue my dreams. I am thankful for the encouragement I have received ever since I was little to challenge stereotypes, to push my limits, to discover the unknown and to develop a curiosity for nature. You were also the reason why I decided to apply my research to help others and I am forever indebted to what you have invested in me.

Lastly, I would like to thank the funding agencies; the National Science Foundation (NSF), the RIFA program and the UC Global Development Lab, UC Graduate Division and the Center for Environmental Science and Technology at UCR, which generous contribution was critical to the execution and success of my projects.

The text of Chapter 2 is a reprint of the material as it appear in the journal of Environmental Science and Technology, Volume 50, Issue 20, 2016, Pages 11137-11144 Technology (DOI: 10.1021/acs.est.6b02684) from the American Chemical Society. This publication was titled "Real-Time Ultrafine Aerosol Measurements from Wastewater Treatment Facilities" by P. Piqueras, F. Li, V. Castelluccio, M. Matsumoto, and A. Asa-Awuku.

The text of the introduction and the closing remark is a partial reprint of the material from a policy brief that was written for the United Nations Global Sustainable Development Report (UN GSDR 2016). The text appears in the article "The rapidly growing death toll attributed to air pollution: A global responsibility" by P. Piqueras and A. Vizenor.

The text and results in chapter 3 (with authorship order: P. Piqueras, R. Islam, M. Leigha, B. Stone and A. Asa-Awuku), chapter 3 (with authorship order: P. Piqueras, K. Curnyn and A. Asa-Awuku) and chapter 4 (with authorship order: P. Piqueras, A.B. Nstele, R. Garland and A. Asa-Awuku) will soon be submitted to separate journals for publication. Chapter 4 will also be disclosed (partially or in full) in regional and national air quality reports within South Africa.

ABSTRACT OF DISSERTATION

Urban Air Pollution: Wastewater Treatment Sources and Impacts on Agriculture

by

Pedro Manuel Piqueras

Doctor of Philosophy, Graduate Program in Chemical and Environmental Engineering
University of California, Riverside, June 2017
Dr. Akua Asa-Awuku, Chairperson

The risks associated with exposure to emissions from wastewater treatment plants (WWTP) are currently uncertain and require more research, stronger regulatory frameworks and safer design consideration. Known toxic compounds, bacteria, fungi, endotoxins and viruses have been observed near WWTP the past, but their concentration and classification are still dubious. The airborne exposure route is also still poorly established due to the lack of information on aerosol characterization and transport.

The first portion of this dissertation attempts to fill some of the gaps in scientific literature by establishing a relationship between WWTP aerated basin coverage, source emission flux, particle composition, size and distribution as well as the dispersion of aerosolized particulates in Southern California. On-line measurements and filter sample collection were executed at Orange County Sanitation District (OCSD) and at two other locations along the Santa Ana River Watershed; Redlands Wastewater Treatment Plant (RWWTP) and Western Municipal Wastewater Treatment Plant (WMWWTP) for comparison. A laboratory bioreactor was also created to measure Chemical Oxygen

Demand (COD), Total Organic Carbon (TOC) and Total Suspended Solids (TSS) and consequently develop a theoretical model, which will later serve as a guide to estimate real world WWTP aerosol number emission fluxes from laboratory data. In addition, the role of hygroscopic growth (CCN activity) in viral wet deposition was investigated at a relative humidity representative of the respiratory system (the upper airways and lungs). The outcome of this analysis provided critical information to further understand the probability of disease via inhalation of pathogens in WWTP aerosol. Results will provide science to aid the design of potential regulatory laws to further implement a safe and non-polluting environment when treating wastewater.

The last chapter of this dissertation provides a phytotoxic assessment on four major crops (wheat, maize, sorghum and soybean) in Mpumalanga province, the fourth-biggest contributor to South Africa's GDP and a region with a horticultural industry that the country heavily relies on. This work highlights the importance of sulfur dioxide emissions and ozone formation in the Highveld Priority Area (HPA) in terms of stressors on agriculture and food security (measured as crop yield losses). The study also compares the phytotoxic results with the potential risk to human health through the inhalation of these pollutants and it presents a monetary value for the total revenue loss within the region.

Table of Contents

List of Figures

List of Tables

List of Acronyms

AA	Annual Average
ARB	Air Resources Board (California)
AERMOD	AMS/EPA Regulatory Model
AERMET	AERMOD Meteorological Preprocessor
AIDS	Acquired Immune Deficiency Syndrome
ALRI	Acute Lower Respiratory Tract Infections
AQA	Air Quality Act
AQMP	Air Quality Management Plan
AOT	Accumulated Ozone over Threshold
ATCC	American Type Culture Collection
AYL	Average Yield Loss
bCOD	Biochemical Oxygen Demand
CA	California
CAPIA	Cross Border Air Pollution Assessment (study)
CAMx	Comprehensive Air Quality Model with Extensions
CBD	Central Business District
CBG	Coomassie blue G (dye)
CCAM	Conformal Cubic Atmospheric Model
CCN	Cloud Condensation Nuclei
CCNC	Cloud Condensation Nuclei Counter
CLRTAP	Convention on Long-range Transboundary Air Pollution
CPC	Condensation Particle Counter
CO	Carbon Monoxide
COD	Chemical Oxygen Demand
COPD	Chronic obstructive pulmonary disease
CSIR	Council of Scientific and Industrial Research
DEA	Department of Environmental Affairs (South Africa)
DI	Deionized
DMT	Droplet Measurement Technologies
Dp_c	Critical Diameter
EPA	Environmental Protection Agency
ft	Feet
GCMS	Gas chromatography–mass spectrometry
GDP	Gross Domestic Product
GIS	Geographic information system
GSA	Growing Season Annual Average
h	hour
HCN	Health Council of the Netherlands
HEPA	High Efficiency Particulate Air
HPA	Highveld Priority Area
IEUA	Inland Empire Utilities Agency

IHD	Ischemic Heart Disease
LAL	Limulous Amoebocyte Lysate
m	Meter
MGD	Million Gallons per Day
MHPA	Mpumalanga Highveld Priority Area
min	Minute
MLSS	Mixed Liquor Suspended Solids
MWe	Megawatt electrical
NAAQS	(South African) National Ambient Air Quality Standards
nm	Nanometer
NOx	Nitrogen oxides
NPN	Non Protein Nitrogen
NSF	National Science Foundation
NRC	National Research Council
O_3	Ozone
OCSD	Orange County Sanitation District
OCWD	Orange County Water District
OECD	Organization for Economic Co-operation and Development
OF	Orange (County) Field Sample
OL	Orange (County) Laboratory Sample
PAH	Polycyclic Aromatic Hydrocarbon
PBS	Phosphate-Buffered Saline
PF	Pyrogen-free
pg	Picogram
PM	Particulate Matter
PTFE	Polytetrafluoroethylene
RF	Redlands Field Sample
RIFA	Research and Innovation Fellowship for Agriculture
RL	Redlands Laboratory Sample
RNA	Ribonucleic Acid
RWWTP	Redlands Wastewater Treatment Plant
SA	South Africa
SAAQIS	South African Air Quality Information System
SAWPA	Santa Ana Watershed Project Authority
SAWS	South African Weather Service
S_c	Critical Supersaturation
SCAQMD	South Coast Air Quality Management District
SBVMWD	San Bernardino Valley Municipal Water District
SCFM	Standard Cubic Feet per Minute
SLCP	Short Lived Climate Pollutants
SMCA	Scanning Mobility CCN Analysis
SMPS	Scanning Mobility Particle Sizer
SO_2	Sulfur Dioxide
SOA	Secondary organic aerosol

TAL	Total Average Loss
TMS	Trimethylsilyl
TOC	Total Organic Carbon
TSB	Tryptic Soy Broth
TSS	Total Suspended Solids
UC	University of California
UNECE	United Nations Economic Commission for Europe
VOC	Volatile Organic Compound
WF	Western (Municipal) Field Sample
WGS	World Geodetic System
WHO	World Health Organization
WL	Western (Municipal) Laboratory Sample
WWTP	Wastewater Treatment Plant
WMWD	Western Municipal Water District
WMWWTP	Western Municipal Wastewater Treatment Plant
ºC	Celsius
µg	Micrograms
µm	Micrometers

Chapter 1: Introduction

Urban air pollution is a growing problem due to the rapid population growth and high energy demands that our society is increasingly experiencing. Emissions from the industrial and transportation sector have been studied the past few decades and their burden has been found to result in regional and global harm on health, climate and vegetation. However, unregulated sources still exist and they may aggravate the economic and social welfare of those that suffer their repercussions, thus impeding prosperity and development in many corners around the world.

According to estimates published by the World Health Organization, 7 million people died as a result of air pollution exposure in 2012 (WHO, 2014). This number signifies one out of eight total global deaths, confirming that air pollution is now the world's largest single environmental health risk, killing more people than malaria and AIDS. Air pollution is not just the concern of a single nation; the matter calls for universal cooperation, as air is a natural resource that does not obey geopolitical boundaries.

High concentrations of atmospheric pollutants are the product that results from unsustainable regional policies and the lack of affordable green technology transfer (Piqueras, P. and Vizenor, A., 2016). The areas that are mostly affected by polluted air have seen a myriad of life-threatening diseases (Pope, 1989; Schwartz et al., 1992; Bruce et al., 2000; Sunyer et al., 2000; Peters et al., 2001; Brunekreef et al., 2002; Brook et al., 2004; Arden Pope et al., 2004; Dominici et al., 2006; Hoek et al., 2013; Loomis et al.,

2013; Jerret et al., 2013; Guarnieri et al., 2014; Newby et al., 2015; Ritz et al., 2016; Thurston et al., 2016; Heroux et al., 2017; Frostad et al., 2017) as well as damage to vegetation (Farmer, 1997; Fuhrer et al 1997; Emberson et al. 2001; van Tienhoven and Scholes, 2003; Smidt and Herman, 2004; Zunckel et al., 2006; Felzer, 2007 Fuhrer, 2009; van Dingenen et al., 2009; Avnery et al., 2011; Yuan et al., 2015) while solar radiation gets trapped in the Earth's atmosphere (Satterthwaite et al.,; 2008; Matthews et al., 2009; Friedlingstein, 2009; Dai, 2012; McGlade et al., 2015; Tubiello et al., 2015; Spracklen, 2016; Quilcaille et al., 2016; Manoli et al., 2016;).

Outdoor air pollution specifically contributes to 3.3 million premature deaths worldwide per year and it is estimated that the number of deaths will double by 2050 if the issue remains unattended (Lelieveld et al, 2015). Globally, the production of energy for commercial and residential use is the main source of emitted atmospheric pollutants. The Western Pacific region, followed by the eastern part of the Mediterranean and Southeast Asia suffer the highest mortality rate per capita in the world, with 70% of total deaths occurring in South and East Asia. China, India and Pakistan account for the highest death toll (1.36 million, 645,000 and 111,000 respectively). Of the Western countries, the United States ranks highest, with a mortality rate of 54,905. (Lelieveld et al, 2015).

Southern California is infamous for its poor air quality (Jerrett et al., 2013). A study published by the American Thoracic Society in 2016 mentioned that the Los Angeles area has the deadliest air in the United States, with 1,451 yearly deaths due to pollution. The Riverside-San Bernardino-Ontario metropolitan area is the second worst,

with 808 deceased every year. The Santa Ana-Irvine area lays in third place with 64 estimated deaths from air pollution on a yearly basis (Cromar et al., 2016). These results appear to be conservative as the health-care professionals did not count deaths from cancers that take decades to develop or deaths from the exacerbation of other chronic illnesses such as diabetes.

The death toll attributed to air pollution in Southern California is alarming, but it is relatively low when it is compared to third world countries. Developing countries tend to have higher risks due to the lack of regulations and their exponential economic growth. South Africa, for example, a country that is considered to have similar climate to California, has a larger pollution burden even though its population is less abundant. It is considered to be one of the most economically advanced countries in Africa (Shahbaz et al., 2013), but its source of emission remains heavily unregulated. Research from the World Bank established that 20,000 deaths occur in South Africa due to air pollution, costing the country at total of R 300 million ($22.6 million) (World Bank, 2016). A South African national analysis indicated that indoor air pollution and urban air pollution are ranked fifteenth and seventeenth, respectively, as risk factors causing the national burden of disease, and the associated air pollution health effects, namely tuberculosis and lower respiratory tract infections, were ranked third and sixth, respectively, in terms of disease prevalence in the country (Norman et al., 2007; MRC, 2008).

In many areas of South Africa where air quality is monitored, international standards are exceeded on a regular basis. This is mainly due to the usage of low-grade

and fossil fuels that the country needs to produce to meet the high electricity demands. Most of the country's energy is produced in the Highveld Area, where many large cities, including Johannesburg and Pretoria, are located (Philander, 2012; Mathu et al., 2013). The high elevation of the Highveld makes the oxygen level 20% less than the oxygen level in the coast, which results in an incomplete combustion of fossil fuels. A severe nocturnal temperature inversion also occurs; which results in smoke being trapped in the air near the surface (Mathee et al., 2003).

Pollutants are emitted from a myriad on sources. They can be gaseous or in the particulate phase and their composition and concentration is the key factor to understand their level of toxicity and pathogenicity. Chronic obstructive pulmonary disease (COPD), ischemic heart disease (IHD), acute lower respiratory illness (ALRI) and lung cancer have been associated with most air pollution related deaths (WHO, 2014). IHD, ALRI and lung cancer have been associated with the inhaling of fine particles (PM or particulate matter), while COPD is mainly caused by ozone (WHO, 2014).

1.1 Particulate matter

Particulate matter (PM), are microscopic particles suspended in the air that can be emitted by human activities or natural events. These particles can be primary (emitted directly from a source) or secondary (forming from the reaction of existing gaseous pollutants in the atmosphere). $PM_{2.5}$, particles of 2.5 micrometers in diameter or less, are much smaller than a grain of sand and even twenty times thinner than a human hair. They

are small enough to enter the lungs and directly penetrate into the blood stream. Exposure to $PM_{2.5}$ has been shown to be the largest contributor to the adverse cardiovascular effects that result in increased hospitalizations and emergency visits for heart attacks, strokes and death (Shah et al., 2015). Although all $PM_{2.5}$ is detrimental to health, carbonaceous $PM_{2.5}$ from combustion of fossil fuels, such as gasoline and coal, are more toxic than natural particles like dust or small sand fragments (Tuomisto et al., 2008). However, while PM research has expanded exponentially over the past decades and mitigation technologies (such as filters and catalysts) have been implemented in many regions around the world, there are still a large amount of sources that remain misunderstood and unregulated.

1.1.1 Bioaerosols and airborne pathogens

Bioaerosols, a subcategory of particulate matter, compromise fragments of biological origin or activity with may affect living things through infectivity, allergenicity, toxicity or other characteristics (Cox and Wathes, 1995). Many processes in nature generate bioaerosols outdoors (e.g. air turbulence, bursting of bubbles, irrigation…etc.). These range from allergens to bacteria, viruses, droplet nuclei, pollens, etc. The sources can be human animal, plant and their composition may vary depending on the source. Some of these may compromise respiratory pathogens which may pose a serious risk through infection (Cox and Wathes, 1995).

The ability to successfully monitor these sources has not yet been fully developed and only a few occupational exposure limits have been set for environments where bioaerosols are found. For example, the Health Council of the Netherlands, recommends

health-based occupational exposure limits for endotoxins (Feron et al., 1998). However, endotoxins are naturally occurring substances and have not been classified and labeled by the European Union or the United States yet. Further assessment and efficient regulation requires a holistic and meaningful data collection as well as characterization of bioaerosols.

Past studies have evaluated the biological risks of aerosols by determining the concentrations of living microorganisms and by using different detection and sampling methods (Fannin et al., 1985; Bauera et al., 2002; Karra and Katsivela, 2007). However, bioaerosol conclusions in past literature often results in confusing and conflicting perspective. Methodology on how to measure or sample sources as well as analytical techniques in the laboratory are not fully established as the sampling efficiency is not yet accurate (Zhao et al., 2011). Samplers are also not fully calibrated as calibration techniques for bioaerosols are not well developed.

WWTP employees and those who live nearby WWTP have been shown to be at a higher risk of developing a large variety of work-related symptoms including respiratory and gastrointestinal effects as well as fatigue and headache (Douwes et al., 2001; Rylander, 1999; Thorn and Beijer, 2004). Previous reports of municipal WWTP particulates have shown that high levels of bioaerosols including bacteria and fungi indoor of the WWTP facilities (Brandi et al., 2000; Sánchez-Monedero et al., 2008). Occupational exposure to the airborne particulates that contain microorganisms and chemical compounds of concern could explain part of the work-related illnesses. This

dissertation provides a collection of investigations that attempt to understand bioaerosols from WWTP and to provide guidance on physical an, biological and chemical properties.

1.2 Ozone and SO_2

Ozone (O_3) is a gas that forms as a product of chemical reactions between anthropogenic nitrogen oxides (NOx) and volatile organic compounds (VOC) in the presence of sunlight. Although ozone is beneficial in the stratosphere to protect the earth from harmful solar radiation (McClaure-Begley et al, 2014), ground-level or tropospheric ozone can trigger a variety of health problems, particularly for children and the elderly. It can also lead to an increase in markers of morbidity such as asthma attacks, hospital admissions, and death.

SO_2 emissions, especially from coal fired power plants and the coal industry, continues to be a serious issue in my developing countries (Held et al. 1996; Arndt et al. 1997; UNECE, 2010). Unlike ozone, it is a pollutant that is directly emitted from the source. The burning of coal in households in developing countries also contributes to ambient SO_2 concentrations and it harms the health of women and children who are exposed to high levels of this pollutant indoors (Osborne et al., 2016). This is mostly due to the fact that many families rely on coal and biomass in the form of wood, dung and crop residues for domestic energy. SO_2 may also forms sulfuric and sulfurous aerosol acid in presence of water vapor that is later part of the so-called acid rain (Wesely and Hicks 1977; Kuylenstierna and Chadwick 1989; Whelpdale and Kaiser 1996; Kuylenstierna et al. 1995, 2001; Kuylenstierna and Hicks 2002; Josipovic et al., 2007).

1.2.1 Impacts on agriculture

The potential for ambient ozone and sulfur dioxide to damage agricultural crops and vegetation is well documented in literature (Farmer, 1997; Fuhrer et al 1997; Emberson et al. 2001; van Tienhoven and Scholes, 2003; Smidt and Herman, 2004; Zunckel et al., 2006; Felzer, 2007 Fuhrer, 2009; Avnery et al., 2011; van Dingenen et al., 2009; Fuhrer 2009; Yuan et al., 2015). The two gaseous compounds enter the plant through its open stomata and make its way to the interior of the leaf (Reich, 1987). Damage to plants is shown by visible leaf injury, flecking and reduced photosynthesis which results in reduced growth rate (Krupa et al., 1998; Mauzerall and Wang 2001; Morgan et al., 2006; Felzer et al., 2007). Thus the yield and growth of the plant become suppressed and nutrition capacity weakens.

Agriculture is one of the main sources of income of many households and is central to food security in South Africa and the African continent at large. As a result, society is extremely vulnerable because agricultural enterprises, whether they focus on crop production, animal husbandry, fruit production or pasture, are extremely sensitive to weather, climate variability and change. Ambient ground level ozone (O_3) concentrations have doubled since the 1900s globally (Osborne et al., 2016), yet there are very few studies in South Africa that focus on ozone and its impacts on agriculture (van Tienhoven et al., 2003, Zunckel et al., 2004; Zunckel et al., 2006; van Tienhoven et al., 2006).

1.3 The climate-health connection

While air pollution is a known threat to human health and agriculture, it also poses a threat to global climate. Most are aware of the warming of the planet due to anthropogenic carbon dioxide (CO_2) emissions. Nonetheless, these emissions only affect human health indirectly by intensifying climate change's catastrophic aftermath. Breathing carbon dioxide is not harmful to humans. However, short-lived climate pollutants (SLCP), such as particulate matter, methane (CH_4) and tropospheric ozone, can cause harmful health effects as previously mentioned, while also affecting climate. Their relative climate potency, when measured in terms of how they heat the atmosphere, can be tens, hundreds, or even thousands of times greater than that of CO_2 (ARB, 2015), but they do not remain in the atmosphere as long. The potential benefits from reducing SLCPs are similar to those of CO_2 reduction. Mitigating SLCP emissions could lead to climate benefits as it will assist the slowdown of global warming and consequently reduce sea level rise while improving regional air quality. It will also benefit economic well-being by reducing disease and protecting endangered ecosystems worldwide (ARB, 2015).

Atmospheric aerosols (another term for particulate matter) may act as cloud condensation nuclei (CCN) upon which liquid droplets can form. This process can also take place in supersaturated environments within the body; when airborne particles enter the respiratory tract, condensational particle growth may occur (Tang et al., 2012). This growth, also called hygroscopic growth, is determined by the uptake of water vapor of the air (humidity) in the respiratory tract by hygroscopic components in the particles. This

growth is also described as cloud condensation nuclei (CCN) activity and it is influenced by the size and composition of the particles (Petters and Kreidenweis, 2007).

Indeed in the context of a changing climate, these ambient air pollution drivers change as well. Sources (i.e. emissions) may be altered due to changes in their spatial distribution or activity brought about by climate change. Atmospheric chemistry is also impacted since reactions are dependent on temperature and solar radiation. For example, a change in the timing, duration and intensity of the high pressure system over north eastern South Africa will affect the number of clear sky days (characteristic of the high pressure cell induced subsidence), thereby changing the amount of solar radiation available for ozone formation. Similarly, regional transport of pollutants will be impacted as the subsidence induced by the high pressure creates stable layers where pollutants may be trapped and concentrated. Additionally, changing rainfall patterns will change where and when pollutants may be rained out. Thus, in order for air quality management to be effective into the future, it is needed to understand the potential impact that climate change may have on air pollution.

The potential linkages between air pollution, climate and resultant impacts are complex and multi-faceted and as such, it is critical for policy-makers to have the necessary analytical support to make informed decisions and understand the potential trade-offs. Due to the large potential impacts of air quality, its linkages to the climate, and the complexities discussed above, it is important to understand the impact of policies, interventions and management decisions from multiple sectors and policies on air pollution and its resultant impacts. The end goal of this dissertation is to provide

frameworks to assist in analyzing the impact of policies on climate change, air pollution, human health and ecosystems.

1.4 Outline of dissertation

Chapter 2 presents a study of the quantification of ultrafine particulate emissions from WWTP as well as a bioreactor development procedure to estimate how aeration flow affects particle concentration flux. The correlations between wastewater parameters (Total Organic Carbon (TOC), Chemical Oxygen Demand (COD) and Total Suspended Solids (TSS)), aeration flow rate and particle concentrations were also explored. A theoretical model was also developed to compare real world WWTP aerosol number emission fluxes with laboratory data.

Chapter 3 discusses the results of chemical characterization of the particulates found at three WWTP, which were collected through filters samples. A model is also presented to understand the transport of the particulates once they escape the basins and several mitigation coverage options are investigated.

Chapter 4 provides a new method development for CCN activity of active viral particles. Aerosolized bioreactor particles through sludge conventional aeration in a laboratory bioreactor are compared to the size and hygroscopicity of MS2 bacteriophage, a commonly used model for human viruses. Viral propagation reagents (agar, PBS and TSB solution) were also explored.

Chapter 5 outlines a phytotoxic assessment of sulfur dioxide and ozone in the Mpumalanga Highveld Priority area. AOT40 values, a threshold used by the European

Union to estimate crop yield los, were calculated by utilizing a multi-year data set provided by three monitoring networks; the South African Department of Environmental Affairs, Eskom (a national public utility) and Sasol (a petrochemical corporation).

Chapter 6 concludes the findings in this dissertation and chapter proposes future work.

1.5 References

Arden Pope, C. et al. "Cardiovascular Mortality and Long-Term Exposure to Particulate Air Pollution." *Circulation* 109.1 (2004): 71–77. Print.

Arndt, Richard L. et al. "Sulfur Dioxide Emissions and Sectorial Contributions to Sulfur Deposition in Asia." *Atmospheric environment* 31.10 (1997): 1553–1572. Print.

Avnery, Shiri et al. "Global Crop Yield Reductions due to Surface Ozone Exposure: 1. Year 2000 Crop Production Losses and Economic Damage." *Atmospheric environment* 45.13 (2011/4): 2284–2296. Print.

Bauer, H. et al. "Bacteria and Fungi in Aerosols Generated by Two Different Types of Wastewater Treatment Plants." *Water research* 36.16 (2002): 3965–3970. Print.

Brandi, G., M. Sisti, and G. Amagliani. "Evaluation of the Environmental Impact of Microbial Aerosols Generated by Wastewater Treatment Plants Utilizing Different Aeration Systems." *Journal of applied microbiology* 88.5 (2000): 845–852. Print.

Brook, Robert D. et al. "Air Pollution and Cardiovascular Disease." *Circulation* 109.21 (2004): 2655–2671. Print.

Bruce, N., R. Perez-Padilla, and R. Albalak. "Indoor Air Pollution in Developing Countries: A Major Environmental and Public Health Challenge." *Bulletin of the World Health Organization* 78.9 (2000): 1078–1092. Print.

Brunekreef, Bert, and Stephen T. Holgate. "Air Pollution and Health." *The Lancet* 360.9341 (2002): 1233–1242. Print.

Cohen, Aaron J. et al. "Estimates and 25-Year Trends of the Global Burden of Disease Attributable to Ambient Air Pollution: An Analysis of Data from the Global Burden of Diseases Study 2015." *The Lancet* (2017): n. pag. Web.

Cox, Christopher S., and Christopher M. Wathes. *Bioaerosols Handbook*. CRC Press, 1995. Print.

Cromar, Kevin R. et al. "American Thoracic Society and Marron Institute Report. Estimated Excess Morbidity and Mortality Caused by Air Pollution above

American Thoracic Society--Recommended Standards, 2011--2013." *Annals of the American Thoracic Society* 13.8 (2016): 1195–1201. Print.

Dai, Aiguo. “Increasing Drought under Global Warming in Observations and Models.” *Nature climate change* 3.1 (2012): 52–58. Print.

Dominici, Francesca et al. “Fine Particulate Air Pollution and Hospital Admission for Cardiovascular and Respiratory Diseases.” *JAMA: the journal of the American Medical Association* 295.10 (2006): 1127–1134. Print.

Emberson, L. D. et al. “Impacts of Air Pollutants on Vegetation in Developing Countries.” *Water, air, and soil pollution* 130.1-4 (2001): 107–118. Print.

Fannin, K. F., S. C. Vana, and W. Jakubowski. “Effect of an Activated Sludge Wastewater Treatment Plant on Ambient Air Densities of Aerosols Containing Bacteria and Viruses.” *Applied and environmental microbiology* 49.5 (1985): 1191–1196. Print.

Farmer, Andrew. *Managing Environmental Pollution*. Abingdon, UK: Taylor & Francis, 1997. Print.

Felzer, Benjamin S. et al. “Impacts of Ozone on Trees and Crops.” *Comptes rendus: Geoscience* 339.11–12 (2007): 784–798. Print.

Feron, V. J. et al. “Endotoxins: Health-Based Recommended Occupational Exposure Limit.” (1998): n. pag. Web. 26 Apr. 2017.

Fuhrer, Jürg. “Ozone Risk for Crops and Pastures in Present and Future Climates.” *Die Naturwissenschaften* 96.2 (2009): 173–194. Print.

Fuhrer, J., L. Skärby, and M. R. Ashmore. “Critical Levels for Ozone Effects on Vegetation in Europe.” *Environmental pollution* 97.1-2 (1997): 91–106. Print.

Guarnieri, Michael, and John R. Balmes. “Outdoor Air Pollution and Asthma.” *The Lancet* 383.9928 (2014): 1581–1592. Print.

Held, G. et al. “The Climatology and Meteorology of the Highveld.” *Air pollution and its impacts on the South African Highveld. Johannesburg: Environmental Scientific Association* (1996): 60–71. Print.

Hoek, Gerard et al. “Long-Term Air Pollution Exposure and Cardio- Respiratory Mortality: A Review.” *Environmental health: a global access science source* 12.1 (2013): 43. Print.

Héroux, Marie-Eve et al. "Response to: Premature Deaths Attributed to Ambient Air Pollutants: Let Us Interpret the Robins–Greenland Theorem Correctly." *International journal of public health* 62.3 (2017): 339–341. Print.

Jerrett, Michael et al. "Spatial Analysis of Air Pollution and Mortality in California." *American journal of respiratory and critical care medicine* 188.5 (2013): 593–599. Print.

Josipovic, Miroslav et al. "Concentrations, Distributions and Critical Level Exceedance Assessment of SO2, NO2 and O3 in South Africa." *Environmental monitoring and assessment* 171.1-4 (2010): 181–196. Print.

Karra, Styliani, and Eleftheria Katsivela. "Microorganisms in Bioaerosol Emissions from Wastewater Treatment Plants during Summer at a Mediterranean Site." *Water research* 41.6 (2007): 1355–1365. Print.

Krupa, S. V., M. Nosal, and A. H. Legge. "A Numerical Analysis of the Combined Open-Top Chamber Data from the USA and Europe on Ambient Ozone and Negative Crop Responses." *Environmental pollution* 101.1 (1998): 157–160. Print.

Kuylenstierna, J., and K. Hicks. "Air Pollution in Asia and Africa: The Approach of the RAPIDC Programme." *Proceedings of the 1st Open Seminar on the Regional Air Pollution in Developing Countries*. Vol. 4. N.p., 2002. Print.

Kuylenstierna, J. C. I. et al. "Terrestrial Ecosystem Sensitivity to Acidic Deposition in Developing Countries." *Water, air, and soil pollution* 85.4 (1995): 2319–2324. Print.

Kuylenstierna, Johan C. I., and Michael J. Chadwick. "The Relative Sensitivity of Ecosystems in Europe to the Indirect Effects of Acidic Depositions." *Regional Acidification Models*. Springer, Berlin, Heidelberg, 1989. 3–21. Print.

Lelieveld, J. et al. "The Contribution of Outdoor Air Pollution Sources to Premature Mortality on a Global Scale." *Nature* 525.7569 (2015): 367–371. Print.

Loomis, Dana et al. "The Carcinogenicity of Outdoor Air Pollution." *The lancet oncology* 14.13 (2013): 1262–1263. Print.

Manoli, Gabriele, Gabriel G. Katul, and Marco Marani. "Delay-Induced Rebounds in CO2 Emissions and Critical Time-Scales to Meet Global Warming Targets." *Earth's Future* (2016): n. pag. Web.

Mathee, Angela, and Yer von Schirnding. "Air Quality and Health in Greater Johannesburg." *Air pollution and health in developing countries. Earthscan Publications, London* (2003): 206–219. Print.

Mathu, Ken, and Richard Chinomona. "South African Coal Mining Industry: Socio-Economic Attributes." *Mediterranean Journal of Social Sciences* 4.14 (2013): 347. Print.

Matthews, H. Damon et al. "The Proportionality of Global Warming to Cumulative Carbon Emissions." *Nature* 459.7248 (2009): 829–832. Print.

Mauzerall, Denise L., and Xiaoping Wang. "Protecting Agricultural Crops from the Effects of Tropospheric Ozone Exposure: Reconciling Science and Standard Setting in the United States, Europe, and Asia." *Annual Review of Energy and the Environment* 26.1 (2001): 237–268. Print.

McClure-Begley, A., I. Petropavlovskikh, and S. Oltmans. "NOAA Global Monitoring Surface Ozone Network, 1973--2014, National Oceanic and Atmospheric Administration, Earth Systems Research Laboratory Global Monitoring Division, Boulder, CO." *Boulder, CO, doi* 10 (2014): V57P8WBF. Print.

McGlade, Christophe, and Paul Ekins. "The Geographical Distribution of Fossil Fuels Unused When Limiting Global Warming to 2 [deg] C." *Nature* 517.7533 (2015): 187–190. Print.

Morgan, Patrick B. et al. "Season-Long Elevation of Ozone Concentration to Projected 2050 Levels under Fully Open-Air Conditions Substantially Decreases the Growth and Production of Soybean." *The New phytologist* 170.2 (2006): 333–343. Print.

Newby, David E. et al. "Expert Position Paper on Air Pollution and Cardiovascular Disease." *European heart journal* 36.2 (2015): 83–93b. Print.

Norman, Rosana, Brendon Barnes, et al. "Estimating the Burden of Disease Attributable to Indoor Air Pollution from Household Use of Solid Fuels in South Africa in 2000." *South African medical journal = Suid-Afrikaanse tydskrif vir geneeskunde* 97.8 Pt 2 (2007): 764–771. Print.

Norman, Rosana, Eugene Cairncross, et al. "Estimating the Burden of Disease Attributable to Urban Outdoor Air Pollution in South Africa in 2000." *South African medical journal = Suid-Afrikaanse tydskrif vir geneeskunde* 97.8 Pt 2 (2007): 782–790. Print.

Osborne, Stephanie A. et al. “Has the Sensitivity of Soybean Cultivars to Ozone Pollution Increased with Time? An Analysis of Published Dose–response Data.” *Global change biology* 22.9 (2016): 3097–3111. Print.

Peters, A. et al. “Increased Particulate Air Pollution and the Triggering of Myocardial Infarction.” *Circulation* 103.23 (2001): 2810–2815. Print.

Petters, M. D., and S. M. Kreidenweis. “A Single Parameter Representation of Hygroscopic Growth and Cloud Condensation Nucleus Activity.” *Atmospheric Chemistry and Physics* 7.8 (2007): 1961–1971. Print.

Philander, S. George, ed. “United Nations Framework Convention on Climate Change.” *Encyclopedia of Global Warming & Climate Change*. 2455 Teller Road, Thousand Oaks California 91320 United States : SAGE Publications, Inc., 2012. Print.

Piqueras, Pedro, and Ashley Vizenor. “The Rapidly Growing Death Toll Attributed to Air Pollution: A Global Responsibility.” n. pag. Web.

Pope, C. A., 3rd. “Respiratory Disease Associated with Community Air Pollution and a Steel Mill, Utah Valley.” *American journal of public health* 79.5 (1989): 623–628. Print.

Quilcaille, Yann et al. “Uncertainty in Projected Climate Change Caused by Methodological Discrepancy in Estimating CO2 Emissions from Fossil Fuel Combustion.” *EGU General Assembly Conference Abstracts*. Vol. 18. adsabs.harvard.edu, 2016. 10549. Print.

Reich, P. B. “Quantifying Plant Response to Ozone: A Unifying Theory.” *Tree physiology* 3.1 (1987): 63–91. Print.

Ritz, Beate et al. “Traffic-Related Air Pollution and Parkinson’s Disease in Denmark: A Case--Control Study.” *Environmental health perspectives* 124.3 (2016): 351. Print.

Satterthwaite, David. “Cities’ Contribution to Global Warming: Notes on the Allocation of Greenhouse Gas Emissions.” *Environment and Urbanization* 20.2 (2008): 539–549. Print.

Schwartz, J., and D. W. Dockery. “Increased Mortality in Philadelphia Associated with Daily Air Pollution Concentrations.” *The American review of respiratory disease* 145.3 (1992): 600–604. Print.

Shah, Anoop S. V. et al. “Short Term Exposure to Air Pollution and Stroke: Systematic Review and Meta-Analysis.” *BMJ* 350 (2015): h1295. Print.

Shahbaz, Muhammad, Aviral Kumar Tiwari, and Muhammad Nasir. “The Effects of Financial Development, Economic Growth, Coal Consumption and Trade Openness on CO2 Emissions in South Africa.” *Energy policy* 61 (2013): 1452–1459. Print.

Smidt, Stefan, and Friedl Herman. “Evaluation of Air Pollution-Related Risks for Austrian Mountain Forests.” *Environmental pollution* 130.1 (2004): 99–112. Print.

Solomon, Susan et al. “Irreversible Climate Change due to Carbon Dioxide Emissions.” *Proceedings of the National Academy of Sciences of the United States of America* 106.6 (2009): 1704–1709. Print.

Spracklen, Dominick V. “Global Warming: China’s Contribution to Climate Change.” *Nature* 531.7594 (2016): 310–312. Print.

Sunyer, J. et al. “Patients with Chronic Obstructive Pulmonary Disease Are at Increased Risk of Death Associated with Urban Particle Air Pollution: A Case-Crossover Analysis.” *American journal of epidemiology* 151.1 (2000): 50–56. Print.

Sánchez-Monedero, M. A. et al. “Effect of the Aeration System on the Levels of Airborne Microorganisms Generated at Wastewater Treatment Plants.” *Water research* 42.14 (2008): 3739–3744. Print.

Tang, Xiaochen et al. “The Effects of Mainstream and Sidestream Environmental Tobacco Smoke Composition for Enhanced Condensational Droplet Growth by Water Vapor.” *Aerosol science and technology: the journal of the American Association for Aerosol Research* 46.7 (2012): 760–766. Print.

Thurston, George D. et al. “Ischemic Heart Disease Mortality and Long-Term Exposure to Source-Related Components of US Fine Particle Air Pollution.” *Environmental health perspectives* 124.6 (2016): 785. Print.

Tubiello, Francesco N. et al. “The Contribution of Agriculture, Forestry and Other Land Use Activities to Global Warming, 1990–2012.” *Global change biology* 21.7 (2015): 2655–2660. Print.

Tuomisto, Jouni T. et al. “Uncertainty in Mortality Response to Airborne Fine Particulate Matter: Combining European Air Pollution Experts.” *Reliability Engineering & System Safety* 93.5 (2008): 732–744. Print.

Van Dingenen, Rita et al. "The Global Impact of Ozone on Agricultural Crop Yields under Current and Future Air Quality Legislation." *Atmospheric environment* 43.3 (2009/1): 604–618. Print.

Van Tienhoven, A. M., and M. C. Scholes. "Air Pollution Impacts on Vegetation in South Africa." *Air pollution impacts on crops and forests: a global assessment. Imperial College Press, London* (2003): 237–262. Print.

Wesely, M. L., and B. B. Hicks. "Some Factors That Affect the Deposition Rates of Sulfur Dioxide and Similar Gases on Vegetation." *Journal of the Air Pollution Control Association* 27.11 (1977): 1110–1116. Print.

Whelpdale, Douglas Murray, and M. S. Kaiser. *Global Acid Deposition Assessment*. World Meteorological Organization, Global Atmosphere Watch, 1997. Print.

Yuan, Xiangyang et al. "Assessing the Effects of Ambient Ozone in China on Snap Bean Genotypes by Using Ethylenediurea (EDU)." *Environmental pollution* 205 (2015): 199–208. Print.

Zhao, Yang et al. "Investigation of the Efficiencies of Bioaerosol Samplers for Collecting Aerosolized Bacteria Using a Fluorescent Tracer. I: Effects of Non-Sampling Processes on Bacterial Culturability." *Aerosol science and technology: the journal of the American Association for Aerosol Research* 45.3 (2011): 423–431. Print.

Zunckel, M., K. Venjonoka, et al. "Van Tienhoven, AM. 2004a. Surface Ozone over Southern Africa: Synthesis of Monitoring Results during the Cross Border Air Pollution Impact Assessment Project." *Atmospheric environment* 38 6139–6147. Print.

Zunckel, M., A. Koosailee, et al. "Modelled Surface Ozone over Southern Africa during the Cross Border Air Pollution Impact Assessment Project." *Environmental Modelling & Software* 21.7 (2006/7): 911–924. Print.

MRC, 2008. 17 Risk Factors South African Comparative Risk Assessment, South African Medical Research Council. http://www.mrc.ac.za/bod/crasumrpt.pdf

WHO, 2014. "Burden of Disease from Ambient Air Pollution for 2012." n.d. (http://www.who.int/phe/health_topics/outdoorair/databases/AAP_BoD_results_March2014.pdf)

WHO, 2014. “Household (Indoor) Air Pollution.” 2014, November. World Health Organization. (http://www.who.int/indoorair/en/)

WHO, 2014. “WHO | 7 Million Premature Deaths Annually Linked to Air Pollution.” 2014, March. World Health Organization. (http://www.who.int/mediacentre/news/releases/2014/air-pollution/en/)

World Bank, 2016. *The Cost of Air Pollution: Strengthening the Economic Case for Action*. N.p., 2016. Print.

UNECE, 2010. Mapping Critical Levels for Vegetation. Manual on Methodologies and Criteria for Modelling and Mapping Critical Loads & Levels and Air Pollution Effects, Risks and Trends. *United Nations Economic Commission for Europe* (UNECE). Convention on Long-range Transboundary Air Pollution, 2010. Web.

Chapter 2: Real-time Ultrafine Aerosol Measurements from Wastewater Treatment Facilities

2.1 Abstract

Airborne particle emissions from wastewater treatment plants (WWTP) have been associated with health repercussions but particulate quantification studies are scarce. In this study, particulate matter (PM) number concentrations and size distributions in the ultrafine range (7-300 nm) were measured from two different sources: a laboratory-scale aerobic bioreactor and the activated sludge aeration basins at Orange County Sanitation District (OCSD). The relationships between wastewater parameters (Total Organic Carbon (TOC), Chemical Oxygen Demand (COD) and Total Suspended Solids (TSS)), aeration flow rate and particle concentrations were also explored. A significant positive relationship was found between particle concentration and WWTP variables (COD: $r(10)=.876$, $p<.001$, TOC: $r(10)=.664$, $p<.05$, TSS: $r(10)=.707$, $p<.05$, aeration flow rate: $r(8)=.988$, $p<.0001$). A theoretical model was also developed from empirical data to compare real world WWTP aerosol number emission fluxes with laboratory data. Aerosol number fluxes at OCSD aerated basins (9.8×10^4 #/min·cm^2) and the bioreactor (7.95×10^4 #/min·cm^2) were calculated and showed a relatively small difference (19%). The ultrafine size distributions from both systems were consistent, with a mode of ~48 nm. The average mass concentration (7.03 μg/cm^3) from OCSD was relatively small compared to other urban sources. However, the in-tank average number concentration of airborne particles (14,480 #/cm^3) was higher than background ambient concentrations.

2.2 Introduction

Wastewater treatment is a crucial component of maintaining the quality of natural water resources and it is increasingly important for developing alternative municipal water sources through reuse practice. However, whether current technologies are adequate to safeguard communities and workers from airborne chemicals and pathogens generated from the wastewater treatment plants (WWTPs) has yet to be determined (Walls, 2015). The risks associated with exposure to emissions from WWTPs are uncertain and require more research, stronger regulatory frameworks and safer design consideration.

Biological processes are used in municipal WWTPs for the removal of biodegradable organics (Tchobanoglous et al., 1991). During the secondary treatment process, microbes degrade organics aerobically (with oxygen) and/or anaerobically/anoxically (without oxygen). Organic components are measured as chemical and biochemical oxygen demand (COD & bCOD) and the values decrease with organic degradation. Aerobic processes have an enhanced effluent quality, high organic removal rates and efficiency, low temperature sensitivity, and operational stability (Chan et al., 2009). Anoxic systems do not require additional oxygen and are typically used after the aerobic system for the removal of nitrate. Anaerobic systems are used for the treatment of high concentrations of organic material (Leverenz et al., 2002). Anaerobic treatment is a net energy producer via methane generation and is enclosed to collect the gas (Glassmeyer et al., 2005). Therefore the exposure of airborne emissions from anaerobic and anoxic WWTP sources may be negligible. In contrast, aerobic tanks (even

covered ones) have outlets that allow the excess air mass to be released into the atmosphere. Open aerated basins are more likely to contribute to ambient particles and are thus the focus of this study.

The aerated basins contain a mixture of wastewater and activated sludge (mixed liquor). The activated sludge process can be described as a suspension of highly concentrated microorganisms in which organics rich wastewater is degraded in a continuous-flow manner (Tchobanoglous et al., 1991). Air is injected into the bottom of the aeration tank, which transfers oxygen into the mixed liquor as it rises upward. Fine bubble diffusers dominate the market in urban settings (Rosso and Stentrom, 2005). Previous work has shown that bubbles at the bottom of the basins are ~600 μm in diameter. Once the bubble has reached the surface, it bursts and ejects approximately five droplets of ~60 μm diameter. The droplets rise to a height of ~8 cm above the surface and may evaporate to form windborne aerosol particles (Fannin et al., 1985). The number and real-time size distribution of these particles once they leave the basin are not well understood and require in-situ measurements to understand changes in the aerosol physical properties. Epidemiological studies, biological assays and filter data suggests that airborne emissions from WWTP exist and impact health and regional air quality (Fannin et al., 1985; Clark et al., 1987; Carducci et al., 1995; Khuder et al., 1998; Bauer et al., 2002; Radke and Herrman, 2003; Radke, 2005; Smit et al., 2005; Beck et al., 2006; Carducci et al., 2008; Krzeniewska , 2001; Uhrbrand et al., 20112; Jebri et al., 2012; Upadhyay et al., 2013; Malakootian et al., 2013; Masclaux et al., 2014; Li et al., 2015; Niazi et al., 2105). However, little literature is available on the concentration and the

distribution of $PM_{0.1}$ emitted by aerobic processes. Furthermore, there is no published relationship between the previous emission data and parameters that describe the process of organic removal in WWTPs. This study fills that gap by presenting data from the systematic study of real-time particle concentrations and emission rates to wastewater parameters and organic degradation.

2.3 Methods

Particle concentrations, size distributions and aerosol fluxes from a laboratory batch bioreactor and the aeration tanks in OCSD were measured in this study. An Ultrafine Condensation Particle Counter (CPC, TSI 3776) measured total particle concentration (Agarwal et al., 1980). The TSI 3776 CPC has a lower particle detection size limit of 2.5 nm, was operated at a flow rate of 0.3 lpm and provided data at 1 Hz. A Scanning Mobility Particle Scanner or SMPS (TSI classifier 3080 with a TSI CPC 3772 operated in tandem) measured the electrical mobility diameter and number distribution. The SMPS is a common aerosol tool for real-time particle measurement and its operation and theoretical framework has been described in detail by Wang et al, 1989. The electrical mobility particle size ranged from 7 nm to 320 nm over 135 seconds. The sheath to aerosol ratio was maintained at 10 to 1. Particles were assumed to be spherical. Particles emitted were wet. Once emitted, they were exposed to subsaturated conditions (RH <100%). This likely initiated efflorescence (particle drying). No electric arcing occurred in the SMPS, thus the data is robust and represents real world WWTP

emissions. The difference between wet and dry particles is shown in the appendix (figure A2.1).

2.3.1 Laboratory Setup

The laboratory bioreactor setup consists of a 5-gal (18.9 L) cylinder with an air diffuser at the bottom of the reactor (figure 2-1a). The air source for the diffuser was filtered with a HEPA filter (Pall Corporation HEPA Capsule) as shown in figure 2-1a. The diffuser produced "particle free" bubbles homogeneously throughout the entire volume of the mixed liquor. The mixed liquor sludge was obtained from the Orange County Sanitation District (OCSD, Fountain Valley, CA) aerated basins. A molasses based synthetic wastewater was used as the organic feed. The synthetic molasses-based wastewater contained mainly sugar (sucrose $C_{12}H_{22}O_{11}$), making 50% of the total molasses mass content; 20% of the molasses mass consisted of non-sucrose organic matter; non-protein nitrogen (NPN) containing substances, such as betaine. The remaining composition contained other minor carbohydrates such as glucose, fructose, raffinose and other oligo- or polysaccharides as well as some minerals such as potassium, sodium, calcium and magnesium (OECD, 2015). Molasses was diluted with DI water to set the influent COD to the desired strength. The incoming bioreactor feed COD was 380 mg/L in each experiment, similar to OCSD influent wastewater COD levels. After a 2-day organic degradation, the COD removal was 79%.

The bioreactor was operated on a sequencing-batch mode, a variation of the activated sludge process, using a two-day feeding cycle. The sequencing batch cycle had

four phases: feed, react, settle, and decant. During the feed cycle 5 L of synthetic wastewater was added and followed by 44 hours of aerated reaction time. At the end of the reaction period, the contents were allowed to settle for 4 hours. 5 L of the reactor supernatant were decanted at the end of the settling period. Thereafter, the batch treatment cycle was reinitiated. The pH, alkalinity and temperature remained stable during the course of the experiments. Monitored bioreactor alkalinity was maintained at 150 mg/L of $CaCO_3$ via periodic addition of sodium bicarbonate. The pH was held at 7.2 and the reactor was kept at room temperature. Experiments were conducted in the fume hood and the average relative humidity was less than 25%.

Aerosols were measured within the enclosed headspace, 10 inches (25.4 cm) above the surface of the mixed liquor where bubble bursting occurred. Particle properties were measured with a 3 foot long (0.9 m), 1/8 inch (0.3 cm) diameter copper line split to the CPC 3776 and the SMPS. Particle size and total particle number measurements were taken in tandem (figure 2-1a). The aerosol measurement set-up conducted in the laboratory was the same at OCSD (Section 2.3.2). Particle losses in copper tubing were negligible at the flow rate, which both the CPC and SMPS were operated (0.3 lpm to 1.5 lpm) (Reineking et al., 1986).

2.3.1.1 COD, TOC and TSS

COD, TOC and TSS are parameters that are commonly used in water quality to describe the condition of the mixed liquor. COD degradation was observed over 48 hours and the EPA's dichromate method 410.4 obtained COD values (EPA, 1993). The monitoring began right after the feeding process. A 25 mL sample of the bioreactor's

mixed liquor was collected every hour to measure COD. The sample was filtered through a filter (Millipore 0.45 μm) to eliminate large particles.

A separate 48-hour experiment was conducted to understand the relationship between Total Suspended Solids (TSS), the degradation of Total Organic Carbon (TOC), and the particle concentrations emitted. TSS were determined using EPA Approved Method 2540 D of the Standard Methods (American Public Health Association, 2010), while the Total Organic Carbon (TOC) was measured following Part 5310 of Standard Methods. A 1088 Rotary Autosampler and an Aurora 1030 TOC Analyzer were used to process the samples.

2.3.1.2 Aeration flow rate

The bioreactor particle concentrations and particle size distributions were measured with 10 different airflows ranging from 0 L min^{-1} (anaerobic setting) up to 5 L min^{-1}. The airflow was monitored using a rotameter and calibrated with a flow meter. Total particle concentration measurements were conducted in triplicate. The bioreactor had a 48-hour degradation cycle; particle concentration data was recorded after 24 hours for 30 minutes. Each 30-minute experiment was performed three times on three different days and the average and standard error of the three data sets are presented. The percentage difference in particle counts outside of the SMPS range (below 7 nm or above 320 nm) and the total particles counted by the CPC were calculated and graphed for different airflows (figure A2.2).

2.3.2 Field set up

Orange County Sanitation District (OCSD) serves an area of 479 square miles in central and northwest Orange County with a population of ~2.5 million people, making it a large water treatment facility as it serves more than 50,000 people (Davies et al., 1997). It consists of two plants; plant 1, located in Fountain Valley, and plant 2 in Huntington Beach. Both plants treat around 230 million gallons (870 million liters) of wastewater per day altogether (OCSD, 2016). This study focuses on emissions from plant 1.

There are 16 individual aerated basins separated into two buildings. The first building from south to north contains tanks 1-10 and the second building has tanks 11-16. All tanks are covered with a concrete slab. As mentioned previously, there are openings for the aerated air mass to exit. These openings are 15 by 15 feet (4.6 by 4.6 m) in area as shown in figure 2-1b and 2-1c. For the purpose of this work, in regards to air quality, we define them as "semi-covered". This study measured emissions from tanks 11-16. These tanks are 250 feet (76.2 m) in length and 45 feet (13.7 m) in width and hold a volume of 1.39 million gallons (5.2 million liters) of mixed liquor. The headspace in the tanks was 3 to 4 feet (0.9 to 1.2 m).

Particle measurements were taken in three locations: 1) inside the headspace of the aerated basin, 2) 10 feet (3 m) upwind of the tank openings, and 3) 10 feet (3 m) downwind of the tank openings as seen in figure 2-1b and 2-1c. The openings were situated 30 feet (9.1 m) from each other. The concrete slab covered the 6 operating tanks with continuous headspace. Thus emissions from these tanks were in the collective

headspace. OCSD aerated basins also had fine bubble diffusers; the incoming airflow to the tank's diffuser was 2,500 SCFM (1.18 m^3/s). There were two air filters before the pump, which provided "particle free" air to the diffusers. Field measurements were taken at 10 am in the morning of November 18th, 2015. Wind direction and cloud coverage remained constant throughout the experiment. The ambient average relative humidity was 48%.

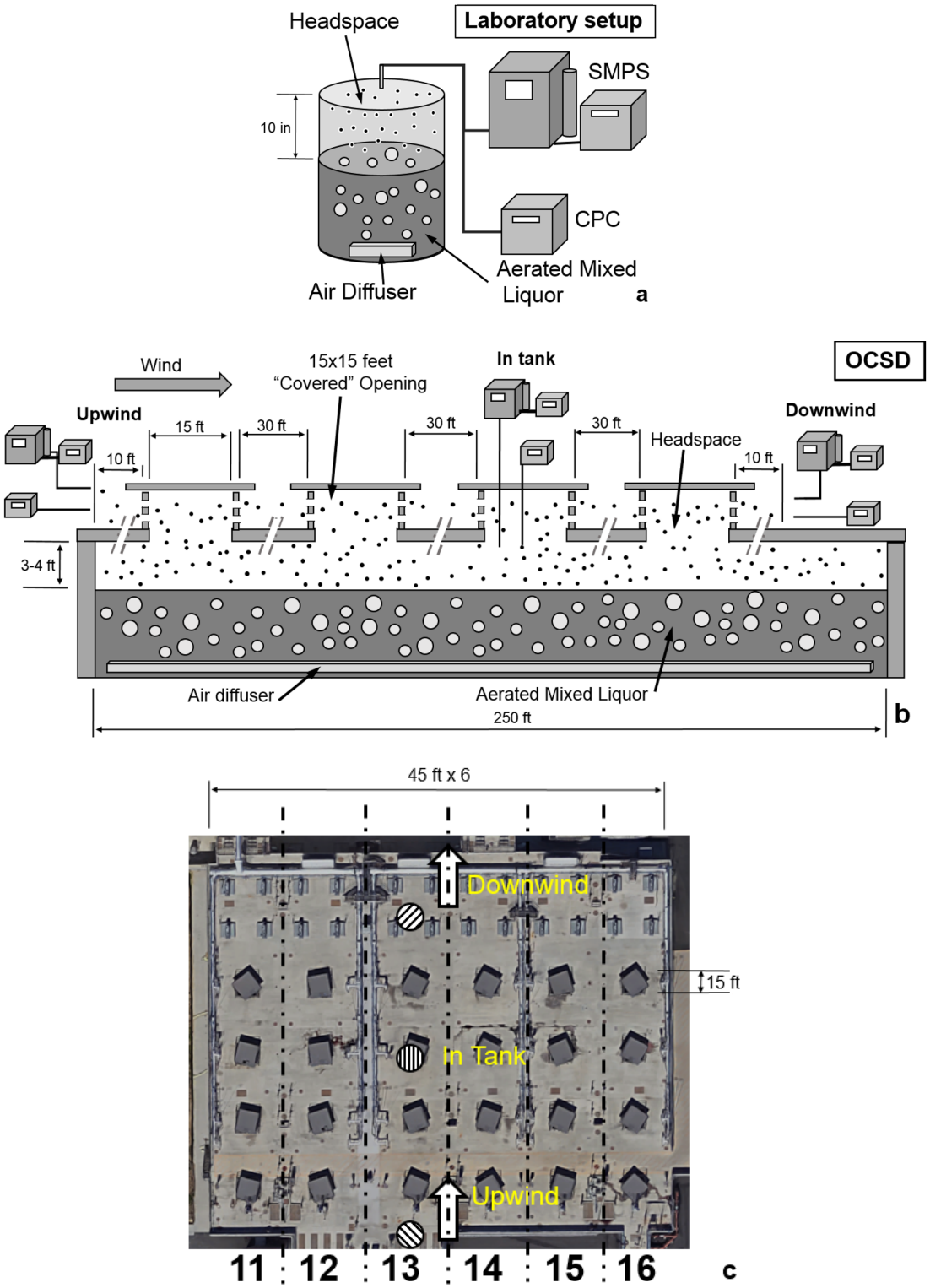
Headspace
Laboratory setup
SMPS
10 in
CPC
Aerated Mixed Liquor
Air Diffuser
a
OCSD
Wind
15x15 feet "Covered" Opening
In tank
Upwind
Downwind
15 ft
30 ft
30 ft
30 ft
Headspace
10 ft
10 ft
3-4 ft
Air diffuser
Aerated Mixed Liquor
250 ft
b
45 ft x 6
Downwind
15 ft
In Tank
Upwind
11
12
13
14
15
16
c

Figure 2-1. Experimental set-up at both sites: a) Laboratory bioreactor set up; Particles are sampled within the headspace of the 5 gallon bioreactor. b) North-south cross-section of OCSD's semi-covered aerated basin number 13. Particles are sampled in 3 different locations; 10 feet upwind from the first opening, in tank and 10 feet downwind after the fourth opening. Openings were 30 feet apart. Distance breaks are shown with grey dashed lines. c) Aerial view of aerated basins; Sampling locations: In tank (top to bottom stripes), upwind and dowwind (side to side stripes). Arrows indicate wind direction. Dashed black lines show divisions between tanks.

2.4 Results and discussion

2.4.1 Field data from OCSD

Figure 2-2 shows field particle measurements from three locations at OCSD: inside the aerated tanks, 10 feet (3 m) upwind from the first opening, and 10 feet (3 m) downwind from the last opening. Identical instruments were placed at the three locations and were operated at the same time. These measurements were carried out simultaneously for 70 minutes. The average total particle concentration is 3,200 #/cm^3 upwind, 5,550 #/cm^3 downwind and 14,480 #/cm^3 in tank (see figure 2-2a). Concentrations in the tank varied from 7,000 #/cm^3 to 18,000 #/cm^3 over each of the 70-minute sampling periods. Downwind concentrations were 73% higher than upwind concentrations and were influenced by particles emitted from the tanks. This increase of 2,200 #/cm^3 between downwind and upwind particle concentrations confirms that ultrafine particles are emitted into the atmosphere by the process. Thus further studies on the transport of WWTP particles are warranted.

Figure 2-2b shows the ultrafine size distributions upwind, in tank and downwind. All had similar monomodal distributions, however the downwind and the in tank size distributions had particles of larger sizes and are shifted to the right of the upwind data set. In tank particles of larger ultrafine sizes contributed to the size distribution observed downwind. The mode of the three locations (upwind, in tank and downwind) were within a few nanometers of 48 nm (bioreactor mode, see figure 2-2b yellow rectangle and section 2.4.3). The mode of the size distribution in the tank was 45 nm and larger than the

mode of the size distribution upwind (38 nm). The downwind mode diameter was 40 nm, which suggests that the ultrafine particle size distribution measured downwind is influenced by the size distribution emitted in the tank. The concentration and size information provided here can be used to model the dispersion of primary ultrafine particles in the WWTP and neighboring areas where particles can potentially affect the health of people living downwind of the source.

The field data confirms that "covered", here semi-covered, aeration tanks emit airborne particles. The processes that govern secondary wastewater treatment vary per location and thus the concentrations from this field study are location specific. However, if we understand wastewater treatment design (e.g. COD, TOC, TSS & aeration rate), we may be able to relate process parameters to airborne particle generation and apply our results to other WWTP sites.

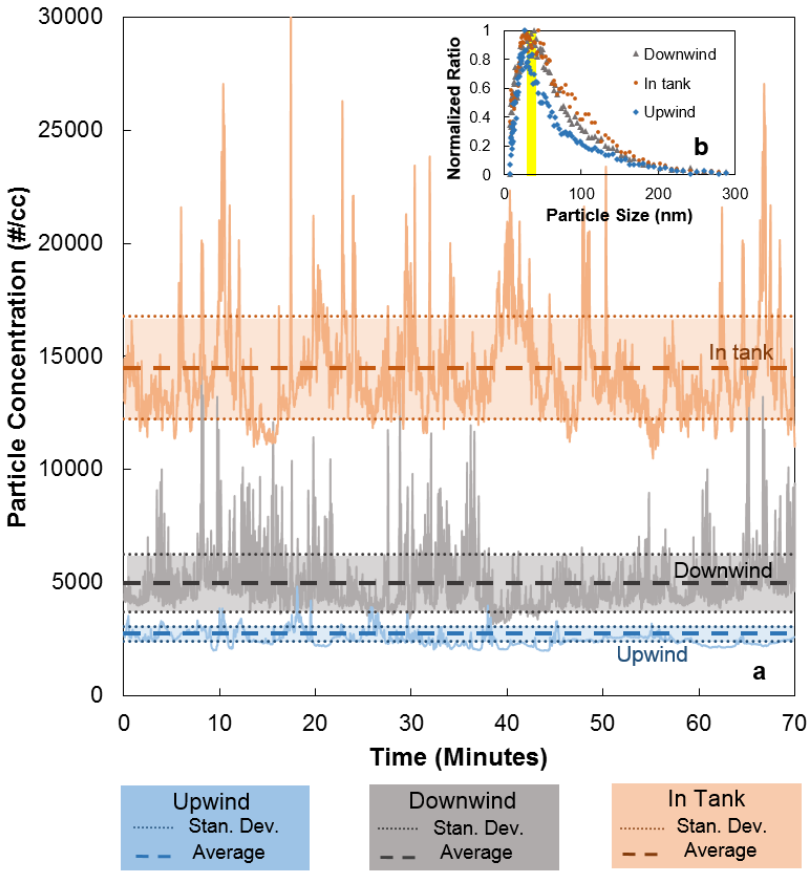

Figure 2-2: a) Particle concentrations at OCSDP: Measurements are taken in triplicate over 70-minute sampling periods. The particle concentration in tank (orange), 10 feet downwind (grey) and 10 feet upwind (blue) are the average of data triplicates collected simultaneously. The average value (dashed line) and standard error (shaded regions) are shown for comparison. b) Normalized particle size distributions: The average size distribution from 96 SMPS scans in tank (orange), downwind (grey) and upwind (blue). Laboratory size peak mode diameter (48 nm, yellow rectangle) is shown for comparison.

2.4.2 COD, TSS & TOC effect on particle concentration

A laboratory bioreactor was used to study the effects of WWTP parameters on particle emissions. The rate of O_2 uptake is a function of COD concentration and degradation rate. When COD is high and degrading, the O_2 transfer from the air bubbles is greater (OCSD, 2016). Due to this effect, the volume of the bubbles shrinks as it rises. Thus, when O_2 transfer rate is high, the bubbles tend to be small (Vasconcelos et al., 2002). Sludge grows as COD is degraded; there is an increase in mixed liquor suspended solids or total suspended solids (MLSS or TSS) (Zheng et al., 2006). Figure 2-3a shows the average particle concentration versus the COD degradation of three experiments over 48 hours in the bioreactor. The initial and final bioreactor COD values were similar to OCSD's. 79% of the COD was removed during the first 20 hours of the cycle. A 25% increase in particle concentration was observed after this.

Figure 2-3b shows a decrease in TOC values while both particle concentration and TSS increased with degradation. The TSS values in the controlled bioreactor were similar to the TSS values inside OCSD's aerated tank. TOC values decreased from 38 ppm to 6 ppm and the TSS values in the bioreactor were 4,250 mg/L and 5,050 mg/L at the beginning and end of the cycle. Hourly TSS increases were observed during the first ~10 hours and plateaued after 16 hours. TOC values also plateaued after 16 hours. The average particle concentration ranged from ~4000 #/cm^3 to ~7000 #/cm^3. This trend suggests biomass suspension growth during the reaction process may influence the number of airborne particles.

COD, TSS and TOC reach steady state values before the 20 hour mark. Thus changes in particle measurements taken after this time will not be influenced by degradation, but by reactor physical properties (e.g. aeration rate and surface area). Figure 2-3c shows COD, TOC and TSS versus average particle concentration. Trends exist with all three parameters. There is a significant positive relationship between the particle concentration and TSS, $r(10)=0.705$, $p<.05$ ($\alpha=.05$), between the particle concentration and TOC, $r(10)=0.664$, $p<.05$ ($\alpha=.05$) and between particle concentration and COD: $r(10)=.876$, $p<.001$ ($\alpha=.001$). The standard errors of the best fit regression lines are 44.25 mg/L, 6.96 ppm, and 484.82 mg/L for COD, TOC and TSS, respectively.

R^2 values with these parameters are less than 0.8 with a significance level of $\alpha=.05$ and suggest no strong correlation between particle concentrations and the change in composition of the mixed liquor. Therefore, in subsequent tests, we measure the impact of aeration flow rate 20 to 28 hours (yellow shaded areas in figures 2-3a and 2-3b into the degradation cycle). This will provide clear evidence of the aeration contribution to particle emissions with minimal impact by organic composition in the sludge.

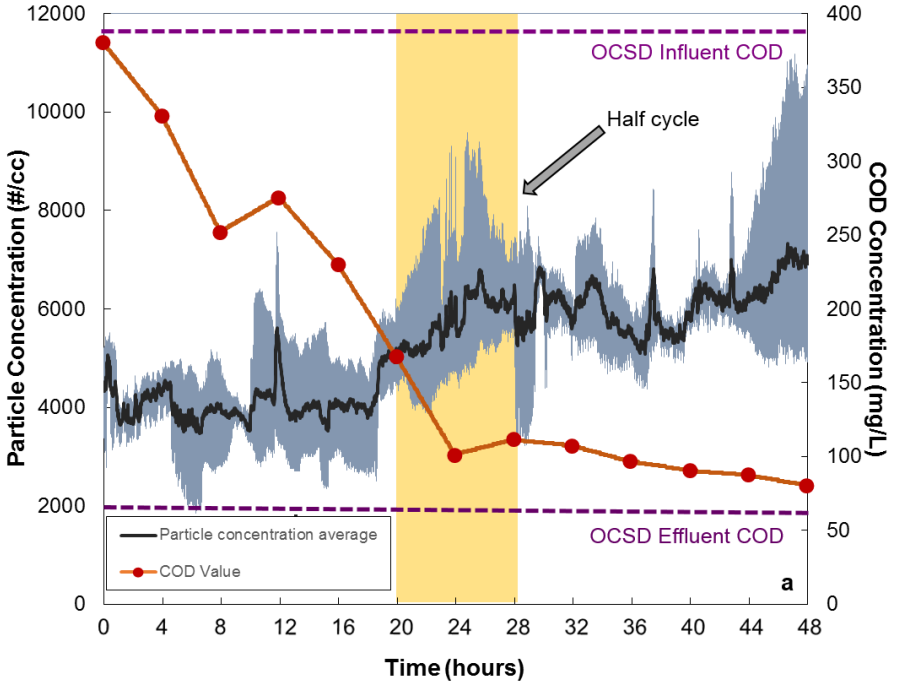
OCSD Influent COD
Half cycle
OCSD Effluent COD
Particle concentration average
COD Value
a
Particle Concentration (#/cc)
COD Concentration (mg/L)
Time (hours)

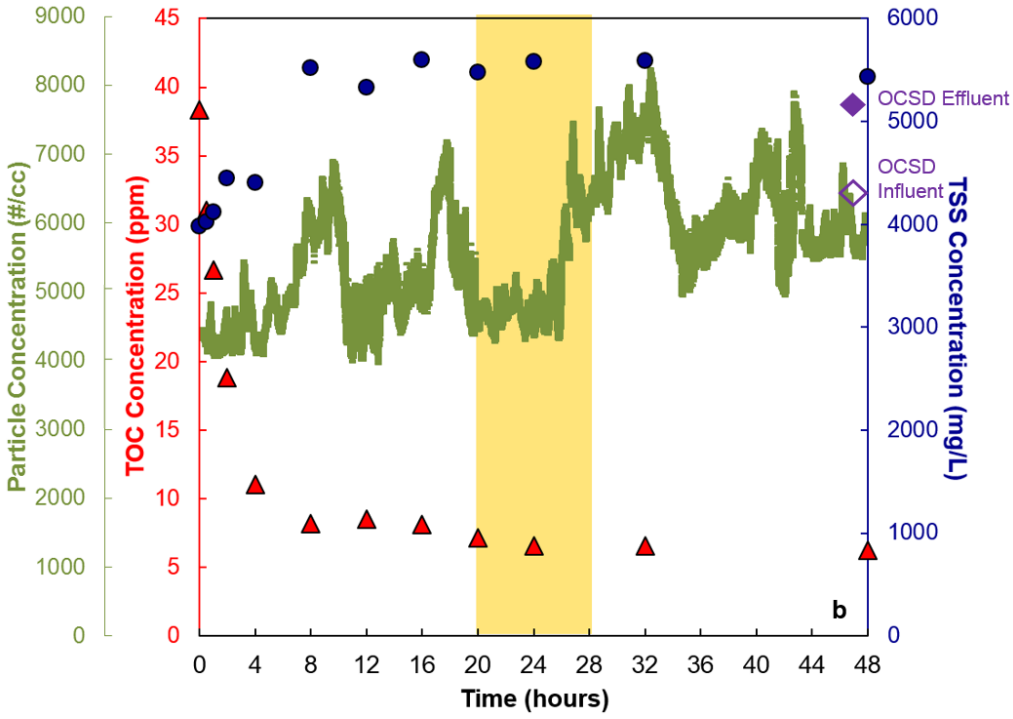
OCSD Effluent
OCSD Influent
b
Particle Concentration (#/cc)
TOC Concentration (ppm)
TSS Concentration (mg/L)
Time (hours)

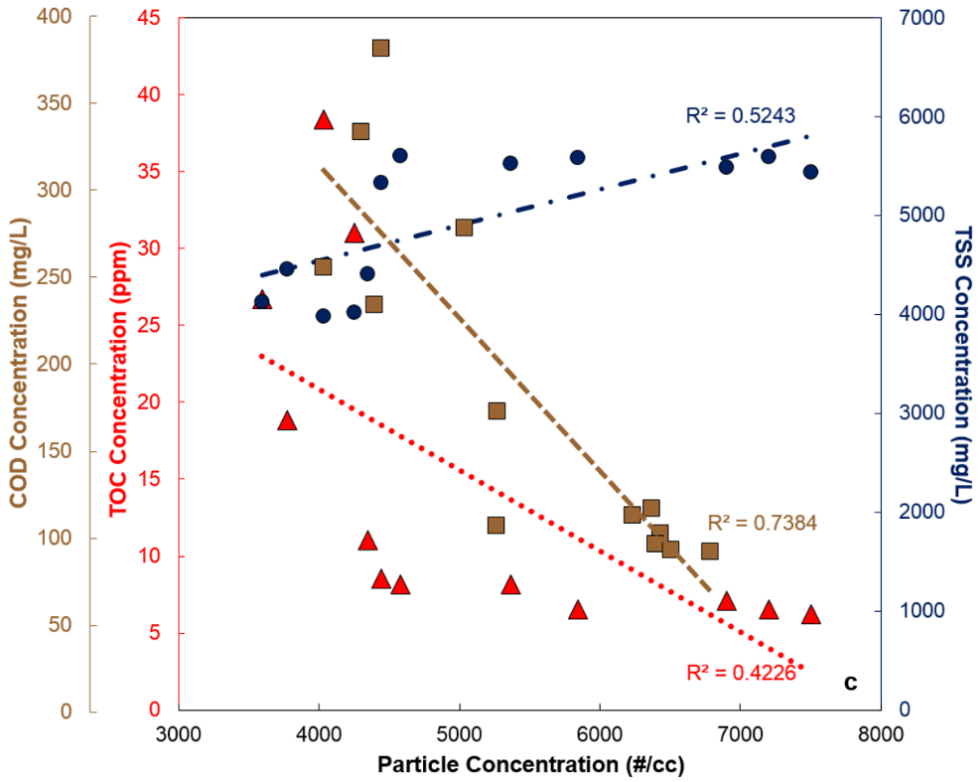
COD Concentration (mg/L)
TOC Concentration (ppm)
TSS Concentration (mg/L)
Particle Concentration (#/cc)
R² = 0.5243
R² = 0.7384
R² = 0.4226
c

Figure 2-3: Changes in mixed liquor parameters (COD, TOC and TSS) and particle concentration during degradation. The organic degradation slows down after yellow shaded area: a) Average particle concentrations over 48 hours for 3 experiments (black). The shaded grey area indicates maximum and minimum concentration values. COD degradation over 48 hours is plotted (orange circles). OCSD influent and effluent COD data (purple dashed line) is plotted for comparison. b) Particle concentration over 48 hours (green) plotted with TOC degradation (red triangles), and TSS in the bioreactor (blue circles). The open purple diamond represents the value of OCSD's influent TSS value (mg/L) and the closed diamond represents the effluent TSS value (mg/L). c) COD (brown squares), TOC (red triangles) & TSS (blue circles) versus particle concentration. Dashed lines are linear fits of the data and correlations are shown.

2.4.3 Air diffuser flow rate effect on particle concentration

Ultrafine particle size distributions and number concentrations from the laboratory bioreactor are shown in Figures 2-4a and b. Particle size distributions are presented for specific flow rates in figure 2-4b. The peak mode diameter (~48 nm) of each laboratory run was within +/- 7% difference of the average field size distribution mode (~45 nm) measured in the tanks at OCSD. The mode diameter of ultrafine particles did not change when airflows varied. Particles larger than 320 nm, not measured by the SMPS but counted by the CPC, were formed with increasing airflow (figure A2.2). This indicates that larger particles are emitted; however, the total particle concentration is dominated by particles below 320 nm. Larger particles are not in the ultrafine range and are less likely to exit the tank and travel far distances.

Air was not diffused into the system during anaerobic operation; anaerobic sludge from a separate biodigestor was used and few particles were measured (figure 2-4a). Airflow is increased in the aerobic bioreactor and more particles were emitted. An empirical correlation describes the relationship between flow rate and particle concentration. The y-intercept was not forced to zero because anaerobic systems were not particle free. The linear equation has an R^2 value of ~0.98 with a statistically significant relationship $r(8)=0.988$, $p<.0001$ (α =.0001), a much stronger correlation with a higher significance level than the mixed liquor organic degradation parameters in figure 2-3 (α =.05 for TOC & TSS and α =.001 for COD). The calculated standard error for aeration flow rate is 896.47 #/cc.

Small but observable increases of particle concentrations were noted over a 2-day batch treatment cycle. The statistical regression between water quality parameters (COD, TOC, TSS) and particle concentration is weaker ($R^2 < 0.8$) than aeration. In other words, aeration is the main source of ultrafine particle number emissions from wastewater treatment processes. The particle concentration downwind of OCSD is likely influenced by the flow rate of diffused air (figure 2-1). This is a potential concern because most aerated tanks (even "covered" ones) can be open to the ambient and aeration flow rates are not regulated. Additional chemical speciation may be required to understand the toxicity and whether organic degradation affects the resulting aerosol composition. The correlation presented in figure 2-4a can be used to estimate ultrafine emission fluxes from WWTPs.

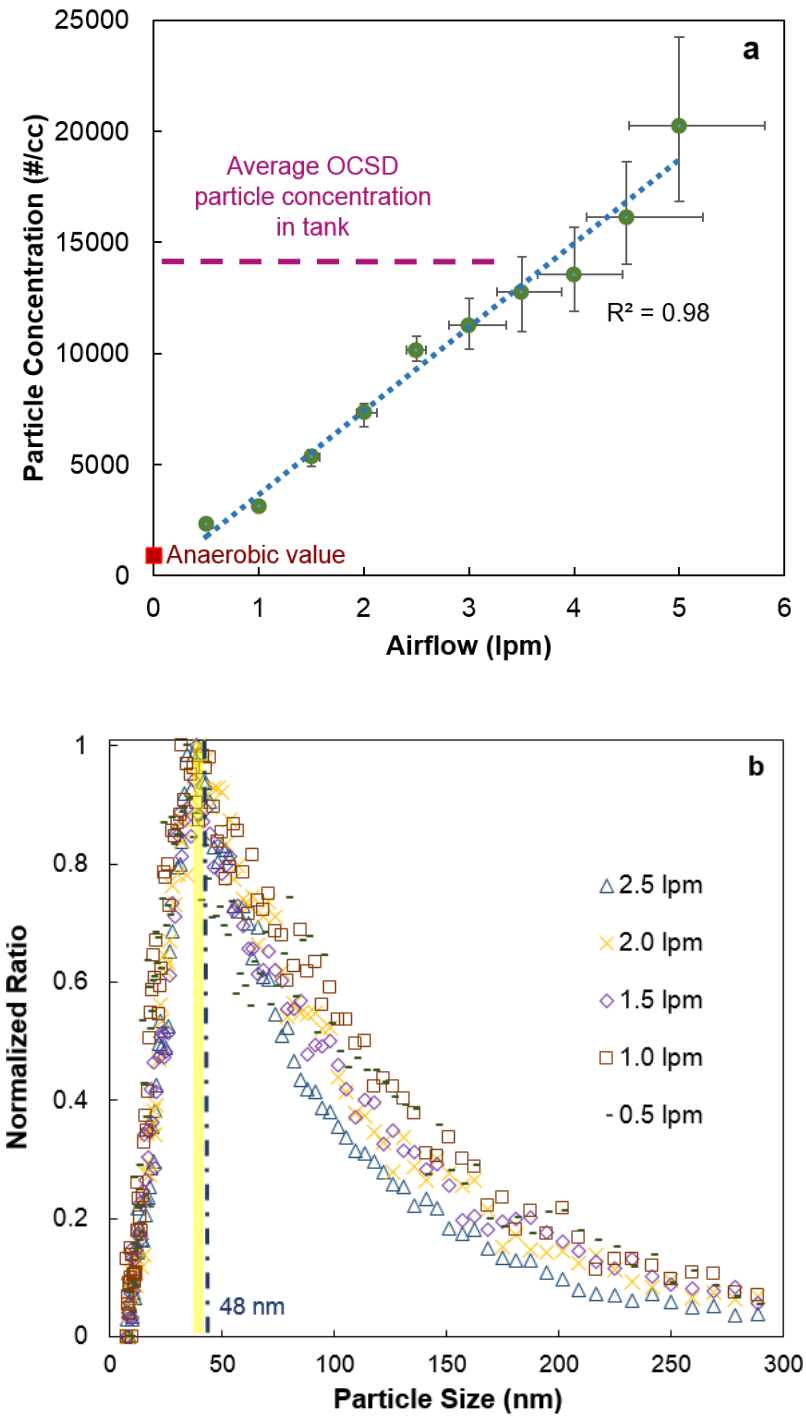
a
Particle Concentration (#/cc)
Airflow (lpm)
Average OCSD
particle concentration
in tank
Anaerobic value
R² = 0.98
25000
20000
15000
10000
5000
0
0
1
2
3
4
5
6
b
Normalized Ratio
Particle Size (nm)
2.5 lpm
2.0 lpm
1.5 lpm
1.0 lpm
0.5 lpm
48 nm
1
0.8
0.6
0.4
0.2
0
0
50
100
150
200
250
300

Figure 2-4. The effect of air flowrate on particle number & size: a) Particle number concentration versus airflow rate. An empirical correlation between particle concentration and airflow rate is provided (dashed blue line). The anaerobic data (red square) was not fit in the data regression. The average OCSD total particle concentration in tank (horizontal purple dashed line) is the same as the average value presented in figure 2-1. b) Normalized size distributions for different airflows. The average peak mode diameter of the bioreactor is 48 nm (blue dashed line) and the average OCSD peak mode diameter is within 6% of this value (yellow shaded region)

2.4.4 Aerosol flux & emission rates

Airflow rate had the strongest correlation with particle concentrations compared to water quality parameters measured in our study. A theoretical approach was considered to compare the aerosol flux of laboratory and field data based on aeration flow rate and particle concentration. The aerosol number flux model is similar to the aerosol mass flux equation presented in Upadhyay et al. 2013. Upadhyay et al used the outgoing vent flow of air, V_t. Given the strong correlation between injected airflow rate and particle concentration, the incoming airflow rate diffused, α, is used in this model instead. For most water treatment plants, α is readily known and monitored whereas V_t must be measured. The aerosol number flux, ϕ_i, is estimated with surface area, S, particle number concentration, C_i, and airflow rate, α, as follows:

$$\text{Equation 2-1:} \qquad \varphi_i = \frac{C_i \alpha}{S}$$

Table 2-1 provides values used to calculate aerosol number flux from both systems. The airflow diffused through OCSD's aerated basins (2,500 SCFM per tank) was multiplied by the average in-tank C_i in figure 2-1 and subsequently divided by the S of one tank (10.5 x 10^6 cm^2). The ϕ_i of one tank at OCSD and the ϕ_i from the bioreactor are compared. There is a 19% difference between the calculated aerosol number fluxes (Table 2-1). This study is the first to show that the ultrafine aerosol number flux measured at the small scale (7.95x10^4 #/min·cm^2, bioreactor) is comparable to large scale (9.8x10^4 #/min·cm^2, OCSD) values. This validates the use of ultrafine particle data

collected in bioreactor settings to predict and understand real world WWTP particle emissions.

Table 2-1: Parameters for Aerosol Number Flux

	Bioreactor	**OCSD (per tank)**
C_i	14,480 #/cm^3	14,480 #/cm^3
α	3,880 cm^3/min	70,792,120 cm^3/min
S	706.5 cm^2	10.5 x 10^6 cm^2
φ_i	7.95x10^4 #/min·cm^2	9.8x10^4 #/min·cm^2

*shaded area = calculated values from (*Equation 4-1*)

Mass emission rates were also calculated assuming a unit density. The average ultrafine aerosol mass rate per basin (2.8417x10^{-7} g/s) had an average mass concentration of 7.03 μg/cm^3. Relative humidity differences between the lab and the field did not likely affect the calculations as the wet and dry particle size modes were found to be within 3 nm from each other (see figure A2.1).

The mass concentration and emission rates of WWTP are relatively low compared to other urban ultrafine emission sources (Zhu et al., 2002). However, the number concentrations in this study (approximately 1.45x10^3 #/cm^3 in-tank) are the same order of magnitude as ambient number concentrations in urban cities (Park et al., 2008; Maskey et al., 2012). There are a significant number of very small particles (< 100 nm) with low

mass and this further suggests that WWTP emissions contribute to the local $PM_{0.1}$ budget. In general, ultrafine particulates are known to impact health. They have been shown to have very little contribution to the overall ambient mass PM concentration, but they can be very high in number (Dennekamp et al., 2002).

The impact of these respirable particles remains unclear. Research to date has examined the health effects pertaining to WWTPs (Fannin et al., 1985; Khuder et al., 1998; Bauer et al., 2002; Radke and Herrmann, 2003; Smit et al., 2005). Many of these studies have focused on the exposure of plant workers and surrounding neighborhoods. Authors have reported illnesses in workers that are new to WWTP facilities.[8,10,14,23] These illnesses were characterized by symptoms of weakness, headaches, fever, diarrhea and abdominal pains. The current body of literature shows a significant association between proximity to WWTP and the incidence of enteric illnesses. However, no direct evidence with ultrafine particle measurement exists to date.

The pathogenicity of WWTP aerosols has been a concern since the 1980's, however there are still no guidelines or laws regarding WWTP emissions. PM_{10} and $PM_{2.5}$ filter data has confirmed the presence of airborne toxic compounds, bacteria, fungi, endotoxins and viruses near WWTP (Carducci et al., 1995; Khuder et al., 1998; Bauer et al., 2002; Radke and Herrman, 2003; Radke, 2005; Smit et al., 2005; Beck et al., 2006; Carducci et al., 2008; Krzeniewska , 2001; Uhrbrand et al., 20112; Jebri et al., 2012; Upadhyay et al., 2013; Malakootian et al., 2013; Masclaux et al., 2014; Li et al., 2015; Niazi et al., 2105). Much of the research has focused on bacteria and fungi as well as endotoxins (Bauer et al., 2002; Korzeniewska et al., 2011; Malakootian et al., 2013; Li et

al., 2015; Niazi et al., 2015). Fewer studies have investigated airborne viruses (Carducci et al., 1995; Carducci et al., 2008; Uhrbrand et al., 2011; Jebri et al., 2012; Masclaux et al., 2014), which are pertinent to this study as viral particles are in the ultrafine range (20-300 nm).

This study fills critical gaps in scientific knowledge by providing on-line and real time particulate size distributions, ultrafine particles emission fluxes and rates. The theoretical model can be used to directly compare WWTPs of different scales and predict real world aerosol fluxes of primary particulate emissions. Gases, specifically ammonia, have also been reported from WWTPs (Kampschreur et al., 2009; Dai and Blanes-Vidal, 2013; Daelman et al., 2015; Campos et al., 2016) and have the potential to form ultrafine secondary aerosol that may contribute to the urban aerosol budget Na et al., 2006; Updyke et al., 2012; Wei et al., 2015. Future work will explore the composition of the ultrafine primary and secondary emissions in and downwind of sources.

2.5 Acknowledgements

This work has been supported by the National Science Foundation Award (NSF) 1151893. Its contents are solely the responsibility of the grantee and do not necessarily represent the official views of the NSF. Furthermore, the NSF does not endorse the purchase of any commercial products or services mentioned in the publication. The authors would like to thank undergraduates Colin Eckerle and Tyler Berte for their technical contribution in the lab. The authors would also like to specifically thank the

staff of Orange County Sanitation District for access to the facilities, their assistance and cooperation.

2.6 Appendix

To understand the contribution of water to the wet aerosol size, a dry-wet particle comparison experiment was performed by operating two SMPS simultaneously connected to the bioreactor. One line had a copper heating coil attached to it at 50 °C which dried the particles and the other one did not. The size distribution between the wet and dry particle measurements were minimal (figure A2.1).

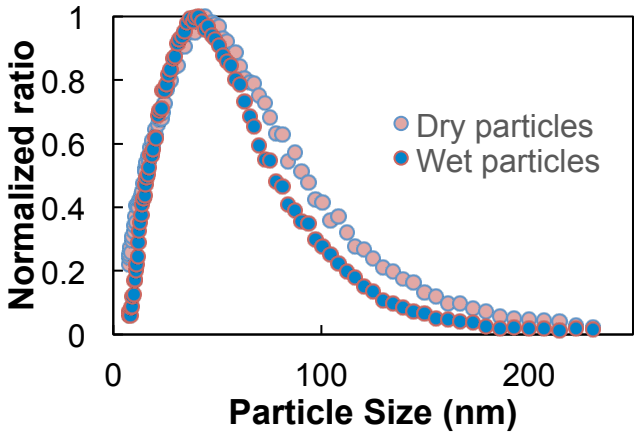

Figure A2.1: Wet and dry particle concentration measurements taken from the bioreactor.

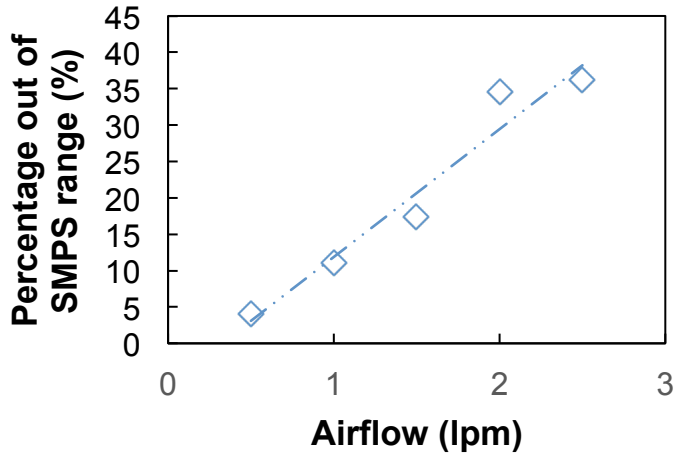

Figure A2.2: Percentage of particles measured outside of the SMPS range as airflow increased. A significant positive relationship is observed ($r(4)=0.94$, $p<0.05$) with a standard error of 5.25%.

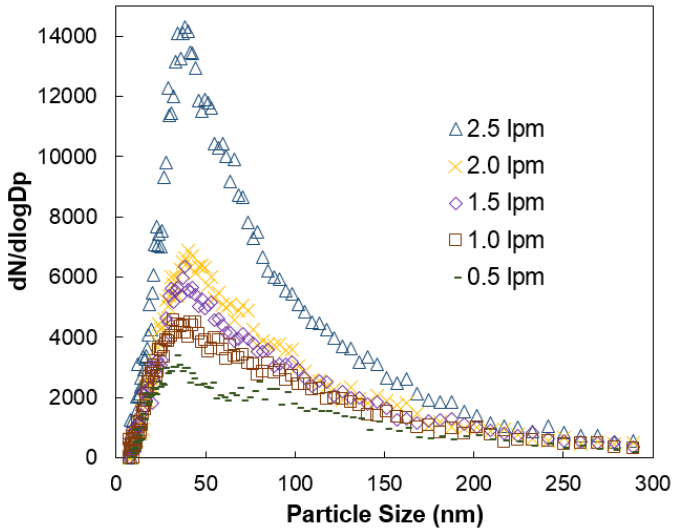

Figure A2.3: Non-normalized particle size distributions in the bioreactor at different airflow rates.

2.7 References

Agarwal, Jugal K., and Gilmore J. Sem. "Continuous Flow, Single-Particle-Counting Condensation Nucleus Counter." *Journal of aerosol science* 11.4 (1980): 343–357. Print.

American Public Health Association. *Standard Methods for the Examination of Water and Wastewater*. General Books LLC, 2010. Print.

Bauer, H. et al. "Bacteria and Fungi in Aerosols Generated by Two Different Types of Wastewater Treatment Plants." *Water research* 36.16 (2002): 3965–3970. Print.

Beck, Melanie, and Michael Radke. "Determination of Sterols, Estrogens and Inorganic Ions in Waste Water and Size-Segregated Aerosol Particles Emitted from Waste Water Treatment." *Chemosphere* 64.7 (2006): 1134–1140. Print.

Campos, J. L. et al. "Greenhouse Gases Emissions from Wastewater Treatment Plants: Minimization, Treatment, and Prevention." *Journal of chemistry and chemical engineering* 2016 (2016): n. pag. Web. 26 May 2016.

Carducci, A., S. Arrighi, and A. Ruschi. "Detection of Coliphages and Enteroviruses in Sewage and Aerosol from an Activated Sludge Wastewater Treatment Plant." *Letters in applied microbiology* 21.3 (1995): 207–209. Print.

Carducci, A. et al. "Study of the Viral Removal Efficiency in a Urban Wastewater Treatment Plant." *Water science and technology: a journal of the International Association on Water Pollution Research* 58.4 (2008): 893–897. Print.

Chan, Yi Jing et al. "A Review on Anaerobic–aerobic Treatment of Industrial and Municipal Wastewater." *Chemical engineering journal* 155.1–2 (2009): 1–18. Print.

Chylek, Petr, and J. Wong. "Effect of Absorbing Aerosols on Global Radiation Budget." *Geophysical research letters* 22.8 (1995): 929–931. Print.

Clark, C. Scott. "Potential and Actual Biological Related Health Risks of Wastewater Industry Employment." *Journal - Water Pollution Control Federation* 59.12 (1987): 999–1008. Print.

Daelman, Matthijs R. J. et al. "Seasonal and Diurnal Variability of N 2 O Emissions from a Full-Scale Municipal Wastewater Treatment Plant." *The Science of the total environment* 536 (2015): 1–11. Print.

Dennekamp, Martine et al. “Exposure to Ultrafine Particles and PM2. 5 in Different Micro-Environments.” *The Annals of occupational hygiene* 46.suppl 1 (2002): 412–414. Print.

Fannin, K. F., S. C. Vana, and W. Jakubowski. “Effect of an Activated Sludge Wastewater Treatment Plant on Ambient Air Densities of Aerosols Containing Bacteria and Viruses.” *Applied and environmental microbiology* 49.5 (1985): 1191–1196. Print.

Glassmeyer, Susan T. et al. “Transport of Chemical and Microbial Compounds from Known Wastewater Discharges: Potential for Use as Indicators of Human Fecal Contamination.” *Environmental science & technology* 39.14 (2005): 5157–5169. Print.

Jebri, Sihem et al. “Presence and Fate of Coliphages and Enteric Viruses in Three Wastewater Treatment Plants Effluents and Activated Sludge from Tunisia.” *Environmental science and pollution research international* 19.6 (2012): 2195–2201. Print.

Kampschreur, Marlies J. et al. “Nitrous Oxide Emission during Wastewater Treatment.” *Water research* 43.17 (2009): 4093–4103. Print.

Keene, William C. et al. “Chemical and Physical Characteristics of Nascent Aerosols Produced by Bursting Bubbles at a Model Air-Sea Interface.” *Journal of geophysical research* 112.D21 (2007): n. pag. Web.

Khuder, S. A. et al. “Prevalence of Infectious Diseases and Associated Symptoms in Wastewater Treatment Workers.” *American journal of industrial medicine* 33.6 (1998): 571–577. Print.

Korzeniewska, Ewa. “Emission of Bacteria and Fungi in the Air from Wastewater Treatment Plants - a Review.” *Frontiers in bioscience* 3 (2011): 393–407. Print.

Li, Yuan et al. “Health Effects Associated with Wastewater Treatment, Reuse, and Disposal.” *Water environment research: a research publication of the Water Environment Federation* 87.10 (2015): 1817–1848. Print.

Malakootian, Mohammad et al. “Bacterial-Aerosol Emission from Wastewater Treatment Plant.” *Desalination and water treatment* 51.22-24 (2013): 4478–4488. Print.

Masclaux, Frédéric G. et al. “Assessment of Airborne Virus Contamination in Wastewater Treatment Plants.” *Environmental research* 133 (2014): 260–265. Print.

Maskey, Shila et al. "Ultrafine Particle Events in the Ambient Atmosphere in Korea." *Asian Journal of Atmospheric Environment* 6.4 (2012): 288–303. Print.

Mårtensson, E. M. et al. "Laboratory Simulations and Parameterization of the Primary Marine Aerosol Production." *Journal of geophysical research* 108.D9 (2003): 4297. Print.

Na, Kwangsam, Chen Song, and David R. Cocker III. "Formation of Secondary Organic Aerosol from the Reaction of Styrene with Ozone in the Presence and Absence of Ammonia and Water." *Atmospheric environment* 40.10 (2006/3): 1889–1900. Print.

Niazi, Sadegh et al. "Assessment of Bioaerosol Contamination (bacteria and Fungi) in the Largest Urban Wastewater Treatment Plant in the Middle East." *Environmental science and pollution research international* 22.20 (2015): 16014–16021. Print.

Park, Kihong et al. "Seasonal and Diurnal Variations of Ultrafine Particle Concentration in Urban Gwangju, Korea: Observation of Ultrafine Particle Events." *Atmospheric environment* 42.4 (2008/2): 788–799. Print.

Radke, Michael. "Sterols and Anionic Surfactants in Urban Aerosol: Emissions from Wastewater Treatment Plants in Relation to Background Concentrations." *Environmental science & technology* 39.12 (2005): 4391–4397. Print.

Radke, Michael, and Reimer Herrmann. "Aerosol-Bound Emissions of Polycyclic Aromatic Hydrocarbons and Sterols from Aeration Tanks of a Municipal Waste Water Treatment Plant." *Environmental science & technology* 37.10 (2003): 2109–2113. Print.

Reineking, A., and J. Porstendörfer. "Measurements of Particle Loss Functions in a Differential Mobility Analyzer (TSI, Model 3071) for Different Flow Rates." *Aerosol science and technology: the journal of the American Association for Aerosol Research* 5.4 (1986): 483–486. Print.

Rittmann, Bruce E. "Aerobic Biological Treatment. Water Treatment Processes." *Environmental science & technology* 21.2 (1987): 128–136. Print.

Rosso, Diego, and Michael K. Stenstrom. "Comparative Economic Analysis of the Impacts of Mean Cell Retention Time and Denitrification on Aeration Systems." *Water research* 39.16 (2005): 3773–3780. Print.

Smit, Lidwien A. M., Suzanne Spaan, and Dick Heederik. "Endotoxin Exposure and Symptoms in Wastewater Treatment Workers." *American journal of industrial medicine* 48.1 (2005): 30–39. Print.

Tchobanoglous, George, F. L. Burton, and D. H. Stensel. "Wastewater Engineering (Treatment, Disposal and Reuse), New York, Metcalf and Eddy." *Inc. p* 1334 (1991): n. pag. Print.

Tyree, Corey A. et al. "Foam Droplets Generated from Natural and Artificial Seawaters." *Journal of geophysical research* 112.D12 (2007): D12204. Print.

Uhrbrand, Katrine, Anna Charlotte Schultz, and Anne Mette Madsen. "Exposure to Airborne Noroviruses and Other Bioaerosol Components at a Wastewater Treatment Plant in Denmark." *Food and environmental virology* 3.3-4 (2011): 130–137. Print.

Upadhyay, Nabin et al. "Characterization of Aerosol Emissions from Wastewater Aeration Basins." *Journal of the Air & Waste Management Association* 63.1 (2013): 20–26. Print.

Vasconcelos, Jorge M. T., Sandra P. Orvalho, and Sebastião S. Alves. "Gas–liquid Mass Transfer to Single Bubbles: Effect of Surface Contamination." *AIChE journal. American Institute of Chemical Engineers* 48.6 (2002): 1145–1154. Print.

Walls, Kelvin. "Health Implications of Increasing Reuse of Wastewater as an Adaption to Climate Change." *journal of Environmental Engineering and Ecological Science* 4.1 (2015): 2. Print.

Wang, Shih Chen, and Richard C. Flagan. "Scanning Electrical Mobility Spectrometer." *Journal of aerosol science* 20.8 (1989): 1485–1488. Print.

Wei, Lianfang et al. "Gas-to-Particle Conversion of Atmospheric Ammonia and Sampling Artifacts of Ammonium in Spring of Beijing." *Science China. Earth Sciences* 58.3 (2014): 345–355. Print.

Zheng, Yu-Ming et al. "Formation and Instability of Aerobic Granules under High Organic Loading Conditions." *Chemosphere* 63.10 (2006): 1791–1800. Print.

Zhu, Yifang et al. "Concentration and Size Distribution of Ultrafine Particles near a Major Highway." *Journal of the Air & Waste Management Association* 52.9 (2002): 1032–1042. Print.

OECD. Safety Assessment of Foods and Feeds Derived from Transgenic Crops, Volume 1, Novel Food and Feed Safety, *OECD Publishing*. **2015**, 64-70

EPA. *The Determination of Chemical Oxygen Demand by Semi-Automated Colorimetry*. Method 410.4, Rev. 2.0. *http://water.epa.gov/*. 1993

OCSD. Facilities, 2016. http://www.ocsd.com/about-ocsd/general-information/facilities.

Chapter 3: Transport and Characterization of Particulate Emissions from Three Wastewater Treatment Facilities in Southern California

3.1 Abstract

Wastewater treatment plants (WWTP) are proliferating in urban environments and their aerosol emissions have been associated with local and regional health burden. Toxic compounds and pathogens have been detected in neighborhoods surrounding the facilities but their concentration and classification are still dubious. The airborne exposure route is also still poorly understood due to the lack of information on aerosol characterization and transport. This study presents a WWTP particulate dispersion analysis through the AMS/EPA Regulatory Model (AERMOD) and establishes a relationship between basin coverage, source emission flux and dispersion: Three coverage scenarios (fully covered basin, semi-covered and covered) were modeled with annual, monthly and daily meteorological data. In addition, filter samples were collected at three WWTP along the Santa Ana River Watershed in Southern California: Orange County Sanitation District (OCSD) in Fountain Valley, Western Municipal Wastewater Treatment Plant (WMWWTP) in Riverside, and the City of Redlands Wastewater Treatment Plant (RWWTP). Filter measurements were taken at four distances from the source (50 m, 100 m and 200 m downwind, as well as 100 m upwind). Filters were further analyzed to quantify and characterize organic compounds, endotoxins, fungal glucans and proteins. The data was later compared to additional filter samples obtained

from a laboratory bioreactor in which mixed liquor (wastewater and sludge mixture) from each WWTP was aerosolized through aeration diffusion in a controlled environment.

AERMOD outcomes show that partial coverage of the basins does not efficiently reduce the particulate emissions as previously thought. Therefore a full coverage of the basin is advised to mitigate WWTP aerosols. Characterization results also confirm that compounds of concern and biological materials that are generated through aerobic processes and bubble bursting in aerated basins are transported away from the WWTPs: Fecal sterols with concentrations as high as 202.5 ± 43.04 ng/m^3 (cholesterol, 50 m downwind from WMWWTP) were observed. Cholestanol/coprostanol was also found at a residential home 860 meters downwind from OCSD (1.09 ± 0.88 ng/m^3). Some poly-aromatic hydrocarbons (PAHs) and levoglucosan were detected in a few WWTP and laboratory bioreactor air samples. However, it was concluded that PAHs and levoglucosan may have come from a different source near the sampling sites (e.g. burning activities).

Endotoxins (a trace for bacteria) were also found as far as 200 m downwind from the source (maximum of 130 EU/m^3 at WMWWTP, 20 EU/m^3 at OCSD and 2.17 EU/m^3 at RWWTP). Protein levels reached 1.10 μg/m^3 at 100 m downwind of WMWWTP and fungal glucan concentrations ranged from 0.01 (100 m upwind from RWWTP) to 1.07 μg/m^3 (100 m upwind from OCSD). It was surmised that the aerated basins at the three locations contribute to protein and endotoxin concentrations but not glucans. Further particle characterization studies are suggested to uncover the origin of fungal elements in the samples as well as other sources of protein and endotoxin within the WWTP.

3.2 Introduction

Wastewater treatment plants (WWTP) are a crucial component of urban planning but their airborne emissions have been associated with the deterioration of regional air quality and detrimental health implications. Previous epidemiological studies have mentioned several diseases that may be caused by WWTPs particulate emissions (Sorber et al., 1979; Clark, 1987; Heng et al., 1994; Chylek et al., 1995; Khuder et al., 1998; Smit et al., 2005; Beck at al., 2006; Radke et al. 2006; Masclaux et al., 2014; Yuan et al., 2015). However, the transport and characterization of these particulates remains elusive and there are still no guidelines or laws regarding their regulation (Walls et al 2015).

Past studies have shown that aerated basins are a main source of particulate emissions in the facilities (Piqueras et al 2016). The aeration is performed in the secondary stage of water treatment to remove the biodegradable organics in the influent (Metcalf and Eddy, 2003). Particulates emitted during this process consist a mixture of solid sludge constituents and liquid water (Upadhyay et al 2013) and they are known to exist in the ultrafine size range (Piqueras et al 2016); including relevant sizes of viral particles (Carducci et al, 1995).

Partial basin coverage has been considered as a solution to the odorous emissions that result in community complaints (Lebrero et al., 2011). Current basin coverage options consist of a concrete slab over the basin where a number of openings are kept to prevent pressure build-up and to allow injected air to escape to the ambient. Most WWTP have uncovered basins as shown in figure 3-1a (ITA, 2003). Partially covered basins are

only typical in upper/middle class urban areas, such as OCSD (shown in Figure 3-1b). Particulates may be reduced through impaction on these concrete surfaces. However, particles may escape if an opening remains; partial coverage mitigation efficiency is unknown and there is also no existent proof that covers used for odor reduction mitigate particulate emissions from the basin. Understanding the dispersion of the WWTP aerosols with different coverage scenarios is critical to assess their contribution to the already existing high concentration of urban pollutants. In the following work, we integrate modeling, laboratory work and field campaigns to provide a holistic view of WWTP emissions in Southern California. Specifically, dispersion modeling estimates the seasonal spread of WWTP in an urban environment. The dispersion modeling guides the sampling locations in the field and controlled laboratory bioreactor studies are conducted to support the analysis of field samples collected.

Figure 3-1: Pictures of a) an open aerated basin and b) a semi-covered aerated basin at Orange County Sanitation District (OCSD). The open basin allows all particulates to escape into the atmosphere while the semi-covered basin may reduce a small portion of particulate emissions due to particle impaction on the basin ceiling. Figure 3-1a source: Marnette Federis (Public Radio International).

3.3 Methodology

3.3.1 Dispersion model

A dispersion model was considered to analyze the transport of particulates emitted from WWTP with different coverage options. AERMOD (the AMS/EPA Regulatory Model) was selected because it is recommended by several regulatory agencies (EPA, 2016; SCAQMD, 2006). This modeling system consists of two regulatory components: AERMET, a meteorological data processor based on planetary boundary layer turbulence structure and scaling concepts that incorporates air dispersion, and AERMAP, a terrain data preprocessor that uses USGS Digital Elevation Data. The model was developed by the American Meteorology Society and the Environmental Protection Agency for regulatory purposes and it has been used in numerous case studies to explore the impact of source pollutants at distances less than 50 km (EPA, 2016). In this analysis, AERMOD is executed with the U.S. EPA regulatory default option with urban conditions, as specified by the South Coast Air Quality Management District (SCAQMD) policy for all air quality impact analyses in its jurisdiction (SCAQMD, 2006). Within this study, the grid spacing is reduced to 100 meters to identify the maximum impacted receptors and the selected area of modeling was set at 4 x 4 km. Equations 4-1 through 4-3 were utilized to calculated model inputs.

Equation 3-1: $A_e = C \cdot V_x$

Equation 3-2: $P_e = C \cdot V_x \cdot A$

Equation 3-3: $V_x = \frac{F}{A}$

In these functions A_e is the area emission rate in g/(s-m^2). P_e is shown for point emission rate in g/s, C for concentration, V_x for exit velocity (m/s), A for exit area and area of the basin of one point source and F for typical air flow that is injected into one aerated tank.

3.3.1.1 Study Area

Orange County Sanitation District (OCSD) was selected as the source of emissions in the model because of its proximity to public spaces, schools and houses. The WWTP is located in a middle class suburb in Fountain Valley, California, right next to the Santa Ana river. The plant is considered to be a large treatment facility as it serves 21 cities with a population of ~2.5 million people (Davies et al., 1997; OCSD, 2016). The district covers an area of 479 square miles in central and northwest Orange County and it consists of two plants; plant 1 and plant 2 which treat about 230 million gallons of wastewater per day (MGD) altogether (Piqueras et al., 2016; OCSD, 2016). The modeling in this study will focus on emissions from plant 1, the farthest one upstream.

OCSD Plant 1 operates 16 individual aerated basins separated into two buildings. The first building from south to north (containing tanks 1-10) and the second building (containing tanks 11-16) are partially covered with a concrete slab. The slab has openings for the aerated air mass to exit. These openings are 15 by 15 feet (4.6 by 4.6 m) in area as shown in figure 3-1b. The openings were situated 30 feet (9.1 m) from each other. A full diagram of these aerated basins can be found in Piqueras et al., 2016. The basins are 250 feet (76.2 m) in length and 45 feet (13.7 m) in width and they hold a volume of 1.39

million gallons (5.2 million liters) of mixed liquor (wastewater and sludge mixture). The headspace from the surface of the mixed liquor to the surface of the concrete slab is 3 to 4 feet (0.9 to 1.2 m) (Piqueras et al., 2016). The injected air into OCSD aerated basins utilized a fine bubble diffuser.

Source measurements and equations developed in Piqueras et al, 2016 were used to estimate particle mass fluxes at each basin. Three different configurations were performed in AERMOD; covered (with small openings), semi-covered (with large openings), and fully uncovered. The covered configuration is represented with 336 point sources, the semi-covered option is assumed to have 84 square area sources and the fully uncovered scenario considers 16 rectangle area sources. All three runs were modeled without deposition and they were later compared by using meteorological data during two selected days in winter and summer (February 15th and August 15th, 2012), four months (January, May, August and November 2012) and over the entire length of 2012. The source height of was measured to be 5.79 m, and the source temperature was assumed to be the same as the temperature of the mixed liquor (37 ºC).

3.3.2 Field campaign

Three WWTP along the Santa Ana River Watershed were considered for the field investigation. All facilities posses aerated basins, but the size and capacity of each plant as well as the composition of the sludge and type of aerator differ at each location.

The Santa Ana River is the largest river in Southern California. It extends a length of 96 miles (154 km) and its watershed drains an area within four counties of 2,650

square miles (6,900 km^2). The watershed has an arid climate in the Inland Empire section and a Mediterranean climate in the coastal plain of Orange County (Westman et al., 1981). The river is a collection site for treated wastewater, precipitation and urban runoff. By the time the river reaches the Pacific Ocean, it has been treated by 18 wastewater districts that serve nearly 6 million residents (SAWPA, 2015). The population is predominantly located in the urban centers of San Bernardino, Redlands, Anaheim and Santa Ana. Most of the flow in the river, below the city of San Bernardino (the city next to RWWTP), consists of effluent from 45 wastewater treatment plants (NRC, 1999). The river is included on the U.S. Environmental Protection Agency's (EPA) list of "304 toxic hot spots list of impaired waterways" (NRC, 1999). Since it is a river that is crucial to many people, the Santa Ana Water Project Authority (SAWPA) was created to establish water management policies and to ensure cooperation among competing water districts (see figure 3-2). Filter samples were collected at OCSD, (explained in section 3.3.1.1), located near the river outlet into the Pacific, the Western Municipal Wastewater Treatment Plant (WMWWTP), situated on the river's mid-course and the City of Redlands Wastewater Treatment Plant (RWWTP), positioned the furthest upstream.

WMWWTP is a tertiary treatment facility located 42 miles upstream of OCSD. The plant is operated by the Western Municipal Water District and it has a design capacity for 3 MGD. It treats water at a tertiary level and it provides sewer treatment services to the community and recycles water for reuse purposes. There are 3 fully uncovered aerated basins that are 117 feet (35 meters) long by 70 feet (21 meters) wide and it is located in a semi-rural setting with a freeway and corporation yards next to it.

This plant has surface aerators; a hollow shaft with a propeller that rotates on ball bearings. Aeration of the water occurs below the surface of the water as air is pushed down into the basin where it is turbulently combined with the mixed liquor.

The RWWTP is located in the city of Redlands near the mountains where the Santa Ana River source is. It currently processes about 6 million gallons per day and it is capable of treating 9.5 MGD (RWWTP, 2016). Effluent from the primary is pumped to a meter controlled distribution system that divides the flow between the MBR and conventional treatment systems (Water Reuse, 2015). The plant has 6 uncovered aerated basins with a surface area of 30,000 ft^2 (2787.09 m^2). Each basin holds 333,333 gallons (1261802.67 liters) and it has rubberized fine air diffusers (same as OCSD). The airflow to the conventional activated sludge can vary between 3,000 and 6,000 SCFM and the airflow into the MBR may vary between 500 and 1100 SCFM.

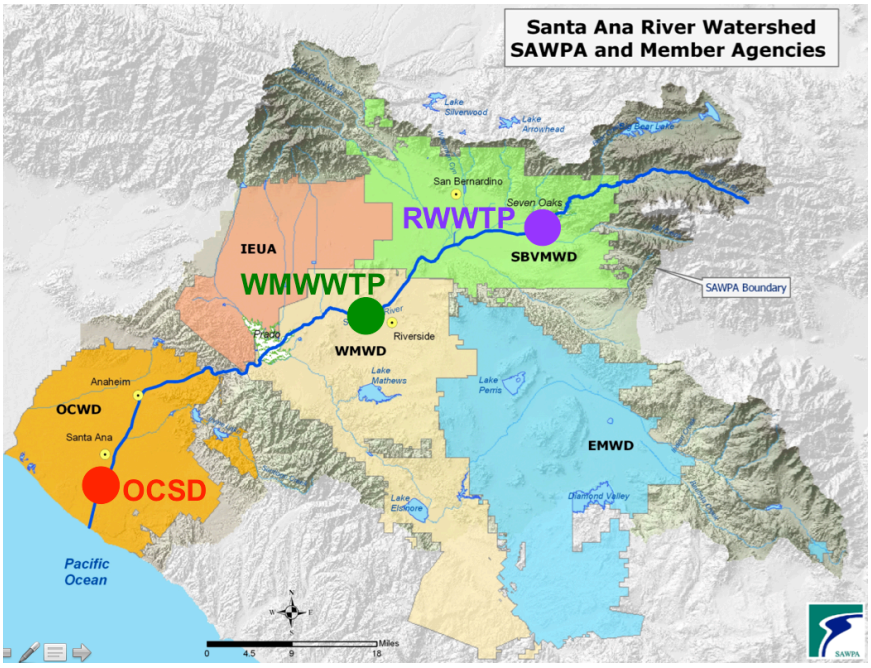

Figure 3-2: Geographical representation of the three wastewater treatment plants that were considered for this study. RWWTP is located upstream (shown with a purple circle), WMWWTP plant is located in mid-course of the river (shown with a green circle) and OCSD plant is situated at the end of the Santa Ana River Watershed (red circle). Colored regions represent the water districts within the watershed. SBVMWD (San Bernardino Valley Municipal Water District), where RWWTP is located, is represented in green. The blue district displays the area of IEUA (Eastern Municipal Water District). The orange region shows the Inland Empire Utilities Agency and the yellow zone establishes the WMWD (Western Municipal Water District), where the WMWWTP plant is located. The orange section represents the OCWD (Orange County Water District) where OCSD is located. The blue line outlines the Santa Ana river course. Source: SAWPA.

Particle filter samples were taken at four locations in each WWTP: 1) 50 meters downwind from the source (RF1, WF1 and OF1), 100 meters downwind from the source (RF2, WF2 and OF2, 200 meters downwind (RF3, WF3 and OF3) and 100 meters upwind (RF4, WF4 and OF4). Two additional filter samples were taken at Robert Gisler Elementary School, located 635 meters from OCSD (OF5) and at a house 860 meters downwind of OCSD (OF6). Table 3-1 shows the exact location of each filter holder during each sampling run. Aerosol samples were collected onto Zefluor 47 mm 0.5 μm supported PTFE filters. Pump flow rate ranged from 16.50 L/min to 25.24 L/min as specified in table 3-1. Sampling time was roughly 4 hours during each run (except at the school and at the house, where sampling time was 7 hours). Flow rate and sampling times were taken into consideration for concentration calculations. Wind direction and cloud coverage remained constant throughout the measurements. Each filter sample was take in triplicate.

Table 3-1: Filter name, location, sampling flow rate (S. flow rate) and sampling time (S. time) during field campaigns at the RWWTP, WMWWTP and OCSD

Name*	Location	Coordinates	S. flow rate	S. time
		RWWTP		
	Source	*34.091172, -117.214500*	*N/A*	*N/A*
RF1	50 m d.	34.091197, -117.212972	21.00 L/min	4 h and 04 min
RF2	100 m d.	34.091301, -117.213458	25.24 L/min	3 h and 55 min
RF3	200 m d.	34.091710, -117.212520	22.80 L/min	4 h and 02 min
RF4	100 m u.	34.090864, -117.215548	16.50 L/min	3 h and 58 min
		WMWWTP		
	Source	*33.866974, -117.265640*	*N/A*	*N/A*
WF1	50 m d.	33.867158, -117.265150	22.80 L/min	4 h and 03 min
WF2	100 m d.	33.867522, -117.264783	25.24 L/min	4 h and 01 min
WF3	200 m d.	33.867564, -117.263717	21.00 L/min	3 h and 45 min
WF4	100 m u.	33.866523, -117.266543	21.00 L/min	4 h and 00 min
		OCSD		
	Source	*33.689819, -117.942108*	*N/A*	*N/A*
OF1	50 m d.	33.690192, -117.941955	25.24 L/min	4 h and 55 min
OF2	100 m d.	33.690582, -117.941663	21.00 L/min	4 h and 50 min
OF3	200 m d.	33.691411, -117.941213	22.80 L/min	4 h and 42 min
OF4	100 m u.	33.688933, -117.942464	16.50 L/min	4 h and 38 min
OF5	635 m d. (school)	33.693394, -117.947835	28.3 L/min	7 h and 00 min
OF6	860 m d. (house)	33.693682, -117.933996	28.3 L/min	7 h and 00 min

** Filter Name XF#, where X refers to the WWTP location, F refers to the field, # refers to the field sampling location. The source coordinates are at the center. D stands for downwind and U. stands for upwind.*

3.3.3 Laboratory bioreactor

Isolating WWTP aerosols in the field is a complex process as there is always a risk of ambient particle influence from other sources. Therefore a simulation laboratory bioreactor was constructed to characterize and compare sludge aerosol emissions. The bioreactor was operated on a sequencing-batch mode, a variation of the activated sludge process, using a two-day feeding cycle. Piqueras et al 2016 showed that the particle size distribution and particle concentrations from a laboratory-controlled bioreactor are comparable to emissions measured in the field. The bioreactor methods as they pertain to subsequent experiments are briefly described here and additional information on the bioreactor can be found in Piqueras et al 2016.

The laboratory bioreactor setup consisted of a 5-gal (18.9 L) cylinder with an air diffuser at the bottom of the sludge mixture (shown in figure 3-3). A molasses based synthetic wastewater was used as the feed that provided the organic supply for degradation. The air source for the diffuser was filtered with a HEPA filter (Pall Corporation HEPA Capsule) that provided "particle free" air. The diffuser created bubbles of < 600 μm (Fannin et al., 1985) homogeneously throughout the entire volume of the mixed liquor. Three bioreactor filter samples were collected when the mixed liquor was aerosolized. The mixed liquor consisted of the feed and sludge from the three WWTP described in section (3.3.2) (RL1 for RWWTP, WL1 for WMWWTP and OL1 for OCSD). A sample from the lab air was also taken for background concentration analysis (LL1). Aerosol samples were collected onto Zefluor 47 mm 0.5 μm supported PTFE filters (Pall Corporation, P/N R2PJ047) with 1 ft^3/min flow rate.

The bioreactor was operated in a controlled environment at constant temperature, pressure and humidity. Aerosols were measured within the enclosed headspace, 10 inches (25.4 cm) above the surface of the mixed liquor where bubble bursting occurred. Filter samples were obtained with a 3-foot long (0.9 m), 1/8 inch (0.3 cm) diameter copper line that was attached to the filter holder. Particle losses in copper tubing were negligible at the flow rate, which the pump was operating (1 ft^3/min or 28.3 L/min). Air was filtered before it was released through the exhaust to prevent particulates from escaping into the lab air ventilation (as shown in figure 3-3). Filter sampling was conducted for 24 hours each. Once the sample was completed, the filters and the particulates collected in them were placed in petri dishes and shipped for characterization. A photograph of the final filter product is displayed in figure 3-4.

Table 3-2: Filter name, sludge collection locations for each laboratory run in the bioreactor and filter sampling flow rate and sampling time.

Filter name	Sludge collection location	S. flow rate	S. time
RL1	RWWTP	28.3 L/min	24 h and 00 min
WL1	WMWWTP	28.3 L/min	24 h and 00 min
OL1	OCSD	28.3 L/min	24 h and 00 min
LL1	N/A (lab air)	28.3 L/min	24 h and 00 min

** Filter samples were run while the mixed liquor was aerated. Filter Name XL#, where X refers to the WWTP location, L refers to the laboratory, # refers to the sampling location*

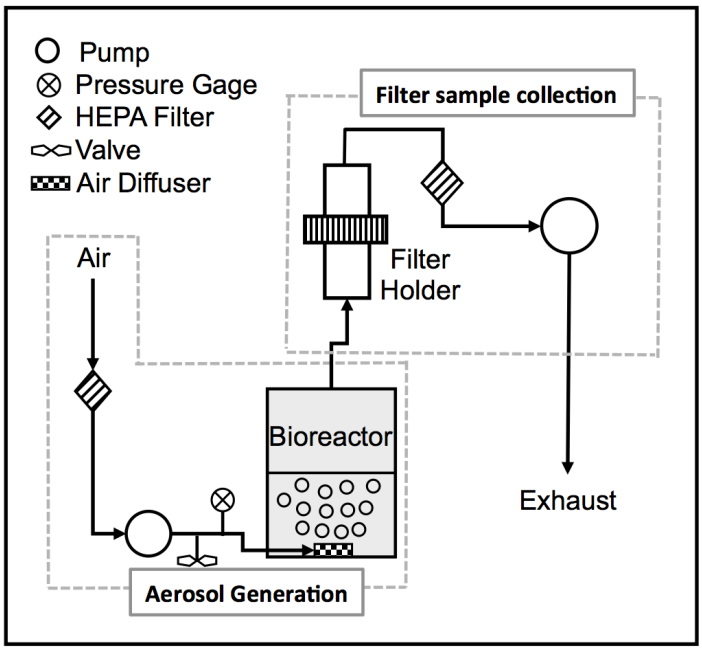

Figure 3-3: Schematic of bioreactor particulate filter collection. Particle free air entered the bioreactor to aerosolize the wastewater and sludge mixture. Particulates collected in the bioreactor headspace were then pumped into the filter holder and the air was filtered before exiting the system.

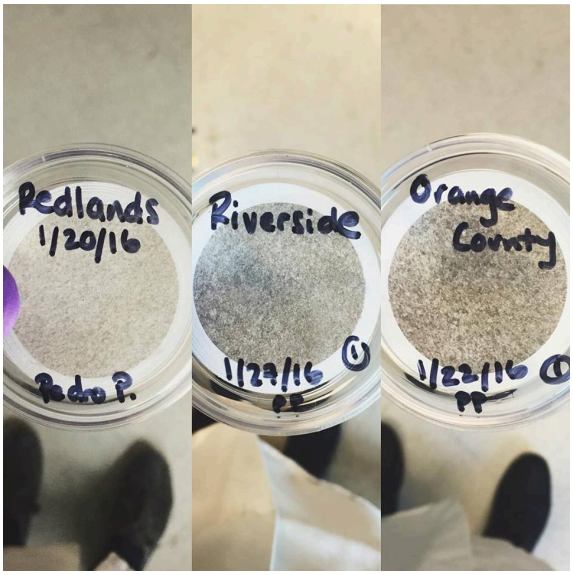

Figure 3-4: Photograph of three filter samples after particulate emission (RL1, WL1 and OL1). A color difference was observed for each filter sample.

3.3.4 Characterization and quantification of samples

Zefluor filters samples from the bioreactor (RL1, WL1 and OL1), lab air (LL1), RWWTP (RF1, RF2, RF3, RF4), WMWWTP (WF1, WF2, WF3, WF4) and OCSD (OF1, OF2, OF3, OF4, OF5 and OF6) were investigated for organic compounds through GCMS, endotoxins through LAL assay, fungal glucans by immunoassay and total proteins by the Bradford method. Detailed methodology procedures are explained in the following subsections.

3.3.4.1 Organic molecular markers (GC-MS)

Gas chromatography mass spectrometry was used to complete a quantitative analysis of the filter samples for several volatile organic compounds (VOC). The samples discussed in this paper were characterized by following the procedure in Stone et al., 2008 for solvent-extractable organic species, in which the filters are spiked with isotopically labeled internal standards and ketopinic acid prior to sequential extraction with dichloromethane and methanol. In this study we used PTFE filters and slightly modified the analysis process as described below:

All filters were spiked with isotopically labeled internal standards for quantification and extracted according to the procedure described in Al-Naiema et al., 2015. The filters were sonicated in two 20 mL portions of each hexane and acetone for removal of polar and nonpolar compounds and the resulting extract was reduced to ~1mL using a high purity nitrogen flow by a turbo evaporator (Zymark Turbo Vap II, LV, Caliper Life Science). The extracts were filtered through a .2 μm PTFE filter (Whatman, GE Health Care Life Sciences) and reduced to 100 μL with a mini evaporator (Reacti-Thermo III, Thermo Scientific). Extracts were analyzed by GC-MS (Agilent Technologies GC-MS 7890A) equipped with an Agilent DB-5 column (30m x .25mm x .25 um) and electron ionization source. Polar species were analyzed after trimethylsilyl (TMS) derivatization method described in Stone et al., 2012 to replace active hydroxyl groups and eliminate error related to hydrogen bonding. This reaction involved nitrogen blowing 10 uL of the sample to dryness and adding 20 μL of the silylation agent N,O-

bis(trimethylsilyl)trifluoroacetamide and 10uL of pyridine, then heating the mixture at 70 °C for 3 hours.

Each extraction batch contained quality control samples including a lab blank filter and a spike recovery filter spiked with known concentrations of analytes. Spike recovery was calculated as a percent of the blank subtracted recovered concentrations to the standard concentration. GC-MS analyte responses were normalized to the corresponding internal standards and quantified using a five-point linear calibration curves ($R^2 \geq .995$).

3.3.4.2 Endotoxins by the LAL assay

Biomarkers were analyzed in extracts from the remaining of the PTFE filters: Filters were extracted via shaking into 2 mL of sterile pyrogen-free (PF) water for 1 h at 22 °C. Extracts were then centrifuged (5 min at 600g at 4 °C) as described in (Rathnayake et al., 2017). To analyze endotoxins, an aliquot of the previously described supernatant was subjected to the kinetic chromogenic Limulusamebocyte lysate assay (LAL) (Thorne et al., 2000). The 12-point calibration 5 curve was generated utilizing endotoxin standard (Escherichia coli 055:B5) at concentrations ranging from 0.024-50 Endotoxin Units (EU) m/L. The solution absorbance was measured at 405 nm (SpectraMax M5, Molecular Devices).

3.3.4.3 Fungal glucans by the immunoassay

For analysis of fungal glucans, a second aliquot of the supernatant was transferred into a PF borosilicate tube, mixed with 10x PF phosphate buffered Saline. This solution contained 0.05% Tween-20 (a surfactant). It was shaken for 1 hour and autoclaved for another hour, then it was shaken for 20 min shaking, and then centrifuged for (600g at 4°C) 20 minutes. Glucans were later quantified by enzyme immunoassay as previously described by Blanc et al., 2005.

3.3.4.4 Total proteins by the Bradford method

The CBG (Coomassie blue G) binding method for protein assay that was originally introduced by Bradford and Sedmak et al was utilized to measure proteins. The preparation of protein reagent was executed as explained in Bradford et al.,1976: Coomassie Brilliant Blue G-250 (100 mg) (previously dissolved in 50 ml 95% ethanol) was added to 100 ml 85% (w/v) phosphoric acid. Final concentration was diluted to attain a total 0.01% (w/v) Coomassie Brilliant Blue G-250, 4.7% (w/v) ethanol, and 8.5% (w/v) phosphoric acid.

Protein assay (standard method) was also followed as specified in Bradford et al., 1976: The protein sample was introduced into the test tube and adjusted with appropriate buffer. Five milliliters of protein reagent was added to the test tube and the contents mixed through vortexing. The absorbance at 595 nm was measured after 2 minutes and before 1 hour in 3 ml cuvettes. A reagent blank was prepared from 0.1 ml of the

appropriate buffer and 5 ml of the protein reagent. The weight of protein was plotted against the corresponding absorbance and compared the results to a previously developed standard curve.

3.3.4.5 Point source buffer analysis

WWTP particulate concentration maps were created in ArcMaps 10.4.1 (ESRI© ArcGIS 10.4.1). GPS coordinates corresponding to the locations of air samplers upwind and downwind of the study site were projected onto a WGS 1984 Mercator street basemap. Buffer zones from the site were created by freehand on-screen digitizing polygons around each sampling site mimicking the direction of wind rather than equidistant circles. Results of the organic compound characterization in section 3.4.2 were joined into the attribute tables of the polygons for the thematic mapping. Dot density description was established at 0.2 pg/m^3 for levoglucosan, sterols and stanols, 0.2 μg/m^3 for protein and fungal glucans and 0.2 EU/m^3 for endotoxins.

3.4 Results and discussion

3.4.1 Basin coverage outputs

3.4.1.1 Annual average concentration

Covered (point sources), semi-covered (area sources) and uncovered aerated basins (rectangle sources) were modeled with meteorically data from 2012. The annual average concentrations were revealed and compared in figure 3-5. A different dispersion pattern was observed for point sources and area sources. Although the area sources have

different dimensions, results suggest that partial coverage does not substantially reduce the emissions. The maximum emission rate of semi-covered scenario (0.0156μg/m^3) was found to be marginally higher than the covered point source scenario (0.0213μg/m^3). The uncovered scenario had the highest value of all cases (0.0240μg/m^3).

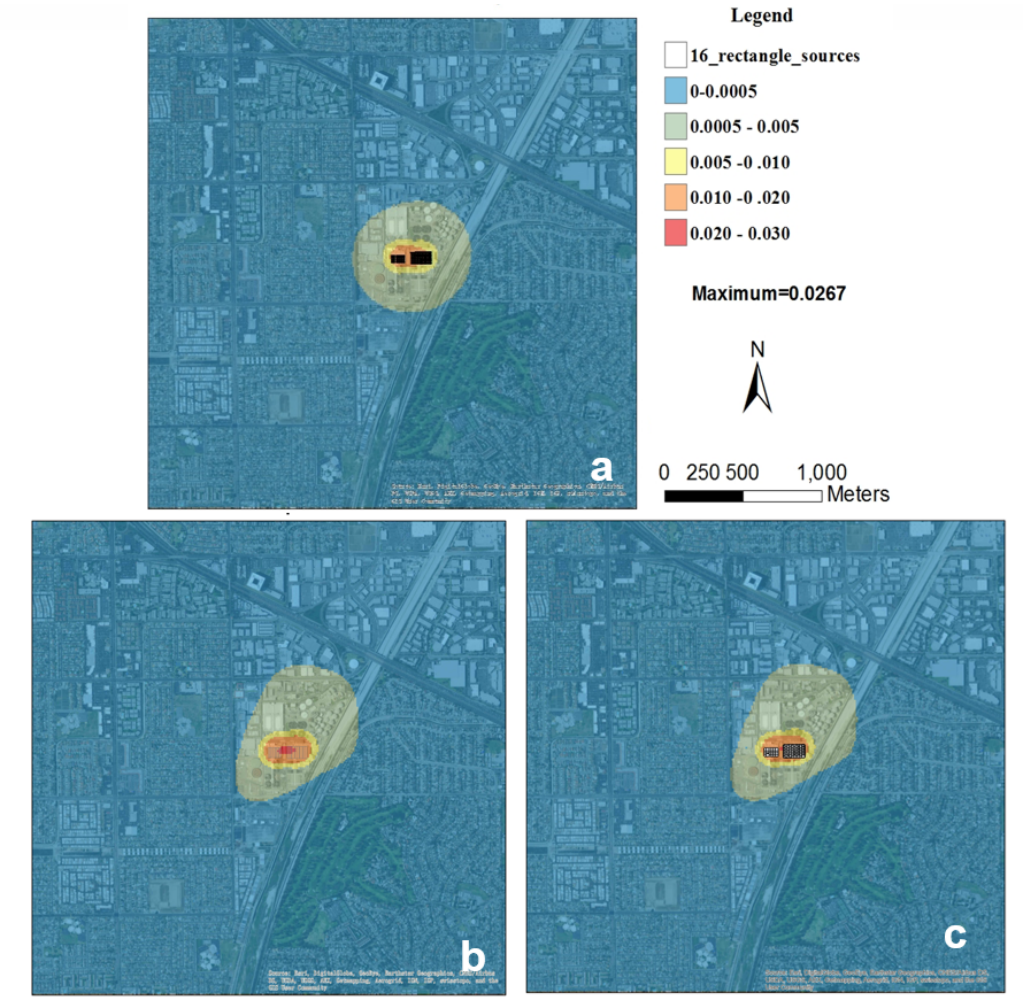

Figure 3-5: Modeled annual average concentrations of covered, semi-covered and uncovered scenarios. Runs were executed with 2012 meteorological data and sources emissions of a) 336 point sources b) 84 semi-covered squares and c) 16 uncovered rectangles.

3.4.1.2 Seasonal average concentrations

Concentration zones of the covered basin scenario (point sources) resulted in seasonaly different strengths throughout the WWTP. However, these areas keep a similar in contour profile (shown by Figure 3-6). The maximum calculated ambient concentrations in winter were obtained at 0.0180$\mu g/m^3$ and 0.0178$\mu g/m^3$ during the spring. The latter was found to be higher than the concentrations calculated during summer of 2012 (0.0135$\mu g/m^3$) and fall (0.0146$\mu g/m^3$).

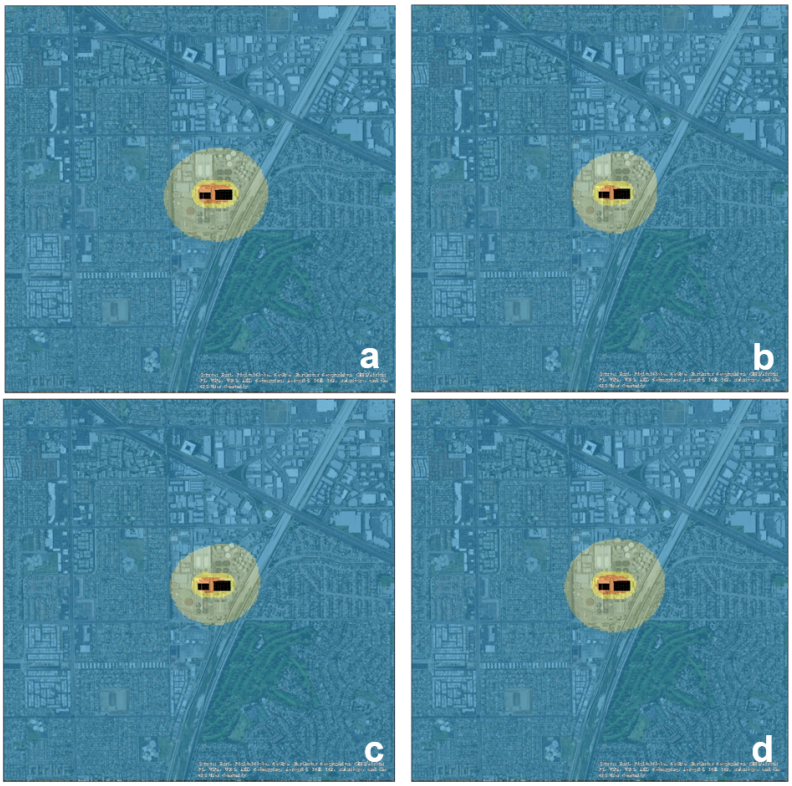

Figure 3-6: Modeled monthly average concentrations of 336 point sources. Legend remains consistent with figure 3-8. Runs were executed with 2012 meteorological data in a) January b) May c) August and d) November.

Modeled monthly average concentrations were obtained with 2012 meteorological data in winter (January), spring (May), summer (August) and fall (November). Figure 3-7 and figure 3-8 respectively display greatly diverse contour profiles of the semi-covered scenario (square sources) and the uncovered scenario (rectangle sources) during the four seasons. The maximum value of calculated ambient concentrations for the semi-covered scenario in spring was 0.0247$\mu g/m^3$ and 0.0242$\mu g/m^3$ for the winter. These two outcomes were clearly higher than the concentrations of summer (0.0177$\mu g/m^3$) and fall (0.0167$\mu g/m^3$). The maximum value of calculated ambient concentrations for the uncovered scenario was spring (0.0267$\mu g/m^3$) and then winter (0.0257$\mu g/m^3$). These two seasons were higher in concentrations than those of summer (0.0183$\mu g/m^3$) and fall (0.0175$\mu g/m^3$). Comparably, the maximum value of the semi-covered scenario is higher than the result obtained for the covered and lower than the uncovered scenario for all seasons.

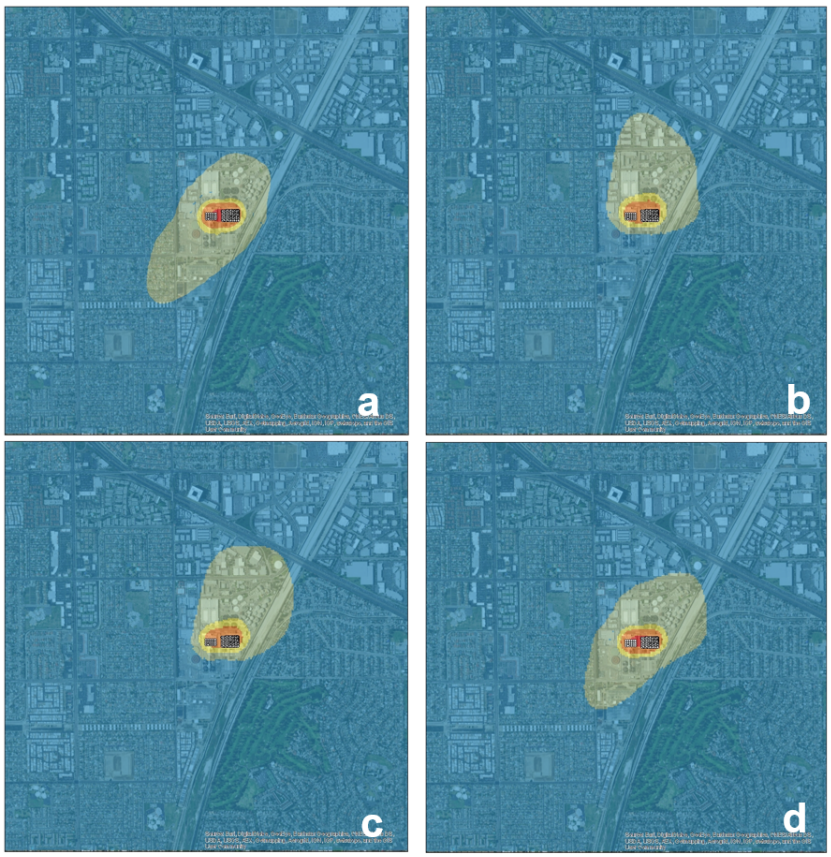

Figure 3-7: Modeled monthly average concentrations of 84 square sources. Legend remains consistent with figure 3-8. Runs were executed with 2012 meteorological data in a) January b) May c) August and d) November.

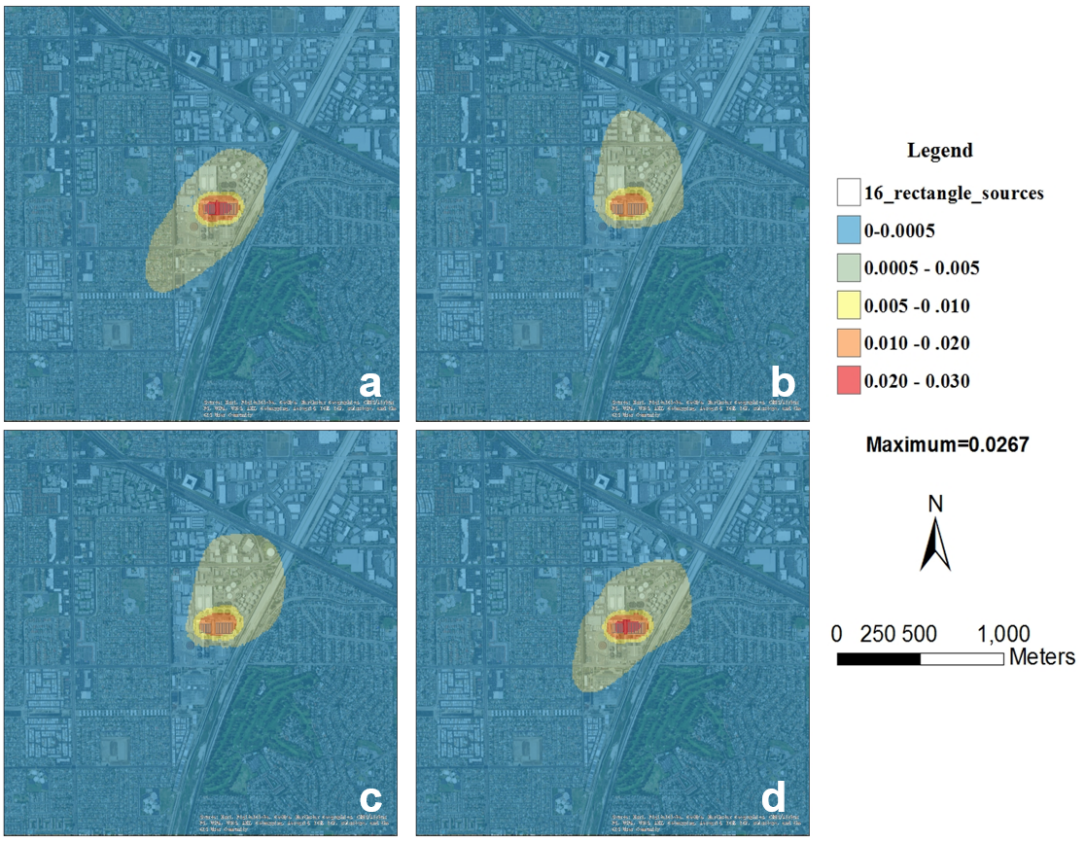

Figure 3-8: Modeled monthly average concentrations of 16 rectangle sources. Runs were executed with 2012 meteorological data in a) January b) May c) August and d) November.

3.4.1.3 Daily average concentrations

Figure 3-9, 3-10 and 3-11 show the modeling results of the three scenarios for two days (24 hour model run). One winter day (February 15^{th,} 2012) and one summer day (August 15th, 2012) were selected for this run. In all three modeling scenarios, ambient concentrations calculated for February 15th are higher than those for August 15th. This occurrence was especially obvious in the semi-covered and uncovered scenario. Ambient

concentrations calculated for the semi-covered scenario resulted in much higher than those obtained for the covered scenario yet they remain lower than uncovered scenarios.

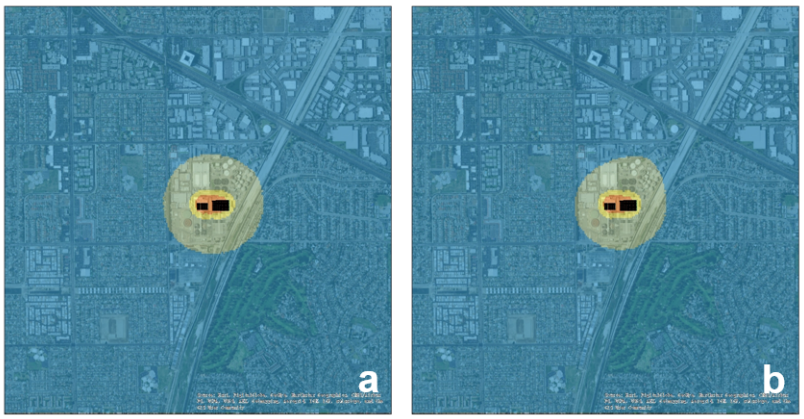

Figure 3-9: Modeled daily average concentrations of 336 point sources. Legend remains consistent with figure 3-11. Runs were executed with 2012 meteorological data on a) February 15th and b) August 15th.

Figure 3-10: Modeled daily average concentrations of 84 semi-covered square sources. Legend remains consistent with figure 3-11. Runs were executed with meteorological data on a) February 15th, 2012 and b) August 15th, 2012.

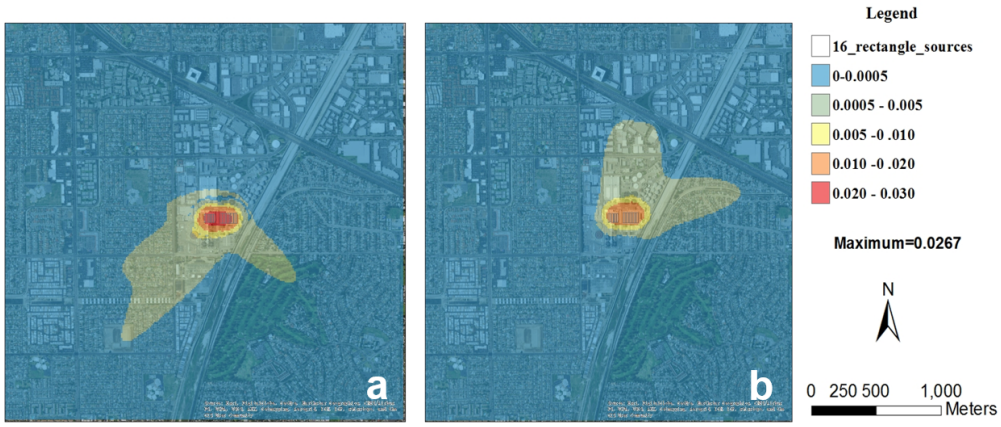

Figure 3-11: Modeled daily average concentrations of 16 uncovered rectangle sources. Runs were executed with meteorological data on a) February 15th, 2012 and b) August 15th, 2012.

3.4.2 Field filter results

Fecal sterols were detected in samples collected downwind of the wastewater treatment plants (WWTP) for all samples and a decrease in concentration was observed when the samples were collected farther away from the WWTP (Figure 3-12): The WWTP that had the highest concentration of sterols was WMWWTP where cholesterol was the most abundant sterol (WF1 = 202.50 ± 43.04 ng/m^3, WF2 = 153.85 ± 32.85 ng/m^3 and WF3 = 13.91 ± 2.90 ng/m^3 at 2), as shown in figure 3-12 a through c. Cholesterol concentrations at RWWTP (RF1 = 14.99 ± 3.12 ng/m^3, RF2 = 10.03 ± 2.10 ng/m^3 and RF3 = 3.25 ± 0.77 ng/m^3 at 200 m) were found to be an order of magnitude lower than those at WMWWTP and almost 10 ng/m^3 lower than OCSD (OF1 = 18.52 ± 3.83 ng/m^3, OF2 = 17.95 ± 3.72 ng/m^3 and OF3 = 8.16 ± 1.71 ng/m^3).

The second most abundant sterol was b-sitosterol (WF1 = 78.3 ± 17.2 ng/m^3, WF2 = 58.61 ± 13.02 ng/m^3 and WF3 = 12.64 ± 3.09 ng/m^3; OF1 = 9.86 ± 2.29 ng/m^3, OF2 = 12.52 ± 2.89 ng/m^3 and OF3 = 7.42 ± 1.96 ng/m^3 as well RF1 = 6.77 ± 2.08 ng/m^3, RF2 = 5.24 ± 1.71 ng/m^3 and RF3 was below the detection limit (BDL)), followed by campesterol (WF1 = 40.65 ± 8.50 ng/m^3, WF2 = 30.19 ± 6.36 ng/m^3 and WF3 = 7.06 ± 2.20 ng/m^3; OF1 = 5.74 ± 1.58 ng/m^3, OF2 = 6.29 ± 1.82 ng/m^3, OF3 = 4.10 ± 1.48 ng/m^3 and BDL at RF1, RF2 and RF3). Campesterol is only found in feces (Upadhyay et al., 2013), therefore the trend is an obvious indication that emitted WWTP aerosols are traveling as far as 100 m in WMWWTP and OCSD. The campesterol concentration at RWWTP was undetectable on site.

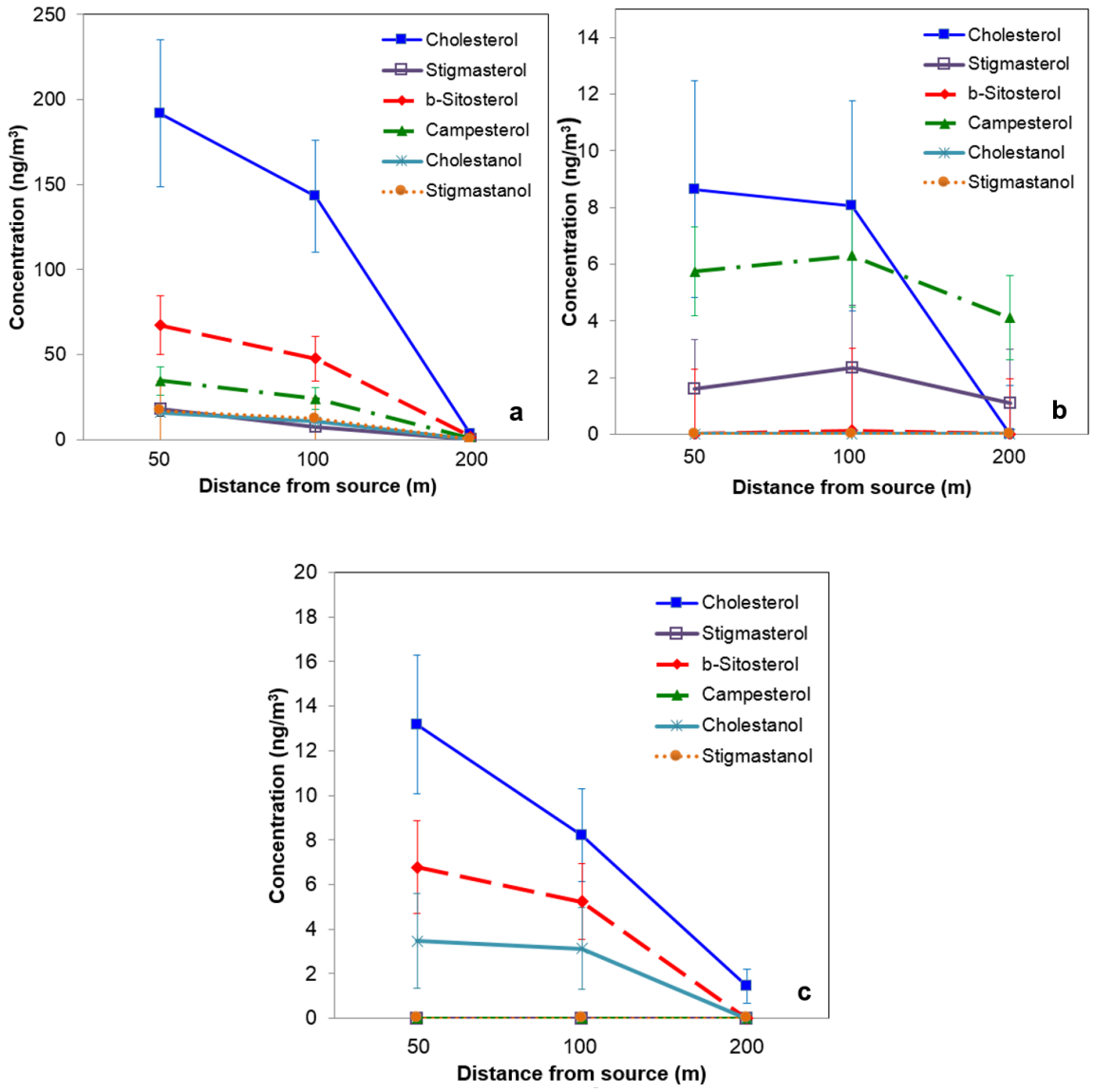

Figure 3-12: Sterol concentrations at a) WMWWTP b)RWWTP and c) OCSD at 50 meters, 100 meters and 200 meters downwind. The upwind concentrations were subtracted to visualize the total sterol concentration contribution of the WWTPs.

Figure 3-13 displays the sterol concentrations at 100 m upwind and in areas passed 200 m (a house and a school in a nearby neighborhood near OCSD, 860 m and 635m respecitively from the source). Cholesterol and b-sitosterol are found upwind at WMWWTP (WF4 = 10.64 ± 2.23 ng/m^3 for cholesterol and WF4 = 11.01 ± 2.79 ng/m^3 for b-sitosterol), OCSD (OF4 = 9.89 ± 2.09 ng/m^3 for cholesterol and OF4 = 12.39 ± 3.08 ng/m^3 for b-sitosterol) and RWWTP (RF4 = 1.82 ± 0.64 ng/m^3 and RF4 = BDL for b-sitosterol). The source of these sterols are unknown, but they are commonly found in nature (Demel et al., 1976; Law et al., 2000; Xu et al., 2001; Jong et al., 2003). Stigmasterol (WF4 = 1.22 ± 2.44 ng/m^3) and campesterol (WF4 = 6.09 ± 1.99 ng/m^3) are also found upwind. However, cholestanol/coprostanol (another fecal sterol) is also found 860 meters downwind from OCSD (at the house location; OF6 = 1.09 ± 0.88 ng/m^3). This indicates that the WWTP particulates could be transported to nearby residental locations, potentially inhaled by local inhabitants. Cholesterol and b-sitosterol were also found in the school (OC5 = 6.09 ± 1.27 ng/m^3 for cholesterol, OC5 = 0.25 ± 0.66 ng/m^3 for b-sitosterol) and outside the local house (OC6 = 14.23 ± 2.94 ng/m^3 for cholesterol, OC6 = 2.89 ± 0.89 ng/m^3 for b-sitosterol) but no stigmasterol, campesterol or stigmastanol was found at either location. It was surmised that WMWWTP had higher concentrations than OCSD because of the surface aerators.

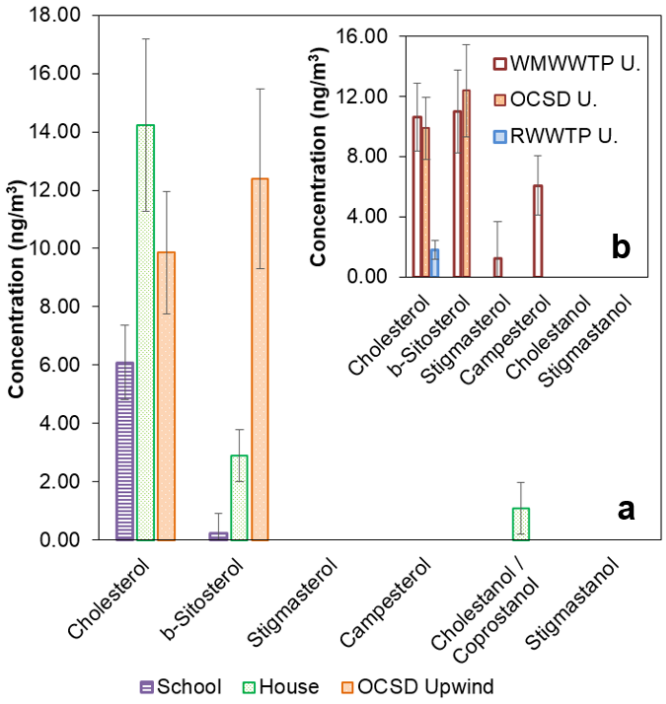

Figure 3-13: a) Sterol concentrations at the school (OF5, purple stripped column) and house (OF6, solid light green column) near OCSD compared to OCSD's upwind values. b) Upwind sterol concentrations at RWWTP (RF4, solid light blue columns), WMWWTP (WF4, white columns with red border lines), and OCSD (OF4, orange columns).

Statistical relationships between fungal glucan, endotoxin and protein concentrations versus distance from the source were investigated (shown in figure 3-14). The highest concentration of endotoxins was found at WMWWTP (WF1 = 14.33 EU/m^3, WF2 = 131.85 EU/m^3, WF3 = 2.27 EU/m^3 and WF4 = 1.43 EU/m^3) with an order of magnitude higher with endotoxin concentrations at RWWTP (RF1 = 1.27 EU/m^3, RF2 =

2.17 EU/m^3, RF3 = 1.35 EU/m^3 and RF4 = 0.38 EU/m^3 upwind) and two orders of magnitude higher than endotoxins concentration at OCSD (OF1 = 0.29 EU/m^3, OF2 = 0.48 EU/m^3, OF3 = 6.48 EU/m^3 and OF4 = 0.34 EU/m^3). A positive increasing trend as distance increased was observed for endotoxins at OCSD (R^2=0.71) and RWWTP (R^2=0.77). The cause of this increase may be that other sources of endotoxins apart from the aerated basins within the WWTP exist (e.g. clarifiers, digesters, primary settling ponds...etc.). Future research is required to unmask other possible sources of endotoxins within these locations. WMWWTP (R^2=0.03) showed no significant relationship and it had a relatively similar concentration of endotoxins throughout the distanced where filters were collected.

Proteins also showed a positive relationship at RWWTP (R^2=0.82). However, no significant relationship was found for WMWWTP (R^2=0.01) or OCSD (R^2=0.01). The increase in protein concentration over distance at RWWTP could be possibly related to the increase in concentration of endotoxins in the same location. Fungal glucan concentrations showed a slightly different trend at WMWWTP with a high correlation value as distance increased (R^2 = 0.90). Similar glucan relationship was also observed RWWTP (R^2 = 0.65) and a slight or no significant relationship was found at OCSD (R^2 = 0.65). Glucans had higher concentrations upwind at WMWWTP (WF1 = 0.17 μg/m^3, WF2 = 0.20 μg/m^3, WF3 = 0.31 μg/m^3 with WF4 = 0.38 μg/m^3 upwind,) and at RWWTP (RF1 = 0.23 μg/m^3, RF2 = 0.90 μg/m^3, RF3 = 0.34 μg/m^3 and RF4 = 0.35 μg/m^3 upwind). Therefore it was concluded that a source of glucans are present upwind of both WWTP. This was not the case of proteins or endotoxins; upwind concentrations at each

WWTP (WF1 = 0.44 $\mu g/m^3$, WF2 = 1.10 $\mu g/m^3$, WF3 = 0.56 $\mu g/m^3$ with WF4 = 0.85 $\mu g/m^3$); OF1 = 0.29 $\mu g/m^3$, OF2 = 0.48 $\mu g/m^3$, OF3 = 6.48 $\mu g/m^3$ and OF4 = 0.34 $\mu g/m^3$ and RF1 = BDL, RF2 = 0.20 $\mu g/m^3$, RF3 = 0.19 $\mu g/m^3$ and RF4 = BDL) were greatly lower than downwind concentrations. It was surmised that the aerated basins at the three locations contribute to protein and endotoxin concentrations but not fungal glucans. Further particle characterization studies are suggested to uncover the other sources of protein and endotoxin within the plant that are contributing to concentrations downwind of the aerated basins.

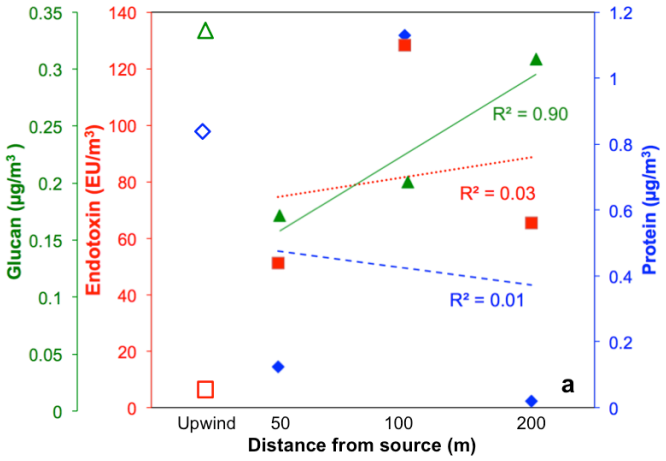
Glucan (µg/m³)
Endotoxin (EU/m³)
Protein (µg/m³)
R² = 0.90
R² = 0.03
R² = 0.01
a
Upwind
50
100
200
Distance from source (m)

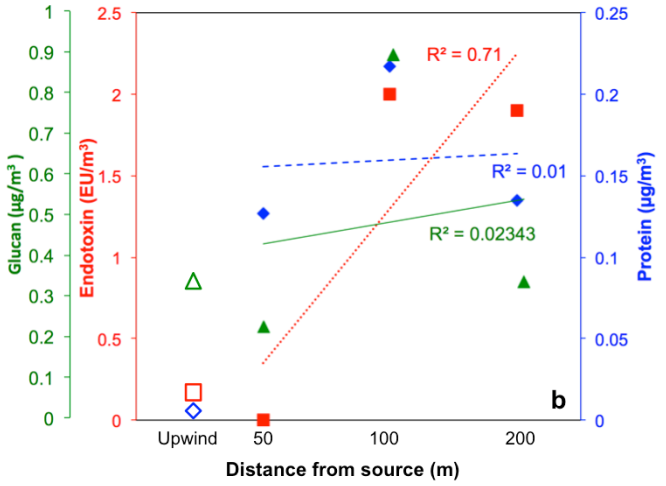
Glucan (µg/m³)
Endotoxin (EU/m³)
Protein (µg/m³)
R² = 0.71
R² = 0.01
R² = 0.02343
b
Upwind
50
100
200
Distance from source (m)

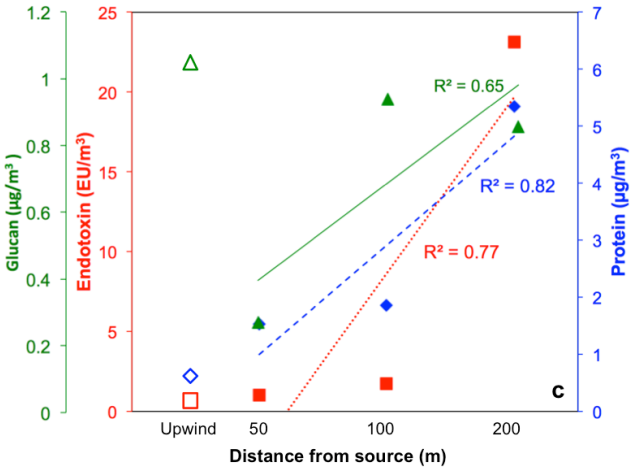
Glucan (µg/m³)
Endotoxin (EU/m³)
Protein (µg/m³)
R² = 0.65
R² = 0.82
R² = 0.77
c
Upwind
50
100
200
Distance from source (m)

Figure 3-14: Fungal glucan (green triangles), endotoxin (red squares) and protein (blue diamonds) concentrations in the filter samples 50 meters, 100 meters and 200 meters downwind from the source at a) WMWWTP, b) RWWTP and c) OCSD. Upwind concentrations are displayed with void green triangles for glucans, void red squares for endotoxin and void diamonds for proteins.

Bioassay characterization was also performed on filter samples obtained at Robert Gisler School (635 m Northwest of OCSD) and at a house in a nearby neighborhood (860 m Southeast of OCSD) to explore biological materials from OCSD are reaching public areas (shown in figure 3-15). Results suggest that endotoxins (OF5 = 0.16 EU/m^3 and OF6 = 1.57 EU/m^3), proteins (OF5 = BDL and OF6 = 0.80 $\mu g/m^3$) and glucans (OF5 = 0.42 $\mu g/m^3$ and OF6 = 0.11 $\mu g/m^3$) are found at both locations. However, these are relatively low when compared to WWTP measurements (three orders of magnitude when compared to WMWWTP, two order of magnitude when compared to RWWTP and one order of magnitude of OCSD).

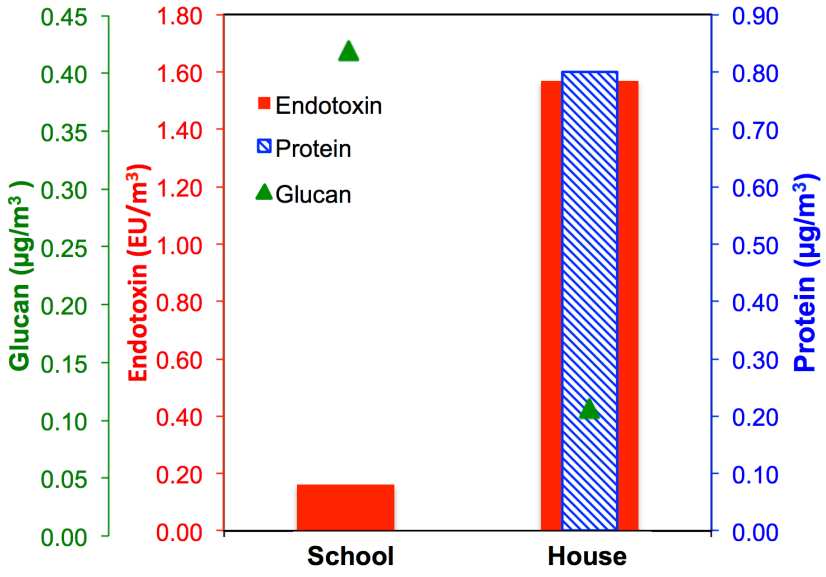

Figure 3-15: Bioassay results from filter samples obtained at Robert Gisler School (OF5, 635 m Northwest of OCSD) and at a house (OF6, 860 m Southeast of OCSD). Endotoxin levels are displayed with red solid columns, proteins are shown with stripped blue columns and fungal glucans are represented with green triangles.

Levoglucosan, a chemical tracer for biomass burning and PAHs were found in the samples. However, no relationship was determined between their concentration, WWTP particulate emissions and their transport to specific distances. It was concluded that the source of these organic compounds was not the WWTP and future characterization work is necessary to understand their origin. These have been included in the appendix for future consideration (figure A3.1 and A3.2).

The final element of the characterization process was to spatially visualize the concentrations of the organic compounds of concern, endotoxins, glucans and proteins throughout the area surrounding the WWTP. Figure 3-16 (a-c) shows the result of the point source buffer analysis in ArcMaps 10.4.1 (ESRI© ArcGIS 10.4.1). Results show that stanols, cholesterol, endotoxins and proteins are found up and downwind. In OCSD's case endotoxins and cholesterol (one of the sterols found in feces) are transported to the school and the house nearby (figure 3-16a). It is also noticeable that as the distance increases the concentration of all components decrease, as is expected. RWWTP had the least dense population of "dots" both up and downwind, which indicates that it is the plant that has the least concentration of endotoxins and cholesterols of all three WWTP. The results of this analysis are similar the outcomes modeled by AERMOD. However, future studies should be evaluated to expand the dates of investigation. A multi year analysis is also suggested to visualize the concentrations of these elements of concern over time.

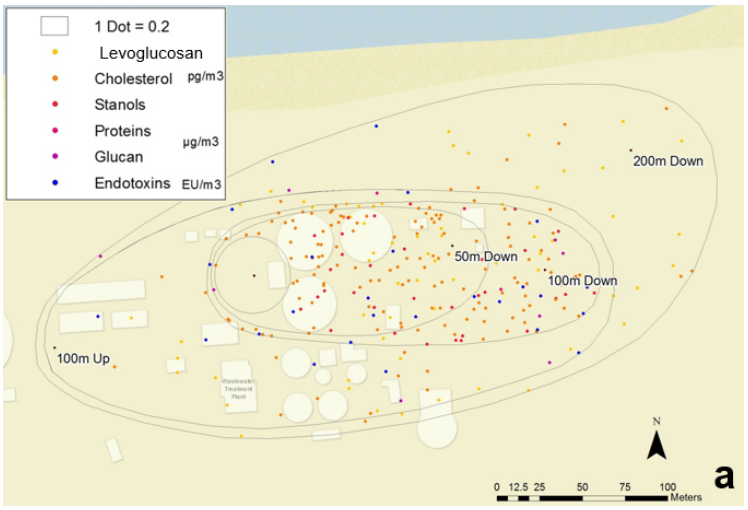
1 Dot = 0.2
Levoglucosan
Cholesterol pg/m3
Stanols
Proteins
Glucan µg/m3
Endotoxins EU/m3
200m Down
50m Down
100m Down
100m Up
N
0 12.5 25 50 75 100 Meters
a

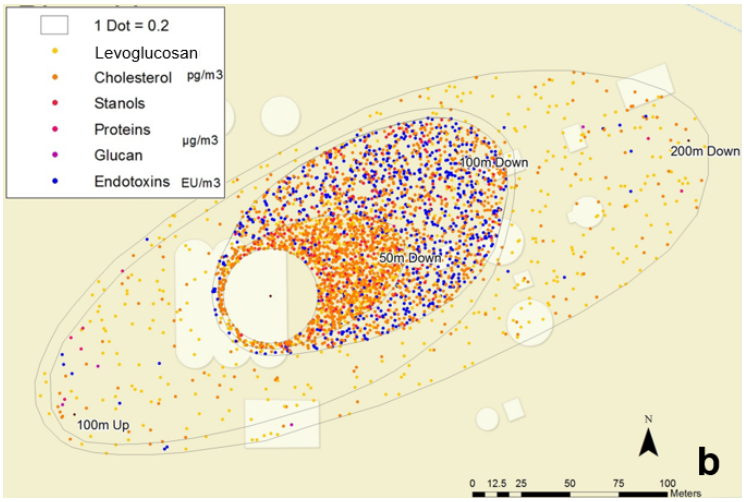
1 Dot = 0.2
Levoglucosan
Cholesterol pg/m3
Stanols
Proteins
Glucan µg/m3
Endotoxins EU/m3
100m Down
200m Down
50m Down
100m Up
N
0 12.5 25 50 75 100 Meters
b

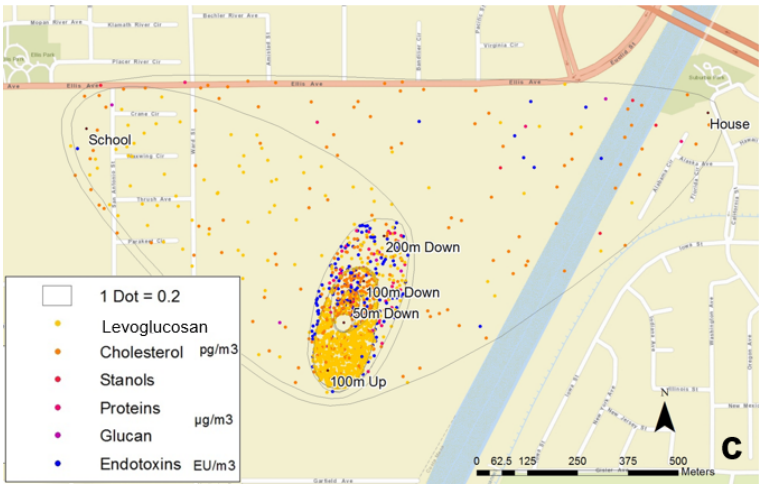
School
House
200m Down
100m Down
50m Down
100m Up
1 Dot = 0.2
Levoglucosan
Cholesterol pg/m3
Stanols
Proteins
Glucan µg/m3
Endotoxins EU/m3
N
0 62.5 125 250 375 500 Meters
c

Figure 3-16: Spatial display of organic compound concentrations at a) RWWTP (collected on filter RL1), b) WMWWTP (collected on filter WL1) and c) OCSD (collected on filter OL1). A colored dot represents 0.2 pg/m^3 for levoglucosan (yellow), cholesterol (light orange), and stanols (red), and µg/m3 for the bacteria protein (light pink) and glucan (blue). Endotoxin concentrations (blue) are also shown with a dot for 0.2 EU/ m^3.

3.4.3 Bioreactor filter results

Filter measurements collected in the laboratory were compared to results obtained in the field to investigate if the source of the sterols is indeed the aerosolization of the mixed liquor in aerated basins. This analysis was also performed to provide additional support to the conclusion presented in previous sections (shown in figure 3-17). Laboratory filter data showed that sterols are present in all samples and the most abundant sterols were also cholesterol (RL1 = 1.20 ng/m^3, WL1 =0.96 ng/m^3 and OL1 = 0.81 ng/m^3) and b-Sitosterol (RL1 = 1.17 ng/m^3 ,WL1 = 1.17 ng/m^3 and OL1 = 1.83 ng/m^3). Cholestanol/coprostanol was also found (RL1 = 1.18 ng/m^3, WL1 = 0.35 ng/m^3 and OL1 = 0.02 ng/m^3). PAH and levoglucosan were also observed and the results have been included in the appendix (figure A3.3 and A3.4) as an additional discussion.

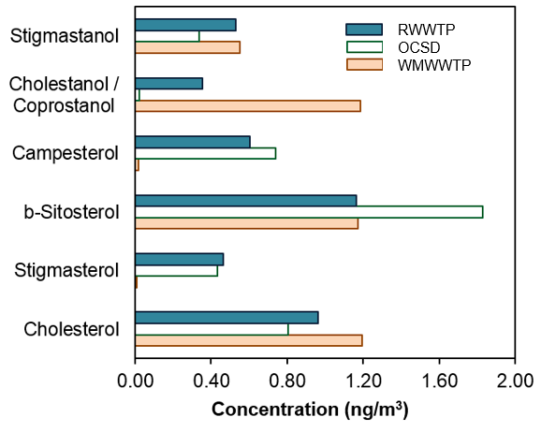

Figure 3-17: Sterol concentrations in laboratory bioreactor aerosolized sludge filter samples. Redlands Wastewater Treatment Plant sludge (RWWTP, filter RL1) levels are shown with blue columns Orange County Sanitation District sludge (OCSD, filter OL1) in Fountain Valley with white columns and Riverside sludge (WMWWTP, filter WL1) is represented with orange columns.

Sterol results are an evident indication that the sterols measured in the field may have come directly from the aerated basins since no source of contamination was possible in the bioreactor. Previous literature has indicated that sterols are an appropriate tracer for WWTP aerosols (Upadhyay et al., 2013). However, additional tracers were also investigated to identify unique markers that could provide more information on the field particle source and potential toxicity: Excess protein and endotoxins are suggested to be a diagnostic marker for biological causes of impaired air quality as well as viruses and bacteria present in the particle (Poruthoor et al., 1998). Laboratory results show high concentration of endotoxin (shown in figure 3-18), especially when the sludges from RWWTP and WMWWTP were aerosolized (RL1 = 22.99 EU/m^3, OC1 = 255.02 EU/m^3 and WL1 = 264.27 EU/m^3). It was also concluded that the levels of proteins in the samples are substantial (OL1 = 3.42 μg/m^3, WL1 = 1.605 μg/m^3 and RL1 = 0.3 μg/m^3).

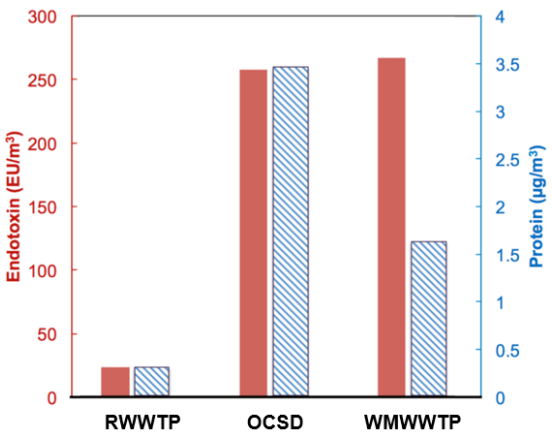

Figure 3-18: Endotoxin concentration in endotoxin units (EU) per cubic meter (red columns) and protein concentration (blue stripped columns) within laboratory filter samples. Sludge from Redlands Wastewater Treatment Plant (RWWTP, collected on filter RL1), Orange County Sanitation District (OCSD, collected on filter OL1) and Western Municipal Wastewater Treatment Plant (WMWWTP, collected on filter WL1) was aerated.

It is expected that fecal matter and consequently sewage contain endotoxin since the human digestive system contains a very high level of endotoxins (Epstein, 2008). However, there are no current regulations of endotoxins in the United States or Europe but there are suggested guidelines: In the Netherlands, the Exposure Standards Setting Committee is proposing a personal inhalable exposure weighted average of 200 EU/m^3 (measured as an eight hour time) (HCN, 2010). Previous literature demonstrates that endotoxin exposure may produce acute effects; they have been proven to cause mucous membrane irritation at 20–50 ng/m^3 (200-500 EU/m^3). At concentrations of 100–200 ng/m^3 (1000-2000 EU/m3) endotoxins cause acute broncho-constriction. In the high

range, at 1000–2000 ng/m^3 (10,000-20,000 EU/m^3), endotoxins can induce organic dust toxic syndrome (Melbostad, et al., 1994; Rylander, 1999); Douwes et al., 2001; Thorn and Beijer, 2004; Thorn and Kerekes, 2001). These concentrations are above the WWTP results presented in this work, but cumulative chronic exposure to those who are at risk should be investigated.

The outcomes of this study indicate that biological material and WWTP tracers (sterols) are present within filter samples and may be a cause for disease, particularly for workers within the plant. Proper hygienic practices (including the complete coverage of aerated basins) is advised prevent some of the symptoms previously reported by WWTP workers and residents living near the plants. Future particle characterization studies are also suggested to uncover the origin of the observed levoglucosan, PAHs and other industrial chemicals, well as other possible sources of protein, glucans and endotoxin within the facilities.

3.5 Acknowledgements

This work has been supported by the National Science Foundation Award (NSF) 1151893. Its contents are solely the responsibility of the grantee and do not necessarily represent the official views of the NSF. Furthermore, the NSF does not endorse the purchase of any commercial products or services mentioned in the publication. The authors would like to thank the staff from the City of Redlands, Western Municipal Water District and Orange County Sanitation District for their contribution to the study,

access to facilities and support and they would also like to express their gratitude to Jill Luo for her assistance with AERMOD modeling.

3.6 Appendix

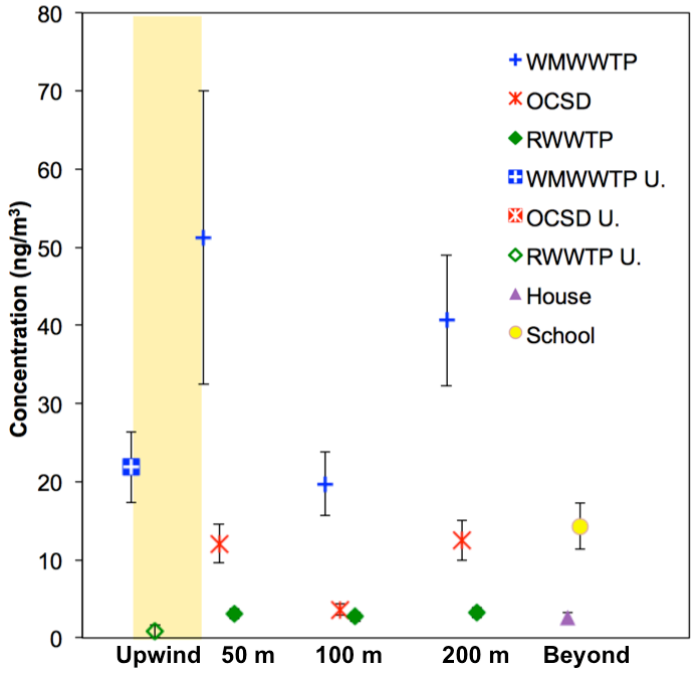

Figure A3.1: Levoglucosan concentrations at 50 meters, 100 meters and 200 meters downwind from the source at WMWWTP (WF1, WF2 and WF3 are shown with blue cross), OCSD (OF1, OF2 and OF3 are shown with a red asterisk) and RWWTP (RF1, RF2 and RF3 are represented with solid green diamond). Upwind concentrations are shown in a yellow region. The filters samples collected at a house (OC5, 635 meters downwind) and school (OC6, 860 meters downwind) near OCSD are also shown for comparison.

Polyaromatic hydrocarbons (PAHs) are generic markers of combustion processes and are likely the result of anthropogenic processes. PAHs were detected in few samples at much lower concentrations indicating the presence of burning actives around the sampling sites or combustion waste found in the WWTP sludge. Previous studies have shown that some PAH may be direct skin irritants. Characterization outcomes suggest that anthracene, benzo(a)pyrene and naphthalene are present in the laboratory sample. Anthracene and benzo(a)pyrene are known to cause allergic response and they're labeled as skin sensitizers. Naphthalene can cause the breakdown of red blood cells if inhaled or ingested in large amounts (Becking and Chen, 1998). Mixtures of PAHs are also known to cause skin irritation and inflammation.

The ability of PAHs to induce short-term health effects in humans is not clear (Abdel-Shafy and Mansour, 2016). Occupational exposures to high levels of pollutant mixtures containing PAHs have resulted in symptoms such as eye irritation, nausea, vomiting, diarrhea and confusion (Rengarajan et al., 2015). However, it is not known which components of the mixture were responsible for these effects and other compounds commonly found with PAHs may be the cause of these symptoms. EPA has classified some of these PAH as carcinogens when respirated chronically. These include benzo(a)pyrene, benzo(b)fluoranthene, benzo(k)fluoranthene (EPA, 2000). The OSHA permissible exposure levels for PAHs in the workplace are 0.2 mg/m^3 for 8-hour time-weighted average.

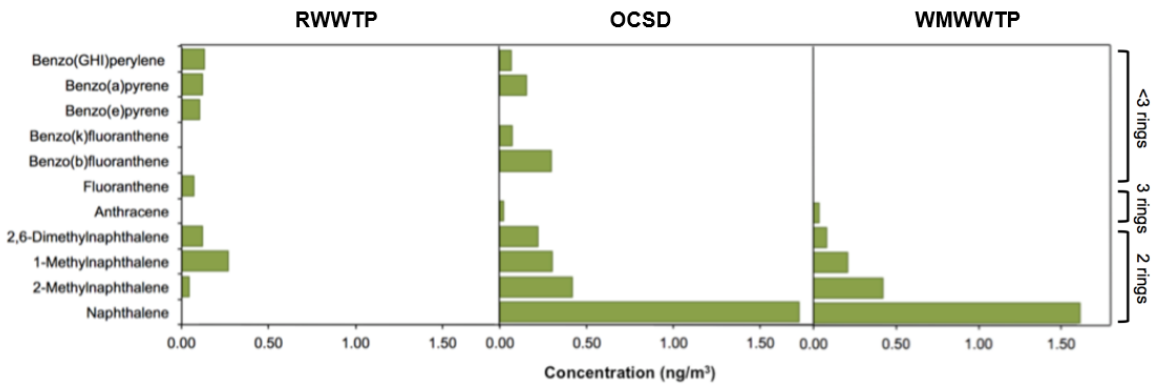

Figure A.3.2: PAH concentrations in filter samples collected through the aerosolization of the sludge of the three WWTP: Redlands Wastewater Treatment Plant (filter RL1), Western Municipal Wastewater Treatment Plant (filter WL1) and Orange County Sanitation District (filter OL1).

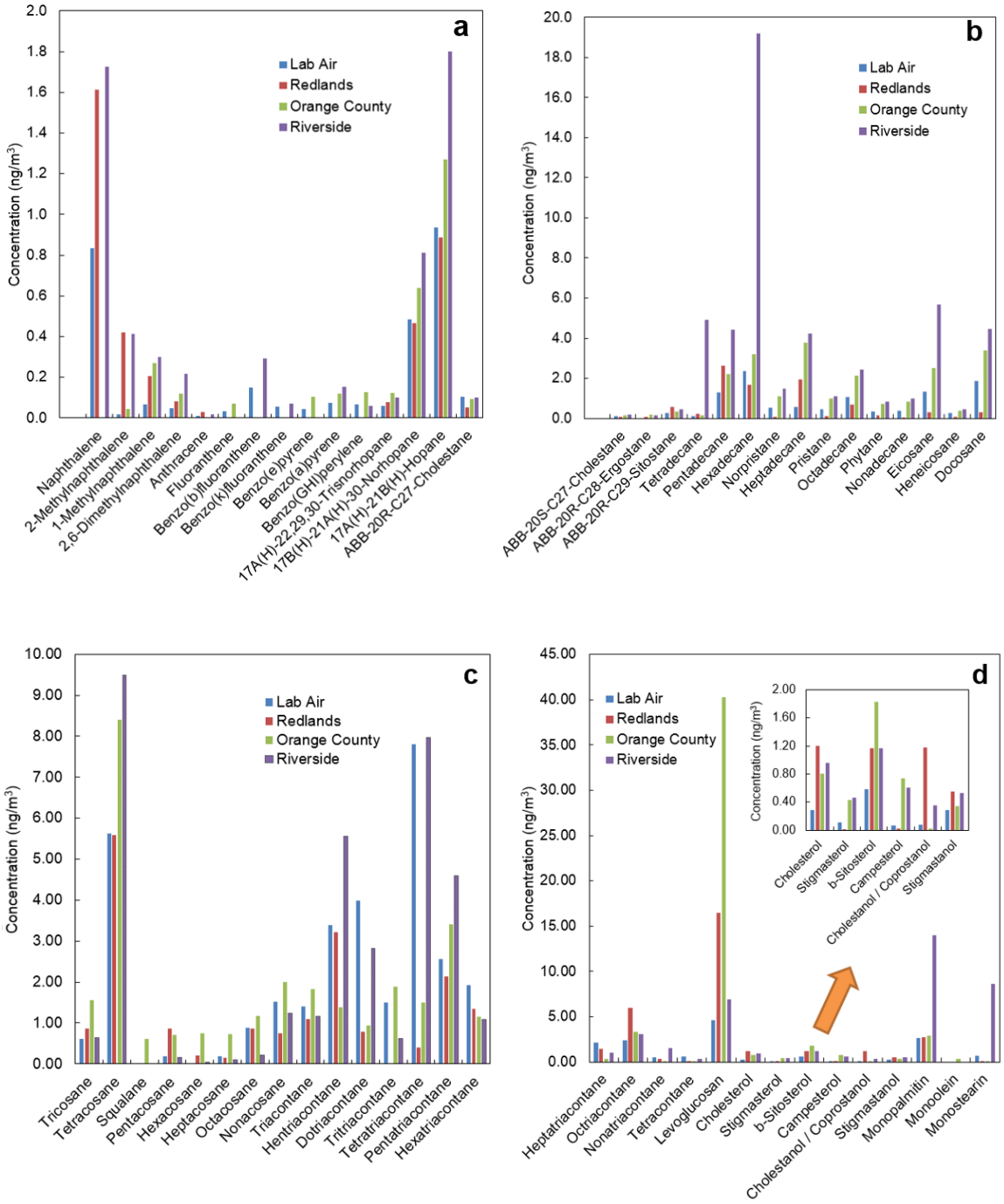
a
Lab Air
Redlands
Orange County
Riverside
Concentration (ng/m3)
Naphthalene
2-Methylnaphthalene
1-Methylnaphthalene
2,6-Dimethylnaphthalene
Anthracene
Fluoranthene
Benzo(b)fluoranthene
Benzo(k)fluoranthene
Benzo(e)pyrene
Benzo(a)pyrene
Benzo(GHI)perylene
17A(H)-22,29,30-Trisnorhopane
17B(H)-21A(H)-30-Norhopane
17A(H)-21B(H)-30-Hopane
ABB-20R-C27-Cholestane
b
Lab Air
Redlands
Orange County
Riverside
Concentration (ng/m3)
ABB-20S-C27-Cholestane
ABB-20R-C28-Ergostane
ABB-20R-C29-Sitostane
Tetradecane
Pentadecane
Hexadecane
Norpristane
Heptadecane
Pristane
Octadecane
Phytane
Nonadecane
Eicosane
Heneicosane
Docosane
c
Lab Air
Redlands
Orange County
Riverside
Concentration (ng/m3)
Tricosane
Tetracosane
Squalane
Pentacosane
Hexacosane
Heptacosane
Octacosane
Nonacosane
Triacontane
Hentriacontane
Dotriacontane
Tritriacontane
Tetratriacontane
Pentatriacontane
Hexatriacontane
d
Lab Air
Redlands
Orange County
Riverside
Concentration (ng/m3)
Cholesterol
Stigmasterol
b-Sitosterol
Campesterol
Cholestanol / Coprostanol
Stigmastanol
Heptatriacontane
Octriacontane
Nonatriacontane
Tetracontane
Levoglucosan
Cholesterol
Stigmasterol
b-Sitosterol
Campesterol
Cholestanol / Coprostanol
Stigmastanol
Monopalmitin
Monoolein
Monostearin

Figure A3.3: Complete chemical speciation data of laboratory filter samples. Lab air is shown with blue columns, RWWTP (RL1) concentrations are displayed with red columns, OCSD (OL1) samples are represented with green columns and WMWWTP (WL1) are marked with blue. Fecal sterols are emphasized in figure d to clarify.

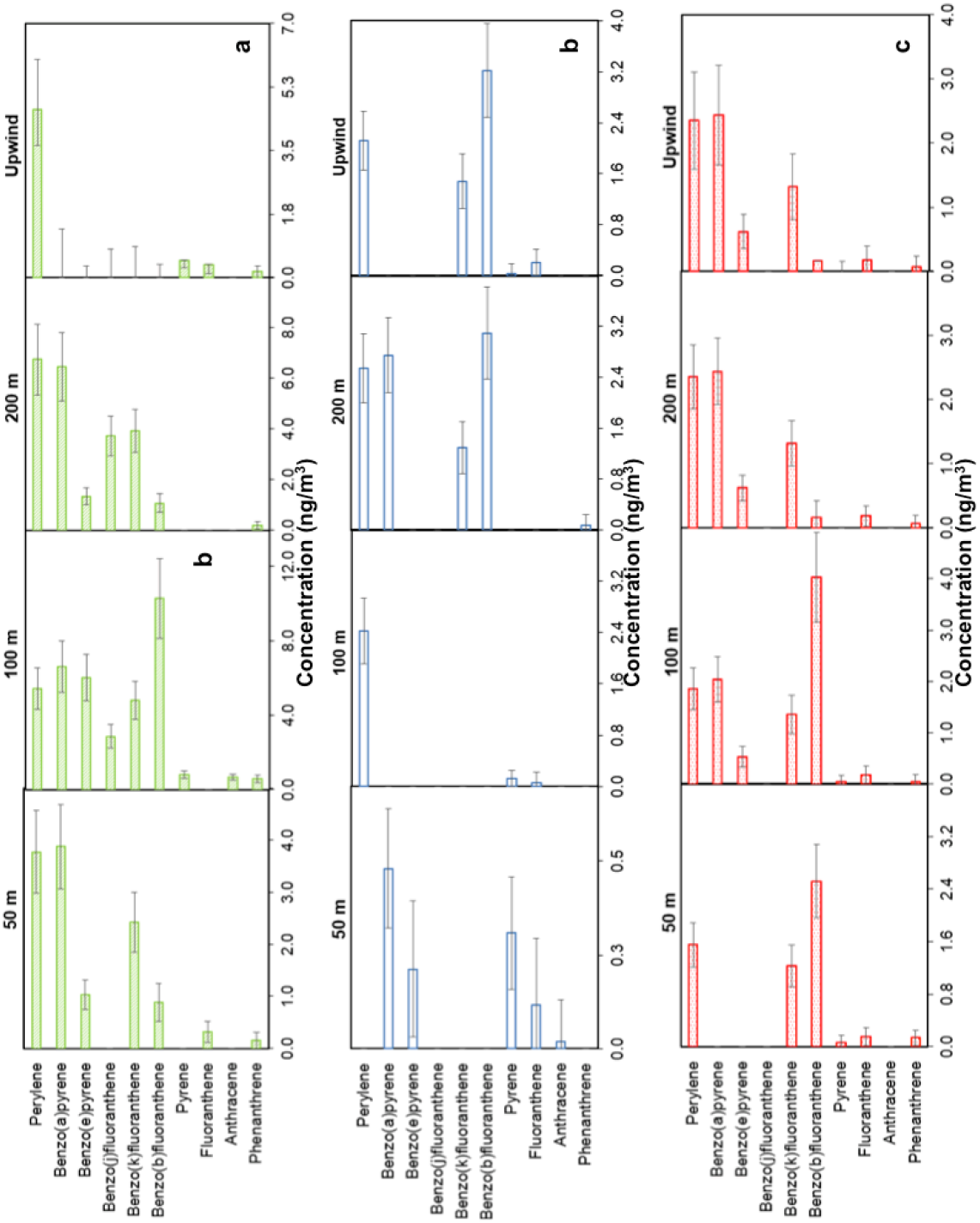
Upwind
200 m
100 m
50 m
a
b
c
Concentration (ng/m3)
Perylene
Benzo(a)pyrene
Benzo(e)pyrene
Benzo(j)fluoranthene
Benzo(k)fluoranthene
Benzo(b)fluoranthene
Pyrene
Fluoranthene
Anthracene
Phenanthrene

Figure A3.4: PAH concentrations at a) RWWTP b) WMWWP and c) OCSD collected 50 meters downwind (RF1, WF1 and OF1), 100 meters downwind (RF2, WF2 and OF2) and 200 meters downwind (RF3, WF3 and OF3). The upwind concentrations are also included as a reference (RF4, WF4 and OF4).

3.7 References

Abdel-Shafy, Hussein I., and Mona S. M. Mansour. "A Review on Polycyclic Aromatic Hydrocarbons: Source, Environmental Impact, Effect on Human Health and Remediation." *Egyptian Journal of Petroleum* 25.1 (2016/3): 107–123. Print.

Al-Naiema, Ibrahim et al. "Impacts of Co-Firing Biomass on Emissions of Particulate Matter to the Atmosphere." *Fuel* 162 (2015): 111–120. Print.

Beck, Melanie, and Michael Radke. "Determination of Sterols, Estrogens and Inorganic Ions in Waste Water and Size-Segregated Aerosol Particles Emitted from Waste Water Treatment." *Chemosphere* 64.7 (2006): 1134–1140. Print.

Becking, G. C., and B. H. Chen. "International Programme on Chemical Safety (IPCS) Environmental Health Criteria on Boron Human Health Risk Assessment." *Biological trace element research* 66.1-3 (1998): 439–452. Print.

Blanc, Paul D. et al. "Impact of the Home Indoor Environment on Adult Asthma and Rhinitis." *Journal of occupational and environmental medicine / American College of Occupational and Environmental Medicine* 47.4 (2005): 362–372. Print.

Bradford, M. M. "A Rapid and Sensitive Method for the Quantitation of Microgram Quantities of Protein Utilizing the Principle of Protein-Dye Binding." *Analytical biochemistry* 72 (1976): 248–254. Print.

Carducci, A., S. Arrighi, and A. Ruschi. "Detection of Coliphages and Enteroviruses in Sewage and Aerosol from an Activated Sludge Wastewater Treatment Plant." *Letters in applied microbiology* 21.3 (1995): 207–209. Print.

Chylek, Petr, and J. Wong. "Effect of Absorbing Aerosols on Global Radiation Budget." *Geophysical research letters* 22.8 (1995): 929–931. Print.

Clark, C. Scott. "Potential and Actual Biological Related Health Risks of Wastewater Industry Employment." *Journal - Water Pollution Control Federation* 59.12 (1987): 999–1008. Print.

Davies, Clive et al. "USEPA's Infrastructure Needs Survey." *Journal - American Water Works Association* 89.12 (1997): 30. Print.

de Jong, Ariënne, Jogchum Plat, and Ronald P. Mensink. “Metabolic Effects of Plant Sterols and Stanols (Review).” *The Journal of nutritional biochemistry* 14.7 (2003): 362–369. Print.

Demel, R. A., and B. De Kruyff. “The Function of Sterols in Membranes.” *Biochimica et biophysica acta* 457.2 (1976): 109–132. Print.

Douwes, Jeroen et al. “Fungal Extracellular Polysaccharides, β (1→ 3)-Glucans and Culturable Fungi in Repeated Sampling of House Dust.” *Indoor air* 11.3 (2001): 171–178. Print.

EPA, U. S., and OAR. “Air Quality Dispersion Modeling - Preferred and Recommended Models.” (2016): n. pag. Web. 10 May 2017.

Epstein, Eliot. "Endotoxins." US Composting Concil (2008): n. pag. Web.

Fannin, K. F., S. C. Vana, and W. Jakubowski. “Effect of an Activated Sludge Wastewater Treatment Plant on Ambient Air Densities of Aerosols Containing Bacteria and Viruses.” *Applied and environmental microbiology* 49.5 (1985): 1191–1196. Print.

Heng, B. H. et al. “Prevalence of Hepatitis A Virus Infection among Sewage Workers in Singapore.” *Epidemiology and infection* 113.1 (1994): 121–128. Print.

Khuder, S. A. et al. “Prevalence of Infectious Diseases and Associated Symptoms in Wastewater Treatment Workers.” *American journal of industrial medicine* 33.6 (1998): 571–577. Print.

Kumar, Awkash et al. “Assessment of Impact of Unaccounted Emission on Ambient Concentration Using DEHM and AERMOD in Combination with WRF.” *Atmospheric environment* 142 (2016): 406–413. Print.

Law, M. R. “Plant Sterol and Stanol Margarines and Health.” *The Western journal of medicine* 173.1 (2000): 43–47. Print.

Lebrero, Raquel et al. “Odor Assessment and Management in Wastewater Treatment Plants: A Review.” *Critical reviews in environmental science and technology* 41.10 (2011): 915–950. Print.

Masclaux, Frédéric G. et al. “Assessment of Airborne Virus Contamination in Wastewater Treatment Plants.” *Environmental research* 133 (2014): 260–265. Print.

Melbostad, Erik et al. "Exposure to Bacterial Aerosols and Work-Related Symptoms in Sewage Workers." *American journal of industrial medicine* 25.1 (1994): 59–63. Print.

Metcalf, and Inc Eddy. "Wastewater Engineering: Treatment and Reuse." 2003: n. pag. Print.

NRC (National Research Council) et al. *New Strategies for America's Watersheds*. National Academies Press, 1999. Print.

OCSD. "Facilities." *General Information*. N.p., 2016. Web.

Piqueras, P. et al. "Real-Time Ultrafine Aerosol Measurements from Wastewater Treatment Facilities." *Environmental science & technology* 50.20 (2016): 11137–11144. Print.

Rathnayake, Chathurika M. et al. "Influence of Rain on the Abundance of Bioaerosols in Fine and Coarse Particles." *Atmospheric Chemistry and Physics* 17.3 (2017): 2459–2475. Print.

Rylander, R. "Indoor Air-Related Effects and Airborne (1 --> 3)-Beta-D-Glucan." *Environmental health perspectives* 107 Suppl 3 (1999): 501–503. Print.

Smit, Lidwien A. M., Suzanne Spaan, and Dick Heederik. "Endotoxin Exposure and Symptoms in Wastewater Treatment Workers." *American journal of industrial medicine* 48.1 (2005): 30–39. Print.

Stone, Elizabeth A., Tony T. Nguyen, et al. "Assessment of Biogenic Secondary Organic Aerosol in the Himalayas." *Environmental chemistry* 9.3 (2012): 263–272. Print.

Stone, Elizabeth A., David C. Snyder, et al. "Source Apportionment of Fine Organic Aerosol in Mexico City during the MILAGRO Experiment 2006." *Atmospheric Chemistry and Physics* 8.5 (2008): 1249–1259. Print.

Thorn, Jörgen, and Lena Beijer. "Work-Related Symptoms and Inflammation among Sewage Plant Operatives." *International journal of occupational and environmental health* 10.1 (2004): 84–89. Print.

Thorn, J., and E. Kerekes. "Health Effects among Employees in Sewage Treatment Plants: A Literature Survey." *American journal of industrial medicine* 40.2 (2001): 170–179. Print.

Thorne, Peter S. et al. “Evaluation of the Limulus Amebocyte Lysate and Recombinant Factor C Assays for Assessment of Airborne Endotoxin.” *Applied and environmental microbiology* 76.15 (2010): 4988–4995. Print.

Trivedi, Bhavini, Cherry Valerio, and Jay E. Slater. “Endotoxin Content of Standardized Allergen Vaccines.” *The Journal of allergy and clinical immunology* 111.4 (2003): 777–783. Print.

Upadhyay, Nabin et al. “Characterization of Aerosol Emissions from Wastewater Aeration Basins.” *Journal of the Air & Waste Management Association* 63.1 (2013): 20–26. Print.

US EPA, OAR, Office of Air Quality Planning and Standards. “Preferred/Recommended Models | TTN - Support Center for Regulatory Atmospheric Modeling | US EPA.” N.p., n.d. Web. 25 Aug. 2016.

Walls, Kelvin. “Health Implications of Increasing Reuse of Wastewater as an Adaption to Climate Change.” *journal of Environmental Engineering and Ecological Science* 4.1 (2015): 2. Print.

Westman, Walter E. “Factors Influencing the Distribution of Species of Californian Coastal Sage Scrub.” *Ecology* 62.2 (1981): 439–455. Print.

Xu, X. et al. “Effect of the Structure of Natural Sterols and Sphingolipids on the Formation of Ordered Sphingolipid/sterol Domains (rafts) Comparison of Cholesterol to Plant, Fungal, and ….” *Journal of Biological* (2001): n. pag. Web.

Yuan, Xiangyang et al. “Assessing the Effects of Ambient Ozone in China on Snap Bean Genotypes by Using Ethylenediurea (EDU).” *Environmental pollution* 205 (2015): 199–208. Print.

"HCN: Endotoxins" Health-based Recommended Occupational Exposure Limit (n.d.): n. pag. Minister of Social Affairs and Employment. No. 2010/04OSH, The Hague, 15 July 2010. Web.

“Polycyclic Organic Matter (POM) - US EPA.” n. pag. Web.

"RWWTP Wastewater Treatment." City of Redlands. N.p., n.d. Web. 15 Sept. 2016.

SAWPA. Santa Ana Watershed Project Authority, 7 June 2015. Web. 10 Jan. 2017.

“SCAQMD Modeling Guidance for AERMOD.” N.p., n.d. Web. 10 May 2017.

"WRCWTP and WWRF." Wastewater in California. Western Municipal Water District, n.d. Web. 10 Oct. 2016.

"Water Reuse Case Studies." Urban Water Reuse Handbook (2015): 915-16. Redlands Wastewater Treatment. CH2MHill. Web.

Chapter 4: A Method Development for Condensational Growth Quantification of Airborne Viral Pathogens from Wastewater Treatment Plants

4.1 Abstract

Supersaturated conditions in the respiratory tract can cause inhaled aerosols to grow in size (hygroscopic growth), which significantly increase particle deposition efficiency. Particle deposition in the respiratory tract increases the probability of infection and thus the transmission of disease if viruses are present within the aerosol. To further explore this process, the size and hygroscopicity of MS2 bacteriophage, a commonly used model for human viruses, and viral propagation reagents (agar, phosphate-buffered saline (PBS) solution and tryptic soy broth (TSB) were investigated. Results suggest that the most hygroscopic element in the MS2 stock solution is PBS (κ = 1.46, very hygroscopic), followed by TSB (κ = 0.42, medium hygroscopicity) and the lastly agar (κ = 0.06, non-hygroscopic but wettable). The hygroscopicity of the mixed MS2 stock was determined at κ = 0.84, which suggests that viral particles may form droplets in supersaturated environments, such as the upper airways (104.5 % humidity) and lungs (95.5 % humidity). The diameter where 50% of the particle population active (Dp_{50}) for upper airways saturations was calculated at 24.55 nm for the MS2 stock, 20.24 nm for PBS, 31.97 nm for TSB and 54.26 nm for agar. Dp_{50} in the lungs resulted in 25.39 nm for the heterogeneous MS2 stock solution, 20.88 nm for PBS, 33.02 nm for TSB and 56.71 nm for agar.

To further understand the role of hygroscopicity in viral deposition, a known urban source of airborne pathogens was considered: Particles from wastewater treatment plants (WWTP) were aerosolized through conventional aeration of sludge in a laboratory bioreactor. Cholesterol, a common sterol found in WWTP, was also explored through atomization. WWTP aerosol constituents ranged from medium to high hygroscopicity (κ = 0.12 for atomized cholesterol solution and κ = 0.21 aerosolized heterogeneous WWTP sludge). These values indicate that WWTP aerosols may undergo condensational growth by water vapor under supersaturated conditions (Dp_{50} = 39 nm at 1.18 % SS, Dp_{50} = 53 nm at 0.78 % SS) and may cause disease due to wet particle deposition of the viruses within the particle.

4.2 Introduction

Particulate matter causes adverse lung diseases and other health effects when deposited in the respiratory track during inhalation (Kampa et al., 2008). Particularly, inhalation of microbes such as viruses and bacteria contribute significantly to pulmonary infections (Bosch et al., 2013; Kreyling et al., 2006). Particle size is the single most important determinant for deposition in the lungs (Lippmann et al., 1980; Heyder et al., 1986). Previous literature shows that infection occurs when bacteria and virus containing particles are inhaled in the submicron size (<1 μm) (Edwards et al , 2004; Fabian et al. 2008; Fabian et al. 2008; Chen et al 2009; Cowling et al., 2013) . The airborne transport of fine particles in the environment is effective (Oberdorster et al., 2005; Fabian et al 2008; Halloran et al 2012; Cowling et al., 2013). However, the deposition of ultrafine

particles (<100 nm) in the respiratory track has a very low probability and low deposition efficiencies. Most of the particles inhaled in the ultrafine range are exhaled (Hinds, 1991; Oberdorster et al., 2005; Tellier, 2009; Hoppentocht et al., 2014; Jinxiang et al., 2015). Nevertheless, this may be the case if particles increase in size inside the respiratory track through condensational (hygroscopic) growth.

4.2.1 The role of hygroscopicity on lung deposition

Ambient aerosols may act as cloud condensation nuclei (CCN) upon which liquid droplets can form in the atmosphere. This process can also take place in supersaturated environments within the body; when airborne particles enter the respiratory tract, condensational particle growth may occur (Tang et al., 2012). This mechanism, also called hygroscopic growth or cloud condensation nuclei (CCN) activity, is determined by the uptake of water vapor of the air (humidity) in the respiratory tract by hygroscopic components within the particles. Hygroscopicity, the measurement how the particle's ability to absorb the water as a function of humidity, is expressed as a single parameter κ (Petters and Kreidenweis, 2007; Engelhart et al 2012). It is largely influenced by the size and composition of the particles (Petters and Kreidenweis, 2007). In general, aerosols that contain inorganic salts leading to a more hygroscopic particle and organic materials leading to a less hygroscopic particle (Kanji et al., 2017). A particle that act as CCN requires a minimum water vapor supersaturation, or critical supersaturation, S_c, to convert into a cloud droplet. When exposed to supersaturations larger than S_c, particles must grow to a critical diameter, $D_{pc,}$ before reaching a mode of unstable (unconstrained)

growth, otherwise known as activation. Upon activation, water vapor spontaneously condenses onto the particle, which quickly grows to a large size limited only by diffusional kinetics and the availability of water vapor (Roberts and Nenes, 2005). The more oversaturated the air is, the higher probability of hygroscopic growth of the particles (Grasmeijer et al., 2016; Li and Hopke, 1993; Longest and Hindle, 2011; Martonen et al., 1985; Robinson and Yu, 1998; Vu et al., 2015). Relative humidity (RH) in the lung is estimated at 99.5% (Londahl et al. 2009) and more recent work has calculated instantaneous values in the supersaturated range in the upper airways (up to 104.5% RH) (Longest and Xi 2008; Varghese and Gangamma 2009; Longest et al. 2010). These humid environments may provide enough water vapor to particles and this may cause particles as small as a virus to activate.

4.2.2 Wastewater treatment plants and their linkage to disease

Emissions from wastewater treatment plants (WWTP) have been associated with health risks, however there are still no guidelines or laws regarding their regulation (Walls et al 2015). Epidemiological studies and filter data suggest that airborne emissions from WWTPs exist and may impact human health (Sorber et al., 1980; Clark, 1987; Heng et al., 1994; Chylek et al., 1995; Khuder et al., 1998; Smit et al., 2005; Beck at al., 2006; Radke et al. 2006; Masclaux et al., 2014; Yuan et al., 2015). Nevertheless, the inhalation route, transport and disease mechanisms of these particulates remain elusive.

Particulates emitted from WWTP are a mixture of solid sludge constituents and liquid water (Upadhyay et al 2013, Piqueras et al., in preparation). PM_{10} and $PM_{2.5}$ filter data has also confirmed the presence of airborne toxic compounds, bacteria, fungi, endotoxins, and viruses near WWTP (Carducci et al., 1995; Korzeniewka et al., 2011; Uhrbrand et al., 2011; Jebri et al., 2012; Malakootian et al., 2013; Masclaux et al., 2014; Li et al., 2015; Niazi et al., 2015). Past studies show that sludge bubbling from aerated basins are one of the main source of particulate emission from the facilities (Piqueras et al 2016); this process is performed to remove the biodegradable organics in the influent. Aerosols emitted from aerated basins have been shown to be in the ultrafine size range (Piqueras et al 2016). $PM_{0.1}$ filter data also shows that potential pathogens (i.e. viruses) and toxins come directly from the WWTP sludge mixture (Piqueras et al., in preparation). In addition, viral particles found in wastewater are of similar size, 20−300 nm (Carducci et al, 1995). However, particle composition effect on hygroscopicity and droplet growth in the lungs remains unknown. Understanding whether these small viral particles will grow large enough to deposit in the lungs is critical to understanding their probability of infection and their level of virulence.

4.2.3 Particle droplet growth analysis

Active viruses may readily form droplets. To verify this, the size distributions and the hygroscopicity of atomized MS2 propagation components were investigated. The κ-Köhler theory was used to measure CCN activity. This method describes the relationship between particle dry diameter and cloud condensation nuclei (CCN) activity

using the single hygroscopicity parameter κ (Petters and Kreidenweis, 2007). Composition-dependent variables were investigated experimentally using a continuous flow streamwise thermal gradient Cloud Condensation Nuclei counter (DMT CCN 100) and a Scanning Mobility Particle Sizer (SMPS, TSI classifier 3080 with a TSI CPC 3772 operated in tandem) in scanning voltage mode. The residence time at the CCN counter was 20 seconds at 0.5 lpm.

Particle size distributions were measured with the SMPS alone. The SMPS is a common tool used for real-time particle measurement and its operation and theoretical framework has been described in detail by Wang et al, 1989. The instrument created a monodisperse flow from the aerosol sample, which later entered the CCN chamber. The electrical mobility particle size ranged from 7 nm to 320 nm over 135 seconds. The sheath to aerosol ratio was maintained at 10 to 1 and particles were assumed to be spherical. Neither the SMPS nor the CCN concentrations were corrected for multiple charge effects in the beta version of SMCA used in this analysis. The relative uncertainty from neglecting the multiple charges is approximately 3–4 % in internally mixed particles (Rose et al., 2008; Moore et al., 2010).

The Scanning Mobility CCN Analysis, a fast method for measuring size-resolved CCN using the two instruments mentioned above, was used to determine the activation diameters (SMCA; Moore et al., 2010). In the analysis, the activated fraction versus dry mobility diameter was fit to determine the activation diameter. The activation diameter, given a critical supersaturation, was used to calculate κ. The CCN counter supersaturation was calibrated using size-classified ammonium sulfate aerosol following the procedure of

Rose et al., 2008 and Engelhart et al., 2008. Köhler calculations for the effective supersaturation assumed the surface tension and density of water and a temperature equal to the average of the top and bottom temperatures of the column in the CCN counter (Tang et al 2012).

Particles were created from liquid solutions using a custom-built atomizer as shown in figure 4-1. The concentrations of the solutions were controlled to ensure that generated particles had similar normalized size distributions. Particles were dried before entering the SMPS-CCN set up by using a heating coil and a diffusion dryer, a column full of silica fragments.

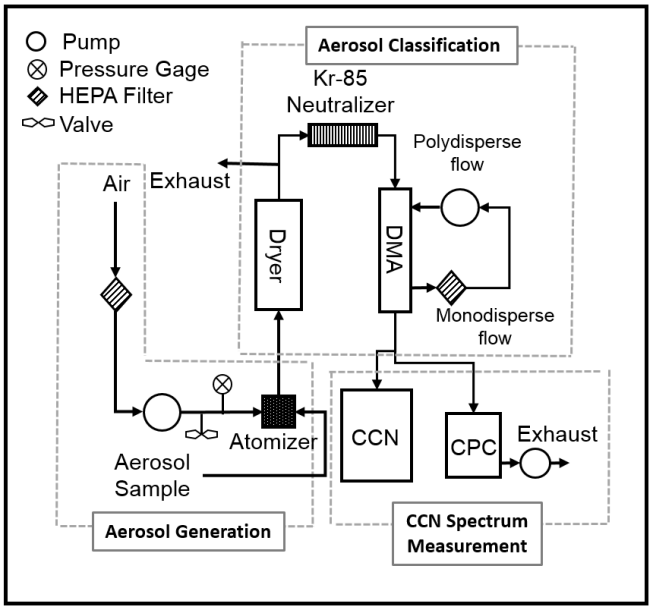

Figure 4-1: Atomizer set up; aerosol liquid sample is atomized by using clean air. Atomized particles pass a silica dryer before entering a differential mobility analyzer (DMA) and a cloud condensation nuclei counter (CCNC) and a condensation particle counter (CPC).

4.2.4 Bacteriophage propagation

Escherichia coli/MS2 was used as the host-pathogen model system as MS2 is easy to work with, harmless to humans, but shares many features with eukaryotic viruses that can be found in WWTPs (Benjamin et al., 1994; Jain et al., 2009). In addition, the bacteriophage is also used as a quantitative marker for the efficiency of water treatment plants and filtration devices (Jolis et al., 1999 and Oppenheimer et al., 1997). MS2 is a 275 Å RNA virus that infects male *Escherichia coli* (Stockley et al., 1993) and its size is in the ultrafine range (23-28 nm) (Kuzmanovic et al., 2003). The bacteriophage has a

simple composition, it is easy to grow and it is also a popular model organism for a number of macromolecular processes including viral replication, translation, infection, and assembly (Peabody and Al-Bitar, 2001; Stockley et al., 1994). Futhermore, the genome-scale metabolic model of *E. coli* is the most comprehensive model at this time (Jain et al., 2009).

In order to analyze MS2's hygroscopicity, a frozen virus stock, obtained from UC Riverside's environmental microbiology laboratory (312 Science Laboratories I), was used for propagation. This stock was a product of a master stock from the American Type Culture Collection (ATCC 15597-B1). Viral strains were kept frozen on dry ice in plastic cryopreservation vials. It was kept at -70°C and -80°C. The virus stock contained 1 mL of solution and it was propagated with its associated agents following the EPA method 1601; male specific (F+) and somatic Coliphage in water by a two-step enrichment procedure (EPA 2001). The stock solution contains virus particles, PBS broth (Peptic digest of animal, NaCl, KCl, Na_2HPO_4, KH_2PO_4 and water), small traces traces (of TSB tryptic soy broth (papaic digest of soybean, dextrose, sodium chloride, pancreatic digest of casein and dipotassium phosphate), agarose and small traces $MgCl_2$.

The MS2 phage was propagated by preparing plates with the soft-agar and host overlay procedure (shown in figure 4-2): To recover the phage, an actively growing broth culture the F_{amp} host strain from a frozen stock was developed through the overnight host and log phase host process (shown in figure 4-2a). Penicillin Streptomycin (amp/strep) antibiotics were introduced in the solution to ensure a single species of bacteria. During

this process, a hard layer of agar surface was overlaid with melted 0.5% agar (same medium, but more diluted) with one drop of the log host. This process is referred to as the double agar layer procedure (DAL, figure 4-2b). After 24 hours incubation, the soft agar was scraped off the surface of the agar plates, as shown in figure 4-3. The scrapped layer was centrifuged at about 1000 rpm for 25 minutes with chloroform to sediment the cellular debris and agar. The supernatant, the top liquid layer after the centrifugation that contains all the MS2 particles, was passed through a .22 um Millipore filter and the filtrate was stored at -80°C in cryotubes until it was needed for CCN experiments.

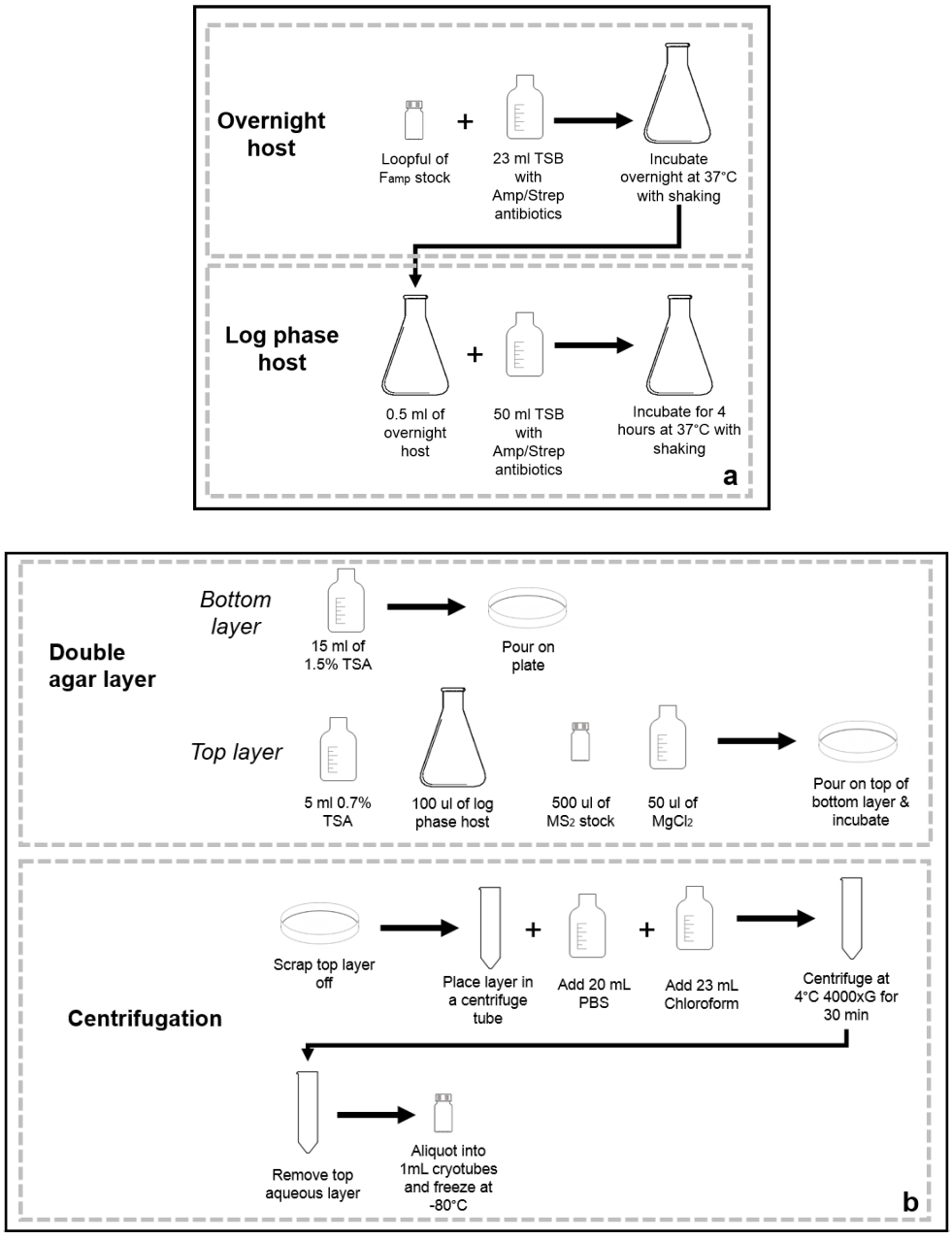

Figure 4-2: (a) F_{amp} overnight and log phase host procedure to create the host broth and (b) MS2 propagation through the double agar layer (DAL) procedure and MS2 supernatant isolation.

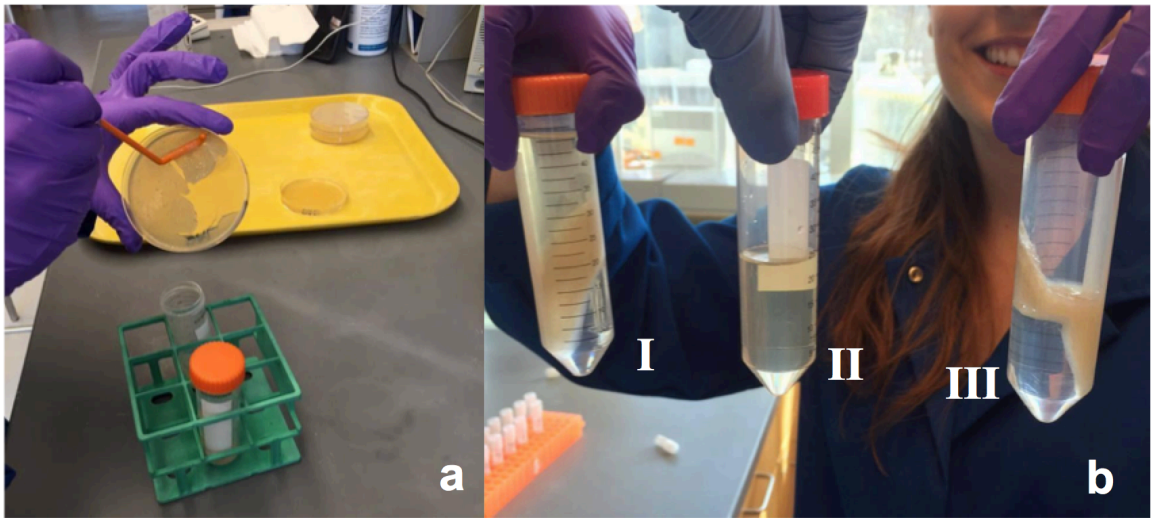

Figure 4-3: (a) Soft agar layer during scrape off and (b) component separation after centrifugation. I) Laboratory tube after centrifugation with the supernatant layer (including MS2 particles) at the top, the debris layer in the middle and the chloroform layer at the bottom. II) Isolated supernatant layer after pouring and III) remaining debris layer with chloroform at the bottom of the centrifuge tube.

The TSB solution that was utilized for this procedure had a total concentration of 30g/L and consisted of 17.0 g/L of tryptone, 3.0 g/L of soytone, 2.5 g/L of dextrose, 5.0 g/L of sodium chloride and 2.5 g/L of dipotassium phosphate. PBS solution (1x concentration) contained 8 g/L NaCl, 0.2 g/L KCl, 1.42 g/L Na_2HPO_4, and 0.24 g/L KH_2PO_4. Agar solution consisted of 0.1 g/L agarose. Since TSA equals to the combination of TSB and agar and its composition is mainly agar (99.6%), it was assumed that all TSB is negligible. The host bacteria volume percentage consisted of 0.3% of the entire solution while PBS encompassed 80% of the volume, glycerol enclosed an 18% and only 2% of the volume was made of TSB. Concentrated stock volume percentage

added up to 80.2% PBS, 1.7% MgCl and only 0.18% of the volume was dominated by MS2 particles.

MS2 was quantified in terms of infectious dose using the standard plaque-based assay method after propagation: The viral concentration in the supernatant stock was analyzed through serial dilution by passing 0.5 mL of the phage into a tube containing 4.5 mL of the broth medium. 100 μL of each dilution was spotted on the surface of the prepared plates agar plates and they were allowed to dry. Lysis was visible after overnight incubation and plaques were counted. The higher the dilution the fewer plaques (shown in figure 4-4). Total concentration was established in the first dilution fold that had no countable plaques (figure 4-4a); the virus concentration was determined at 10^{10} plaque forming units per milliliter (pfu/ml). It was assumed that 1 pfu equals to one virus particle, therefore the total concentration in the stock resulted in 10^{10} active viral particles per milliliter.

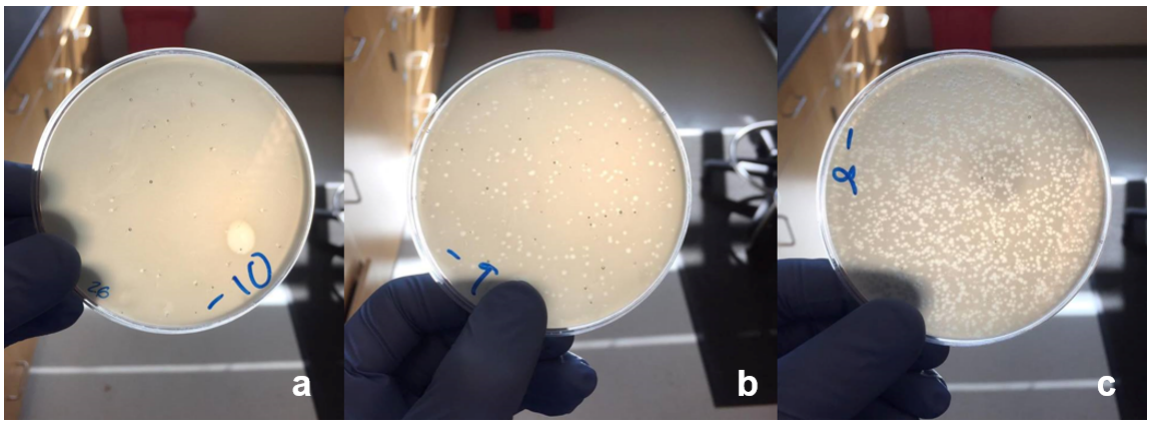

Figure 4-4: Plaque-based assay results showing viral concentration of the MS2 stock (a) with a ten-fold dilution, which indicated the concentration of the stock due to its lack of lysis (b) and a nine-fold dilution and (c) eight-fold dilution. Clear spots are representative of areas where the MS2 virus caused lysis.

4.3 MS2 CCN results and discussion

Particle hygroscopicity was quantitatively characterized by converting direct measurements of a selected particle diameter (D_p) and the critical supersaturation (S_c), where 50% of the particle population has activated) to κ (Kanji et al., 2017). The mobility-equivalent critical diameter is the intersection of a fit curve with the dashed line drawn at an activated fraction of 0.5 (Taylor et al., 2016). These curves are shown for MS2 propagation components and the heterogeneous stock solution in figure 4-5. Supersaturations (SS) were calibrated at 0.25% for 0.2% SS, 0.40% for 0.4% SS, 0.54% for 0.6%S S, 0.73% for 0.8% SS, 0.89% for 1% SS and 1.1776% for 1.2% SS and they were held constant during each run.

At 1.2% SS (shown in figure 4-5a) it was observed that agar had a Dp_{50} of 57.05 nm, PBS had a Dp_{50} of 20.2 nm, TSB showed a Dp_{50} of 29.38, and MS2 solution had a Dp_{50} of 22.97. For comparison, the critical diameter of ammonium sulfate is particle active at 0.5% supersaturation is 27.17 nm. As it was expected, there was an increase in Dp_{50} as supersaturations decrease. At 0.8% SS (shown in figure 4-5c) agar had a Dp_{50} of 74.6 nm while PBS had a Dp_{50} of 26.65 nm, TSB resulted in a a Dp_{50} of 49.95 nm, MS2 solution had a Dp_{50} of 31.73 and a Dp_{50} 35.04 nm was observed for ammonium sulfate. During the lowest SS run the experiment (0.4% SS in figure 4-5c) agar resulted in a Dp50 of 120.94 nm, PBS had a Dp50 of 39.7 nm, TSB showed a Dp50 of 64.56 nm, while MS2 solution displayed a Dp50 of 48.21 and ammonium sulfate resulted in a Dp_{50} 51.47 nm. The supersaturation levels in upper airways and the lungs are known to be between 1.2 SS and 0.8 SS, therefore Dp_{50} values between these two values are expected (see table 4-1).

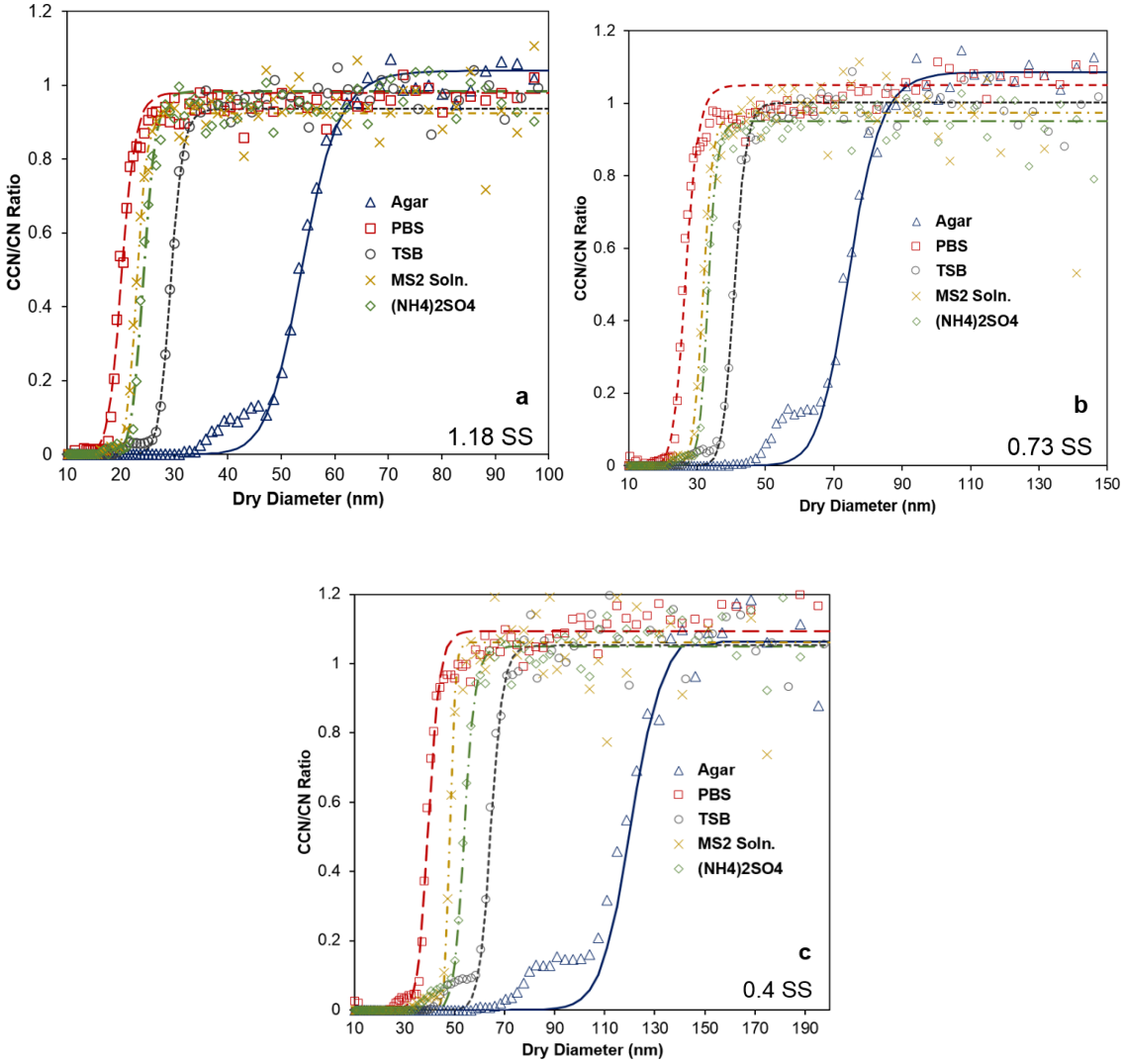
CCN/CN Ratio
Dry Diameter (nm)
Agar
PBS
TSB
MS2 Soln.
(NH4)2SO4
a
1.18 SS
b
0.73 SS
c
0.4 SS

Figure 4-5: CCN activation curves for atomized agar (blue triangles), PBS (red squares), TSB (grey circles) and MS2 solution mixture (yellow "x"). Activation curve from ammonium sulfate was used for comparison (green diamonds). Scanning supersaturation were held constant for each run at (a) 1.18% (b) 0.73% and (c) 0.4%. SS% are representative of the calibrated values. The sigmoid curves are fit to the data points of its corresponding color (solid blue line for agar, dashed grey line for TSB, dashed green line for ammonium sulfate, dashed yellow line for MS2 solution mixture and red dashed line for PSB). Because of its atmospheric relevance, ammonium sulfate was chosen as the inorganic salt for reference and calibration of the CCNC.

Figure 4-6a shows the average size distribution of the atomized MS2 solution measured with a SMPS. The average maximum peak value measured over 50 scans of 135 seconds was 26.9 nm. Virus stock components ranged in hygroscopicity: The agar (polysaccharide polymer) had a low experimental hygroscopicity (κ =0.06), which suggests that it has low hygroscopicity, but it is wettable since κ is above zero. PSB had the highest hygroscopicity value (κ = 1.46). This was expected as the main ingredient of PSB is salts. Values of the hygroscopicity parameter, κ values usually ranged between 0.5 and 1.4 for highly-CCN-active (Petters et al 2007). The heterogeneous virus stock were also in the hygroscopic range (κ = 0.84), however TSB was found to be less hygroscopic (κ = 0.42), confirming that MS2 viral particles are slightly high to high hygroscopicity (shown in figure 4-6b).

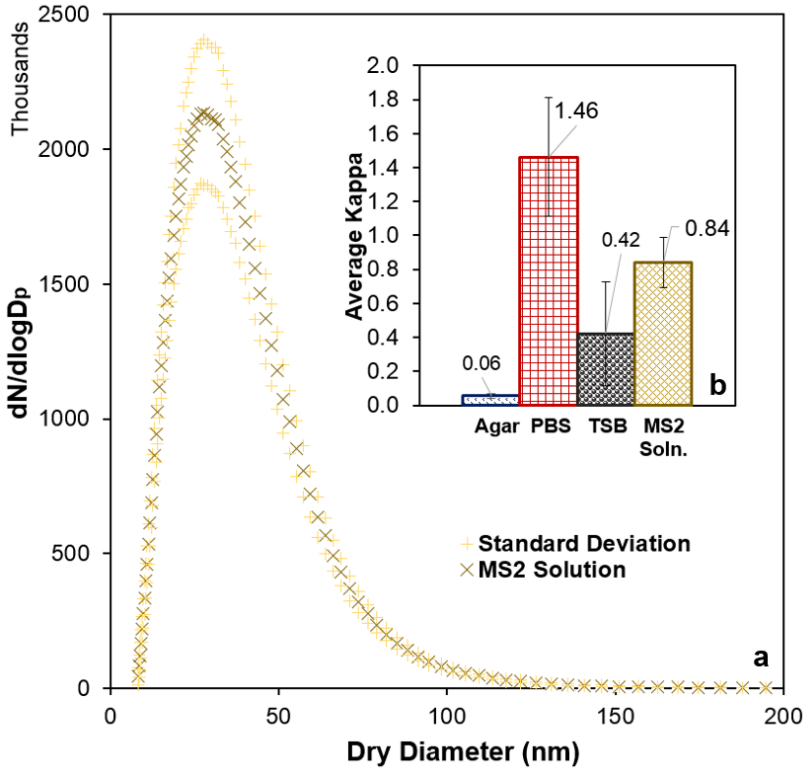

Figure 4-6: (a) Size distributions of MS2 solution (brown "x" signs) with its corresponding standard deviations (yellow "+"). Mode is located around 35 nm (b) Average κ values for agar (blue), PBS solution (red), TSB (grey) and the MS2 solution mixture (yellow).

Figure 4-7a was developed to visualize the changes of critical supersaturation as function of dry particle diameter for the investigated particle compositions from. The data outcomes are plotted as curves in log–log space following the Köhler slope of ammonium sulfate. The dry diameter was adopted from the measured Dp_{50} values at each experimental supersaturation. Particles of agar, PBS, TSB and MS2 could activate into cloud droplets in the investigated supersaturation range (figure 4-7b). The S_c for activation decreased with increasing dry particle diameter while droplet size increased with increasing S_c.

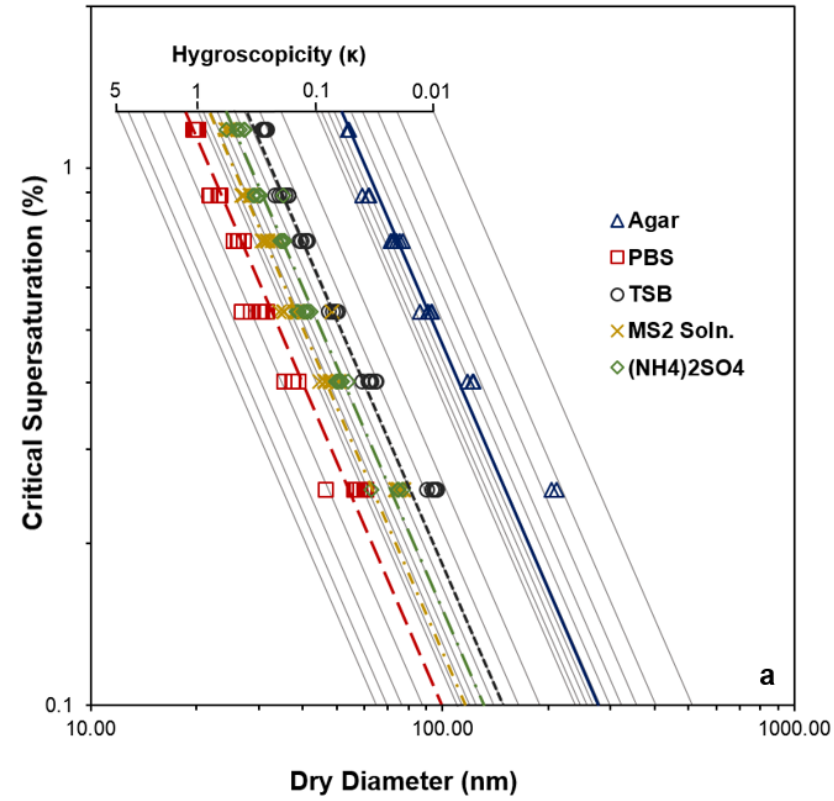
Hygroscopicity (κ)
5
1
0.1
0.01
Critical Supersaturation (%)
1
0.1
10.00
100.00
1000.00
Dry Diameter (nm)
Agar
PBS
TSB
MS2 Soln.
(NH4)2SO4
a

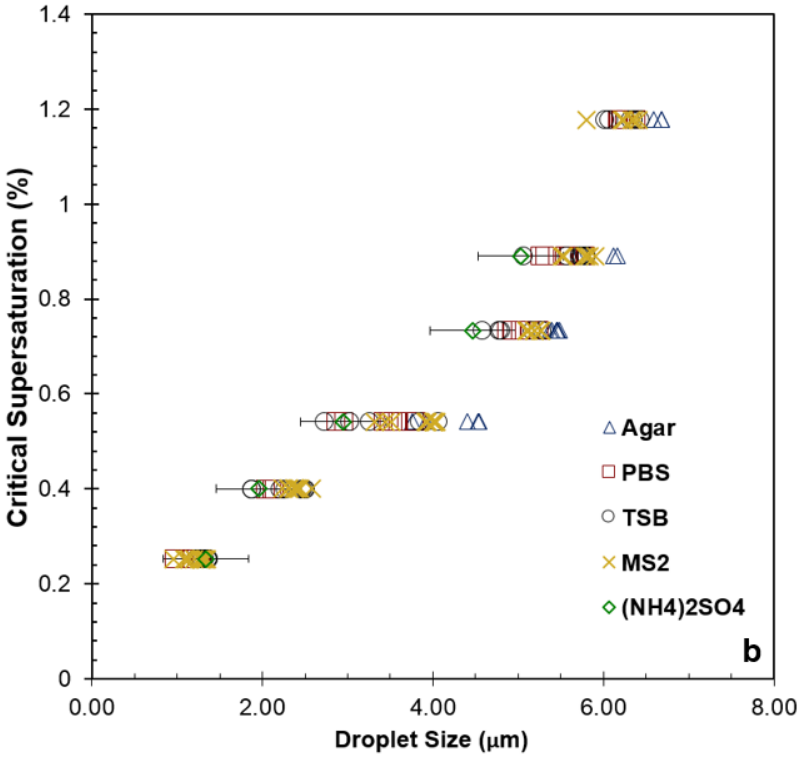
Critical Supersaturation (%)
1.4
1.2
1
0.8
0.6
0.4
0.2
0
0.00
2.00
4.00
6.00
8.00
Droplet Size (μm)
Agar
PBS
TSB
MS2
(NH4)2SO4
b

Figure 4-7: (a) κ curves representative of critical supersaturation, hygroscopicity and dry diameter as well as (b) Critical supersaturation as a function of droplet size. A positive relationship was observed between the two variables for all compositions; Agar (blue triangles), PBS solution (red squares), TSB (grey circles), and MS2 solution (yellow "x"). Ammonium sulfate solution is also graphed as a comparison.

Dp_{50} values were calculated for all components of the MS2 stock using the functions obtained from the linear fit of the data from figure 4-7b. These results are specified in table 4-1. Critical supersaturations in the upper airways (1.04% SS) and lungs (0.99% SS) were utilized for the calculations.

Table 4-1: Calculated critical Dp_{50} (nm) of MS2 propagation constituents in lungs (99.5% saturation) and upper airways (104.5% saturation).

	Lungs	Upper airways
Agar	56.41	54.26
PBS	20.88	20.24
TSB	33.02	31.97
MS2 Soln.	25.39	24.55
$(NH_4)_2SO_4$*	28.21	27.39

**Dp_50 of ammonium sulfate are shown for comparison.*

κ can be estimated assuming that the hygroscopicity of mixtures can be calculated by adding the κ values of the individual mixed compounds when multiplied by their volume percentage in the solution. Equation 4-1 was developed to theoretically determine the hygroscopicity of any viral particle if the κ value of the stock solution, PBS and agar and known. None of the other viral propagation constituents were taken into consideration since their volume is negligible (see section 2.1).

Equation 4-1: $$\boldsymbol{\kappa}_{\mathrm{viral}} = \frac{-(\kappa_{\mathrm{PBS}} * \mathrm{V}_{\mathrm{PBS}}\,\%) - (\kappa_{\mathrm{Agar}} * \mathrm{V}_{\mathrm{Agar}}\,\%) + \kappa_{\mathrm{stock}}}{\mathrm{V}_{\mathrm{viral}}\%}$$

When the experimentally obtained κ values for PBS and agar are utilized in the equation the modified version becomes:

Equation 4-2: $$\boldsymbol{\kappa}_{\mathrm{viral}} = \frac{-(1.46 * \mathrm{V}_{\mathrm{PBS}}\,\%) - (0.06 * \mathrm{V}_{\mathrm{Agar}}\,\%) + \kappa_{\mathrm{stock}}}{\mathrm{V}_{\mathrm{viral}}\%}$$

This equation was used to calculate the theoretical κ value of MS2 particles. However, the volume of viral particles within the stock is negligible when compared to the other components (see section 4.2.4). Therefore, it was concluded that non-viral particle components are the elements that play the most important role in particle hygroscopic growth. Since the laboratory MS2 stock has a chemical composition that is not representative how human viruses exist in nature, a common source of active viruses was explored in section 4.4. Future research should focus on increasing the volume of viruses within the stock to provide more robust estimates on isolated viral particle hygroscopicity.

4.4 Particle hygroscopicity from WWTP

In this study, size distributions and the hygroscopicity of particulates produced by the bubbling of well-mixed WWTP liquor and atomized sterol particulates were explored.

Aerosols from the bioreactor are likely of a heterogeneous complex mixture. However, sterols are currently used as WWTP particulate tracers to evaluate the significance of emissions of wastewater-born organic compounds during wastewater treatment by relating concentrations of these compounds in aerosol sample (Piqueras et al. in preparation, Radke et al 2003, 2005). Therefore cholesterol, the most abundant sterol found in particulate emissions from WWTPs, was examined through atomization. These two sources of aerosols were later compared to the heterogeneous MS2 stock and individual components (PSB, TSB and agar) as presented in section 4.2.

4.4.1 Bioreactor setup

Isolating WWTP aerosols in the field is a complex process as there is always a risk of ambient particle contamination. To avoid this, a laboratory case bioreactor was constructed. This bioreactor was operated on a sequencing-batch mode, a variation of the activated sludge process, using a two-day feeding cycle as explained in Piqueras et al 2016. A molasses based synthetic wastewater was used as the organic feed. The laboratory bioreactor setup consists of a 5-gal (18.9 L) cylinder with an air diffuser at the bottom of the reactor (figure 4-8). The air source for the diffuser was filtered with a HEPA filter (Pall Corporation HEPA Capsule). The diffuser produced "particle free" bubbles homogeneously throughout the entire volume of the mixed liquor. The mixed liquor sludge was obtained from the Orange County Sanitation District (OCSD) aerated basins in Fountain Valley, CA.

The bioreactor was kept in a controlled environment with constant temperature, pressure and humidity. Aerosols were measured within the enclosed headspace, 10 inches (25.4 cm) above the surface of the mixed liquor where bubble bursting occurred. Particle properties were measured with a 3 foot long (0.9 m), 1/8 inch (0.3 cm) diameter copper line split to the CPC 3776 and the SMPS. Particle size and total particle number measurements were taken in tandem. Particle losses in copper tubing were negligible at the flow rate which both the CPC and SMPS were operated (0.3 lpm to 1.5 lpm).

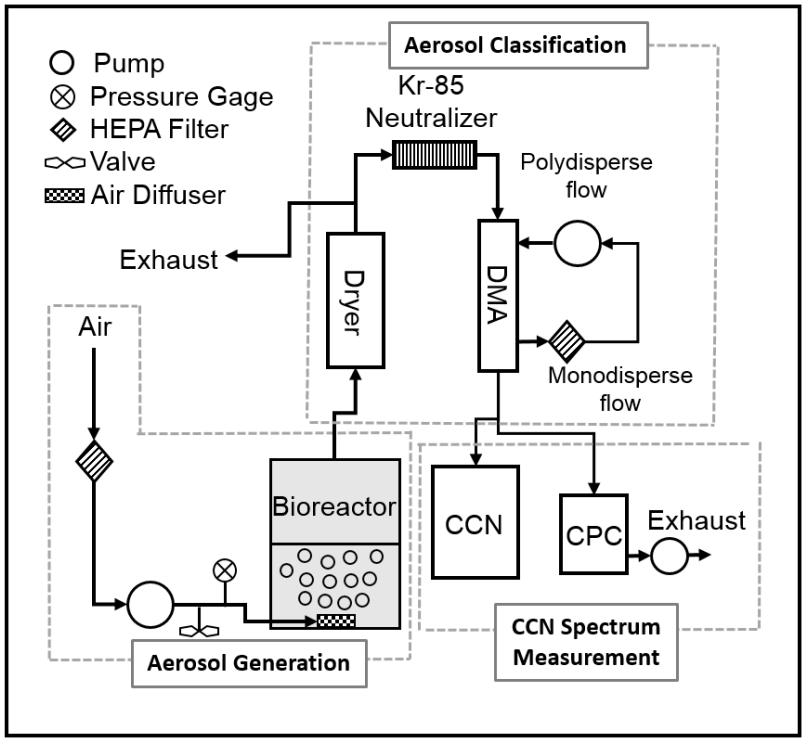

Figure 4-8: Bioreactor set up: Particles are sampled within the headspace of the 5 gallon bioreactor they were later introduced into an SMPS for size measurements and a CCNC for hygroscopicity measurements.

4.5 Bioreactor CCN results and discussion

To understand how WWTP emissions relate to MS2 particles, viral propagation constituents and bioreactor emissions were compared. Results show that bioreactor particles had a size mode of 48 nm, similar to that of cholesterol (45 m). Viral propagation ingredients had slightly smaller size modes (MS2 solution, 20nm; PSB, 28 nm; TSB, 32 nm) except agar, which had a larger size mode (62 nm). MS2 solution particles were measured to be in the lower size range <100 nm, which is an indication that most of the particles that were aerosolized were viral particles (around 28 nm) and the reagents in the solution did not play a big role in the particle size of the aerosolized particles from the virus stock.

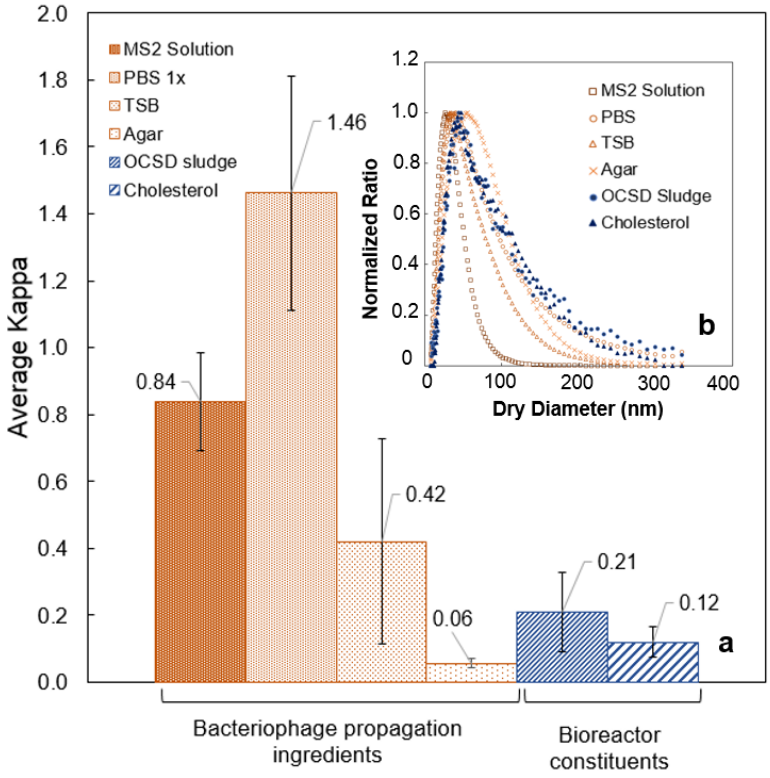

Figure 4-9: (a) κ values of MS2 propagation ingredients (orange columns), bioreactor particles (dotted blue column), atomized cholesterol (stripped blue column) and (b) size distributions of bioreactor particles, atomized cholesterol and MS2 propagation ingredients.

Data outcomes show that the sludge mixture had a size peak at 44.5 nm and was found to be slightly hygroscopic (κ = 0.21). This is the same hygroscopicity range as secondary organic aerosol (SOA) (Petters et al. 2007). Cholesterol had a peak at 47.8 nm and showed to be less hygroscopic with a κ value of 0.12. By comparison, the MS2 solution, κ of 0.84 with 0.15 standard deviation and a size peak of 26.9 nm, which

insinuates that the salts in the solution (PBS with a κ = 0.211.46 with a standard deviation of 0.35) had a large effect in the hygroscopicity. Maximum peak size for TSB was observed at 32.2 nm, PBS at 40 nm and agar with the largest value at 55.2 nm. At 1.18 % SS the sludge particles had a Dp_{50} of 39 nm, while at 0.78 % SS they had a Dp_{50} of 53 nm. The maximum Dp_{50} for WWTP particulate emissions (76 nm) was observed at 0.4% SS. Cholesterol resulted in higher Dp_{50} with an average difference of 10 nm. This may have occurred due to its lower hygroscopicity. Dp_{50} values for cholesterol ranged from 49 nm at 1.18 % SS to 67 nm at 0.78 % SS and 88 nm at 0.4% SS.

Hygroscopicity and particle size results shown in figure 4-9 suggests that aerosols emitted from WWTP are CCN active and could contribute to CCN formation under saturated and supersaturated environments. Although WWTP may be only one source of viruses in urban settings, the data from this study implies that particles from this source can uptake water in the lungs and upper airways. While these particles emitted from aerated basins are in a size range that would cause them to be fully exhaled, condensational growth in the respiratory track may lead to the intensive deposition of human viruses found within these particles and it may cause a higher probability of disease. It is therefore critical to understand the type of viruses that are being volatilized at WWTP and their composition for future hygroscopicity assessments. This evidence should also be taken into consideration when developing future regulations for WWTP emissions mitigation.

4.6 Acknowledgements

This research has been supported by the National Science Foundation Award (NSF) 1151893. Its contents are solely the responsibility of the grantee and do not necessarily represent the official views of the NSF. Furthermore, the NSF does not endorse the purchase of any commercial products or services mentioned in the publication. The authors would like to thank their colleagues Ashley Vizenor and Emmanuel Fofie for their technical contribution in the lab as well as Marylynn Yates for her willingness to collaborate on this project. They would also like to specifically thank the staff of Orange County Sanitation District for access to the facilities, their assistance and cooperation.

4.7 References

Beck, Melanie, and Michael Radke. "Determination of Sterols, Estrogens and Inorganic Ions in Waste Water and Size-Segregated Aerosol Particles Emitted from Waste Water Treatment." *Chemosphere* 64.7 (2006): 1134–1140. Print.

Benjamin W. Lykins, Jr, Wayne E. Koffskey, and Kathleen S. Patterson. "Alternative Disinfectants for Drinking Water Treatment." *Journal of Environmental Engineering* 120.4 (1994): 745–758. Print.

Bosch, Astrid A. T. M. et al. "Viral and Bacterial Interactions in the Upper Respiratory Tract." *PLoS pathogens* 9.1 (2013): e1003057. Print.

Carducci, A., S. Arrighi, and A. Ruschi. "Detection of Coliphages and Enteroviruses in Sewage and Aerosol from an Activated Sludge Wastewater Treatment Plant." *Letters in applied microbiology* 21.3 (1995): 207–209. Print.

Chen, Li-Mei et al. "In Vitro Evolution of H5N1 Avian Influenza Virus toward Human-Type Receptor Specificity." *Virology* 422.1 (2012): 105–113. Print.

Chylek, Petr, and J. Wong. "Effect of Absorbing Aerosols on Global Radiation Budget." *Geophysical research letters* 22.8 (1995): 929–931. Print.

Clark, C. Scott. "Potential and Actual Biological Related Health Risks of Wastewater Industry Employment." *Journal - Water Pollution Control Federation* 59.12 (1987): 999–1008. Print.

Cowling, Benjamin J. et al. "Aerosol Transmission Is an Important Mode of Influenza A Virus Spread." *Nature communications* 4 (2013): 1935. Print.

Edwards, David A. et al. "Inhaling to Mitigate Exhaled Bioaerosols." *Proceedings of the National Academy of Sciences of the United States of America* 101.50 (2004): 17383–17388. Print.

Engelhart, G. J., C. J. Hennigan, et al. “Cloud Condensation Nuclei Activity of Fresh Primary and Aged Biomass Burning Aerosol.” *Atmospheric Chemistry and Physics* 12.15 (2012): 7285–7293. Print.

Engelhart, G. J., A. Asa-Awuku, et al. “CCN Activity and Droplet Growth Kinetics of Fresh and Aged Monoterpene Secondary Organic Aerosol.” *Atmospheric Chemistry and Physics* 8.14 (2008): 3937–3949. Print.

Fabian, Patricia et al. “Influenza Virus in Human Exhaled Breath: An Observational Study.” *PloS one* 3.7 (2008): e2691. Print.

Grasmeijer, Niels, Henderik W. Frijlink, and Wouter L. J. Hinrichs. “An Adaptable Model for Growth And/or Shrinkage of Droplets in the Respiratory Tract during Inhalation of Aqueous Particles.” *Journal of aerosol science* 93 (2016/3): 21–34. Print.

Halloran, Siobhan K., Anthony S. Wexler, and William D. Ristenpart. “A Comprehensive Breath Plume Model for Disease Transmission via Expiratory Aerosols.” *PloS one* 7.5 (2012): e37088. Print.

Heng, B. H. et al. “Prevalence of Hepatitis A Virus Infection among Sewage Workers in Singapore.” *Epidemiology and infection* 113.1 (1994): 121–128. Print.

Heyder, J. et al. “Deposition of Particles in the Human Respiratory Tract in the Size Range 0.005–15 μm.” *Journal of aerosol science* 17.5 (1986): 811–825. Print.

Hinds, William C. *Aerosol Technology: Properties, Behavior, and Measurement of Airborne Particles*. John Wiley & Sons, 2012. Print.

Hoppentocht, M. et al. “Technological and Practical Challenges of Dry Powder Inhalers and Formulations.” *Advanced drug delivery reviews* 75 (2014): 18–31. Print.

Jain, Rishi, and Ranjan Srivastava. “Metabolic Investigation of Host/pathogen Interaction Using MS2-Infected Escherichia Coli.” *BMC systems biology* 3 (2009): 121. Print.

Jebri, Sihem et al. “Presence and Fate of Coliphages and Enteric Viruses in Three Wastewater Treatment Plants Effluents and Activated Sludge from Tunisia.” *Environmental science and pollution research international* 19.6 (2012): 2195–2201. Print.

Kampa, Marilena, and Elias Castanas. “Human Health Effects of Air Pollution.” *Environmental pollution* 151.2 (2008): 362–367. Print.

Kanji, Zamin A. et al. “. (A) CCN Activation Curves for 50 Nm Size Selected Particles... - Figure 2 of 4.” *ResearchGate*. N.p., 24 Feb. 2017. Web. 15 Apr. 2017.

Khuder, S. A. et al. “Prevalence of Infectious Diseases and Associated Symptoms in Wastewater Treatment Workers.” *American journal of industrial medicine* 33.6 (1998): 571–577. Print.

Korzeniewska, Ewa. “Emission of Bacteria and Fungi in the Air from Wastewater Treatment Plants - a Review.” *Frontiers in bioscience* 3 (2011): 393–407. Print.

Kreyling, Wolfgang G., Manuela Semmler-Behnke, and Winfried Möller. “Ultrafine Particle-Lung Interactions: Does Size Matter?” *Journal of aerosol medicine: the official journal of the International Society for Aerosols in Medicine* 19.1 (2006): 74–83. Print.

Kuzmanovic, Deborah A. et al. “Bacteriophage MS2: Molecular Weight and Spatial Distribution of the Protein and RNA Components by Small-Angle Neutron Scattering and Virus Counting.” *Structure* 11.11 (2003): 1339–1348. Print.

Law, Yingyu et al. “Nitrous Oxide Emissions from Wastewater Treatment Processes.” *Philosophical transactions of the Royal Society of London. Series B, Biological sciences* 367.1593 (2012): 1265–1277. Print.

Li, Wei, and P. K. Hopke. “Initial Size Distributions and Hygroscopicity of Indoor Combustion Aerosol Particles.” *Aerosol science and technology: the journal of the American Association for Aerosol Research* 19.3 (1993): 305–316. Print.

Li, Yuan et al. “Health Effects Associated with Wastewater Treatment, Reuse, and Disposal.” *Water environment research: a research publication of the Water Environment Federation* 87.10 (2015): 1817–1848. Print.

Lippmann, M., D. B. Yeates, and R. E. Albert. “Deposition, Retention, and Clearance of Inhaled Particles.” *British journal of industrial medicine* 37.4 (1980): 337–362. Print.

Longest, P. Worth, James T. McLeskey Jr, and Michael Hindle. “Characterization of Nanoaerosol Size Change During Enhanced Condensational Growth.” *Aerosol science and technology: the journal of the American Association for Aerosol Research* 44.6 (2010): 473–483. Print.

Longest, P. Worth, and Michael Hindle. “Numerical Model to Characterize the Size Increase of Combination Drug and Hygroscopic Excipient Nanoparticle Aerosols.” *Aerosol science and technology: the journal of the American Association for Aerosol Research* 45.7 (2011): 884–899. Print.

Löndahl, Jakob et al. “Experimentally Determined Human Respiratory Tract Deposition of Airborne Particles at a Busy Street.” *Environmental science & technology* 43.13 (2009): 4659–4664. Print.

Malakootian, Mohammad et al. “Bacterial-Aerosol Emission from Wastewater Treatment Plant.” *Desalination and water treatment* 51.22-24 (2013): 4478–4488. Print.

Martonen, T. B., A. E. Barnett, and F. J. Miller. “Ambient Sulfate Aerosol Deposition in Man: Modeling the Influence of Hygroscopicity.” *Environmental health perspectives* 63 (1985): 11–24. Print.

Masclaux, Frédéric G. et al. “Assessment of Airborne Virus Contamination in Wastewater Treatment Plants.” *Environmental research* 133 (2014): 260–265. Print.

Moore, Richard H., Athanasios Nenes, and Jeessy Medina. “Scanning Mobility CCN Analysis—A Method for Fast Measurements of Size-Resolved CCN Distributions and Activation Kinetics.” *Aerosol science and technology: the journal of the American Association for Aerosol Research* 44.10 (2010): 861–871. Print.

Niazi, Sadegh et al. “Assessment of Bioaerosol Contamination (bacteria and Fungi) in the Largest Urban Wastewater Treatment Plant in the Middle East.” *Environmental science and pollution research international* 22.20 (2015): 16014–16021. Print.

Oberdörster, Günter, Eva Oberdörster, and Jan Oberdörster. “Nanotoxicology: An Emerging Discipline Evolving from Studies of Ultrafine Particles.” *Environmental health perspectives* 113.7 (2005): 823–839. Print.

Oppenheimer, Joan A. et al. “Testing the Equivalency of Ultraviolet Light and Chlorine for Disinfection of Wastewater to Reclamation Standards.” *Water environment research: a research publication of the Water Environment Federation* 69.1 (1997): 14–24. Print.

Peabody, D. S., and L. Al-Bitar. “Isolation of Viral Coat Protein Mutants with Altered Assembly and Aggregation Properties.” *Nucleic acids research* 29.22 (2001): E113. Print.

Petters, M. D., and S. M. Kreidenweis. “A Single Parameter Representation of Hygroscopic Growth and Cloud Condensation Nucleus Activity.” *Atmospheric Chemistry and Physics* 7.8 (2007): 1961–1971. Print.

Piqueras, P. et al. “Real-Time Ultrafine Aerosol Measurements from Wastewater Treatment Facilities.” *Environmental science & technology* 50.20 (2016): 11137–11144. Print.

Radke, Michael. “Sterols and Anionic Surfactants in Urban Aerosol: Emissions from Wastewater Treatment Plants in Relation to Background Concentrations.” *Environmental science & technology* 39.12 (2005): 4391–4397. Print.

Radke, Michael, and Reimer Herrmann. “Aerosol-Bound Emissions of Polycyclic Aromatic Hydrocarbons and Sterols from Aeration Tanks of a Municipal Waste Water Treatment Plant.” *Environmental science & technology* 37.10 (2003): 2109–2113. Print.

Robinson, R. J., and C. P. Yu. “Theoretical Analysis of Hygroscopic Growth Rate of Mainstream and Sidestream Cigarette Smoke Particles in the Human Respiratory Tract.” *Aerosol science and technology: the journal of the American Association for Aerosol Research* 28.1 (1998): 21–32. Print.

Rose, Diana et al. “Calibration and Measurement Uncertainties of a Continuous-Flow Cloud Condensation Nuclei Counter (DMT-CCNC): CCN Activation of Ammonium Sulfate and Sodium Chloride Aerosol Particles in Theory and Experiment.” *Atmospheric Chemistry and Physics* 8.5 (2008): 1153–1179. Print.

Smit, Lidwien A. M., Suzanne Spaan, and Dick Heederik. “Endotoxin Exposure and Symptoms in Wastewater Treatment Workers.” *American journal of industrial medicine* 48.1 (2005): 30–39. Print.

Sorber, C. A., and B. P. Sagik. “Indicators and Pathogens in Wastewater Aerosols and Factors Affecting Survivability.” *Wastewater Aerosols and Disease; Proceedings of a Symposium*. N.p., 1979. Print.

Stockley, P. G. et al. “Molecular Mechanism of RNA-Phage Morphogenesis.” *Biochemical Society transactions* 21 (Pt 3).3 (1993): 627–633. Print.

Tang, Xiaochen et al. “The Effects of Mainstream and Sidestream Environmental Tobacco Smoke Composition for Enhanced Condensational Droplet Growth by Water Vapor.” *Aerosol science and technology: the journal of the American Association for Aerosol Research* 46.7 (2012): 760–766. Print.

Taylor, Nathan F. et al. “FIG. 3 CCN Activation Curves at 0.5% Supersaturation for NaCl Particles... - Figure 4 of 12.” *ResearchGate*. N.p., 29 Aug. 2016. Web. 15 Apr. 2017.

Tellier, Raymond. “Aerosol Transmission of Influenza A Virus: A Review of New Studies.” *Journal of the Royal Society, Interface / the Royal Society* 6 Suppl 6 (2009): S783–90. Print.

Uhrbrand, Katrine, Anna Charlotte Schultz, and Anne Mette Madsen. “Exposure to Airborne Noroviruses and Other Bioaerosol Components at a Wastewater Treatment Plant in Denmark.” *Food and environmental virology* 3.3-4 (2011): 130–137. Print.

Upadhyay, Nabin et al. “Characterization of Aerosol Emissions from Wastewater Aeration Basins.” *Journal of the Air & Waste Management Association* 63.1 (2013): 20–26. Print.

Varghese, Suresh K., and S. Gangamma. “Particle Deposition in Human Respiratory System: Deposition of Concentrated Hygroscopic Aerosols.” *Inhalation toxicology* 21.7 (2009): 619–630. Print.

Vu, Tuan V., Juana Maria Delgado-Saborit, and Roy M. Harrison. “A Review of Hygroscopic Growth Factors of Submicron Aerosols from Different Sources and Its Implication for Calculation of Lung Deposition Efficiency of Ambien Aerosols.” *Air Quality, Atmosphere and Health* 8.5 (2015): 429–440. Print.

Wang, Shih Chen, and Richard C. Flagan. “Scanning Electrical Mobility Spectrometer.” *Journal of aerosol science* 20.8 (1989): 1485–1488. Print.

Xi, Jinxiang et al. “Growth of Nasal and Laryngeal Airways in Children: Implications in Breathing and Inhaled Aerosol Dynamics.” *Respiratory care* 59.2 (2014): 263–273. Print.

Xi, Jinxiang, and P. Worth Longest. “Numerical Predictions of Submicrometer Aerosol Deposition in the Nasal Cavity Using a Novel Drift Flux Approach.” *International journal of heat and mass transfer* 51.23–24 (2008): 5562–5577. Print.

ATCC. Virology guide. 2016. https://www.atcc.org/~/media/PDFs/Culture%20Guides/Virology_Guide.ashx

EPA. Method 1601, Male-Specific (F^+) and Somatic Coliphage in Water by Two-step Enrichment Procedure. April 2001. https://www.epa.gov/sites/production/files/2015-12/documents/method_1601_2001.pdf

EPA Method 1602, Male-Specific (F^+) and Somatic Coliphage in Water by Single Agar Layer (SAL) Procedure. April 2001. https://www.epa.gov/sites/production/files/2015-12/documents/method_1602_2001.pdf

Chapter 5: Phytotoxic assessment of ozone and sulfur dioxide on four major crops in Mpumalanga, South Africa.

5.1 Abstract

The Highveld Priority Area (HPA) in eastern South Africa is regarded as one of the largest industrialized areas in Africa. Mpumalanga, the province that encompasses this region, heavily relies on agriculture as a source of revenue and it is considered one of the main food baskets of the country. Monitoring data collected over the past seven years shows elevated concentrations of known phytotoxic pollutants (ozone (O_3) and sulfur dioxide (SO_2)) in the province, especially during the growing season. However, the repercussions of these gases on the agricultural enterprises grown in the region remain unknown.

This is the first study in South Africa to quantify the effects of ambient O_3 and SO_2 on four major crops (wheat, maize, sorghum and soybean): AOT40 values were used to calculate yield and revenue losses in different magisterial districts within the Mpumalanga province. These thresholds are currently used in the European Union to estimate crop yield loss by considering O_3 concentrations for daytime hours (06:00 AM to 06:00 PM) during the three-month growing season pertaining to each plant. This work utilizes concentrations from multiple years of ambient O_3 data for AOT40 calculations.

Results suggest that the most affected crop is wheat (multi-year average yield loss (AYL) of 14.21% and multi-year average total annual loss (TAL) of $2.39 million in the

region), followed by maize (AYL of 11.42% and TAL of $49.9 million in the region), sorghum (AYL of 0.55% and TAL of $0.08 million in the region) and soybean (AYL of 0.12% and TAL of $0.32 million in the region). Many of the region's magisterial districts also surpass the international SO_2 standards for agriculture during the growing season, which likely exacerbates the yield losses. This study highlights the importance of air pollutant stressors on agriculture and regional economies in addition to the potential human health risks via their inhalation.

5.2 Introduction

Air pollution is a growing problem in many developing countries; emissions are increasing due to economic growth, industrial development and urbanization. In South Africa, outdoor and indoor air pollution continues to be a serious concern due to high concentrations of sulfur dioxide, particulate matter, nitrogen dioxide, nitrogen oxides, ozone, benzene and VOCs in urban and some rural regions (DEA, 2011). Previous researchers have labeled industrial complexes in South Africa as major hotspot of air pollution in the southern hemisphere (Lourens et al., 2012; Matyssek et al., 2012). As a result, the country's government declared a few heavily polluted regions as Air Quality Priority Areas. These particular districts have been federally established because the air quality currently exceeds or will exceed the South African National Ambient Air Quality Standards (NAAQS) for human health; the Minister of Environmental Affairs believes that air quality management action is necessary to rectify the current situation (SAAQIS, 2017).

Three Priority Areas currently exist in South Africa: the Waterberg Bojanala Priority Area, the Vaal Priority Area and the Highveld Priority Area (shown in Figure 5-1). These regions surround the heavily trafficked cities of Johannesburg and Pretoria, where a large number of industrial processes occur. This study focuses only on Highveld Priority Area, a region that is known to exceed the national and international standards for ozone and SO_2. It is also the only priority area that has a relatively dense quantity of air quality monitoring stations spatially spread out throughout its territory. The data obtained from the monitoring stations has reasonable completeness for risk assessment calculations ($\geq$ 80% data availability). More importantly, the monitoring stations are situated in areas close to agricultural enterprises that contribute to a large portion of the national economy.

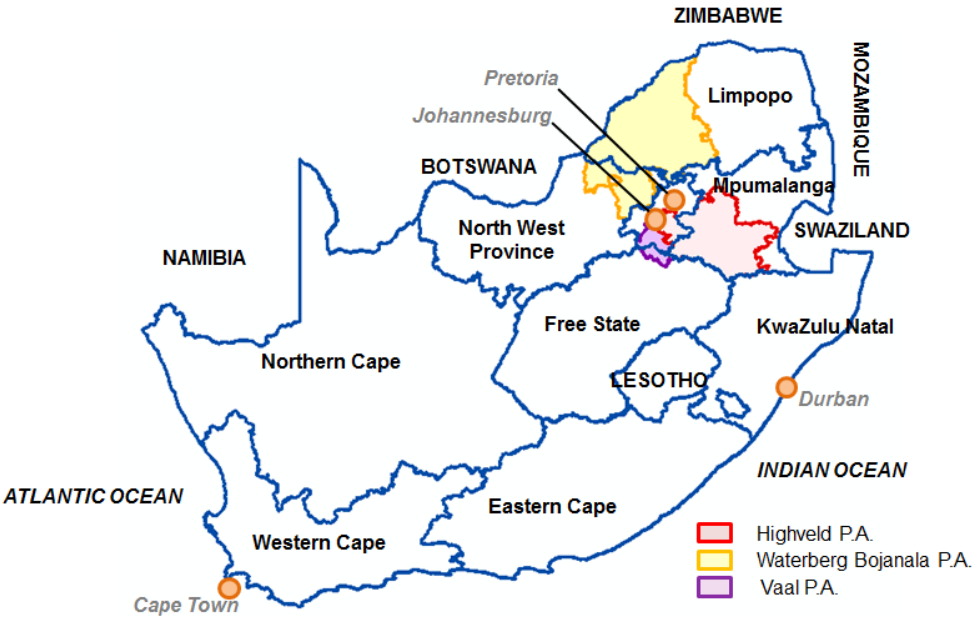

Figure 5-1: Map of South Africa's provinces and 3 highlighted priority areas. The Highveld Priority Area (outlined in red), the Vaal Priority area (purple) and the Waterberg Bojanala Priority Area (yellow) are noted. Major cities are indicated with orange circles.

5.2.1 The Highveld Priority Area

The Highveld Priority Area (HPA) is regarded as one of the largest industrialized regions in Africa (van Tienhoven et al., 2003). The state of ambient air quality in the HPA has been subject to a number of investigations for more than 30 years (Held et al., 1996; Mokgathle et al. 2006; Lourens et al., 2011 and 2012; Balashov et al., 2014). The focus of the monitoring has been the growing power generation industry, mining as well as the petrochemical and the metallurgical sectors. For example, Zunckel et al., 2000, drew attention to the high surface ozone concentrations and precursor emissions in the

region as well as the transport and deposition across Southern Africa. Held et al., 1996, also gathered previous research findings, including SO_2 measurements over the period from 1988 to 1994, through which he described the evolution of air quality in the region when the industrial sector had the fastest growth.

The district covers an area of 31,106 km^2 (12,010 square miles) with a single metropolitan municipality, three district municipalities, and nine local municipalities. The area is contained within the boundaries of: the Ekurhuieni Metropolitan Municipality, Lesedi Local Municipality, Govan Mbeki Local Municipality, Dlpaleseng Local Municipality, Lekwa Local Municipality, Msukaiigwa Local Municipality, Pixley ka Seme Local Municipality, Delmas Local Municipality, Emalahleni Local Municipality, and the Sieve Tshwete Local Municipality (van Schalkwyk, 2007, No. 35072). However, the majority of the population is located in municipalities on the western section of the HPA. The geography of the region is relatively flat and at a elevation of 1500 meters (4921 feet). The higher Drakensberg Escarpment in the east (shown in Figure 5-2) acts as a barrier that collects ground level pollutants in the West.

The HPA is located east of Johannesburg and Pretoria and it encompasses the municipalities in the Southwest region of Mpumalanga province and a small Southeast section of Gauteng. This study only focuses on the Mpumalanga area of the HPA (MHPA), where the agricultural enterprises of interest are located.

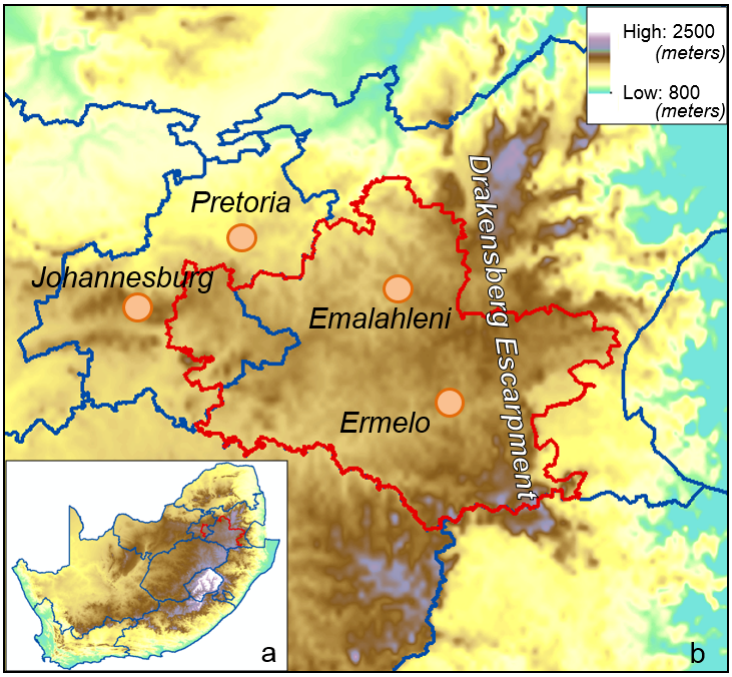

Figure 5-2: (a) National elevation map of South Africa and (b) Elevation map for Mpumalanga and Gauteng (the two provinces that compose the Highveld Priority Area). The HPA is outlined with a red line. The MHPA is is the region is located east of the province border line (blue). The Drakensberg Escarpment acts as a natural border of the Priority Area. Data was obtained from the CSIR and it was mapped in ArcGIS.

As the area overlaps provincial boundaries, the Department of Environmental Affairs (DEA) functions as the lead agent in the management of the priority area. The DEA is required (in terms of Section 19(1) of the National Environmental Management: Air Quality Act (Act 39 of 2004) (AQA)) to develop an Air Quality Management Plan (AQMP) for the priority area (HPA AQMP, 2011).

Mpumalanga is the fourth-biggest contributor to South Africa's GDP. The province's economy is dominated by mining, mostly coal for the Eskom power plants that are also located within the province. The municipalities in the MHPA produce about 80 percent of the country's coal, it is one of the largest production regions for forestry and agriculture. According to the crops and markets report of 2009 published by the Department of Agriculture, 21% of South Africa's maize is produced in Mpumalanga (Mpumalanga, 2017). Agricultural enterprises for local consumption also include wheat, grain sorghum and soybeans (Laban et al., 2015). Planted crop area extends throughout most of the MHPA (see figure 5-3), and it consists of 92% of all harvested crops within the province. Sorghum and soybeans are considered a summer crop in the region (October through January), wheat is considered a winter crop (August through October) and maize grows in the spring (September through November).

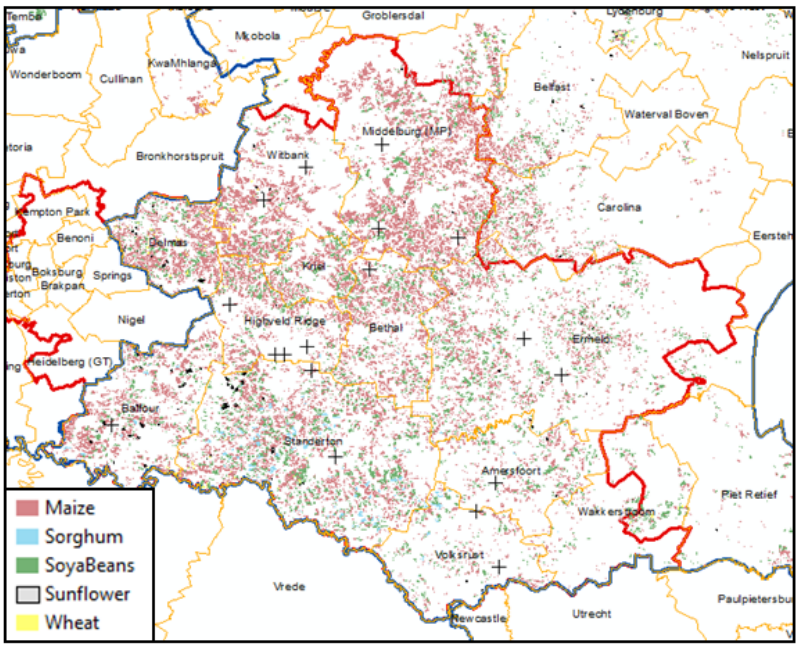

Figure 5-3: (a) Detailed map of the Mpumalanga Highveld Priority Area (MHPA) with planted areas for maize (pink), sorghum (blue), soybean (green), sunflower (grey) and wheat (yellow). Magisterial district borders are represented with yellow lines and provincal borders are represented with blue lines. The HPA is outlined with a red line. Data was obtained from South Africa's Department of Agriculture and it was mapped in ArcGIS.

5.2.2 Ozone and SO_2 as phytotoxic pollutants

Stringent government regulation in Europe and North America has lead to declining SO_2 emissions in their region, where as in developing countries it has not. SO_2 emissions are actually rising in many developing nations across the world, including South Africa (Galloway 1995; Held et al. 1996; McCormick 1997). SO_2 emissions,

especially from the coal industry, continue to be a serious issue in developing countries (Held et al. 1996; Arndt et al. 1997; UNECE, 2010). This is primarily due to fossil fuel emissions and the impact of climate change, among other factors.

Ambient ground level ozone (O_3) concentrations have doubled since the 1900s globally (Osborne et al., 2016). Ozone, as a secondary pollutant, is very challenging to control because it is generated through photochemical reactions of ozone precursors (nitrogen oxides (NO_x) and volatile organic compounds (VOCs) (Jeffries, 1995; Sillman, 1999; van Tienhoven et al., 2003; Penkett et al., 2003). There are two common types of ozone exposure, defined according to extent and concentration: Acute exposure is short-term exposure (hours) of O_3 concentration greater than 120 ppb. Chronic exposure is long-term exposure (three months) at elevated O_3 that peak at 120 ppb (Morgan, 2003).

The potential for ambient ozone and sulfur dioxide to damage agricultural crops and vegetation is well documented in literature (Farmer, 1997; Fuhrer et al 1997; Emberson et al. 2001; van Tienhoven and Scholes, 2003; Smidt and Herman, 2004; Zunckel et al., 2006; Felzer, 2007 Fuhrer, 2009; Avnery et al., 2011; van Dingenen et al., 2009; Fuhrer 2009; Yuan et al., 2015). The two gaseous compounds can enter the plant through open stomata and make its way to the interior of the leaf (Reich, 1987). Damage to plants is shown by visible leaf injury, flecking and reduced photosynthesis which results in reduced growth rate (Krupa et al., 1998; Mauzerall and Wang 2001; Morgan et al., 2006; Felzer et al., 2007). Thus the yield and growth of the plant become suppressed and nutrition capacity weakens.

The aperture of the stomata is controlled by environmental conditions, such as humidity, temperature and light intensity. These external factors thus influence the rate of uptake of sulfur dioxide and ozone and hence the degree of injury (UNECE, 2010). The stomata is closed when it is dark (night time) or in drought conditions. Therefore the plant has a lower degree of susceptibility to injury during a dry year. However, dry years are the periods with the highest amount of solar radiation and higher potential for ozone formation (Jain et al., 2005). Long-term exposure to the gas is cumulative and results in reduced growth and yield often with no clear visible symptoms (UNECE, 2010). The amount of damage depends on time of exposure and crop stage of development; young plants are considered more sensitive and plants that are exposed to high concentrations of ozone and sulfur dioxide for longer periods (over 3 months) suffer the most damage (Teixeira et al., 2009). Acute doses are associated with initial loss of photosynthesis while chronic doses affects plant production (Morgan et al., 2003).

Past studies have quantified average global yield losses due to O_3 for specific crops. Plants range from sensitive (wheat, water melon, pulses, cotton, turnip, tomato, onion, soybean and lettuce), moderately sensitive (sugar beet, potato, oilseed rape, tobacco, rice, maize, grape and broccoli) and resistant (barley and fruit represented by plum and strawberry) (Mills et al., 2007). Soybeans were found to be the most ozone sensitive crop with a loss of 6%-16% based on the analysis for the year 2000. (Osborne et al., 2016). Other researchers have shown evidence of O_3 main hotspots of damage in East China and India (Teixeira *et al*, 2009). The study in India estimated that ozone-induced

national aggregated wheat and rice yield loss was equal to the amount that could feed 94 million people (Ghude et al., 2014).

Sulfur dioxide and ozone concentrations are exceeded in extensive areas throughout MHPA (SAAQIS, 2017). The winter season (November-February) has the highest frequency of exceedances of standards when there are poor dispersion conditions and low-level emissions are trapped near the surface. Seasonal trends are clearly observed for O_3 in the monitoring record, as springtime peaks are easily identified during the growing season (SAAQIS, 2017). Rural and agricultural areas in the country also experience high ozone concentrations as ozone precursors and SO_2 may be transported far from their emission sources (Sillman, 1999; Derwent, 2000; Laban et al., 2015).

In South Africa 12% of the land is used for crop production and about 50% of South Africa's water is used for agriculture, crop farming has economic and societal value in the country (Brand S.A., 2016). However, there are very few studies in South Africa that focus on ozone and its impacts on agriculture (van Tienhoven et al., 2003, Zunckel et al., 2004; Zunckel et al., 2006; van Tienhoven et al., 2006). Currently, the country's attention on air pollution has been on its impact on human health and little is known about its impact on agriculture. A review of surface ozone monitoring showed Mpumalanga Highveld and Botswana to have the highest ozone concentrations in spring time (van Tienhoven., et al. 2006). A similar index was used by Zunckel et al., (2005) in South Africa as part of Cross Border Air Pollution Assessment study (CAPIA). Nevertheless, the emissions inventory used in the CAPIA study lacks many major

sources, its results are underestimated and it is not considered robust enough by the South African scientific community. Josipovic et al, 2009 also provided direct concentration measurements and critical level exceedance assessment of SO_2 and O_3 in the MHPA. However, this study used passive sampling sites to calculate monthly means, and the accumulated hourly intake, the basis a phytotoxic assessment for both gases, was not calculated. Since ambient ozone levels have been shown to be high during the growing season in past studies, even when it was underestimated, it is likely that there is the potential for negative impacts on agriculture. Therefore, it is therefore crucial to quantify the effects of ambient ground-level secondary ozone and primary sulfur dioxide on crops, to evaluate sources and perform risk assessments on food security.

5.2.3 Sources of ozone precursors and SO_2

Industrial sources are by far the largest contributor of total emissions in the MHPA, accounting for 89% of PM_{10}, 90% of NO_x (shown in table 5-1 and figure 5-4a) and 99% of SO_2 (shown in table 5-1 and figure 5-4b). Emission sources in the region mainly consist of power generation (the largest source of emissions in the MHPA), coal mining, metallurgical operations, brick manufacturers, and petrochemical industry, (AQA, 2012). However, additional sources (e.g. traffic, biomass burning…etc.) also contribute to air pollution in the MHPA.

Table 5-1: Sources of NO_x and SO_2 within the Mpumalanga Highveld Priority Area.

Source	NO_x (t/a)	NO_x (%)	SO_2 (t/a)	SO_2 (%)
Ekurhuleni MM industrial	15636	2	25772	2
Mupmalanga Industrial	590	0	5,941	0
Clay Brick Manufacturing	-	-	9,963	1
Power Generation	716,719	73	1,337,521	82
Primary Metallurgical	4,416	0	39,582	2
Secondary Metallurgical	229	0	3,223	0
Petrochemical	148,434	15	190,172	12
Motor Vehicles	83,607	9	10,059	1
Household Fuel Burning	5,600	1	11,422	1
Biomass Burning	3,550	0	-	-
TOTAL HPA	978 781	-	633 655	

**Source: AQA, 2012*

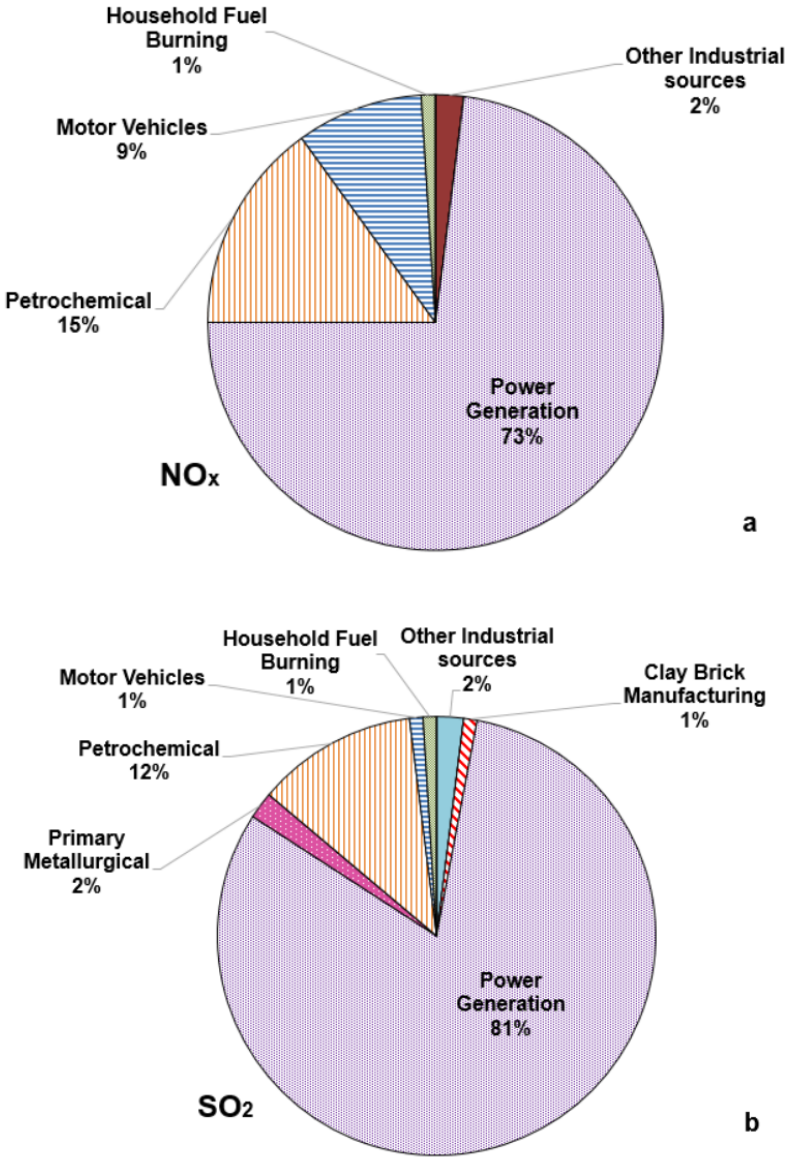

Figure 5-4: Total source of NO_x emissions (a) and SO_2 emissions (b) in the HPA. (Source: AQA, 2012)

5.2.3.1 Power generation and other industrial processes

The generation of electricity in South Africa is largely dependent on coal. The operation of coal-fired power stations results in the emission of pollutants such as particulate matter, sulfur dioxide, nitrogen oxides and mercury. The air quality impacts of these pollutants are largely felt in the regions where most of the coal reserves lie. In the MHPA, the power generation contributes 73% of the total estimated oxides of nitrogen (NO_x) emission of 978,781 tons per annum and 82% of the total estimated SO_2 emission of 1,633,655 tons per annum (HPA AQMP, 2011). Eskom and Sasol are the established energy companies responsible for most of the coal mining and dumping (Mathu et al., 2013)

Eskom

Eskom is South Africa's main public utility and it is currently the largest producer of electricity in Africa. The company supplies 95% of the electricity used nationally (Sanchez, 2017). It has a total of 13 coal-fired power stations that produce 92.5% of all Eskom's electricity, 11 of which are located in Mpumalanga and within the region of this study (shown in table 5-2). The power plants' production range from 764 Megawatts (Medupi plant) to 4416 MWe (Kendal plant), the last one being the 22nd largest coal-fired station in the world and the largest power station of any kind in Africa (Eskom, 2017).

Table 5-2: Name, coordinate location and electricity production of all Eskom coal-fired power plants in the MHPA

Power Plant Name	Coordinates	Electricity production
Kendal	26°5′24″S 28°58′17″E	4116 MWe
Majuba	27°6′2″S 29°46′17″E	4110 MWe
Lethabo	26°44′31″S 27°58′39″E	3708 MWe
Tutuka	26°46′43″S 29°21′7″E	3654 MWe
Matla	26°16′57″S 29°8′27″E	3600 MWe
Duvha	25°57′50″S 29°20′14″E	3600 MWe
Kriel	26°15′15″S 29°10′46″E	3000 MWe
Arnot	25.94384°S 29.78956°E	2400 MWe
Hendrina	26°2′S 29°36′E	2000 MWe
Camden	26°37′13″S 30°5′38″E	1600 MWe
Grootvlei	26°46′S 28°30′E	1200 MWe
Komati	26°05′24″S 29°28′19″E	1000 MWe

**Power plants are listed in order of largest electricity production to least.*

Source: Eskom.

Eskom is planning to build another coal plant in Mpumalanga (Kusile Power Station), which will produce approximately 4800 MWe. The entire project is expected to be completed in 2021 (HPA AQMP, 2011).

Sasol

Sasol Limited is an energy and chemical company based in Johannesburg and it is the world's first oil-from-gas company (Mowatt, 2016). It develops and commercializes technologies, including synthetic fuels technologies, and produces different liquid fuels, chemicals and electricity (Sasol, 2017). The company operates six coalmines that supply feedstock for Secunda, a synthetic fuel plant, (Sasol Synfuels). The plant Secunda develops and manages the group's upstream interests in oil and gas

exploration and production. Sasol's total greenhouse gas emissions total 72.7 Mt CO_2 equivalent per annum (SEPI, 2017). SO_2 emissions from smoldering coal dumps were estimated at more than 54,000 t/a in the Mpumalanga Province's 2001 State of Environment Report (DACE, 2001).

5.2.3.2 Traffic

There is an increase in the number of privately owned vehicles in South Africa. This has resulted in an increase of fuel consumption (Akinboade et al., 2008). Pretoria and Johannesburg are expansive, sprawl in every direction and overflow into each other. The driving culture in both metropolises is unequivocal; each is surrounded and crisscrossed by ribbons of highways, and traffic congestion still are a major issue despite new public transport alternatives. In urban areas within the MHPA, vehicle emissions may be responsible for 90 to 95 % of CO and 60 to 70 % of NO_x within the atmosphere (DEA, 2011). Emissions from vehicles contribute to photochemical smog, especially downwind of areas that experience high traffic density such as central business districts (CBDs) (DEA, 2011).

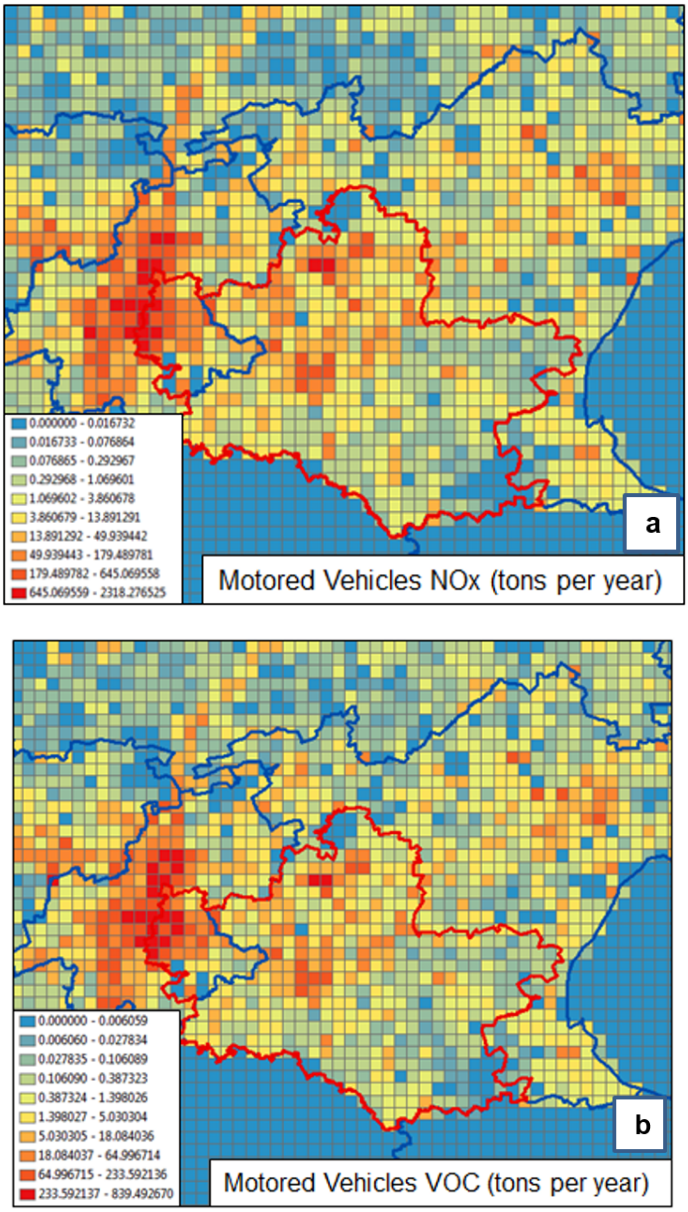

Figure 5-5: 8 km resolution map of the HPA representing total NO_x emissions (a) and VOC emissions (b) from motored vehicles in a year. Agricultural areas are located downwind of NO_x hotspots. The data was obtained from CSIR's most current emissions inventory.

5.2.3.3 Biomass and household burning

Africa is the single largest continental source of biomass burning emissions (Roberts et al 2008). Fire is prevalent throughout the MHPA, where most fires occur in the dry season (July to September) (Archibald et al, 2009). The main gases emitted during the process of biomass burning are CO, CH_4, particulates and NO_x, the last one being a significant ozone precursor (Brocard et al., 1996; Cachier, 1996; Levine, 1996). The natural vegetation in the MHPA is dominantly grassland, which emits low amounts of VOC during combustion (Barker et al., 1996).

Domestic coal and wood combustion within townships, informal settlements and rural areas have also been identified through several studies to be one of the greatest sources of gaseous emissions (including NO_x and SO_2) as well as airborne particulates (Barnes et al., 2002). Small merchants trade around 2% of domestic coal consumption to small businesses and households and about one million tones is sold into a retail market for domestic space heating during the winters. As a result, the combustion of coal generates emissions of criteria pollutants throughout populated areas (Eberhard, 2011). The use of household coal also produces high levels of indoor air pollution and respiratory diseases, which costs the region an estimated $160 million per annum (Balmer, 2007).

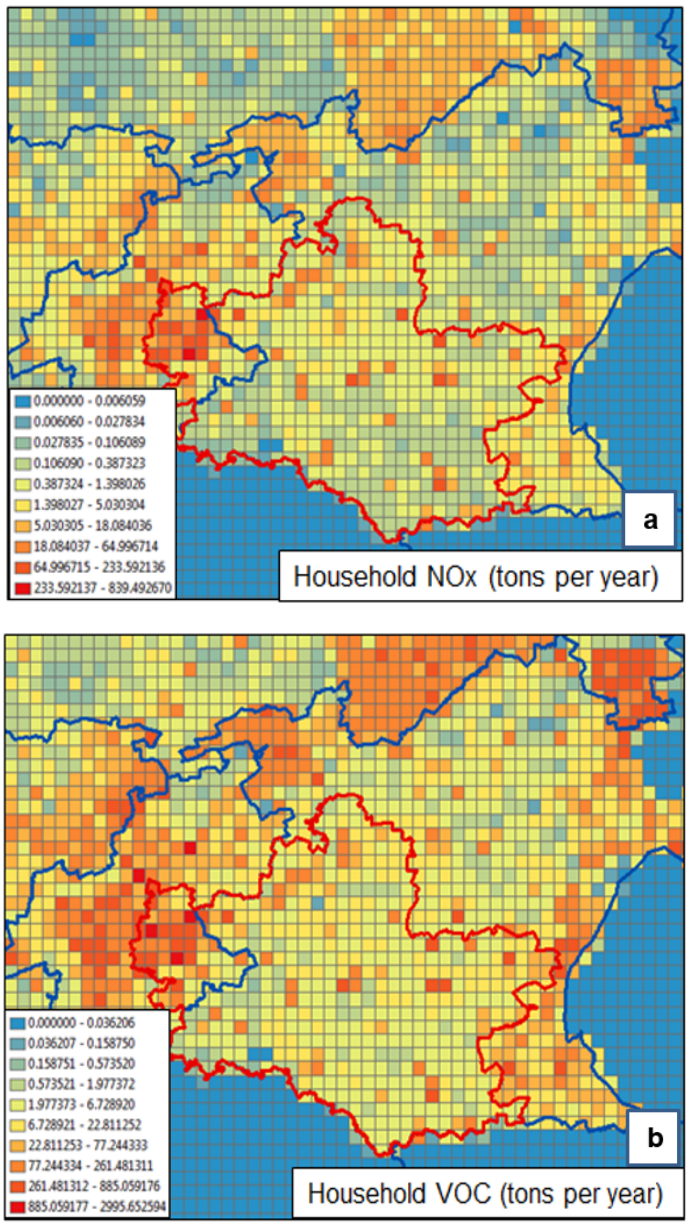

Figure 5-6: 8 km resolution map of the HPA representing total NOx emissions (a) and VOC emissions (b) from household burning in a year. Hotspots are located in populated areas. The data was obtained from CSIR's most current emissions inventory.

The emissions inventory for industrial sources and household emissions was relatively complete and included all industries on the HPA. It is recognized that these sources comprise the major sources, with non-registered sources being very small in comparison. Source categories where emissions could not be determined were landfills, incinerators, wastewater treatment works, tire burning, biogenic sources, odor and agricultural dust. The inventory of motorized vehicle emissions was also not fully complete.

5.2.3.4 Wind transport and meteorology

The winter anticyclonic circulation over the MHPA results in stable atmosphere, weak winds, clear skies and the development of surface temperature inversions at night that continues into the morning (Held et al., 1996). During the day, surface warming enhances the dispersion the nighttime pollution build-up. There is no dispersion of the pollutants that are released at or near ground level. Therefore, pollutants tend therefore to accumulate near their source. This is relevant to low level industrial stacks, domestic fuel burning, motor vehicles and burning coalmines and coal dumps (Held et al., 1996). Convection also occurs and it brings emissions from taller stacks down to ground level. Relatively high ambient concentrations occur especially at night and in the morning when the surface inversions are strongest.

Emissions in the MHPA also affect neighboring regions. Approximately 41% of the pollutants emitted within the MHPA are transported into countries bordering South Africa through either direct or re-circulated transport, as shown in figure 5-7 (Freiman and Piketh, 2003). Transport to Mozambique occurs more than 35% of the time, and

more than 30% of the time to Botswana. Transport to Swaziland, Namibia and Zimbabwe is between 15% and 23% with less to other southern African countries (AQA, 2012).

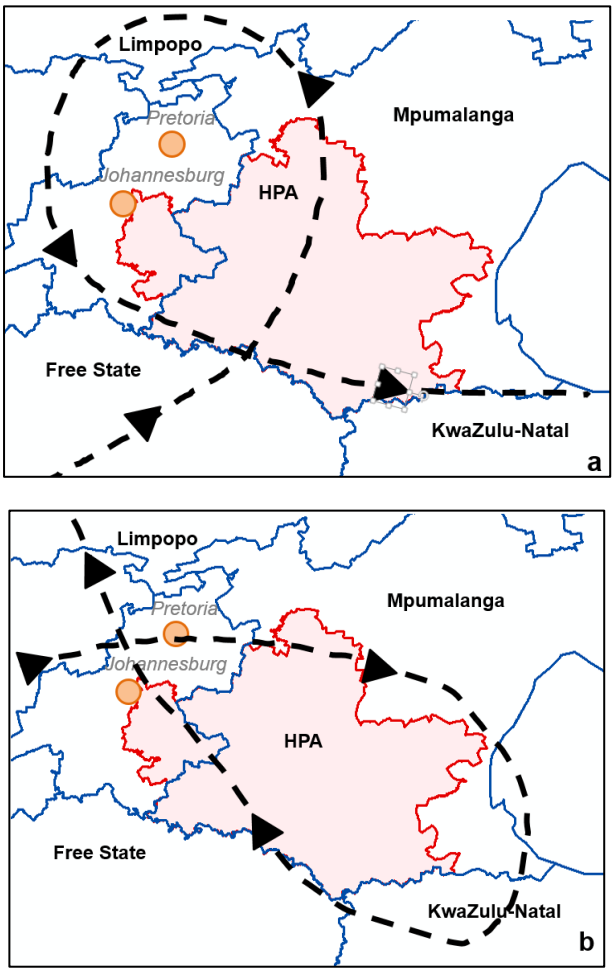

Figure 5-7: Characteristic wind paths during strong anticyclonic ridging in from May to June (a) and August to April (b). The patterns are responsible for the accumulation of phytotoxic pollutants in the MHPA. Source: Held et al 1996.

5.3 Methods

To quantify the potential impact of O_3 on plants requires understanding the crop's response to O_3 and the incorporation of these responses to crop production models (Osborne et al., 2016). Ozone exposure can be represented statistically using indices to summarize O_3 exposure during growing season; these indices are used in collaboration with concentration response relationships to calculate yield losses (Avnery et al., 2011).

Cumulative exposure to ozone is generally considered together with ambient thresholds. A common metric for assessing agricultural risk is determined by using the ozone accumulated exposure over a threshold of 40 ppb for hourly values for a growing season (UNECE, 2010). This index is used in Europe as a standard for protection of vegetation against ozone pollution. Surface ozone concentrations in the country that exceed this concentration should affect plants if the areas where this occurs coincide areas where staple crops grow. The most significant agricultural enterprises in the MHPA and the focus of this study are wheat, maize, grain sorghum and soybean.

5.3.1 Monitoring data

Since the emissions inventory is not as complete as it necessary to make an accurate phytotoxic assessment, an alternative approach was followed by analyzing multi-year monitoring data; SAAQIS (the South African Air Quality Information System) provides data from monitoring stations that measure ambient gaseous and particulate concentrations in compliance with NAAQS. This data is freely available through the Department of Environmental Affairs (DEA) and the South African Weather Service

(SAWS). The monitoring stations are owned by three networks: Sasol, Eskom and the DEA. Each of their stations throughout the MHPA are sparsely located many of them correspond to areas where agricultural activities occur (Zunckel et al., 2004; van Tienhoven et al., 2006, 2003). This area is responsible for 95% of the total agricultural production in the province.

Many air quality-monitoring stations are located in urban and industrial districts and a substantial number are located in the middle townships and in rural areas near crops (shown in figure 5-8 and table 5-3). Hourly ozone concentrations from 2008 to 2015 were collected from the SAAQIS for all DEA and Sasol Stations in the MHPA. Monitoring data from the Eskom stations were obtained directly from the public utility. The hourly mean ozone concentrations were expressed in parts per billion (ppb) in all data sets. It some limitations such as large gaps of missing data, negative figures and extremely large values, which may indicate instrument error, theft or that the monitoring stations is overdue for a calibration. However, these values were quality controlled; negative and extremely large values were omitted.

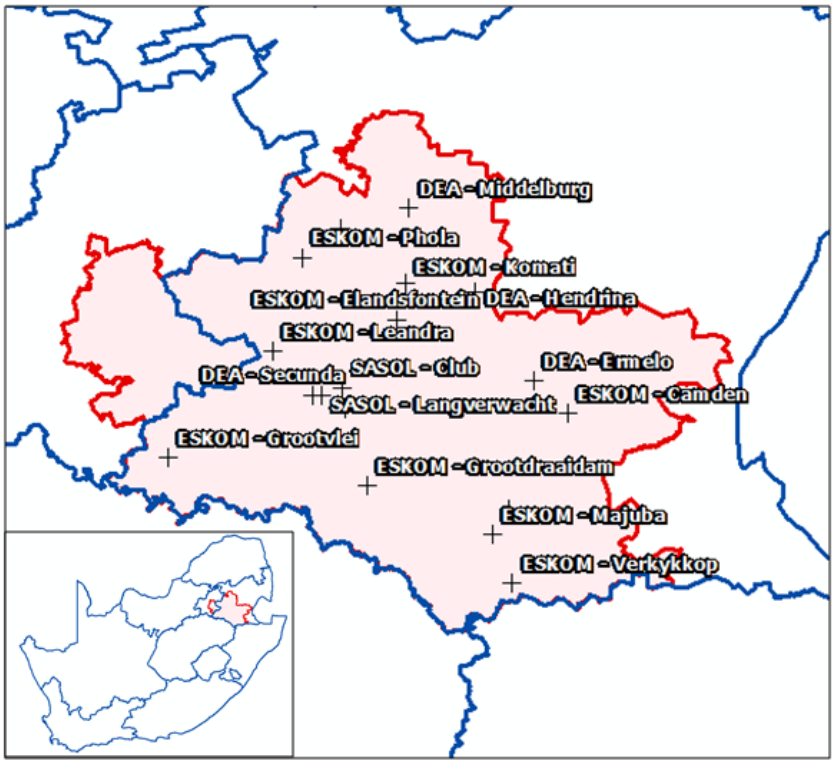

Figure 5-8: Geographical area of the HPA (red). Monitoring stations are indicated with a "+" sign.

Table 5-3: Station name with its corresponding monitoring network, coordinates and location description.

Network	Station Name	Coordinates	Location details
DEA	Secunda	26.548578°S 29.080055°E	In a township
DEA	Witbank	25.877812°S 29.188664°E	In a township
DEA	Hendrina	26.150947°S 29.716789″E	Rural community
DEA	Middelburg	25.796061°S 29.463623°E	Middle class community
DEA	Ermelo	26.493372°S 29.968056°E	In a township
SASOL	Club	26.519579°S 29.194118°E	Upper class club
SASOL	L/Embelenhle	26.551389°S 29.1125°E	Middle class near mines
ESKOM	Amersfoort	27.010167°S 29.867833°E	-
ESKOM	Camden	26.622608°S 30.108976°E	Rural near power station
ESKOM	Phola	25.995670°S 29.038173°E	In a townswhip
ESKOM	Majuba	27.112809°S 29.800300°E	Rural. No population
ESKOM	Verkykkop	26.309091°S 29.881436°E	Rural. No population
ESKOM	Leandra	26.371822°S 28.917127°E	Middle class and township
ESKOM	Elandsfontein	26.245487°S 29.417382°E	Rural. No population
ESKOM	Komati	26.098178°S 29.450542°E	Rural near power station
ESKOM	Grootdraaidam	26.891813°S 29.307802°E	Rural. No population
ESKOM	Grootvlei	26.764677°S 28.480087°E	Rural community
ESKOM	Bossiespruit	26.605833°S 29.210833°E	Rural. No Population

**Source: DEA, Sasol and Eskom*

5.3.2 Data processing

5.3.2.1 AOT40 and yield losses calculation

The AOT40 index (accumulated ozone threshold) is a cumulative exposure limit to place weight on higher concentrations of ozone when calculating yield losses (Tuovinen, 2000). Above this value there is a potential for crop yield loss for all sensitive species (van Tienhoven et al., 2005). The concept of AOT defines long-term ozone exposure above 40 ppb it gives a good linear fit to experimental data from open-top chambers for arable crops (Fuhrer et al., 1997).

AOT40 is calculated for a period of 3 months during the growing season during the daytime (06:00 AM to 06:00 PM). Sunlight hours are used because the plants close their stomata at night thus there is no ozone uptake (van Tienhoven et al., 2005). Single crop values were calculated for their correspondent growing season; wheat (August, September, October), maize (September, October, November), sorghum (October, November, December) and maize (November, December and February).

Only years with data completeness (availability) of 80% were considered. This threshold was chosen to maintain a statistically accurate analysis since AOT40 is a cumulative value. Data completeness was calculated using equation 1. AOT40 was then calculated using equation 2 where C_{O3} is the hourly ozone concentration and 40ppb is the threshold. AOT40 values were only calculated when the hourly ozone concentration was greater than 40 ppb.

Equation 5-1: $$data\ completeness = \frac{number\ of\ valid\ data\ points\ obtained}{total\ number\ of\ data\ points\ in\ the\ averaging}$$

Equation 5-2: $$AOT40 = \sum_{i=1}^{n}(\left[c_{O_3}\right] - 40ppb)$$

Once AOT40 values were determined, previously published response functions were utilized to calculate relative yields for each growing season (shown in table 5-4). These equations for response thresholds for adverse effects of ozone were derived in laboratories with controlled environments for broad categories of economically important species. They were developed using rigorous selection criteria (field-based crop selection, ozone concentrations within European range and full season exposure period) (Mills et al., 2007). However, there is still no derived equation for sorghum to date. Therefore, since maize and sorghum are C4 plants (they uptake gases in a similar way), the same function was utilized to calculate sorghum yield losses (Muchow et al. 1994).

Table 5-4: Previously developed response function fits to relative yields using AOT40 values for each crop species.

Crop	Function (y=relative yield x = AOT40 in ppm.hr)	Reference
Wheat (C3)	*Eq. 5-4.1:* y=-0.0161x+0.99	Fuhrer et al. (1986a) Temple (1990b)
Maize (C4)	*Eq. 5-4.2:* y= -0.0036x+1.02	Rudorff et al. (1996), Mulchi et al. (1995), Kress and Miller (1985)
Soghum (C4)	*Eq. 5-4.3:* y= -0.0036x+1.02 (same as maize)	Rudorff et al. (1996), Mulchi et al. (1995), Kress and Miller (1985)
Soybean (C3)	*Eq. 5-4.4:* y=-0.0116x+1.02	Heagle et al. (1988b), Heggestad et al. (1985, 1988), Mulchi et al. (1995) Heggestad and Lesser (1990), Heagle et al. (1987a, 1998), Fiscus et al. (1997)

**The same equation was used for sorghum and maize. (Source: Mills et al., 2007).*

5.4 Results and discussion

Hourly O_3 concentrations in each station on the HPA are illustrated in Figure 5-9. The ozone ambient concentrations recorded by all DEA, Sasol and Eskom monitoring stations regularly exceed the 8 hourly NAAQS for human health (61 ppb). All stations also had hourly average values of O_3 above the national standard as well as the AOT40 threshold (40 ppb). Therefore, crop damage is expected.

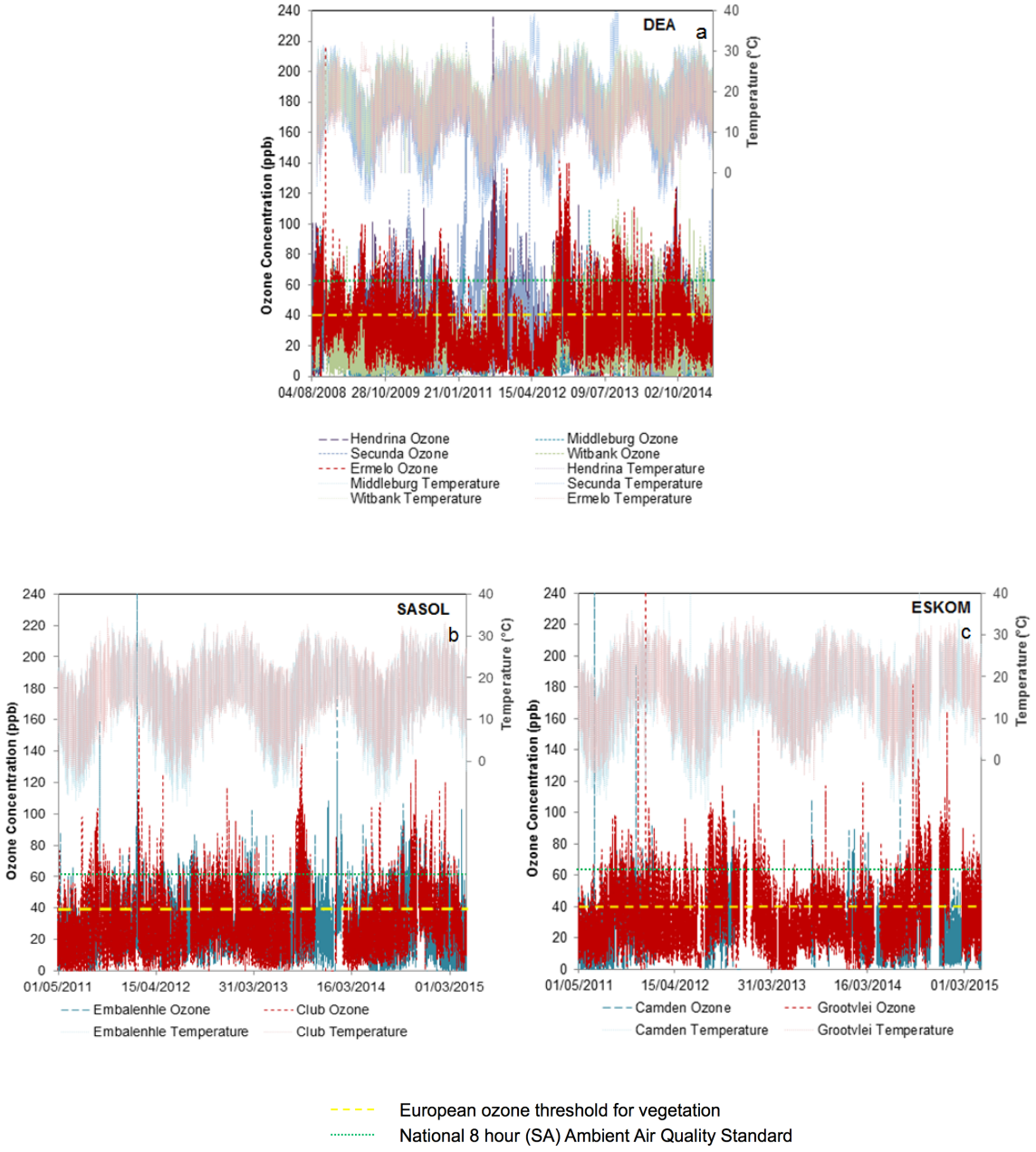

Figure 5-9: Hourly ozone concentrations for the 3 different monitoring networks. (a) Department of Environmental Affairs, (b) Sasol and (b) Eskom and the UN WHO AOT threshold (yellow dashed line) and the South African National ambient air quality standard for 8 hour running average (green dotted line).

Results indicate that dominant northwesterly winds during the growing season transport O_3 precursors from the Secunda complex as well as Eskom power plants, industrial facilities and municipalities in the Southeast. Elevated O_3 concentrations at Amersfoort and Ermelo emerge due to the site location a relatively long distance (10 to 50 kilometers) downwind from its main NO_x source. Stations close to their precursor sources did not have high ozone concentration due to NO_x titration. This is the case of Secunda station, located right outside of the industrial complex, Camden and Hendrina.

5.4.1 AOT40 results

5.4.1.1 DEA Sites

Monitoring stations that belong to the Department of Environmental Affairs included Ermelo, Hendrina, Middelburg, Secunda and Witbank and their data completeness ranged from 5% to 90%. The reason for this disparity changes from station to station. Data was available from 2008 to 2014. Data completeness was calculated according to the availability of the data during the growing months. Since AOT40 values are cummulative, only monitoring stations with appropriate data availability was taken into consideration. Ermelo and Witbank are the stations that showed the highest consistency in data completeness throughout the years and the availability of data from Secunda is the lowest of all stations. AOT40 values were highest in Ermelo and lowest in Secunda but not all years were complete. Ermelo's high concentrations suggest that the source of ozone precursors are the nearby powerplants of Kriel and Matla, which are located upwind during the growing season.

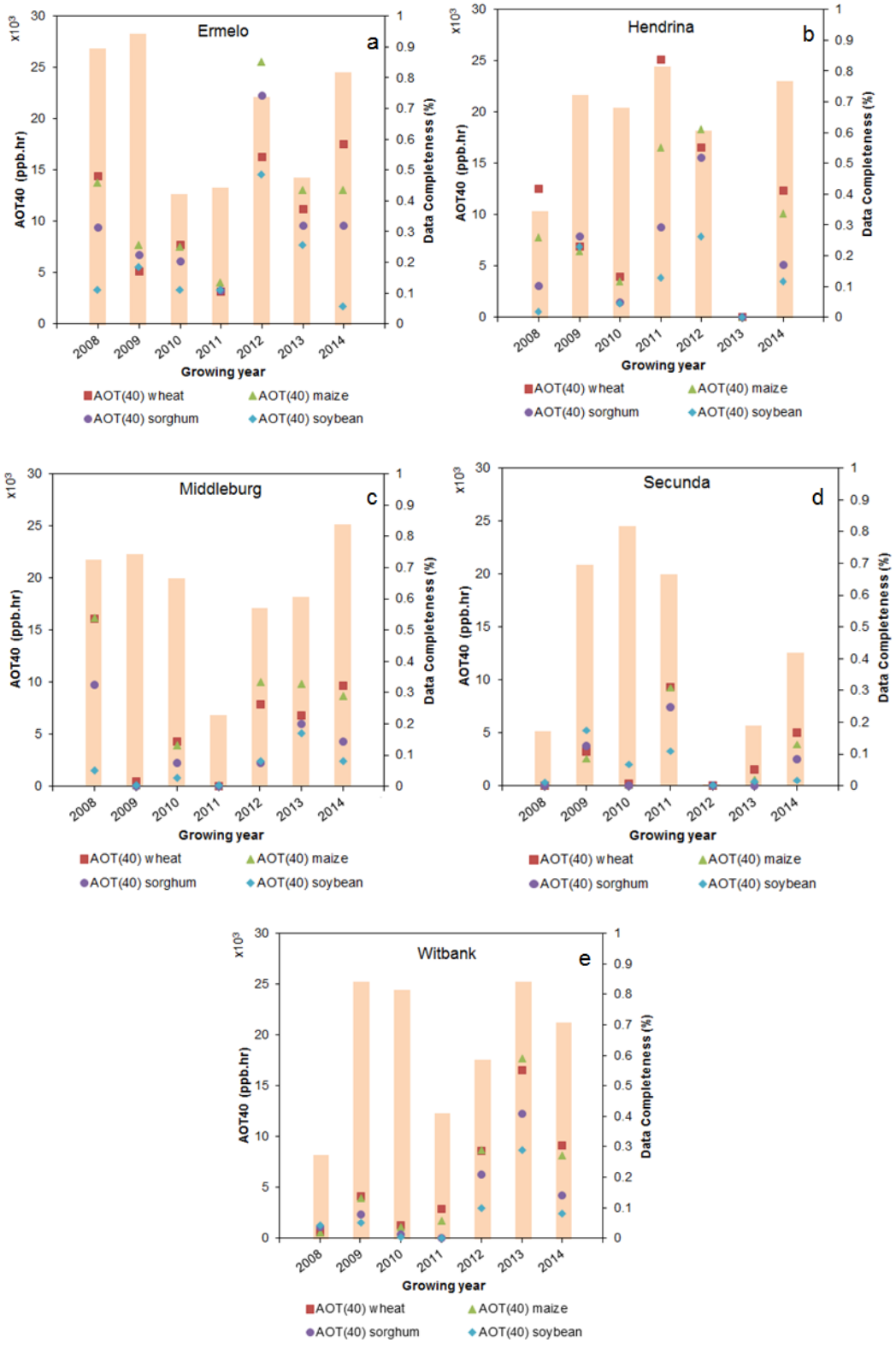
Ermelo
a
Hendrina
b
Middleburg
c
Secunda
d
Witbank
e
x10³
AOT40 (ppb.hr)
Data Completeness (%)
Growing year
2008
2009
2010
2011
2012
2013
2014
AOT(40) wheat
AOT(40) maize
AOT(40) sorghum
AOT(40) soybean

Figure 5-10: Annual cummulative AOT40 values for wheat (red squares), maize (green triangles), sorghum (purple circles), and soybean (blue diamonds) for each station owned by South Africa's Department of Environmental Affair; (a) Ermelo, (b) Hendrina, (c) Middelburg, (d) Secunda and (e) Witbank. Data completeness is represented for each annual data set (orange column).

5.4.1.2 Eskom Sites

The data completeness in Eskom's stations was lower than the data obtained from the Department of Environmental Affairs. Only 2011 through 2014 were considered since they were the only years available. Data completeness values ranged from 6% to 87% in Camden station and from 38% to 82% in Grootvlei station. Only years with data completeness above 80% were considered for AOT40 calculations (same as DEA's station data analysis). No conclusion was established about AOT40 values due to low data availability. Further Eskom data from other stations data was obtained for 2015-2016, and they are discussed in section 5.4.2.

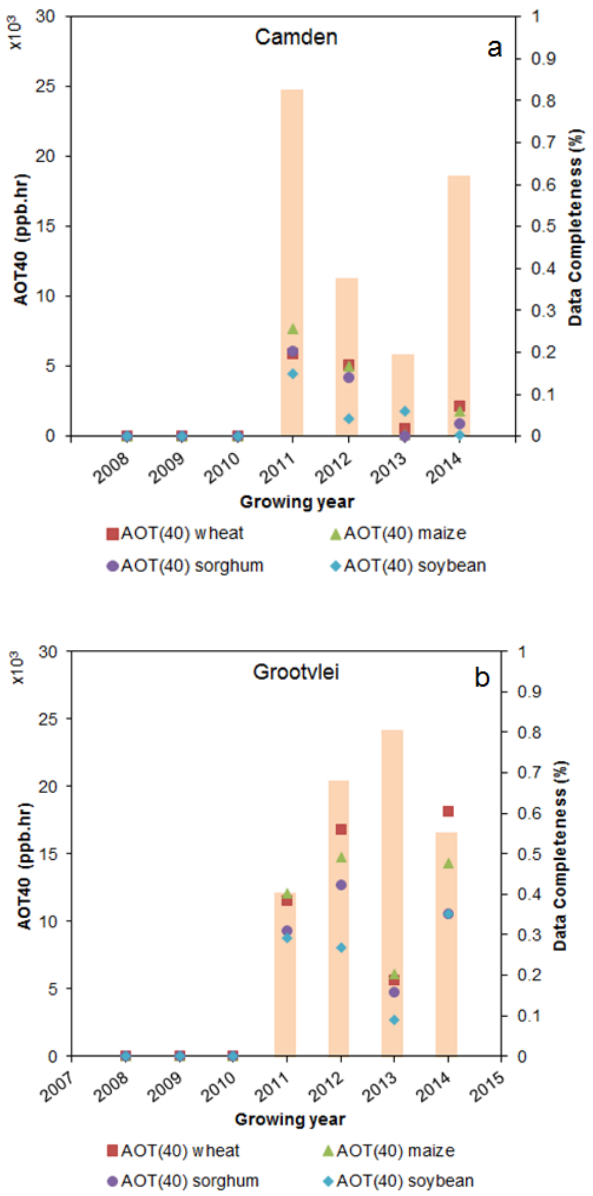

Figure 5-11: Annual cummulative AOT40 values for wheat (red squares), maize (green triangles), sorghum (purple circles), and soybean (blue diamonds) for each station owned by Eskom; (a) Camden and (b) Grootvlei. Data completeness is represented for each annual data set (orange column).

5.4.1.3 Sasol Sites

There was data availability only for two Sasol stations in Club and Embalenhle (Witbank). Data from this network is more robust as it has the highest values of data completeness of all three monitoring networks. However, only the years from 2011 to 2014 were available. Data completeness values ranged from 38% to 83% in Club station and from 76% to 94% in Embalenhle, being the last one the station with highest average data completeness through the four years. AOT40 values were highest in Embalenhle, partially due its high data availability. This was expected because several powerplants and heavily populated municipalities are located upwind.

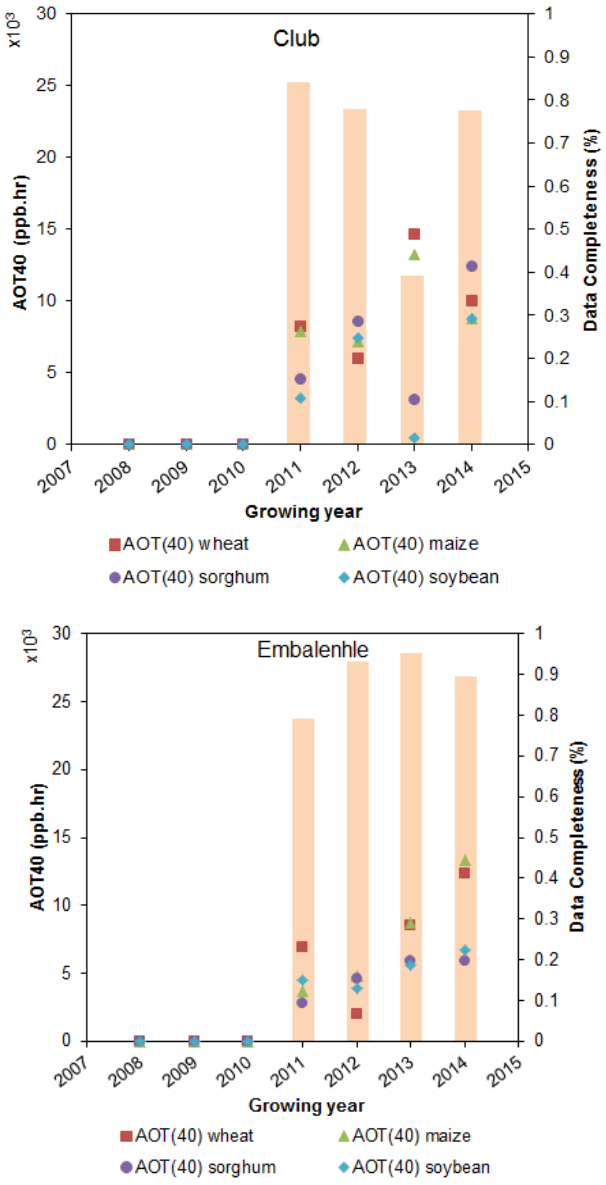

Figure 5-12: Annual cummulative AOT40 values for wheat (red squares), maize (green triangles), sorghum (purple circles), and soybean (blue diamonds) for each station owned by Sasol; (a) Club and (b) Embalenhle. Data completeness is represented for each annual data set (orange column).

The total AOT40 critical level of 3000 ppb.hr for agricultural crops was considered as the general starting point of plant damage origination. This same cumulative threshold is currently used by the European Union to assess wheat, the most sensitive crop in this study (UNECE, 2010). Crop specific critical levels have been developed for the other species (Mills et al., 2007). These are higher than wheat's: Soybean has a critical level of 4300 ppb.hr (Heagle et al., 1986; Heggestad *et al*., 1985; Heggestad *et al*., 1988; Mulchi et al. 1995; Heggestad and Lesser, 1990; Heagle *et al*., 1987 ; Heagle *et al*., 1998; Fiscus et al. 1997). Maize has a critical level of 13,900 ppb.hr (Rudorff et al., 1996; Mulchi et al., 1995, Kress and Miller, 1985). The same critical level as maize (13,900 ppb.hr) was used for sorghum due to the lack of research on the latter. This action was taken because they uptake SO_2 and O_3 similarly since they're both C4 plants. The thresholds and critical levels for each crop, shown in figure 5-13, provide a more accurate value for yield loss assessment.

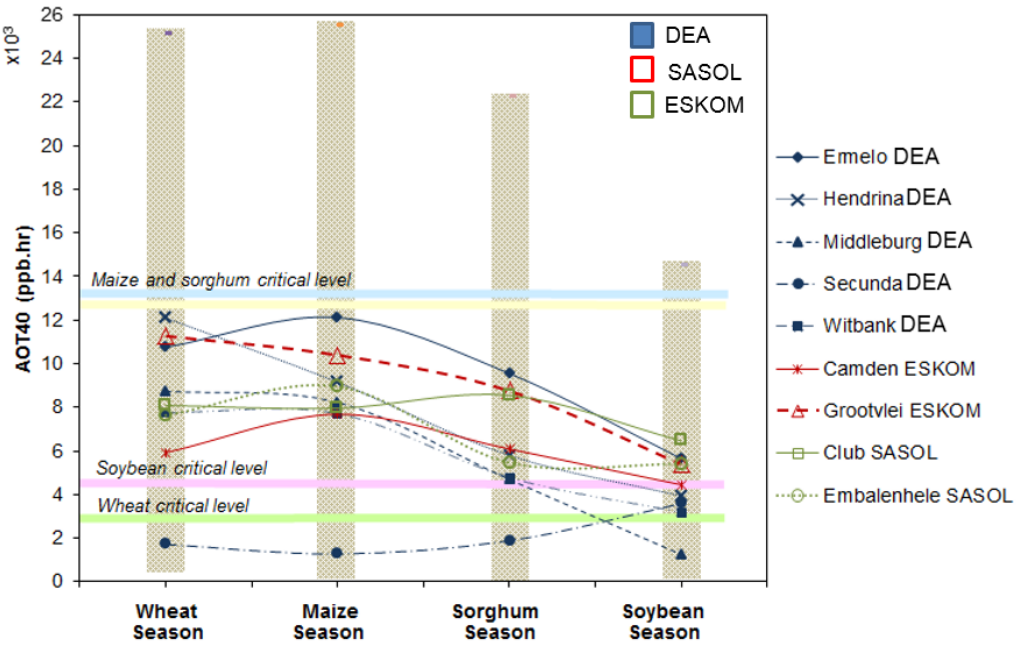

Figure 5-13: All sites average AOT40 values progression over the four growing season. DEA estations are shown in blue, Eskom stations in red and Sasol in green. Growing season AOT40 maximum and minimum values are illustrated with beige columns.

AOT40 results showed inter annual variability, which may be linked to climate factors of the area. A decline was observed in multi-year AOT40 values as the year progressed. The earlier crop (wheat) had the highest AOT40 average and the latest (soybean) had the lowest. Most stations had AOT40 values above the 3000 ppb.hr threshold (wheat's critical level) throughout the study period. Some stations had average values below 3000 ppb.hr, especially during the soybean season. This means that soybean

may experience the least damage due to ozone overall. However, AOT40 maximum values were above all critical levels for all seasons.

5.4.2 Losses due to ozone

Annual crop yield losses were calculated using previously derived response functions from literature described in section 5.3.2. Monitoring stations with data availability from 2015 to 2016 are first shown in figure 5-14. For these two years the crop that was mostly affected was wheat, followed by maize, then sorghum and lastly soybean. Grootdraaidam was the station with the lowest values and Secunda the station with the highest (75% difference). Data completeness is highest in Verkykkop's 2016 data set (92%) and lowest in Amersfoort's 2015 (0%). Grootdraaidam showed the lowest difference in data completeness between the two years (shown in figure 5-14b). The AOT40 values show an overall decreasing trend from the wheat season (the earliest) to the soybean season (the latest), which is equivalent to figure 5-14a. The yield losses also decrease as the season progresses. The highest yield losses are found in Phola station, with values as high as 56% and 55% during the wheat and maize season and 8% and 2 % for the sorghum and soybean season respectively. The lowest losses values were observed in Grootdraaidam with losses of 22% and 14% during the wheat and maize season and as low as 1% during the soybean season.

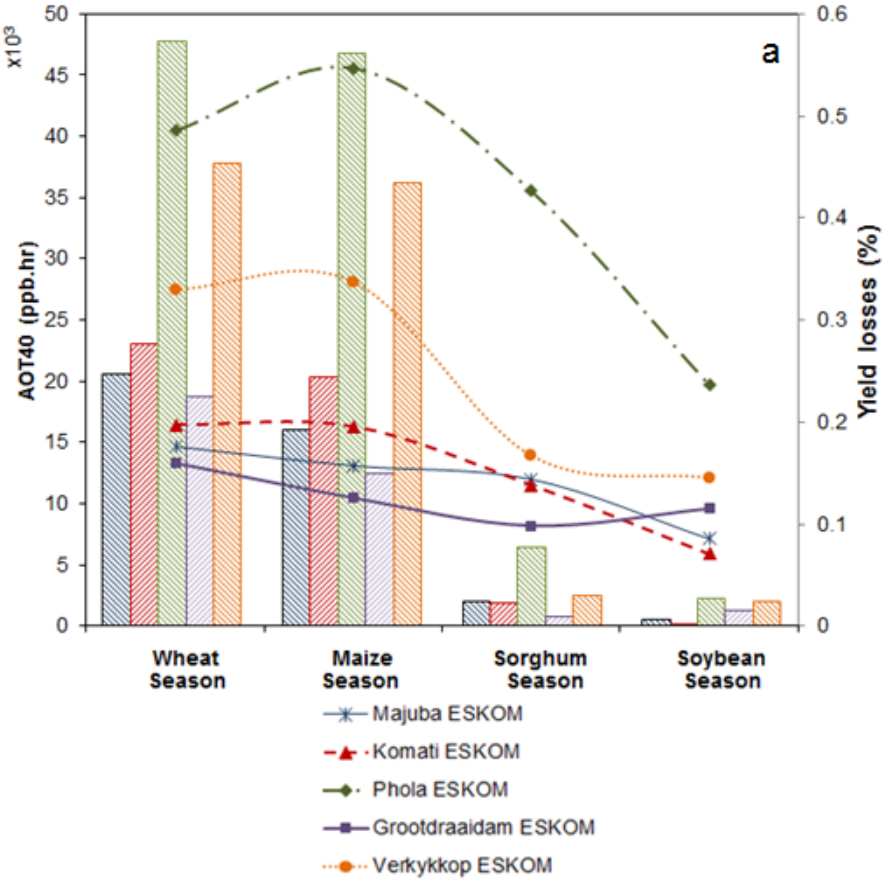
a
x10³
AOT40 (ppb.hr)
Yield losses (%)
50
45
40
35
30
25
20
15
10
5
0
0.6
0.5
0.4
0.3
0.2
0.1
0
Wheat Season
Maize Season
Sorghum Season
Soybean Season
Majuba ESKOM
Komati ESKOM
Phola ESKOM
Grootdraaidam ESKOM
Verkykkop ESKOM

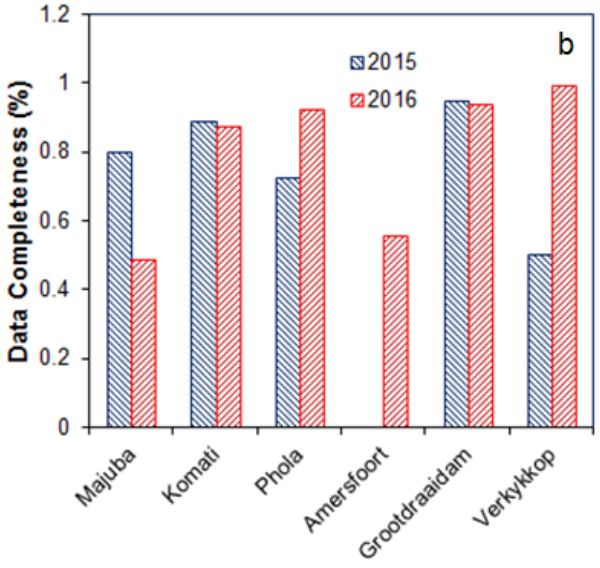
b
2015
2016
Data Completeness (%)
1.2
1
0.8
0.6
0.4
0.2
0
Majuba
Komati
Phola
Amersfoort
Grootdraaidam
Verkykkop

Figure 5-14: (a) Average annual AOT40 values (lines) and yield losses (columns) for the Eskom's stations with 2015-2016 data. Colors correspond to each station; blue is Majuba, red is Komati, green is Phola, purple is Grootdraaidam and orange is Verkykkop and (b) data completeness for each annual data set. Blue colums show data completeness in 2015 and red shows data completeness in 2016.

Crop specific AOT40 and yield losses in stations from the DEA, Sasol and Eskom networks with data from 2011 through 2014 are described in the followig subections.

5.4.2.1 Wheat

Wheat was the crop that showed the highest calculated yield loss percentage. This occurrence was due to the fact that its growing season takes place during the spring when sun radiation is high and the summer rains have not yet arrived. However, Mpumalanga does not grow a lot of wheat. Therefore it does not have a big impact in the local economy (see section 5.2.1). The regions that demonstrated the highest average losses for wheat are Grootvlei (19.1%), Hendrina (20.5%) and Ermelo (18.3%). These stations are located in relatively remote areas with no immediate sources of NO_x, allowing for chemistry to occur since ozone precursor sources are located 10 to 50 kilometers upwind. The lowest average yield loss was observed in Secunda (3.7%). This is mainly due to the proximity of the station to the Sasol Secunda industrial process, where ozone is being titrated by constant NO_x emissions. This station was followed by Camden (10.5%) and Witbank (13.48%).

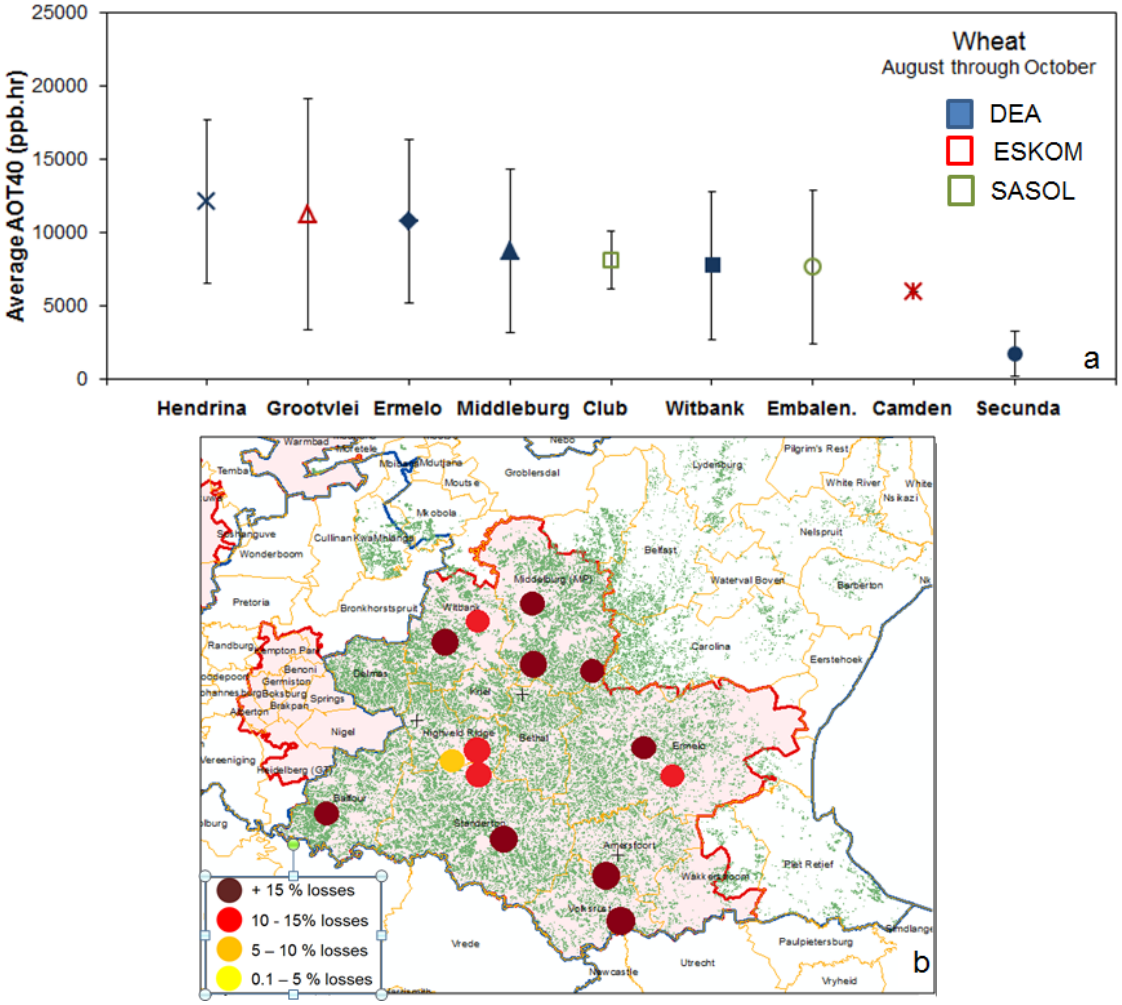

Figure 5-15: (a) AOT40 values in stations with 2011-2104 data during the wheat growing season for the three monitoring networks and (b) wheat crop yield loss map due to ozone across the Mpumalanga Highveld Priority Area. Losses are shown with colored circles for each station; more than 15% crop yield losses (brown), from 10 to 15% yield losses (red), from 5 to 10% yield losses (orange) and from 0.1 to 5% losses (yellow).

While there isn't much wheat in Mpumalanga it is important to understand how this crop is affected by ozone because it is the third most important grain produced in South Africa. In the 2014/15 season, this crop contributed approximately 10% to the gross value of all field crops. The average annual gross value of wheat for the past five years amounts to R4,868 million, compared to R23,347 million for maize, which is the most important field crop (South Africa Agriculture, 2016).

Wheat is also a crop that has severely been affected by drought in the past, especially within the summer rainfall regions (which includes the MHPA). Wheat planted under dryland conditions has been declining and it is expected to continue to decline (South Africa Agriculture, 2016). The reason for wheat producers to decrease the planting is mainly because of a shift from wheat to summer crops such as maize and soybeans. South Africa, a net importer of wheat, relies on imports from Russia, Germany and the Ukraine, among others, to meet its domestic demand. However, crop damage due to drought and ozone will decrease domestic production and increase the imports to meet the demand (South Africa Agriculture, 2016).

5.4.2.2 Maize

Maize is the most important grain crop in South Africa. It's the major feed grain and the staple food of the majority of the country's population. About 47% of the maize produced in South Africa is white and the remaining 53% is yellow maize (2015). White maize is primarily used for human consumption, while yellow maize is mostly used for

animal feed production (South Africa Agriculture, 2016). Most of the maize produced in South Africa is consumed locally; as a result, the domestic market is very important to the industry. In October 2015, the intended maize plantings of South African farmers were 2.55 million ha for the 2015/16 production season, which is 3,8% less than the 2.65 million ha planted during 2014/15.

Wheat was the crop that indicated the highest yield loss, but maize is the crop that is being affected the most by ozone in the MHPA, according to the results of this study. This occurs because of the large amount of corn that is grown in the region. This is a significant finding since the largest contributor towards the gross value of field crops in the province for the past five seasons has been maize (47.3%) (South Africa Agriculture, 2016). Since maize growing season is later in the year by a month, the calculated losses were overall lower than the wheat values. This is due to the increase of rain and cloudy days as crop planting and growing gets closer to the region's rainy season. Results show that there still were regions with very high losses and trends are similar to those obtained in the wheat calculations.

The highest values were observed in Ermelo (17.5%), followed by Grootvlei (14.7%) and Hendrina (12.7%). The lowest values were observed once again in Secunda (1.03%) due to the high NO_x concentrations in the area emitted from the petrochemical plant. This station was followed by Camden (13.4%). These values need further consideration as it is shown that ozone does cause a large amount of maize to be lost in one of the highest producing provinces in the countries.

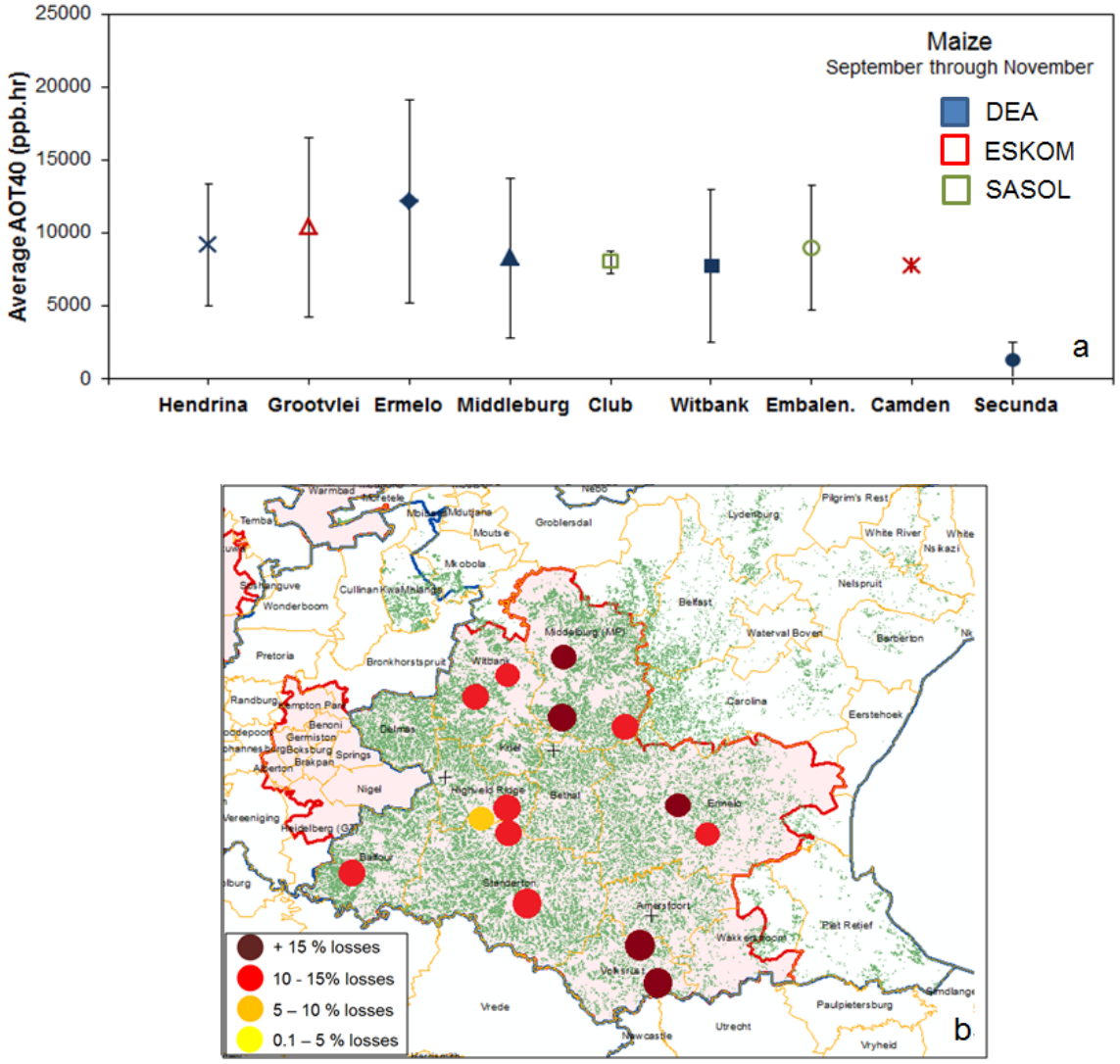

Figure 5-16: (a) AOT40 values in stations with 2011-2104 data during the maize growing season for the three monitoring networks and (b) maize crop yield loss map due to ozone across the MHPA. Losses are shown with colored circles for each station; more than 15% crop yield losses (brown), from 10 to 15% yield losses (red), from 5 to 10% yield losses (orange) and from 0.1 to 5% losses (yellow).

Maize producers in South Africa indicated that they intend to plant less maize for future seasons because they were under pressure of the prevailing dry weather conditions (South Africa Agriculture, 2016). Since the rainfall could still influence farmers' decisions, it is important to also consider ozone's effects for the future. There may be a possible correlation between maize decline and the increase of ozone; there is a lack of rainfall there are longer sunny days, which results in more opportunities for solar irradiation to form the phytotoxic pollutant.

5.4.2.3 Sorghum

Sorghum is native to Africa and it used to be the staple starch before maize was introduced by Portuguese colonists (McCann, 2001). Currently, sorghum grain isn't as highly consumed as wheat and maize, but it is still considered a valuable crop. Crop yield analysis results suggest that this plant species did not have high yield loss values. This is mainly due to the fact that the plant is resistant to ozone and the ozone values aren't as high during its growing season. The same equation was used for sorghum yield losses estimation as maize because they are both C4 plants and they intake ozone through their stomata similarly. However, a source of error is expected.

Losses are overall substantially lower than those of wheat and maize as it can be seen in the map below. No stations had values over 10%. High and low trends were the same as wheat and maize seasons. Results indicate that the highest yield losses values are located in Ermelo (1.5%) and Grootvlei (1.29%). The monitoring station located in

Secunda showed 0%, the lowest value calculated. Witbank and Embalenhle had the second lowest value with 0.08% losses. In order to assess sorghum losses (something that is a major concern in Africa), an equation development in the future is advised for more accurate information.

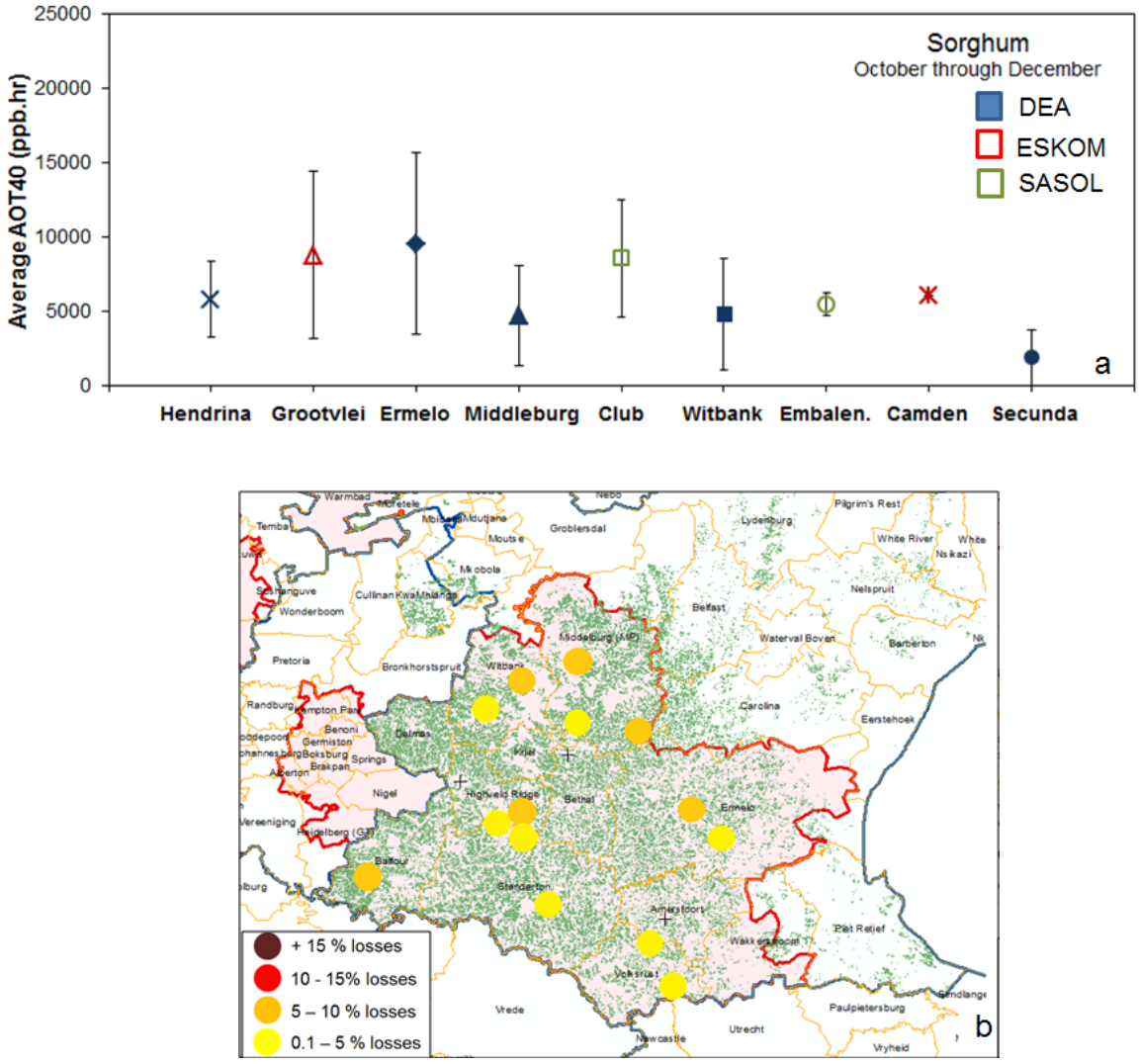

Figure 5-17: (a) AOT40 values in the stations with 2011-2104 data during the sorghum growing season for the three monitoring networks and (b) sorghum crop yield loss map due to ozone across the MHPA. Losses are shown with colored circles for each station; more than 15% crop yield losses (brown), from 10 to 15% yield losses (red), from 5 to 10% yield losses (orange) and from 0.1 to 5% losses (yellow).

5.4.2.4 Soybean

Soybean was the crop that was least affected by ozone in the MHPA. While previous research has shown that the crop is one of the most sensitive species to ozone (Mills et al., 2007), calculated AOT40 values did not show elevated concentrations during its growing season because the crop is cultivated it is in the middle of the region's rainy season. More clouds and less sunlight mean less radiation and therefore less ozone formation. Losses for soybean were negligible when compared to the other crops.

There were several stations whose yield losses appeared to be zero throughout the entire growing season. These include Camden, Middelburg, Witbank and Secunda. This could be due to the close proximity of these stations to industrial sites and larger cities. High and low trends were similar as the other three seasons. The highest yield losses values were observed in Ermelo (0.57%) and Grootvlei (0.45%).

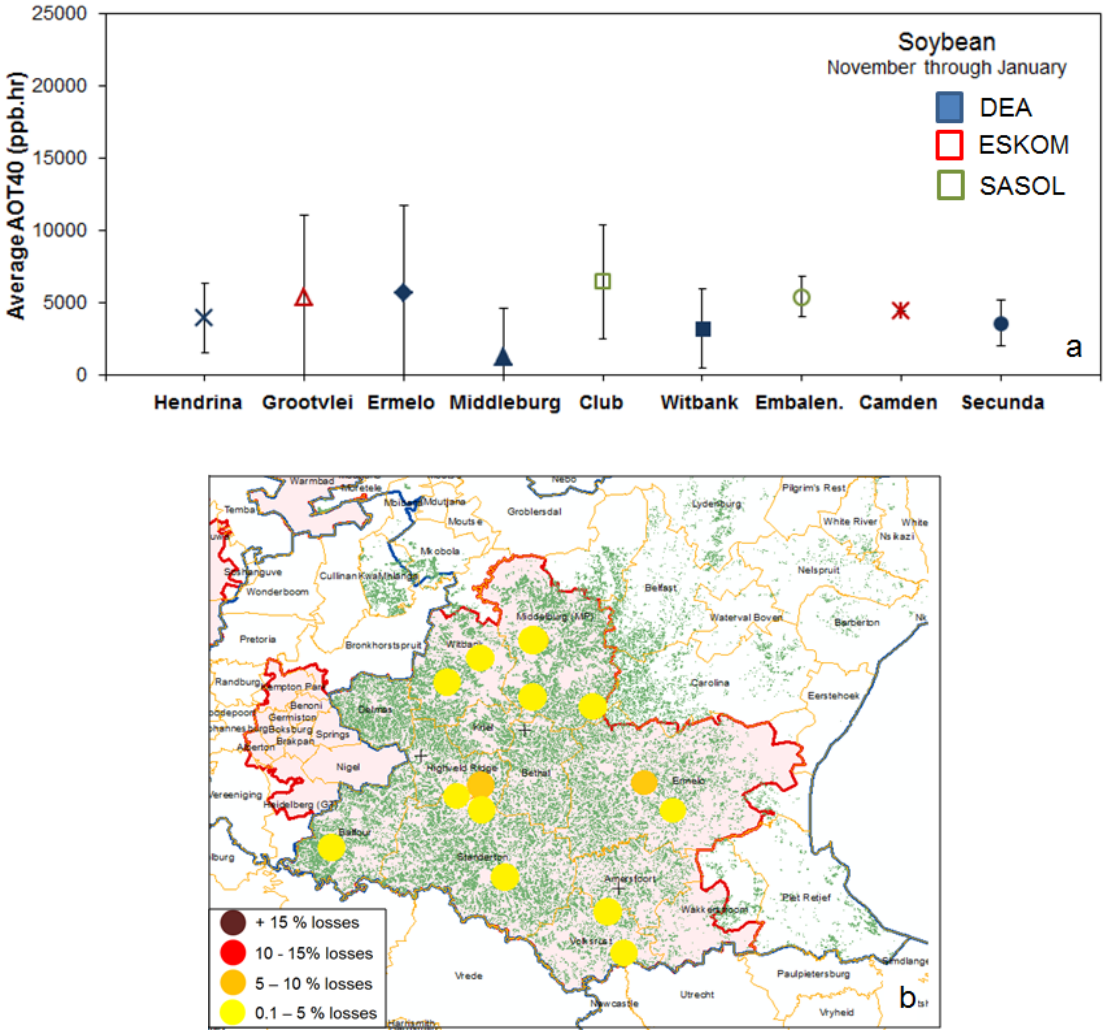

Figure 5-18: (a) AOT40 values in stations with 2011-2104 data during the soybean growing season for the three monitoring networks and (b) soybean crop yield loss map due to ozone across the MHPA. Losses are shown with colored circles for each station; more than 15% crop yield losses (brown), from 10 to 15% yield losses (red), from 5 to 10% yield losses (orange) and from 0.1 to 5% losses (yellow).

5.4.2.5 Multi-crop economic impact

Data from South Africa's Department of Agriculture provided the planted area for each crop in all the magisterial districts within the MHPA. This data set also contained the total revenue earned in the districts per growing year. With the provincial earning information and the outcomes of the crop yield losses calculation discussed in previous sections, revenue losses per magisterial district were calculated.

Ozone caused the most economic damage on maize (648.8 million Rand, $47 million, total losses in the HPA), followed by wheat (31 million Rand, $2.26 million, total losses in the HPA), then soybean (4.14 million Rand, $0.3 million, total losses in the HPA) and lastly sorghum (1.03 million rand, $0.08 million, total losses in the HPA). This is not the same order as percentage losses because the amount of crop grown in Mpumalanga varied from district to district. The magisterial district that had the highest losses for Maize was Middelburg (121.4 million Rand, $8.85 million), followed by Standerton (113.9 million Rand, $8.3 million) and Ermelo (108. 4 million Rand, $7.9 million). The highest revenue loss for wheat was found in Witbank (11.1 million Rand, $0.81 million), followed by Delmas (8.9 million Rand, $0.65 million) and Middelburg (6.8 million Rand, $0.5 million). Soybean was mostly affected in Standerton (1.7 million Rand loss, $0.12 million) and Ermelo with the same revenue loss. Sorghum was the crop that suffered the least amount of revenue losses, with the highest being in Standerton (0.89 million Rand, $0.06 million), followed by Balfour (0.09 million Rand loss, $0.01 million) and Ermelo (0.03 million Rand, roughly $22,000). The magisterial district with the highest total revenue loss for all crops was Middelburg (128.15 million Rand, $9.34

million), followed by Standerton (116.5 million Rand, $8.49 million) and Ermelo (110.09 million Rand, $8.03 million). Amersfoort, Witbank, Balfour, Bethal and Delmas had an order of magnitude lower than the previously mentioned magisterial district, ranging from 16.5 million Rand ($1.2 million) losses in Amersfoort to 67.5 million Rand ($4.92 million) losses in Bethal. The district with the least multi-crop losses was Mkobola (3.5 million Rand loss, $0.26 million).

Percentage losses per magisterial district and total loss per year are shown in figure 5-19. Values are not identical because the percentage losses assume that the total area of the magisterial district is taken entirely by the crop. Results indicate that losses could be greater if larger areas were to be planted in magisterial districts with high concentrations of ozone. For example, yield losses during the wheat season were highest in Witbank and Delmas because wheat grows in those magisterial districts. Other districts like Carolina, Standerton or Waterval-Boven could also have severe losses if wheat was introduced to the region. This information could be utilized by the farmers to estimate which crop would perform best in their region.

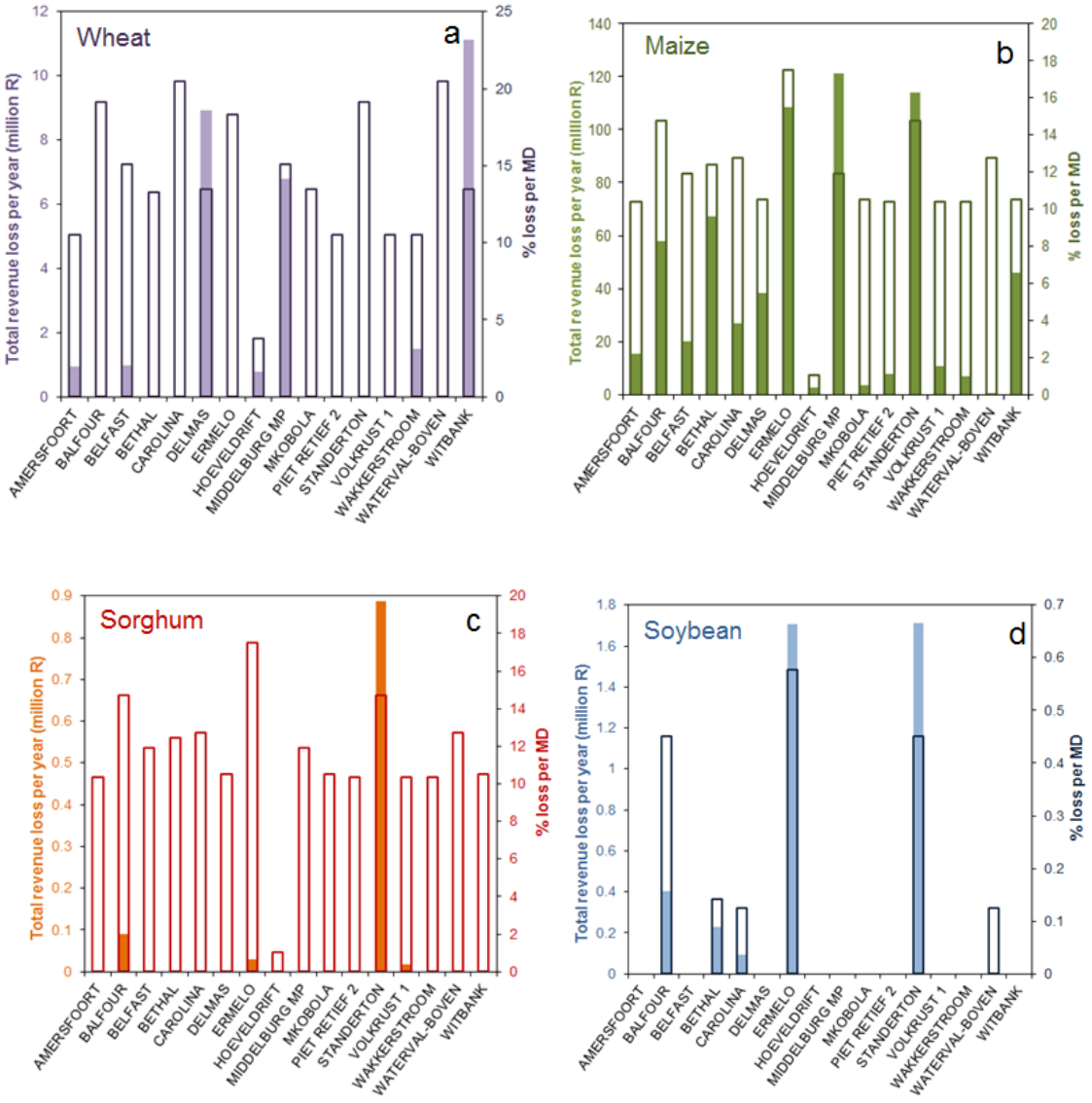
Wheat
a
Total revenue loss per year (million R)
% loss per MD
Maize
b
Total revenue loss per year (million R)
% loss per MD
Sorghum
c
Total revenue loss per year (million R)
% loss per MD
Soybean
d
Total revenue loss per year (million R)
% loss per MD
AMERSFOORT
BALFOUR
BELFAST
BETHAL
CAROLINA
DELMAS
ERMELO
HOEVELDRIFT
MIDDELBURG MP
MKOBOLA
PIET RETIEF 2
STANDERTON
VOLKRUST 1
WAKKERSTROOM
WATERVAL-BOVEN
WITBANK

Figure 5-19: (a) Average revenue and percentage losses due to ozone on wheat crops during one year (purple filled column) and the maximum losses within the magisterial district if more wheat was to be planted (void purple column) (b) Average revenue and percentage losses due to ozone on maize crops during one year (green filled column) and the maximum losses within the magisterial district if more maize was to be planted (void green column). (c) Average revenue and percentage losses due to ozone on sorghum crops during one year (orange filled column) and the maximum losses within the magisterial district if more sorghum was to be planted (void sorghum column). (d) Average revenue and percentage losses due to ozone on soybean crops during one year (blue filled column) and the maximum losses within the magisterial district if more soybean was to be planted (void blue column).

Total revenue losses due to ozone's effects on agriculture were later compared to the national and regional GDP (shown in table 5-5). While the outcome does not show to be a high percentage loss by solely taking ozone's effects into account, higher contributions to the GDP loss are expected when taking SO_2 and droughts into account. This is subject for future research.

Table 5-5: Calculated contribution of crop losses due to ozone pollution compared to Mpumalanga's regional and South Africa's national GDP.

	South Africa	**Mpumalanga**
GDP in 2015 (billion Rands)	4403.98	187.37
Total GDP loss due to SO_2 and O_3 (billion Rands)	0.0156%	0.3656%
% GDP loss due to O_3	0.0156%	0.3656%

**Source: The World Bank*

5.4.2.6 Department of agriculture yields

Globally, agricultural crop production is challenged by water scarcity, soil erosion and degradation, and the impact of climate change (e.g. elevated temperatures and reduced amount of rainfall). Therefore, it is important to also find a relationship between SO_2 and O_3 effects on crops and other parameters that affect the yields. To accomplish

this, the relationship between measured production and calculated AOT40 values was determined.

Measured annual crop yield were obtained from S.A. Department of Agriculture and an indirect relationship was established between the two variables (as AOT40 averages increase, measure crop yield decrease and vice versa). As average AOT40 values decrease from 2012 to 2014 an increase in maize yield was observed. Same case was also noticed for soybean, which AOT40 average peaks in 2012 when the measured production is the lowest and decreases as time passes towards 2014, while measured production increases. Wheat showed a slight increase in production from 2012 to 2013 as AOT40 and a subsequent stable increase occurred after. Sorghum was the only crop that did not show the same relationship as the other three species. The department of agriculture alleges that there are many other factors involved in the measured crop yield, such as drought, ambient temperature…etc., (South Africa Agriculture, 2016). Therefore, since there were only four measured years of data available and there is no information about other climatological factors, no fit equation was established. However, results from this observation have created opportunities for future investigations.

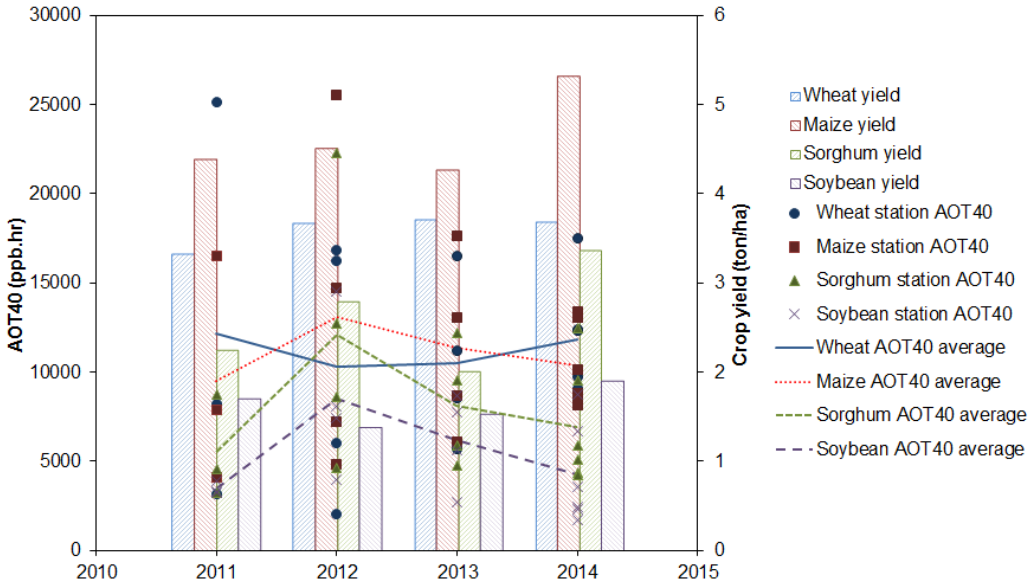

Figure 5-20: Measured crop yields from the South African Department of Agriculture for wheat (blue column), maize (red column), sorghum (green column) and soybean (purple column). Annual AOT40 values for each growing season in each station are shown for wheat (blue circles), maize (brown squares), sorghum (green triangles) and soybean (purple crosses). Annual AOT40 averages for all stations are shown for wheat (blue solid line), maize (red dotted line), sorghum (green dashed line) and soybean (purple dashed line).

5.4.3 SO_2 thresholds

In this study, hourly SO_2 values were collected from each station and concentrations were graphed to examine which stations had values over the hourly national standard. Figure 5-21 shows how all stations from all three monitoring networks. All data sets had values over the hourly national standard for health (134 ppb). There is no noticeable pattern to the vales, but it was observed that the DEA and Eskom stations showed higher data points than Sasol.

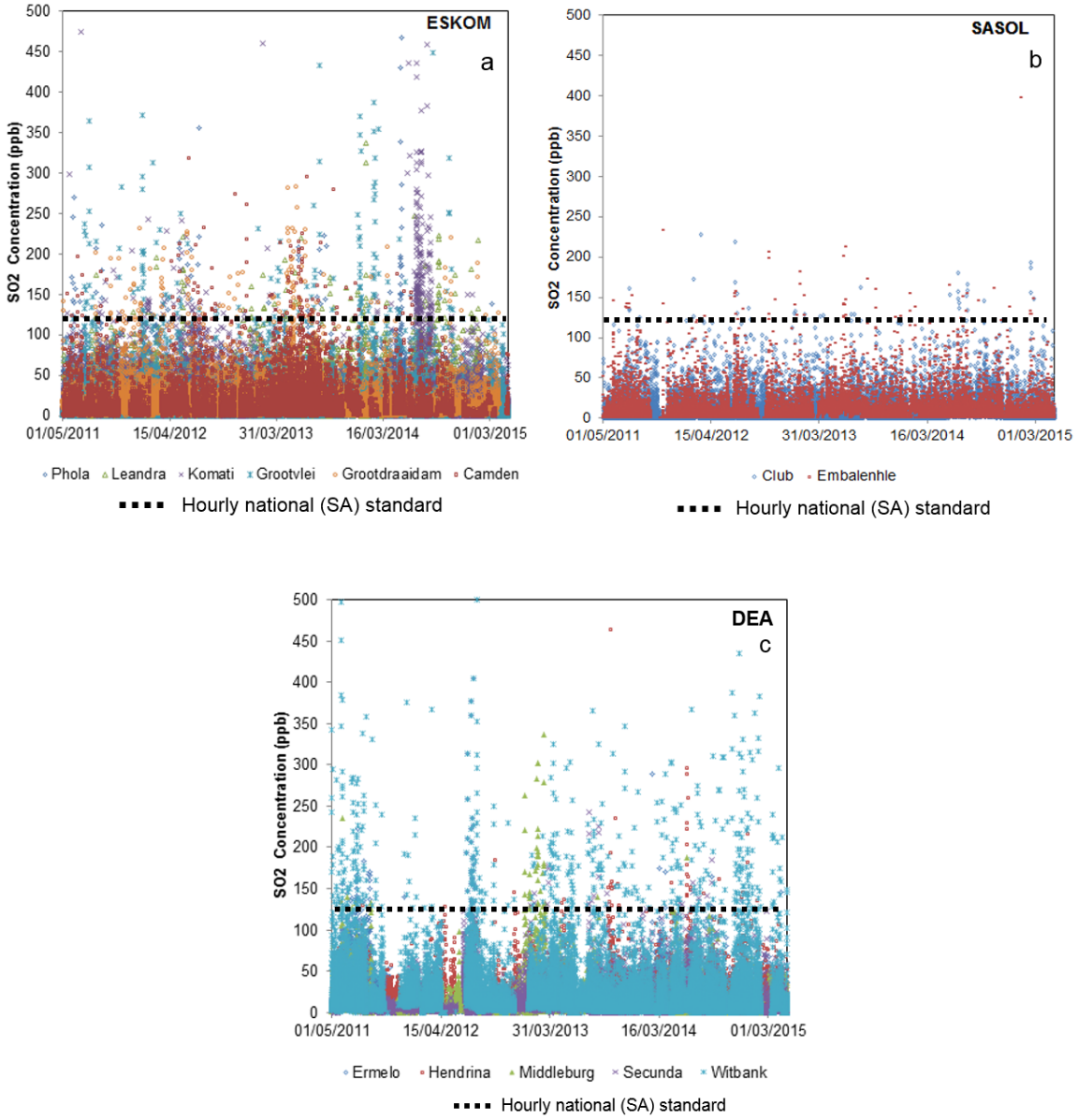

Figure 5-21: Hourly SO_2 for each station within Eskom (a), Sasol (b) and the Department of Environmental Affairs (c). Many values surpass the South African national hourly standard (black dotted line).

Many of the region's magisterial districts also surpass the international SO_2 standards for agriculture from the United Nations Economic Commission for Europe (CLRTAP), especially during the growing season (GSA). However annual average values (AA) are also found to be over the yearly average standard. All stations from the DEA had GSA values over the UNECE CLRTAP for all years except Middelburg from 2010 to 2015 and Secunda in 2008 and 2015. All Eskom stations exceeded the GSA standard except Camden in 2013 and Grootdraaidam in 2015. Sasol had GSA values for both Club and Embalenhle above the GSA standard. National annual average standards for health were exceeded in Komati in 2013 (Eskom station) and Witbank (DEA station) in 2009, 2010, 2011 and 2012.

Multi-year Annual and GSA averages for all three networks were compiled and graphed in figures 5-22a through 5-22c. The multi-year average value for all maximum values were also considered for the assessment (figure 5-22d). It is concluded that while there might be some yearly averages that do not surpass the annual or growing season standard, the maximum peaks are at very high concentrations and several orders of magnitude of those expected in many other polluted regions around the world.

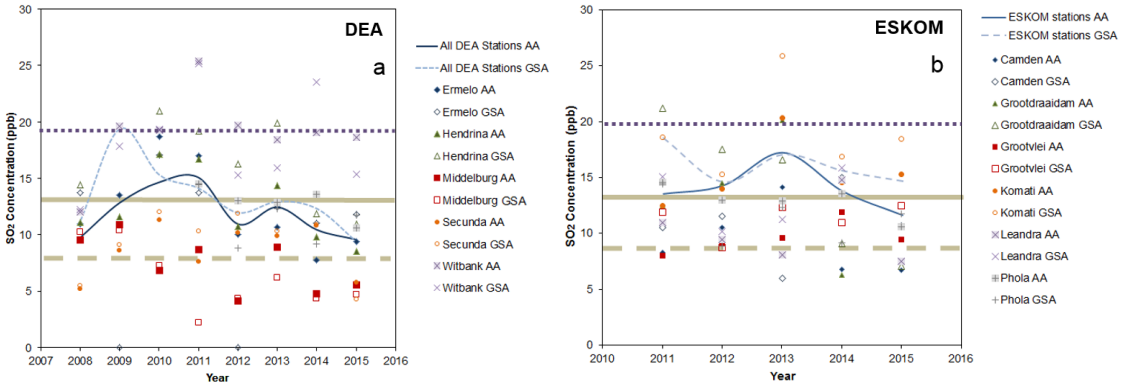
DEA
a
SO2 Concentration (ppb)
Year
All DEA Stations AA
All DEA Stations GSA
Ermelo AA
Ermelo GSA
Hendrina AA
Hendrina GSA
Middelburg AA
Middelburg GSA
Secunda AA
Secunda GSA
Witbank AA
Witbank GSA
ESKOM
b
ESKOM stations AA
ESKOM stations GSA
Camden AA
Camden GSA
Grootdraaidam AA
Grootdraaidam GSA
Grootvlei AA
Grootvlei GSA
Komati AA
Komati GSA
Leandra AA
Leandra GSA
Phola AA
Phola GSA

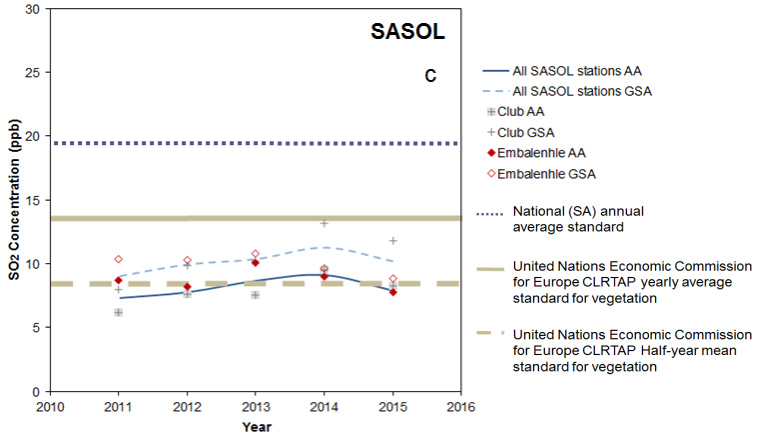
SASOL
c
SO2 Concentration (ppb)
Year
All SASOL stations AA
All SASOL stations GSA
Club AA
Club GSA
Embalenhle AA
Embalenhle GSA
National (SA) annual average standard
United Nations Economic Commission for Europe CLRTAP yearly average standard for vegetation
United Nations Economic Commission for Europe CLRTAP Half-year mean standard for vegetation

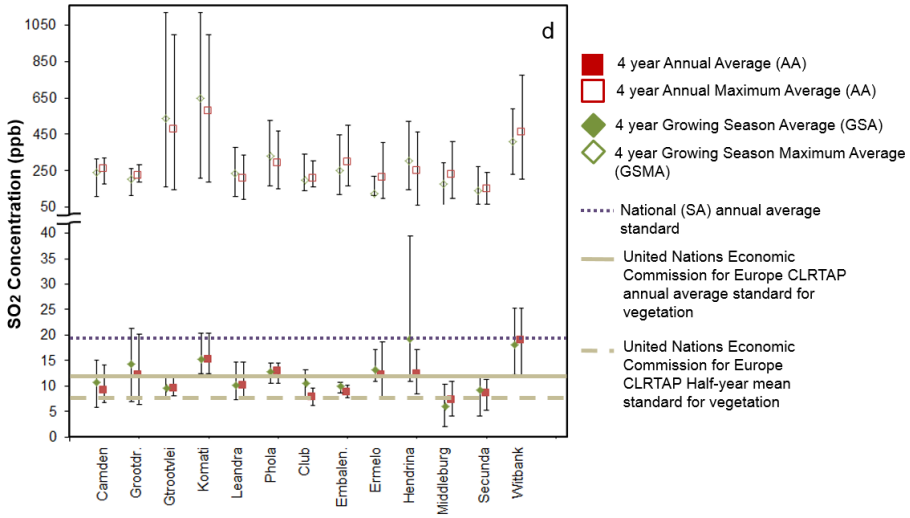
d
SO2 Concentration (ppb)
Camden
Grootdr.
Gtrootvlei
Komati
Leandra
Phola
Club
Embalen.
Ermelo
Hendrina
Middleburg
Secunda
Witbank
4 year Annual Average (AA)
4 year Annual Maximum Average (AA)
4 year Growing Season Average (GSA)
4 year Growing Season Maximum Average (GSMA)
National (SA) annual average standard
United Nations Economic Commission for Europe CLRTAP annual average standard for vegetation
United Nations Economic Commission for Europe CLRTAP Half-year mean standard for vegetation

Figure 5-22: (a) Annual SO_2 average concentrations for each individual station owned by South Africa's Department of Environmental Affairs with the multi station total annual average (solid blue line) and growing season annual average (dashed blue line), (b) Annual SO_2 average concentrations for each individual station owned by Eskom with the multi station total annual average (solid blue line) and growing season annual average (dashed blue line) (c) Annual SO_2 average concentrations for each individual station owned by Sasol with the multi station total annual average (solid blue line) and growing season annual average (dashed blue line) (d) 4 year annual average SO_2 concentrations (AA, red squares) and 4 year growing season average (GSA, green diamonds) plotted for each monitoring station. Filled values represent the data set average and the void values show the four-year maximum average. Beige solid line establishes designates the UNECE-CLRTAP annual average standard for vegetation, the beige dashed line marks the agency's half year standard and the purple dotted line symbolizes the South African national average standard.

Accurate quantification of the losses was not possible in this study due to the lack of response function research for SO_2. Fit equation development research is necessary to fully understand the revenue loss. However, spatial representation of the effects of SO_2 on the four major crops was accomplished in this study by noting which monitoring stations had values over the UNECE CLRTAP annual average standard (AA) and the growing season standard (GSA). Spatial distribution did not follow a similar pattern to the ozone yield losses. It was concluded that while less than half of the stations exceeded the annual average standard (AA), most of the stations surmounted the growing season average standard (GSA). The latter standard (GSA) is what's most relevant to this study and therefore requires further consideration when establishing losses in agriculture in the region.

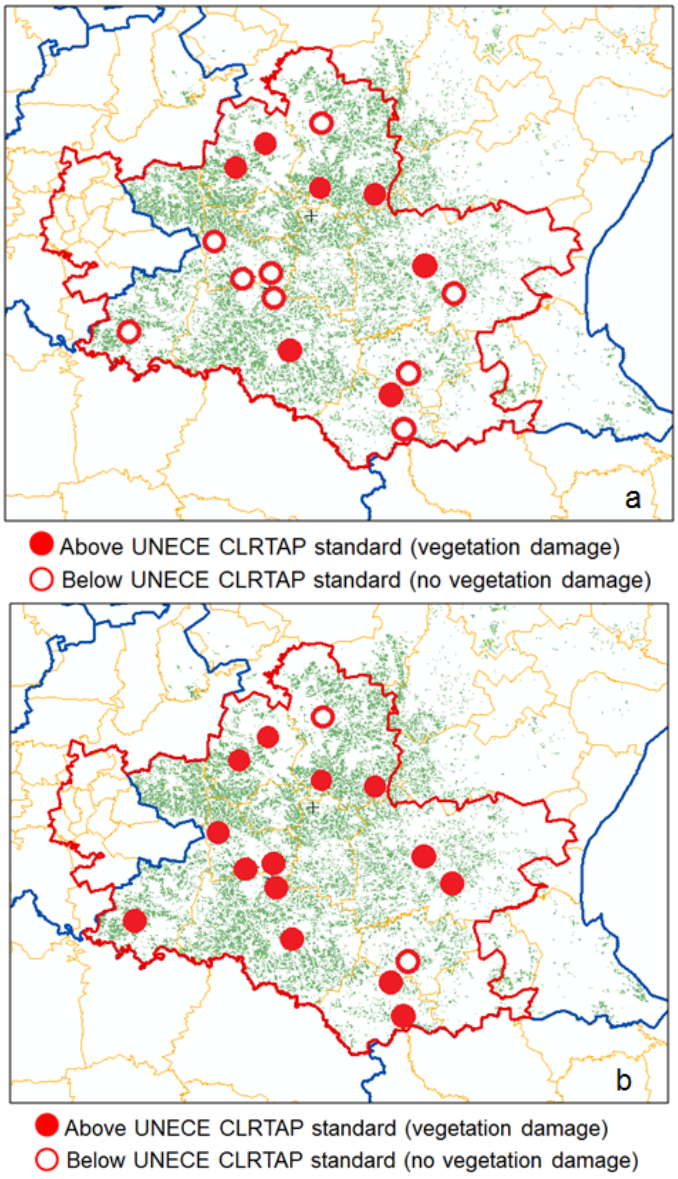

Figure 5-23: Detailed maps that show which stations surpass the UNECE CLRTAP annual average (AA) standard for SO_2 (a), and the UNECE CLRTAP growing season average (GSA) standard (b). Filled red circles represent the stations that surpass the standard, where vegetation damage due to SO_2 is expected, and the void circles mark the stations which are under the standard and where no vegetation damage is expected.

Past research suggest that yield losses may be exacerbated due to SO_2 emissions (Eason et al., 1996). Wheat, maize and soybean damage due to ozone and SO_2 is cumulative and the intake mechanisms (adsorption through the plant‘s stomata) are additive. However, there have been global and local concerns that ecological damage due to acid rain in other regions downwind of large coal-fired power plants and industries exist and may be a more serious concern than gaseous SO_2 intake (Wesely and Hicks 1977; Kuylenstierna and Chadwick 1989; Whelpdale and Kaiser 1996; Kuylenstierna et al. 1995, 2001; Kuylenstierna and Hicks 2002; Josipovic et al., 2007). SO_2 also has the potential to damage plants and acidify soil via acid rain in the HPA. This will most likely affect crops with a rainy summer growing season; this is the case of soybean, sorghum and maize. Sunflower, the crop that produces the most revenue in South Africa (South Africa Agriculture, 2016) is affected by SO_2. However, there isn't much sunflower that is grown in Mpumalanga. Future phytotoxic studies will focus on the sunflower yield losses caused by SO_2 in the Free State and The North West province.

5.5 Health impacts

5.5.1 Community health study

It is estimated that in South Africa, outdoor air pollution caused 3.7% of total mortality from cardiopulmonary disease in adults aged 30 years and older, 5.1% of mortality attributable to cancers of the trachea, bronchus, and lung in adults, and 1.1% of mortality from acute respiratory infections in children under 5 years of age. (Norman et al, 2007). To fully assess the impacts of SO_2 and O_3 in the MHPA, a study on the health

of the residents was also executed. The same data sets obtained from the DEA, Eskom and Sasol for the crop yield loss assessment was used for this investigation.

Table 5-6 (a and b) provides an assessment of the data obtained from SAAQIS. Data from the DEA and Sasol monitoring stations were analyzed for the period 2008 to 2015. Data from the Eskom monitoring stations were examined from 2011 to 2015. The compiled data set was introduced into IGOR Pro, where the data availability of the pollutants, as well as the 50^{th} and 95^{th} percentiles of each parameter were calculated. Thereafter, the acute and chronic averages for all criteria pollutants that have associated national ambient air quality standards (NAAQS) were investigated. Those parameters that had >80% data availability are highlighted in blue. The stations where pollutant concentrations exceeded NAAQS are marked in red. The division between low (green) and medium (yellow) is indicative only, and was selected as the mid-point between zero and the NAAQS value.

It was determined that while gaseous SO_2 and ozone are pollutants of concern in terms of health, the largest threat to the communities in the MHPA is PM_{10} and $PM_{2.5}$. Some of these particulates may have formed from primary gaseous pollutants (including SO_2 and VOCs) to form secondary organic aerosols (Capes et al., 2009; Santiago et al., 2012).

Table 5-6a: Network owners, station names and their location that are monitoring in HPA.

	Pollutant	% Compl.	50th Percentile (Hourly)	95th Percentile (Hourly)	Average (Acute)	Average (Chronic)
Ermelo DEA	SO2 (ppb)	62.2	7.8575	41.0584	12.2852	11.1459
	NO2 (ppb)	68.8	9.48	42.8436	13.676	13.9086
	O3 (ppb)	84.5	28.39	64.3773	31.2222	
	PM10 (µg/m³)	89.8	30.1917	173.721	52.4824	53.0422
	PM2.5 (µg/m³)	89.8	16.1963	86.7621	26.3674	26.5819
Hendrina DEA	SO2 (ppb)	79	9.26167	41.1514	13.6448	14.0024
	NO2 (ppb)	80.7	8.70333	41.6595	13.2642	16.0224
	O3 (ppb)	80	27.8167	68.1831	31.0288	
	PM10 (µg/m³)	70.3	29.15	118.658	43.133	47.4583
	PM2.5 (µg/m³)	70.3	15.6159	57.1034	20.7319	20.7763
Middelburg DEA	SO2 (ppb)	86.1	3.87667	23.5163	7.02341	7.30869
	NO2 (ppb)	81.4	8.83	39.0609	13.9348	15.72
	O3 (ppb)	78.4	18.6083	58.355	22.5496	
	PM10 (µg/m³)	88.5	27.9517	134.69	43.5454	45.5959
	PM2.5 (µg/m³)	88.6	14.5333	60.5702	20.7826	21.4795
Segunda DEA	SO2 (ppb)	78.9	5.43333	28.7597	8.76101	8.49738
	NO2 (ppb)	79.1	11.58	35.9365	14.2275	14.8328
	O3 (ppb)	60.7	25.6608	72.424	30.2874	
	PM10 (µg/m³)	84.6	31.2817	266.611	69.9382	65.6962
	PM2.5 (µg/m³)	84.6	15.6833	122.812	32.3138	30.0923
Witbank DEA	SO2 (ppb)	80.2	10.2	68.0737	19.0092	18.8128
	NO2 (ppb)	73.2	13.2917	50.9835	18.1329	18.1751
	O3 (ppb)	84.7	24.8946	56.4035	26.2594	
	PM10 (µg/m³)	82.8	30.5491	156.852	48.5271	48.0206
	PM2.5 (µg/m³)	82.8	15.5508	87.7615	25.9324	25.7034
Club SASOL	SO2 (ppb)	97.5	3.35572	30.5937	7.55022	7.58484
	O3 (ppb)	91.3	27.385	60.2217	29.6797	
	NO2 (ppb)	96	8.57226	31.1436	11.4396	11.4847
	PM10 (µg/m³)	86.4	23.2193	89.9191	32.033	31.0279
	PM2.5 (µg/m³)	74.6	9.22993	35.5016	12.2398	11.061

Acute	$PM_{2.5}$ (µg/m³)	PM_{10} (µg/m³)	NO_2 (ppb)	SO_2 (ppb)	O_3 (ppb)
Low	0 - 19	0 - 34	0 - 54	0 - 24	0 - 31
Medium	20 - 40	35 - 75	55 - 106	25 - 48	32 - 61
High	> 41	> 75	> 106	> 48	> 61

Chronic	$PM_{2.5}$ (µg/m³)	PM_{10} (µg/m³)	NO_2 (ppb)
Low	0 - 10	0 - 20	0 - 10
Medium	11 - 20	21 - 40	11 - 21
High	> 20	> 40	> 21

Table 5-6b: Continuation of table 5-6a. Network owners, station names and their location that are monitoring in HPA.

	Pollutant	% Compl.	50th Percentile (Hourly)	95th Percentile (Hourly)	Average (Acute)	Average (Chronic)
Embalenhle SASOL	SO2 (ppb)	95.8	3.86271	30.688	8.09225	8.10901
	O3 (ppb)	93.6	25.6817	58.4898	27.8854	
	NO2 (ppb)	91.1	6.89814	29.155	9.72819	9.8579
	PM10 (µg/m³)	67.2	32.0105	172.527	49.7626	47.9637
	PM2.5 (µg/m³)	59.8	10.0732	48.9269	15.1675	12.151
Camden ESKOM	NO (ppb)	79.3	1.439	48.5912		
	NO2 (ppb)	79.4	4.989	24.08	7.67993	7.87348
	SO2 (ppb)	83	4.0625	38.5228	9.59834	9.30413
	O3 (ppb)	54.2	21.8	51.9985	22.9032	
	PM10 (µg/m³)	79.2	28.174	132.221	43.7378	42.9711
Grootdraaidam ESKOM	NO (ppb)	76.7	1.251	7.457		
	NO2 (ppb)	75.5	3.635	14.0107	5.04297	4.97711
	SO2 (ppb)	84.7	26.89	88.613	12.3963	12.1936
	PM10 (µg/m³)	62.8	7.776	40.6514	32.814	35.1093
Grootvlei ESKOM	NO (ppb)	83.4	1.952	12.0592		
	NO2 (ppb)	83.4	6.031	21.165	7.89204	8.20725
	SO2 (ppb)	86.6	5.268	30.363	9.49286	9.59982
	O3 (ppb)	90.7	30.33	64.983	32.8385	
	PM10 (µg/m³)	72.9	29.93	94.9189	38.4996	36.878
Komati ESKOM	NO (ppb)	77.9	2.667	25.2225		
	NO2 (ppb)	77.9	7.205	25.99	9.53538	9.33061
	SO2 (ppb)	81.4	6.128	50.4072	15.1389	13.8375
	PM10 (µg/m³)	85.5	51.92	140.4	60.9111	58.4289
Leandra ESKOM	NO (ppb)	22.7	1.274	5.585		
	NO2 (ppb)	22.7	3.4825	11.5756	4.49215	4.49215
	SO2 (ppb)	88	6.301	35.76	10.7023	11.1293
	PM10 (µg/m³)	64.2	17.499	84.4	26.7061	28.8154
Phola ESKOM	NO (ppb)	83.2	4.238	38.6271		
	NO2 (ppb)	81	7.811	29.4038	10.6161	10.8075
	SO2 (ppb)	87.9	8.516	38.7975	12.9743	12.85
	PM10 (µg/m³)	67.6	34.5825	251.95	68.3232	70.8493

Acute	$PM_{2.5}$ (µg/m³)	PM_{10} (µg/m³)	NO_2 (ppb)	SO_2 (ppb)	O_3 (ppb)
Low	0 - 19	0 - 34	0 - 54	0 - 24	0 - 31
Medium	20 - 40	35 - 75	55 - 106	25 - 48	32 - 61
High	> 41	> 75	> 106	> 48	> 61

Chronic	$PM_{2.5}$ (µg/m³)	PM_{10} (µg/m³)	NO_2 (ppb)
Low	0 - 10	0 - 20	0 - 10
Medium	11 - 20	21 - 40	11 - 21
High	> 20	> 40	> 21

**Acute average concentrations (CO, NO_2 hourly; SO_2, PM_{10}, $PM_{2.5}$ daily) and chronic average concentrations (annual) in the HPA. Stations are color-coded by the initial assessment of whether the stations should be considered (in green) or not (in red) for the community survey.*

In a future study, this health assessment will also include a community survey where questionnaires will be administered. In addition, a children health analysis will be conducted where lung functions will be measured and skin prick tests will be performed to determine allergies. The focus of this effort will be developed in lower income households.

5.6 Air quality modeling

5.6.1 Expanding research to other provinces

The potential impact of ozone on agriculture was appraised using information from monitoring stations, when co-located with agricultural areas of interest. However, if station data does not exist, or only provides information for a limited region or temporal scale, modeled data may suffice to "fill in the gaps". Through modeling, it is also possible to investigate various scenarios (e.g. a changing climate or foreseen changes in emissions sources). As a result of limited spatial extent of the monitored data availability in the country, air quality models can be used to produce air quality information nationwide.

Stations in the MHPA are located near agricultural enterprises. However, there are other regions throughout the country that are considered important for national food security. These include the Northwest Province, the Free State and Limpopo (shown in figure 5-24a). These provinces are also major growers of sunflower and maize but they lack monitoring stations (figure 5-24b). Therefore an alternate approach is necessary to perform phytotoxic and health assessments in the regions.

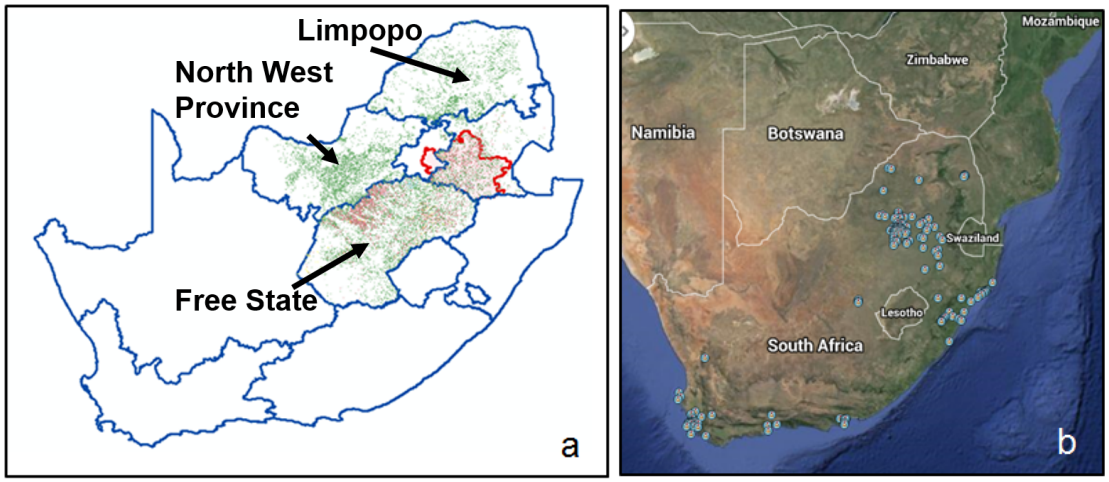

Figure 5-24: (a) Location of agriculture of concern in provinces surrounding Gauteng (green areas) (b) Air quality monitoring stations in South Africa that report data to SAAQIS are labeled with blue pins. Google Imagery 2015, NASA.

Ground level ozone can be modeled on a regional scale using air quality models like CAMx (Comprehensive Air quality Model with Extensions). Dispersion models, such as those used for environmental impact assessments, are not suitable for modeling ozone as the models do not account for the atmospheric chemistry that produces ozone

but they could be applied to further understand SO_2 effects. The CSIR currently uses CAMx to model regional air quality. In CSIR's simulation, pollutant transport and general atmospheric conditions (that impact chemistry) is forced with meteorological output from the CCAM (Conformal Cubic Atmospheric Model) regional climate model. To model and trace O_3 one needs to know how much is being formed and what emission source contribute to O_3 formation (Naidoo, 2015). Therefore a holistic emissions inventory is necessary to accurately perform a phytotoxic assessment using CAMx. The current emissions inventory still needs extensive improvement.

Figure 25 shows an example of the annual average change simulated for surface ozone. It illustrates a general slight increase over the country for 1989-2009 due to changes in meteorology. This climatological change has potential implications for synoptic patterns that may have on the transport and formation of ozone in South Africa in the future.

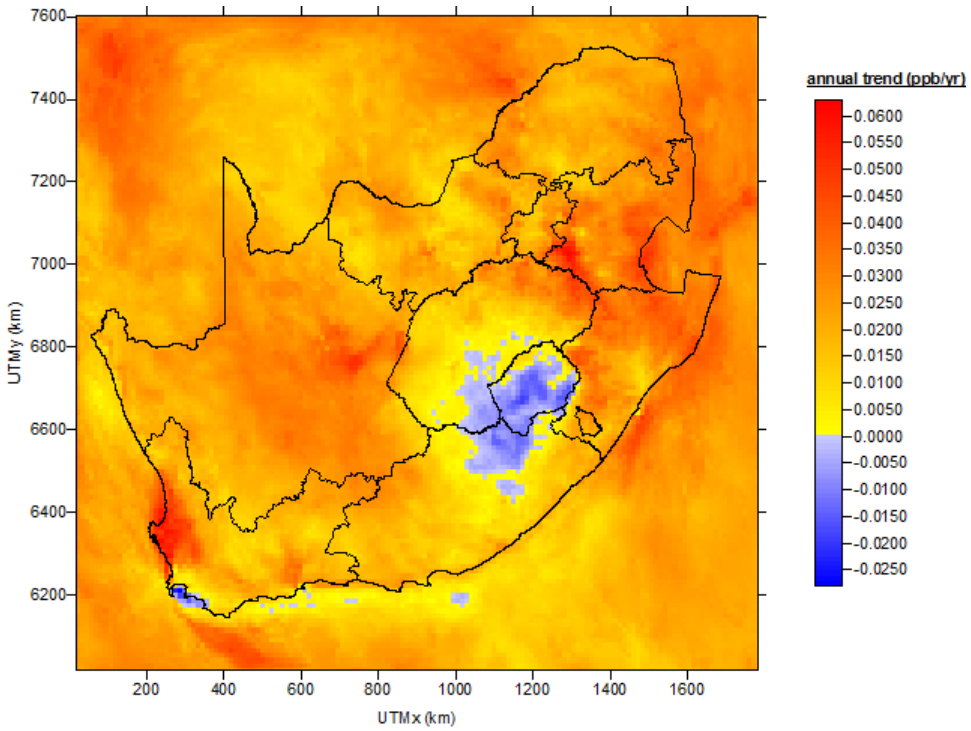

Figure 5-25: Annual average change simulated for surface ozone using a comprehensive emissions inventory for South Africa.

5.7 Acknowledgements

This work has been supported by the RIFA fellowship, sponsored by the UC Global Development Lab. Its contents are solely the responsibility of the grantee and do not necessarily represent the official views of the fellowship. Furthermore, RIFA does not endorse the purchase of any commercial products or services mentioned in the publication. The authors would like to thank Seneca Naidoo for their technical contribution to the report and the staff of SAAQIS, Eskom and Sasol for their assistance obtaining monitoring data and cooperation.

5.8 References

Akinboade, Oludele A., Emmanuel Ziramba, and Wolassa L. Kumo. "The Demand for Gasoline in South Africa: An Empirical Analysis Using Co-Integration Techniques." *Energy Economics* 30.6 (2008): 3222–3229. Print.

Archibald, Sally et al. "What Limits Fire? An Examination of Drivers of Burnt Area in Southern Africa." *Global change biology* 15.3 (2009): 613–630. Print.

Arndt, Richard L. et al. "Sulfur Dioxide Emissions and Sectorial Contributions to Sulfur Deposition in Asia." *Atmospheric environment* 31.10 (1997): 1553–1572. Print.

Avnery, Shiri et al. "Global Crop Yield Reductions due to Surface Ozone Exposure: 1. Year 2000 Crop Production Losses and Economic Damage." *Atmospheric environment* 45.13 (2011/4): 2284–2296. Print.

Avnery, Shiri et al. "Global Crop Yield Reductions due to Surface Ozone Exposure: Year 2030 Potential Crop Production Losses and Economic Damage under Two Scenarios of O3 Pollution." *Atmospheric environment* 45.13 (2011/4): 2297–2309. Print.

Barker, Jerry R., Andrew A. Herstrom, and David T. Tingey. "Formaldehyde: Environmental Partitioning and Vegetation Exposed." *Water, air, and soil pollution* 86.1-4 (1996): 71–91. Print.

Barnes, Brendon, and Angela Mathee. "Reducing Childhood Exposure to Indoor Air Pollution: The Potential Role of Behaviour Change Interventions." *Clean Air Journal, Tydskrif vir Skoon Lug* 11.1 (2002): 14–18. Print.

Balmer, M. "Household Coal Use in an Urban Township in South Africa." *Journal of Energy in Southern Africa (2007)*. Web.

Balashov, Nikolay V. et al. "Surface Ozone Variability and Trends over the South African Highveld from 1990 to 2007." *Journal of Geophysical Research, D: Atmospheres* 119.7 (2014): 2013JD020555. Print.

Brand S.A. "Tax Revenue Points to Growing Economy." *BoaNews.* N.p., 15 Sept. 2016. Web. 25 Jan. 2017.

Brocard, Delphine et al. "Emissions from the Combustion of Biofuels in Western Africa." *Biomass burning and global change* 1 (1996): 350–360. Print.

Cachier, Helene et al. “African Fire Particulate Emissions and Atmospheric Influence.” *Biomass Burning and Global Change* 1.41 (1996): 428–440. Print.

Capes, G., J. G. Murphy, and C. E. Reeves. “Secondary Organic Aerosol from Biogenic VOCs over West Africa during AMMA.” *Atmospheric* (2009): n. pag. Web.

Derwent, R. G. “Ozone Formation Downwind of an Industrial Source of Hydrocarbons under European Conditions.” *Atmospheric environment* 34.22 (2000): 3689–3700. Print.

Eason, Gwendolyn, Richard A. Reinert, and James E. Simon. “Sulfur Dioxide-Enhanced Phytotoxicity of Ozone to Watermelon.” *Journal of the American Society for Horticultural Science. American Society for Horticultural Science* 121.4 (1996): 716–721. Print.

Elashvili, Ilya et al. *Effects of Sample Impurities on the Analysis of MS2 Bacteriophage by Small-Angle Neutron Scattering*. DTIC Document, 2005. Web.

Emberson, L. D. et al. “Impacts of Air Pollutants on Vegetation in Developing Countries.” *Water, air, and soil pollution* 130.1-4 (2001): 107–118. Print.

Eberhard, Anton. “The Future of South African Coal: Market, Investment and Policy Challenges.” *Program on energy and sustainable development* (2011): 1–44. Print.

Farmer, Andrew. *Managing Environmental Pollution*. Abingdon, UK: Taylor & Francis, 1997. Print.

Felzer, Benjamin S. et al. “Impacts of Ozone on Trees and Crops.” *Comptes rendus: Geoscience* 339.11–12 (2007): 784–798. Print.

Fiscus, E. L., C. D. Reid, and J. E. Miller. “Elevated CO2 Reduces O3 Flux and O3-Induced Yield Losses in Soybeans: Possible Implications for Elevated CO2 Studies.” *Journal of Experimental* (1997): n. pag. Web.

Fuhrer, Jürg. “Ozone Risk for Crops and Pastures in Present and Future Climates.” *Die Naturwissenschaften* 96.2 (2009): 173–194. Print.

Fuhrer, J. et al. “Critical Levels for Ozone Effects on Vegetation in Europe.” *Environmental pollution* 97.1-2 (1997): 91–106. Print.

Galloway, J. N. “Acid Deposition: Perspectives in Time and Space.” *Water, air, and soil pollution* 85.1 (1995): 15–24. Print.

Gelang, Johanna et al. “Rate and Duration of Grain Filling in Relation to Flag Leaf Senescence and Grain Yield in Spring Wheat (Triticum Aestivum) Exposed to Different Concentrations of Ozone.” *Physiologia plantarum* 110.3 (2000): 366–375. Print.

Ghude, Sachin D. et al. “Reductions in India’s Crop Yield due to Ozone.” *Geophysical research letters* 41.15 (2014): 5685–5691. Print.

Heagle, Allen S. et al. “Injury and Yield Response of Soybean to Chronic Doses of Ozone and Soil Moisture Deficit.” *Crop science* 27.5 (1987): 1016. Print.

Heagle, A. S., J. E. Miller, and W. A. Pursley. “Influence of Ozone Stress on Soybean Response to Carbon Dioxide Enrichment: III. Yield and Seed Quality.” *Crop science* 38 (1998): 128–134. Print.

Heggestad, H. E., E. L. Anderson, et al. “Effects of Ozone and Soil Water Deficit on Roots and Shoots of Field-Grown Soybeans.” *Environmental pollution* 50.4 (1988): 259–278. Print.

Heagle, A. S. et al. “Response of Soybeans to Chronic Doses of Oxone Applied as Constant or Proportional Additions to Ambient Air.” *Phytopathology* (1986): n. pag. Web.

Heggestad, Howard E., and Virginia M. Lesser. “Effects of Ozone, Sulfur Dioxide, Soil Water Deficit, and Cultivar on Yields of Soybean.” *Journal of environmental quality* 19.3 (1990): 488–495. Print.

Held, G. et al. “The Climatology and Meteorology of the Highveld.” *Air pollution and its impacts on the South African Highveld. Johannesburg: Environmental Scientific Association* (1996): 60–71. Print.

HPA AQMP. *Highveld Priority Area Air Quality Management Plan*. Rep. Department of Environmental Affairs, 2011. Web.

Jain, S. L. et al. “Observational Study of Surface Ozone at New Delhi, India.” *International journal of remote sensing* 26.16 (2005): 3515–3524. Print.

Jeffries, Harvey E. “Photochemical Air Pollution.” *Composition, chemistry, and climate of the atmosphere* (1995): 308–348. Print.

Jenkin, Michael E., and Kevin C. Clemitshaw. “Ozone and Other Secondary Photochemical Pollutants: Chemical Processes Governing Their Formation in the Planetary Boundary Layer.” *Atmospheric environment* 34.16 (2000): 2499–2527. Print.

Josipovic, Miroslav et al. “Concentrations, Distributions and Critical Level Exceedance Assessment of SO2, NO2 and O3 in South Africa.” *Environmental monitoring and assessment* 171.1-4 (2010): 181–196. Print.

Kgabi, Nnenesi A., and Ramotsamai M. Sehloho. “Tropospheric Ozone Concentrations and Meteorological Parameters.” *Global Journal of Science Frontier Research* 12.6-B (2012): n. pag. Web. 5 Apr. 2017.

Kress, L. W., and J. E. Miller. “Impact of Ozone on Grain Sorghum Yield.” *Water, air, and soil pollution* 25.4 (1985): 377–390. Print.

Krupa, S. V., M. Nosal, and A. H. Legge. “A Numerical Analysis of the Combined Open-Top Chamber Data from the USA and Europe on Ambient Ozone and Negative Crop Responses.” *Environmental pollution* 101.1 (1998): 157–160. Print.

Kuylenstierna, Johan C. I., and Michael J. Chadwick. “The Relative Sensitivity of Ecosystems in Europe to the Indirect Effects of Acidic Depositions.” *Regional Acidification Models*. Springer, Berlin, Heidelberg, 1989. 3–21. Print.

Kuylenstierna, J. C. I. et al. “Terrestrial Ecosystem Sensitivity to Acidic Deposition in Developing Countries.” *Water, air, and soil pollution* 85.4 (1995): 2319–2324. Print.

Kuylenstierna, J. C. et al. “Acidification in Developing Countries: Ecosystem Sensitivity and the Critical Load Approach on a Global Scale.” *Ambio* 30.1 (2001): 20–28. Print.

Kuylenstierna, J., and K. Hicks. “Air Pollution in Asia and Africa: The Approach of the RAPIDC Programme.” *Proceedings of the 1st Open Seminar on the Regional Air Pollution in Developing Countries*. Vol. 4. N.p., 2002. Print.

Laban, Tracey L. et al. “Impacts of Ozone on Agricultural Crops in Southern Africa: Commentary.” *Clean Air Journal, Tydskrif vir Skoon Lug* 25.1 (2015): 15–18. Print.

Lee, David S., Michael R. Holland, and Norman Falla. “The Potential Impact of Ozone on Materials in the UK.” *Atmospheric environment* 30.7 (1996): 1053–1065. Print.

Levine, Joel S. *Biomass Burning and Global Change: Remote Sensing, Modeling and Inventory Development, and Biomass Burning in Africa*. MIT Press, 1996. Print.

Lippmann, Morton. “Health effects of Ozone, A Critical Review.” *JAPCA* 39.5 (1989): 672–695. Print.

Lourens, Alexandra S. M. et al. “Re-Evaluating the NO2 Hotspot over the South African Highveld.” *South African journal of science* 108.11-12 (2012): 83–91. Print.

Lourens, Alexandra S. et al. “Spatial and Temporal Assessment of Gaseous Pollutants in the Highveld of South Africa.” *South African journal of science* 107.1-2 (2011): 1–8. Print.

Mathu, Ken, and Richard Chinomona. “South African Coal Mining Industry: Socio-Economic Attributes.” *Mediterranean Journal of Social Sciences* 4.14 (2013): 347. Print.

Matyssek, R. et al. “Forests under Climate Change and Air Pollution: Gaps in Understanding and Future Directions for Research.” *Environmental pollution* 160.1 (2012): 57–65. Print.

Mauzerall, Denise L., and Xiaoping Wang. “Protecting Agricultural Crops from the Effects of Tropospheric Ozone Exposure”: Reconciling Science and Standard Setting in the United States, Europe, and Asia.” *Annual Review of Energy and the Environment* 26.1 (2001): 237–268. Print.

McCann, James. “Maize and Grace: History, Corn, and Africa’s New Landscapes, 1500--1999.” *Comparative studies in society and history* 43.02 (2001): 246–272. Print.

McCormick, John. *Acid Earth: The Politics of Acid Pollution*. Earthscan, 1997. Print.

Mills, G. et al. “A Synthesis of AOT40-Based Response Functions and Critical Levels of Ozone for Agricultural and Horticultural Crops.” *Atmospheric environment* 41.12 (2007/4): 2630–2643. Print.

Mokgathle, Bontle Beauty. “Seasonal and Diurnal Variations of Surface Ozone on the Mpumalanga Highveld.” North-West University, 2006. Web.

Morgan, P. B., E. A. Ainsworth, and S. P. Long. “How Does Elevated Ozone Impact Soybean? A Meta-Analysis of Photosynthesis, Growth and Yield.” *Plant, cell & environment* 26.8 (2003): 1317–1328. Print.

Morgan, Patrick B. et al. “Season-Long Elevation of Ozone Concentration to Projected 2050 Levels under Fully Open-Air Conditions Substantially Decreases the Growth and Production of Soybean.” *The New phytologist* 170.2 (2006): 333–343. Print.

Mowatt, Grant. “10 Pretty Cool Inventions You May Not Have Known Come from South Africa.” *The South African*. N.p., 28 Sept. 2016. Web. 11 Feb 2017.

Muchow, R. C., and T. R. Sinclair. “Nitrogen Response of Leaf Photosynthesis and Canopy Radiation Use Efficiency in Field-Grown Maize and Sorghum.” *Crop science* 34 (1994): 721–727. Print.

Mulchi, C. et al. “Morphological Responses among Crop Species to Full-Season Exposures to Enhanced Concentrations of Atmospheric CO2 and O3.” *Water, air, and soil pollution* 85.3 (1995): 1379–1386. Print. ASA Special Publication.

Naidoo, Mogesh. “Modelling of Ozone over South Africa: Needs and Challenges: Commentary.” *Clean Air Journal, Tydskrif vir Skoon Lug* 25.1 (2015): 13–14. Print.

Osborne, Stephanie A. et al. “Has the Sensitivity of Soybean Cultivars to Ozone Pollution Increased with Time? An Analysis of Published Dose–response Data.” *Global change biology* 22.9 (2016): 3097–3111. Print.

Penkett, Stuart A. et al. “Atmospheric Photooxidants.” *Atmospheric Chemistry in a Changing World*. Ed. Guy P. Brasseur, Ronald G. Prinn, and Alexander A. P. Pszenny. Springer Berlin Heidelberg, 2003. 73–124. Print. Global Change - The IGBP Series.

Reich, P. B. “Quantifying Plant Response to Ozone: A Unifying Theory.” *Tree physiology* 3.1 (1987): 63–91. Print.

Roberts, G., M. J. Wooster, and E. Lagoudakis. “Annual and Diurnal African Biomass Burning Temporal Dynamics.” *Biogeosciences discussions* 5.4 (2008): 3623. Print.

Rudorff, B. F. et al. “Effects of Enhanced O3 and CO2 Enrichment on Plant Characteristics in Wheat and Corn.” *Environmental pollution* 94.1 (1996): 53–60. Print.

Sanchez, Dana. “Which Countries Produce And Consume Most Electricity In Africa?” *AFKInsider*. AFKInsider, 28 Oct. 2014. Web. 3 Apr. 2017.

SAAQIS, *South African Air Quality Information System Home Page*. N.p., 2017. Web.

Santiago, Manuel, Marta García Vivanco, and Ariel F. Stein. “SO2 Effect on Secondary Organic Aerosol from a Mixture of Anthropogenic VOCs: Experimental and

Modelled Results." *International Journal of Environment and Pollution* 50.1/2/3/4 (2012): 224. Print.

Sillman, Sanford. "The Relation between Ozone, NOx and Hydrocarbons in Urban and Polluted Rural Environments." *Atmospheric environment* 33.12 (1999): 1821–1845. Print.

Sinha, B. et al. "Assessment of Crop Yield Losses in Punjab and Haryana Using 2 Years of Continuous in Situ Ozone Measurements." *Atmospheric Chemistry and Physics* 15.16 (2015): 9555–9576. Print.

Smidt, Stefan, and Friedl Herman. "Evaluation of Air Pollution-Related Risks for Austrian Mountain Forests." *Environmental pollution* 130.1 (2004): 99–112. Print.

Solmon, Fabien et al. "Dust Aerosol Impact on Regional Precipitation over Western Africa, Mechanisms and Sensitivity to Absorption Properties." *Geophysical research letters* 35.24 (2008): L24705. Print.

Teixeira, Edmar et al. "Surface Ozone Impact on Global Food Supply: Potential Damage and Adaptation for Soybean Crops." *IOP Conference Series: Earth and Environmental Science*. Vol. 6. adsabs.harvard.edu, 2009. 372043. Print.

Tuovinen, J. P. "Assessing Vegetation Exposure to Ozone: Properties of the AOT40 Index and Modifications by Deposition Modelling." *Environmental pollution* 109.3 (2000): 361–372. Print.

Van Dingenen, Rita et al. "The Global Impact of Ozone on Agricultural Crop Yields under Current and Future Air Quality Legislation." *Atmospheric environment* 43.3 (2009/1): 604–618. Print.

Van Tienhoven, Anna Mieke et al. "Assessment of Ozone Impacts on Vegetation in Southern Africa and Directions for Future Research: Commentary." *South African journal of science* 101.3-4 (2005): 143–148. Print.

Van Tienhoven, A. M., and M. C. Scholes. "Air Pollution Impacts on Vegetation in South Africa." *Air pollution impacts on crops and forests: a global assessment. Imperial College Press, London* (2003): 237–262. Print.

Van Tienhoven, Anna Mieke et al. "Preliminary Assessment of Risk of Ozone Impacts to Maize (Zea Mays) in Southern Africa." *Environmental pollution* 140.2 (2006/3): 220–230. Print.

Van Schalkwyk, M., *South Africa National Environmental Management.* SAAQIS. N.p., 2007. Web.

Wesely, M. L., and B. B. Hicks. "Some Factors That Affect the Deposition Rates of Sulfur Dioxide and Similar Gases on Vegetation." *Journal of the Air Pollution Control Association* 27.11 (1977): 1110–1116. Print.

Whelpdale, Douglas Murray, and M. S. Kaiser. *Global Acid Deposition Assessment*. World Meteorological Organization, Global Atmosphere Watch, 1997. Print.

Yuan, Xiangyang et al. "Assessing the Effects of Ambient Ozone in China on Snap Bean Genotypes by Using Ethylenediurea (EDU)." *Environmental pollution* 205 (2015): 199–208. Print.

Zunckel, M., K. Venjonoka, et al. "Van Tienhoven, AM. 2004a. Surface Ozone over Southern Africa: Synthesis of Monitoring Results during the Cross Border Air Pollution Impact Assessment Project." *Atmospheric environment* 38 6139–6147. Print.

Zunckel, M., A. Koosailee, et al. "Modelled Surface Ozone over Southern Africa during the Cross Border Air Pollution Impact Assessment Project." *Environmental Modelling & Software* 21.7 (2006/7): 911–924. Print.

"Households and the Environment: Energy Use: Analysis." N.p., n.d. Web. 13 Oct. 2016.

"Africa's Population Boom: Will It Mean Disaster or Economic and Human Development Gains?" *World Bank*. N.p., n.d. Web. 12 Oct. 2016.

"DEA State of Air Quality Governance Report." *Department of Environmental Affairs*. N.p., 2011. Web. 05 Jan. 2017.

"Mpumalanga Region." Region Industrial Development Corporation. N.p., n.d. Web. 10 Feb. 2017.

"Sasol Unlimited." Company Overview. N.p., n.d. Web. 20 Jan. 2017.

"SEPI." Sasol Exploration & Production International. N.p., n.d. Web. 20 Jan. 2017.

"WHO Vegetation." Effects of Sulfur Dioxide on Vegetation: Critical Levels (n.d.): World Health Organization Regional Office for Europ, 2000. Web.

"EPA Standards." National Ambient Air Quality Standards (NAAQS). N.p., 2014. Web. 22 June 2015.

"UNECE." Mapping Critical Levels for Vegetation. Manual on Methodologies and Criteria for Modelling and Mapping Critical Loads & Levels and Air Pollution Effects, Risks and Trends. *United Nations Economic Commission for Europe* (UNECE). Convention on Long-range Transboundary Air Pollution, 2010. Web.

"AET", National Strategy on Education And Training For Agriculture And Rural Development. Rep. Department of Agriculture, Conservation and Environment, 2005. Web.

UCAR. "How Does Ozone Damage Plants?" Center for Science Education. N.p., n.d. Web. 22 Jan. 2017.

"AQA, Air Quality Act No. 35072", National Environmental Management: Highveld Priority Area. *Government Gazette*, Government Notice 144. N.p.: n.p., 2012. Print.

"Eskom Company Information." Eskom Holdings SOC. N.p., n.d. Web. 06 Feb. 2017.

"DACE: Nelspruit" Mpumalanga Department of Agriculture, Conservation and Environment. (2001). Mpumalanga State of the Environment Report.

South Africa. Agriculture, Forestry and Fisheries. Directorate Information and Knowledge. Trends in the Agricultural Sector. Pretoria: n.p., 2016. Print.

Chapter 6: Conclusion

6.1 Dissertation summary

The efforts accomplished in this dissertation reveals a misunderstood source of particulate emissions in urban settings and further elaborate on the agricultural impacts of gaseous pollution in one of the fastest growing economical regions in Africa. The aim of the first three chapters of this doctoral thesis was to investigate particulate emissions from wastewater treatment sources and to model their transport. Results from these chapters provide a roadmap to develop solutions that reduce the incidence of disease among WWTP workers and neighboring communities. The final chapter goes beyond expected objectives to provide the first economic assessment on phytotoxic pollutants with monitoring data in the entire African continent. The information provided in this work will serve as a guide for future scientists, researchers and government officials to ensure a safe environment when treating wastewater as and to reinforce resilience in horticultural enterprises in Southern Africa.

Chapter 1 supplied results consisting of particulate number concentrations and size distributions from two different sources: a laboratory-scale aerobic bioreactor and the activated sludge aeration basins at Orange County Sanitation District (OCSD). Relationships between wastewater parameters (Total Organic Carbon (TOC), Chemical Oxygen Demand (COD) and Total Suspended Solids (TSS) and particle concentrations) were established. TOC, COD and TSS levels did not show to have a strong correlation with particle concentrations. Aeration flow proved to have the most significant relationship with particle concentrations increase. Therefore it was established that

aerobic processes generate particles through bubble bursting and that aeration reduction is one of the particle mitigation recommendations. A theoretical approach was also developed from empirical data to compare real world WWTP aerosol number emission fluxes with laboratory data. This will serve as a model to predict real world aerosol fluxes of primary particulate emissions in future studies.

Chapter 2 provided a characterization analysis of filter samples and a dispersion estimation through the AMS/EPA Regulatory Model (AERMOD): The study instituted a relationship between basin coverage, source emission flux and dispersion of particulates and revealed the biological and chemical composition of particulates collected filter samples from three WWTP along the Santa Ana River Watershed in Southern California: Orange County Sanitation District (OCSD) in Fountain Valley, Western Municipal Wastewater Treatment Plant (WMWWTP) in Riverside, and the City of Redlands Wastewater Treatment Plant (RWWTP). Basin coverage efficiency was investigated by modeling three coverage scenarios (fully covered basin, semi-covered and covered) were in the model with annual, monthly and daily meteorological data. Filter samples were collected 100 m upwind and 50 m, 100 m and 200 m downwind from the WWTP to quantify and speciate organic compounds, endotoxins, fungal glucans and proteins. Filter data was later compared with particulate concentrations obtained from a laboratory bioreactor that aerosolizes sludge obtained from each WWTP.

Results in this chapter showed that biological materials (endotoxin, proteins and glucans) and compounds of concern were found within the aerosol at the specified distances. Most of the fecal sterols were detected in samples collected downwind of the

WWTP in WMWWTP and RWWTP. A decrease in organic compound concentration was observed as the distance increased. PAHs were detected in few samples at much lower concentrations indicating the presence of burning activities around the sampling sites. WMWWTP had one order of magnitude higher of endotoxin concentrations because the plant has surface aerators that propel larger volumes mixed liquor into the atmosphere.

OCSD and RWWTP consisted of fine diffuser aeration; therefore lower concentrations of biological material were measured in these plants. An increase of endotoxin concentration was observed as the filter sample was taken further from the aerated basins. The cause of this increase may be that other sources of endotoxins exist downwind of the aerated basins (e.g. clarifiers, digesters, primary settling ponds...etc.) Future research is required to unmask other possible sources of endotoxins within these locations.

Another significant finding in chapter 2 was the discovery of cholestanol/coprostanol at a house in a neighborhood 635 meters downwind from OCSD. This insinuates that the WWTP particulates are reaching the public spaces and they could potentially cause disease in the people inhabiting the area. It was surmised that the aerated basins at the three locations contribute to protein and endotoxin concentrations but not fungal glucans and it was also concluded that partial coverage of the basins did not efficiently reduce the particulate emissions as previously thought. Thus, a basin that

is fully covered and possesses a fine air diffuser is advised to mitigate WWTP aerosols in urban areas.

Chapter 3 presented a novel method for condensational growth quantification of airborne viral pathogens. This investigation was pursued because particle deposition in the respiratory tract impacts lung conditions and increases the probability of viral and infection. This process occurs when supersaturated conditions in the respiratory tract cause inhaled WWTP aerosols to grow in size (hygroscopic growth), which significantly increase particle deposition efficiency. The methodology followed during this portion of the dissertation consisted of the EPA method 1601 for bacteriophage propagation: Male specific (F+) (MS2) and somatic coliphage in water by a two-step enrichment procedure and cloud condensation nuclei (CCN) experiments. The hygroscopicity of MS2 reagents (agar, phosphate-buffered saline (PBS) solution and tryptic soy broth (TSB) were also investigated. Particles from wastewater treatment plants (WWTP) were later aerosolized through conventional aeration of sludge in a laboratory bioreactor (as previously discussed in chapters 1 and 2) for an additional condensational growth studies.

The outcomes of chapter 3 suggest that WWTP aerosols may act as CCN inside the respiratory system, undergo hygroscopic growth and thus cause disease due to wet particle deposition. The most hygroscopic reagent in the MS2 stock solution was PBS, followed by TSB and the lastly agar. WWTP aerosols range from medium to high hygroscopicity. This indicates that viral particles from WWTP may also form droplets in supersaturated environments, such as the upper airways at 104.5 % humidity and lungs (95.5 % humidity).

Chapter 4 highlighted gaseous stressors (ozone and sulfur dioxide) on agriculture and compares them with the potential risk to human health through their inhalation in Mpumalanga, South Africa. This province is regarded as one of the largest industrialized areas in Africa and it heavily relies on agriculture as a source of revenue. AOT40 values, thresholds developed by the European Union, were used to estimate crop yield loss from during multiple years. These values were then used to calculated revenue losses in different magisterial districts within the province. Only O_3 and SO_2 concentrations for daytime hours (06:00 AM to 06:00 PM) during the three-month growing seasons (August through October for wheat, September through November for maize, October through December for sorghum and November through January for soybean) were considered.

Results in this chapter suggested that the most affected crop is wheat (multi-year average yield loss (AYL) of 14.21% and multi-year average total annual loss (TAL) of $2.39 million in the region), followed by maize (AYL of 11.42% and TAL of $49.9 million in the region), sorghum (AYL of 0.55% and TAL of $0.08 million in the region) and soybean (AYL of 0.12% and TAL of $0.32 million in the region). It was also concluded that many of the region's magisterial districts also surpass the international SO_2 standards for agriculture during the growing season, which also exacerbates the yield losses. SO_2 also has the potential to acidify soil and damage the plants via acid. This will most likely affect crops with a rainy summer growing season (soybean, sorghum and maize). It was also determined that while gaseous SO_2 and O_3 are pollutants of concern in terms of health, the largest health threat to the communities in Mpumalanga is PM_{10} and

$PM_{2.5}$; some of these particulates may have been primary gaseous pollutants (including SO_2 and VOCs) that formed secondary organic aerosols (SOA).

6.2 Future work

6.2.1 WWTP airborne emissions research

Future studies should be evaluated to expand the dates of investigation at RWWTP, WMWWTP and OCSD. A multi-year analysis is also suggested to visualize the concentrations of the elements of concern over time. Gases, specifically ammonia, have also been reported from WWTPs (Campos et al., 2009; Dai et al., 2013; Daelman et al., 2015; Campos et al., 2016) and have the potential to form SOA that may contribute to the urban aerosol budget: Future work will explore the composition of the secondary aerosols downwind of sources.

Levoglucosan, a chemical tracer for biomass burning was also observed in the measurements. No relationship was determined between concentration, WWTP particulate emissions and their transport to specific distances as it was concluded that the source of this organic compound was not the WWTP and future work is necessary to understand their source. PAHs were also found in all samples in similar concentrations as the filter samples from the bioreactor and they are also supected to come from a different source.

Further particle characterization studies are suggested to uncover the other sources of protein and endotoxin within the WWTP that are contributing to

concentrations downwind of the aerated basins. There has been concern in the scientific community that harmful viruses like Ebola can be aerosolized in WWTP (Bibby et al., 2017). Therefore biological characterization studies should also focus on the identification of the specific types of viruses and bacteria to understand their level of pathogenicity. Potential work could also expand to other WWTP and to explore how WWTP particulates would behave in different environments (humidity, temperature, etc.). In addition, future efforts should also focus on community education and the communication of the potential risks of living near uncovered aerated basins in neighborhoods that are affected.

The MS2 bacteriophage was not fully isolated in chapter 2 because its volume within the stock was found to be also almost ineligible. A future holistic CCN investigation should require the viral particles to be isolated. Possible work could also expand to investigating the deposition efficiency of viruses in the respiratory airways of mice. Chapter 2 only focused on the MS2 bacteriophage. Yet there are other bacteriophages and viruses with different shape and composition. Obtaining more information on how different viral properties affect CCN activity is critical to fully understand viral deposition in the respiratory airways.

6.2.2 Agriculture and phytotoxic pollution in Africa

The potential impact of SO_2 and O_3 on agriculture was appraised using information from monitoring stations. Stations in the MHPA are located near agricultural enterprises. However, there are other regions throughout the country that are considered

important food baskets yet they lack monitoring. These include the Northwest Province, the Free State, Limpopo and the Western Cape. These provinces are also major growers of sunflower; the crop that produces the most revenue in South Africa (South Africa Agriculture, 2016). This crop is affected by SO_2. Therefore future phytotoxic studies will focus on the sunflower yield losses caused by this pollutant.

Monitoring data is very limited on the African continent. Therefore phytotoxic assessments cannot be accurately developed for the entire South Africa and other countries in the continent. As a result of limited spatial extent of the monitored data availability, air quality models may be used as an alternative. Through modeling, it is possible to investigate various scenarios, e.g. a changing climate or foreseen changes in emissions sources. Ground level ozone may be modeled on a regional scale using air quality models like CAMx (Comprehensive Air quality Model with Extensions). Dispersion models, such as those used for environmental impact assessments, are not suitable for modeling ozone as the models do not account for the atmospheric chemistry that creates the secondary pollutant but they could be applied to further understand SO_2 effects.

The CSIR currently uses CAMx to model regional air quality. In CSIR's simulation, pollutant transport and general atmospheric conditions (that impact chemistry) is forced with meteorological output from the CCAM (Conformal Cubic Atmospheric Model) regional climate model. To model and trace O_3, information on how much of this gas is being formed and what emission source contribute its creation is

critical (Naidoo, 2015). Therefore a holistic emissions inventory is necessary to accurately perform a phytotoxic assessment using CAMx. The current national emissions inventory still needs extensive improvement.

In order to develop an economic assessment of SO_2 effects on the previously mentioned crops, accurate crop response functions are needed (same line as the AOT40 equations). SO_2's effect on agriculture is not as well studied as ozone. Therefore establishing these equations is a crucial step to understand how this phytotoxic pollutant is affecting the crops in developing countries, where SO_2 is still a big concern. Future efforts should also emphasize the necessity of communicating these results to South African farmers. Farmers should be made aware of the pollution levels in their region to assess which crops they should plant. Additionally, substantial regulation and enforcement is necessary in the region in to develop efficient solutions to reduce O_3 precursor and SO_2 emissions.

A health assessment is also in process of being conducted in the Mpumalanga Highveld (where the phytotoxic analysis was perform). This study will include a community survey, where questionnaires will be administered, as well as a children health assessment, where lung functions will be measured and skin prick tests will be performed to determine allergies. This study will be will be performed in lower income households.

6.3 Closing remark

Air pollution research for sustainable development

Understanding the source of urban air pollution, its consequences and establishing partnerships at the local, national and global level are imperative in designing mitigation strategies. In order to advance the United Nations Sustainable Development Agenda, there are a series of objectives that the global community must pursue to overcome the challenges attributed to pollution that the world is currently facing. These include furthering public awareness on air pollution, encouraging scientific progress in regards to air pollution and its subsequent effects on health and climate change, demanding the institution of clean air standards, and protecting our community members by making local efforts to reduce public risks. Endeavors should be focused on marginalized areas where the harm is greatest and technologies haven't yet reached.

Many countries, like South Africa are still in process of industrialization. Therefore, it is important to promote air pollution mitigation technologies such as catalysts, filters and renewable energy replacements to make cities safer and more sustainable. Efforts should identify the opportunities and challenges of air pollution as one of today's predominant issues for global science policy. Universal fundamental principles should therefore be adopted in response to this issue: It is important to globally recognize access to clean air as a crucial component of health and as a service that should be incorporated within the pantheon of essential public health services akin to clean water, vaccinations and primary care.

Monitoring and lessening harmful emissions of both outdoor and indoor air pollution would improve the wellbeing of all citizens while halting climatological variations that could later cause more convoluted complications. Interdisciplinary strategies are necessary to achieve global health standards and to achieve minimum air quality standards by enforcing environmental law. By approaching the issue one community at a time, millions of lives could be saved while axiomatically addressing climate change. It is a nexus that is vital to the survival of our civilization and the planet as a whole.

6.4 References

Bibby, Kyle et al. “Disinfection of Ebola Virus in Sterilized Municipal Wastewater.” *PLoS neglected tropical diseases* 11.2 (2017): e0005299. Print.

Campos, J. L. et al. “Greenhouse Gases Emissions from Wastewater Treatment Plants: Minimization, Treatment, and Prevention.” *Journal of chemistry and chemical engineering* 2016 (2016): n. pag. Web. 26 May 2016.

Daelman, Matthijs R. J. et al. “Seasonal and Diurnal Variability of N 2 O Emissions from a Full-Scale Municipal Wastewater Treatment Plant.” *The Science of the total environment* 536 (2015): 1–11. Print.

Dai, X. R., and V. Blanes-Vidal. “Emissions of Ammonia, Carbon Dioxide, and Hydrogen Sulfide from Swine Wastewater during and after Acidification Treatment: Effect of pH, Mixing and Aeration.” *Journal of environmental management* 115 (2013): 147–154. Print.

Kampschreur, Marlies J. et al. “Nitrous Oxide Emission during Wastewater Treatment.” *Water research* 43.17 (2009): 4093–4103. Print.

Naidoo, Mogesh. “Modelling of Ozone over South Africa: Needs and Challenges: Commentary.” *Clean Air Journal. Tydskrif vir Skoon Lug* 25.1 (2015): 13–14. Print.

South Africa. Agriculture, Forestry and Fisheries. Directorate Information and Knowledge. Trends in the Agricultural Sector. Pretoria: n.p., 2016. Print.